UNITED STATES DEPARTMENT OF COMMERCE
DANIEL C. ROPER, Secretary
NATIONAL BUREAU OF STANDARDS
Lyman J. Briggs, Director

✦

Journal of Research

of the

National Bureau of Standards

✦

Volume 20, No. 3
March 1938

[Published with approval of the Director of the Budget]

UNITED STATES
GOVERNMENT PRINTING OFFICE
WASHINGTON : 1938

For sale by the Superintendent of Documents, Washington, D. C. - - - - - - Price 25 cents
$2.50 per year on subscription

The prices of the separate Research Papers appearing in this JOURNAL are given on the front cover page. If 100 or more copies of any separate are ordered, a discount of 25 percent is allowed. Those who desire copies of separate Research Papers should send their orders and remittances without delay to the Superintendent of Documents, U. S. Government Printing Office, Washington, D. C. This will aid him to determine the number of copies to be printed for sale. Research Papers are not printed from electrotypes, and usually no more reprints can be had when the first and only printing is exhausted.

U. S. DEPARTMENT OF COMMERCE NATIONAL BUREAU OF STANDARDS

RESEARCH PAPER RP1078

Part of Journal of Research of the National Bureau of Standards, Volume 20, March 1938

AN ABSOLUTE ELECTROMETER FOR THE MEASUREMENT OF HIGH ALTERNATING VOLTAGES

By Herbert B. Brooks, Francis M. Defandorf, and Francis B. Silsbee

ABSTRACT

An absolute electrometer of the attracted-disk type is described. It is suitable for the measurement of alternating voltages up to 275,000 volts effective value with an accuracy of a few hundredths of a percent. A set of equally spaced coaxial guard hoops, maintained at equally spaced potentials, serves to produce a uniform field at the disk in spite of the large separation (110 cm) required to avoid spark-over at the high operating voltage. Formulas are derived by which corrections can be applied for any deviation of the individually measured hoop potentials from the ideal equal spacing.

The disk hangs from one arm of a delicate balance which serves to measure the force of attraction. Light reflected from a mirror carried by the balance beam serves to magnify its motion and to indicate to the operator at a safe distance when a condition of equilibrium is reached. It also serves to indicate the height of the disk relative to its surrounding guard ring. The scale reading corresponding to the ideal coplanar condition is obtained from auxiliary measurements made with a pair of special microscopes adapted for measuring distances in the line of sight by a calibrated focus adjustment.

The change in the attractive force as the disk moves away from the coplanar position has been measured and compared with that calculated theoretically. The effects of this change on the sensitivity and on the stability of the balance are worked out in detail.

Trials of this instrument under various conditions, both normal and with certain adverse influences exaggerated, over the range from 10,000 to 100,000 volts, indicate that the probable error of values obtained with it is about 0.01 percent, and that this error will not be greatly increased when the instrument is used at 275,000 volts.

CONTENTS

	Page
I. Introduction	254
II. General description	256
III. Stability and sensitivity	259
IV. Formulation of the working equation	265
V. Precision and accuracy	266
VI. Experimental tests	269
1. Electrical discharges	270
2. Tilt of disk and of lower plate	272
3. Eccentricity of disk in aperture	272
4. Width of gap	272
5. Flatness of disk and of guard ring	273
6. Ventilating holes	276
7. Temperature	277
8. Guard-hoop potentials	277
9. Flatness of lower plate	285
10. Vibration	286
VII. Mechanical details	286
1. Main structure	286
2. Lower plate	288
3. Disks and damping chamber	289
4. Balance	290
5. Potential divider and hoops	293

Page
VIII. Details of operation 294
1. Weighing 294
2. Measurement of coplanarity 295
3. Gaging 297
4. Measurement of diameters 297
5. Survey of the disk 298
6. Measurement of hoop-potential distribution 299
IX. Mathematical details 300
1. Correction for nonuniformity of hoop-potential distribution 300
2. Sources of error in Fourier coefficients, G_k' 305
3. Variation of force with height of disk 309
X. Conclusions and discussion 312
XI. List of principal symbols 315

I. INTRODUCTION

The growth of the electrical industry has been marked for many years by a continued increase in the voltage at which electrical energy is transmitted. This is the natural result of the greater economy of high-voltage transmission for long distances and large amounts of power. The art of measuring alternating voltages and of measuring power and energy at high voltages has kept pace with this growth by extending further and further the methods and types of apparatus originally developed for more moderate voltages.

It seemed desirable to develop an independent method for measuring high voltages with an accuracy approaching 0.01 percent, which would afford a check on the methods at present in use. Such a method should provide a safeguard against any constant and unrecognized errors which tend to creep into the measurements of quantities which are widely different in magnitude from their basic units. Such an independent method for measuring high voltages was felt to be particularly desirable at the National Bureau of Standards, because one function of this Bureau is to check instrument voltage transformers and other apparatus used throughout this country in the commercial measurement of high voltages.

The precise methods in common use for the measurement of effective values of high alternating voltages involve a stepping-up by a factor of about 100,000 from the electromotive force of a standard cell to the voltage to be measured, together with a transfer from direct to alternating current by an instrument of the electrodynamic type. It was felt that the greatest possible contrast to this type of method would be obtained by using an absolute electrostatic instrument to which the entire potential difference to be measured could be directly applied. The attracted-disk type of instrument was adopted because in it the maximum permissible electric field is utilized most effectively, and because it is most adaptable to shielding from external disturbances.

This type of instrument was originally suggested by Sir William Snow Harris [1] in 1834. His rudimentary device, shown in figure 1, consisted of a metal disk d hung from one arm of a balance and a second disk a supported coaxially below the suspended disk. The force of attraction between the disks is proportional to the square of the potential difference between them. Because of the crowding of the electric charges toward the edges of the disk, and because of the

[1] Sir William Snow Harris. *On a new electrometer, and the heat excited in metallic bodies by voltaic electricity.* Trans. Roy. Soc. Edinburgh **12**, 206 (1834).

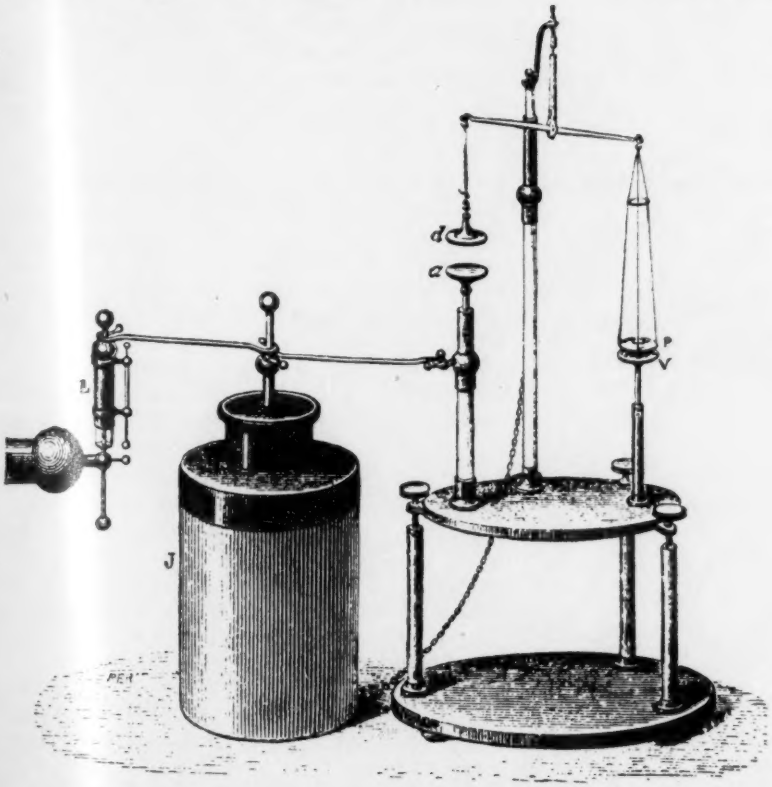

FIGURE 1.—*Attracted-disk electrometer of Sir William Snow Harris, 1834.*

forces exerted by neighboring objects, voltage measurements with the instrument in this form have relative significance only.

To remove this limitation of the Harris electrometer, and to develop it into an instrument suitable for accurate measurements, Lord Kelvin,[2] about the year 1870, surrounded the attracted disk by a fixed "guard ring" electrically connected to the disk, the flat lower surface of the guard ring being in the same plane as the lower surface of the disk. He also increased the diameter of the lower plate to equal the outside diameter of the guard ring. By making this diameter and that of the lower plate several times as great as the separation between these parts, Kelvin greatly reduced the effect of nonuniformity of charge at their edges on the force acting on the disk.

The simple theory of the Kelvin guard ring electrometer considers the disk, guard ring, and lower plate as plane parallel surfaces, and makes further assumptions, some of which, of a geometrical nature, are as follows:

1. That the lower surface of the disk and that of the guard ring are in the same plane.
2. That the clearance between the disk and the guard ring is zero, although the disk is free to move vertically.
3. That the common diameter of the guard ring and of the lower plate is so great in comparison with the distance between these parts that any further increase in this diameter would produce an inappreciable effect upon the electric field acting on the disk and therefore upon the force acting on the disk.

With these assumptions, it may be shown that for an effective difference of potential between the disk and the lower plate of V_s electrostatic units the electric force on the disk is

$$F=\frac{V_s^2 A}{8\pi b^2} \text{ dynes}, \tag{1}$$

where A is the area of the disk and b is the separation between it and the lower plate.

When the condition in assumption 1 is not realized, that is, when the disk either recedes into or protrudes from the guard ring, the electric charge ceases to be uniformly distributed over the surface of the disk and eq 1 must be extended to include a correction for the lack of coplanarity.

The condition in assumption 2 cannot be realized. There must be a gap between the disk and the guard ring. The effect of this gap, when the lower surface of the disk and that of the guard ring are coplanar, has commonly been allowed for by regarding the effective radius of the disk as exceeding the actual radius by one-half of the width of the gap.

The assumption made in condition 3 is not difficult to realize when the voltage to be measured is only a few kilovolts. It is obvious from eq 1 that in any event, to make the electric force to be measured large, the separation b should be small. For any given voltage, however, there is a minimum separation [3] below which sparkover will occur. For the high voltages now in commercial use (220 kilovolts and higher), this minimum value of b is so large as to make it impracticable to use a

[2] Lord Kelvin, Papers on Electrostatics and Electromagnetism, Sect. 360, 2d ed. p. 287 (Macmillan & Co., London, 1884).

[3] Instruments of smaller dimensions immersed in compressed gas have been used successfully by Palm (Z. tech. Physik **1**, 137 (1920); **14**, 390 (1933)) for high-voltage measurement and give large forces, but operation in the open seemed to us to offer greater convenience for studying the effect of various sources of error.

guard ring and a lower plate large enough to satisfy assumption 3. When the present investigation was begun, search was therefore made for some practicable method by which the electric force on the disk could be made to have the same value, to a sufficient approximation, as it would have if the common diameter of the guard ring and the lower plate were four or five times as great as the separation between them. Such an expedient [4] was found in a system of equally spaced coaxial "guard hoops" which enclose the cylindrical space between the guard ring and the lower plate. In operation, these hoops are maintained at equally spaced potentials, intermediate between those of the guard ring and of the lower plate.

In addition to the three geometrical assumptions just discussed, the use of an actual instrument of this type involves the further assumptions that in its construction the theoretical conditions, such as flatness and parallelism of surfaces, squareness of edges, equality of spacing of the hoops and of their potentials, etc., have been realized with sufficient exactness, and also that spurious effects, such as an electric wind from a brush discharge, are not present to a significant extent. In the present work wherever possible, as for example in the case of the hoop potentials, the departures of these various conditions from the ideal have been the subject of auxiliary measurements the results of which, when substituted in theoretically derived equations, give the corrections needed to allow for the departures. In the case of other conditions, such as coplanarity and flatness, our procedure has been to make observations under conditions definitely on either side of the ideal and to obtain the final result by interpolation. For the remaining and more numerous class of conditions, such as lack of parallelism, eccentricity, etc., we have performed check experiments with the disturbing condition present to an exaggerated degree, and from the smallness of the resulting effect on the indication of the instrument we have felt justified in neglecting the error present under normal operating conditions.

An absolute electrometer embodying these principles has accordingly been designed and built at the National Bureau of Standards for measurements up to 275,000 volts. It is the purpose of the present paper to describe this instrument in detail and to give the fundamental basis on which its indications depend and experimental data showing its possibilities and limitations. The comparison of results obtained with it and those obtained by the conventional method of measuring high voltages is treated in another paper.[5]

II. GENERAL DESCRIPTION

The general appearance of the electrometer with its capacitance potential divider is shown in figure 2. It is about 1 m in diameter and 3 m high. The lower plate is adjustable in height to give separations up to 110 cm.

The fundamental features of the instrument are shown schematically in the center of figure 6. It is evident that ideally the disk forms the central part of the upper plane equipotential boundary of a cylindrical space, the lower plate forms the other parallel equi-

[4] Chester Snow. *Effect of clearance and displacement of attracted disk, and also of a certain arrangement of conducting hoops upon the constant of an electrometer.* BS J. Research **1**, 514 (1928) RP17.

[5] Francis B. Silsbee and Francis M. Defandorf. *A transformer method for measuring high alternating voltages and its comparison with an absolute electrometer.* J. Research NBS **20**, 317 (1938) RP1079.

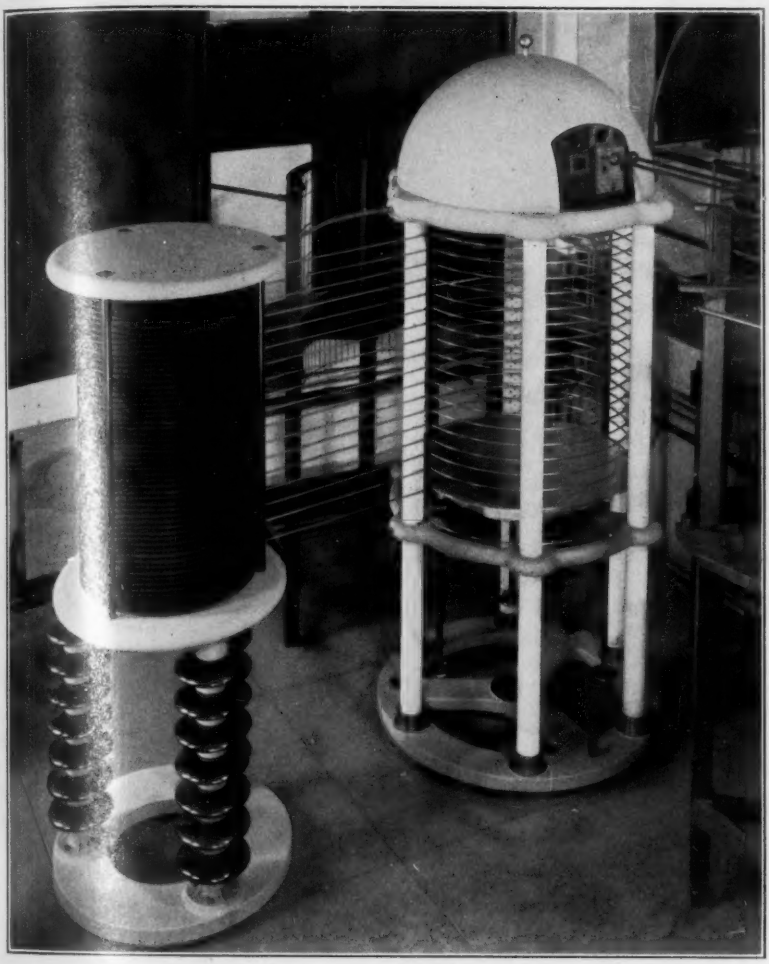

FIGURE 2.—*Electrometer (right) and capacitance potential divider (left).*
Hoops are here shown spaced at 6 cm instead of at the normal 2 cm.

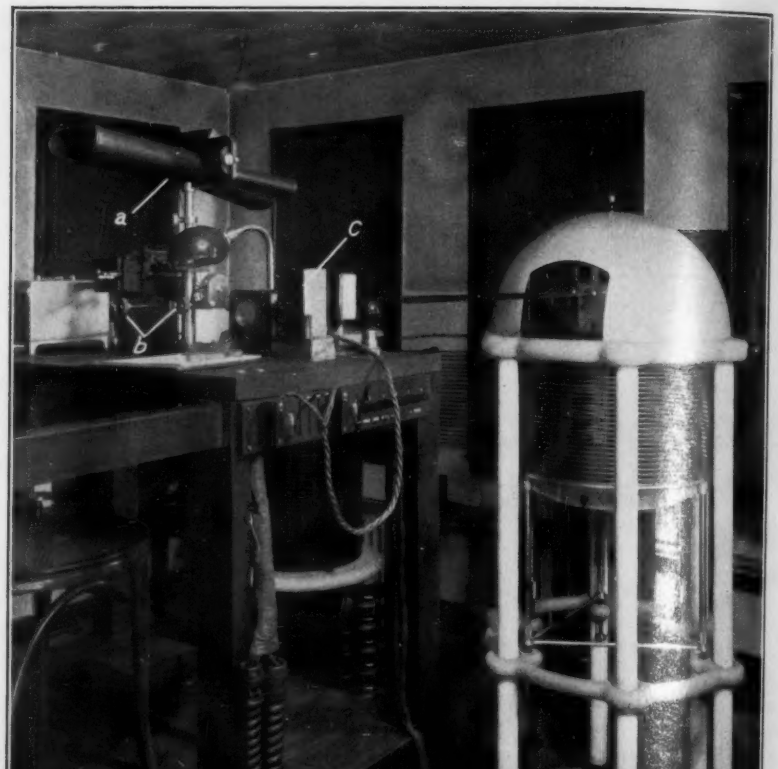

FIGURE 3.—*Electrometer (right) and observer's control station (left).*
a, Mounting for ground-glass scale; *b*, control-rod handles; and *c*, voltage-control box.

potential boundary, while the cylindrical boundary surface is forced by the charged hoops to have a potential gradient which is uniform (except for a slight ripple near the hoops which has a negligible effect at the disk). The dome-shaped metal cover protects the balance and the upper surface of the disk from electrostatic forces and also from air currents and dust.

The upper plate, disk, and dome are at a high potential above ground when the electrometer is in use. To assure the safety of the operator the mechanisms for arresting and controlling the balance are operated by long insulating rods and the balance is read by an optical lever system.

In use, the counterpoise is adjusted for equilibrium. Known weights are then removed from a pan on the disk arm. Voltage is applied and adjusted to restore equilibrium by producing an electrostatic force equal to the weight just removed. The motion of the balance is nearly critically damped by the piston action of the disk, and the observer adjusts for an exact balance at the scale zero instead of using the more customary procedure of observing the successive turning points in the swings of an undamped balance.

A more detailed idea of the construction of the electrometer can be obtained from figure 27, which will be found facing p. 314. This figure is in effect a vertical cross section through the axis of the instrument, but many of the smaller parts are drawn to an exaggerated scale and others, particularly parts of the optical system, have been so shifted in azimuth as to more clearly indicate their function.

The attracted disk (1) hangs in an aperture in the guard ring, which consists of the upper plate (4) and the bushing (3) which fits into it. The disk is electrically connected to the guard ring by gold ligaments (17) which conduct the charging current of the disk around the agate knife-edges. The guard ring is supported by six hollow pillars (36) of fused silica which rest on the base ring (43). An intermediate ring (42), rigidly attached to the silica pillars, carries the three rods (38) which support the lower plate (35) and also carries the jack screws (41) of coarse pitch which are used only in making large changes in the height of the lower plate. The support rods (38), of invar, which support the lower plate when the instrument is in use, rest on three micrometer screws (40) of fine pitch. These screws are used in the final adjustment of the lower plate to the proper level.

The silica pillars also support the guard hoops (31), each of which rests on three horizontal wooden pegs (32) inserted in equally spaced holes drilled in three of the six silica pillars. The leads connecting each hoop to the appropriate tap in the potential divider are seen in figure 2.

The more essential features of the balance mechanism are shown schematically and enlarged above the guard ring in figure 27. The weights, aggregating 0.1 to 2.5 g, rest on a weight pan (16) which can be lowered onto the stirrup when the instrument zero is to be read, or raised by the lifter (15) when voltage is to be measured. The counterweight is at (20) and the fine gold chain (21), one end of which is attached to the beam, while the other can be moved vertically by the arm, serves as a fine adjustment of the mass on the counterweight arm of the balance.

The stabilizing arm (22), on which may be placed weights such as that shown, provides the stabilizing effect required to offset the

inherently unstable action which would otherwise result from the variation of the electrostatic force. Under extreme conditions a stabilizing mass of 15 g at a distance of 12 cm below the central knife-edge is required. Arrestments are provided: (a) For lifting the beam off its central knife-edge; (b) for lifting the stirrup, which carries the disk and weight pan, off the end knife-edge; and (c) for clamping the stem of the disk, while the weight pan is being raised or lowered by its lifter. This procedure of clamping the stem (clamp 12) obviates any relative shift of the knife-edges with respect to their bearings between the time when the voltage is measured with the weights removed and the time when the zero is observed with the weights on the stirrup and the voltage removed. The clamp and weight lifter, as well as the "chainomatic" arm, can be controlled through long insulating rods from the observer's station. (See fig. 3.)

To indicate the position of the beam and thus the height of the attracted disk, the mirror (18) attached to the balance beam reflects the image of an illuminated reticle (27) onto the ground-glass electrometer scale at the observer's station. This optical method is equivalent to the use of a pointer 5 m long. For clearness, in figure 27 the prism (13) has been drawn in a position turned 90°, about a vertical axis, from that in which it is actually located. Its position in the electrometer is such that a tilt of the beam through a vertical angle produces a horizontal motion of the image. A second image of the illuminated scale is formed by reflection from a second mirror (19) rigidly supported near the beam mirror. The position of the beam image relative to this fiducial image gives a true indication of the position of the beam and disk and is unaffected by any motion of the observer's platform and its scale relative to the electrometer proper.

Four bushings (3) have been provided, each of which accurately fits the central opening in the upper plate and reduces it to a diameter suitable for a disk of 10, 12, 14, or 16 cm diameter, respectively. To permit the required accurate shaping of the edge and of the flat surface at the important region adjacent to the disk, a ring (2) of stainless steel 20 cm in outside diameter is inserted at the inner edge of each bushing.

The vertical separation between the guard ring and the lower plate is measured by gage rods (33) inserted through holes in the bushing, the relative heights of the top of the rod and of the block (6) being shown by a sensitive surface gage (5).

In order to correlate readings on the electrometer scale with the height of the disk relative to the guard ring, auxiliary measurements of this height are made for some particular scale reading, using the coplanarity microscope (29). The optical system of one of these instruments is indicated schematically in figure 27 and is described in more detail in section VIII–2. For this measurement, before and after each series of weighings, a mounting containing a pair of such microscopes is clamped to the under side of the guard ring. These microscopes are focused alternately on the lower surface of the disk and on that of the guard ring, and the difference in height is derived from the observed difference in focus adjustment.

III. STABILITY AND SENSITIVITY

The functioning of the electrometer depends essentially on a balance between the electrostatic and the mechanical forces acting on the disk, and hence its sensitivity and even its stability are vitally affected by the manner in which these forces vary with the position of the disk. A downward displacement of the disk from its normal position will increase the force of attraction; first, because of the increase in the electric gradient with the decrease in the distance to the lower plate, and second, because of the tendency for electric charge to redistribute itself, its density increasing on the protruding disk at the expense of that on the adjacent portions of the guard ring. The first, and more obvious, effect varies inversely as the separation between the guard ring and the lower plate, and becomes negligible at the widest spacings. The second effect, however, though less evident on first consideration, is so large as to predominate except at very small separations, and increases slowly with separation. The resultant effect is consequently very appreciable at all separations. The attractive force F for a given (constant) voltage may be expressed in the form

$$F=F_0\,(1-fh), \tag{2}$$

where F_0 is the force when the disk and the guard ring are coplanar, h is the height of the disk above the plane of the guard ring, and f is a coefficient which depends somewhat on h and on the proportions of the instrument. Under most conditions used in the present work, the force changes between 10 and 20 percent for 1-mm displacement of the disk so that f in cgs units lies between 1 and 2. This large value of f, and hence rapid change in the attractive force with displacement, has two effects on the operation of the electrometer. First, it makes it necessary to determine with high accuracy the true zero (i. e., the position of the spot of light for which the disk and the guard ring are truly coplanar); and second, it reduces the stability [6] of the balance to such an extent that the moving system would be unstable under most conditions if some stabilizing device were not added.

Considering first the precision required in measuring h, we find from eq 2 that, for a constant voltage

$$\frac{1}{F}\frac{dF}{dh}=-f \text{ approx.}$$

For the scale magnification by the optical lever of 80 and for the typical value of 1.6 for f, a precision of 1 percent in voltage requires that the height h of the disk be known to ⅛ mm and that the scale be read merely to 1 cm. On the other hand, for a precision of 0.01 percent in voltage the scale must be read to 0.1 mm and the height of the disk relative to the guard ring must be known to about 1 μ. Except at very small separations, this latter requirement is materially more exacting than the precision required in measuring the vertical separation c between the guard ring and the lower plate. For example, when the separation is 50 cm, the height of the disk above the guard ring must be known 25 times as precisely as its height above the lower plate.

[6] This tendency toward instability was discussed by Kelvin and more particularly by Abraham and Lemoine, J. phys. [3] **4**, 463 (1895).

For a precision of 0.01 percent the permissible error in the measurement of h is in fact less than the unavoidable bulging and irregularities in the lower surface of the disk, and the question arises, which parts of this surface should be measured to determine the mean values used for the separation and for the displacement. Except when the separation is small, the major part of the term involving fh results from the increase or diminution of electrostatic flux near the edge of the disk.

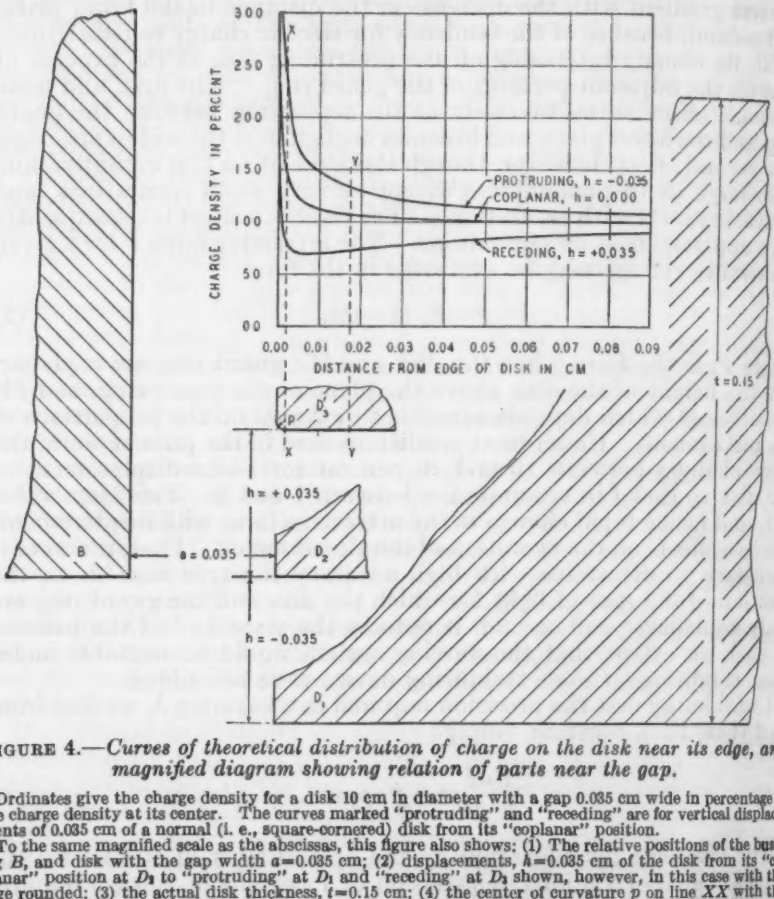

FIGURE 4.—*Curves of theoretical distribution of charge on the disk near its edge, and magnified diagram showing relation of parts near the gap.*

Ordinates give the charge density for a disk 10 cm in diameter with a gap 0.035 cm wide in percentage of the charge density at its center. The curves marked "protruding" and "receding" are for vertical displacements of 0.035 cm of a normal (i. e., square-cornered) disk from its "coplanar" position.

To the same magnified scale as the abscissas, this figure also shows: (1) The relative positions of the bushing B, and disk with the gap width a=0.035 cm; (2) displacements, h=0.035 cm of the disk from its "coplanar" position at D_1 to "protruding" at D_3 and "receding" at D_2 shown, however, in this case with the edge rounded; (3) the actual disk thickness, t=0.15 cm; (4) the center of curvature p on line XX with the edge of the disk at D_3 shown rounded as in test of table 2, set C; and (5) intersection of line YY with lower surface of disk which is the average position both of the center of the portion of the disk sighted when the coplanarity microscopes are used, and of the finger of the optical indicator when used in surveying the rim of the disk.

The graphs of figure 4 show the theoretical distribution of charge near the edge of the electrometer disk. These graphs are based on a paper by Snow.[7] His equation 8 has here been applied to the case of a 10-cm disk with a separation of 28 cm, and a gap between the disk and the edge of the opening in the guard ring of 0.035 cm, which is somewhat larger than that normally used. The ratio of the density of charge at any point on the surface to that at the center of the disk has been

[7] Chester Snow. *Effect of clearance and displacement of attracted disk, and also of a certain arrangement of conducting hoops upon the constant of an electrometer.* BS J. Research 1, 513 (1928) RP17.

plotted as ordinate against distance inward from the edge of the disk as abscissa, for three different positions of the disk. It is evident from these graphs that the major part of the excess or deficiency of charge, as compared with the ideal case in which there is no gap or displacement, occurs mainly on a peripheral belt a few millimeters wide around the circumference of the disk. Hence h should be taken as the mean vertical displacement between the adjacent edges of the disk and the guard ring, and the term involving f should vanish when h is zero.

Hitherto we have considered only a perfectly plane disk, which cannot be exactly realized in practice. If the actual disk were indented so that on the average its surface were higher than its rim by an amount h_d, then, when the edges were coplanar the mean distance from the disk to the lower plate would be $c+h_d$ and the force would be expected to be less than that on a plane disk by the factor $c^2/(c+h_d)^2$. Hence the use of the quantity $c+h_d$ in place of c for the separation, as is indicated in the factor affecting the right-hand member of eq 12 below, would be expected to correct for such a deviation of the surface of the disk from an ideal plane, if the resulting increase in distance were the only effect. As is shown below, however (see fig. 9), this procedure is not sufficient and a further correction, determined from experiments using nonplanar disks as described in section VI–5, must be applied as indicated by the term $\varphi_1(h_d/r_d)$ in eq 12.

The second effect of the rapid variation of attractive force with disk height, namely, the effect on the stability of the balance, is best treated in connection with the following general consideration of the behavior of the balance during the weighing procedure. In any balance certain factors, such as the height of the central knife edge above the center of gravity of the beam and above the line joining the end knife-edges, introduce a restoring moment which increases approximately in proportion to the tilt of the beam and opposes the moment caused by the unbalance of the weights. In this electrometer two other restoring moments contribute to the stability of the balance. One is produced by the "chainomatic" device and is proportional to the tilt, to the mass of the chain per unit length, and to the square of the distance from the central knife-edge to the point of attachment of the chain. The other, and much the largest moment of all, is produced by stabilizing weights which may be attached as desired at definite distances along an aluminum rod which extends downward from the center of the beam. The total effective mechanical "stiffness" (i. e. restoring moment per unit angle) resulting from all these effects may be designated by P, and expressed in dyne-centimeters per radian. The turning moment produced by these stabilizing effects will be proportional to the angular tilt of the beam away from some particular (though unknown) position at which their resultant is zero. Let the reading of the spot of light on the electrometer scale for this hypothetical position be S_D. Then, when the scale reading has some other value, S, the increase in tilt in radians will be $(S-S_D)/L$, where L is the effective pointer length [8] of the optical system, and the torque tending to reduce this tilt will be $P(S-S_D)/L$.

The process of weighing consists essentially in two operations. In the first, with no voltage applied to the instrument, a mass M_r,

[8] This effective pointer length is approximately twice the distance from the mirror to the scale but is somewhat less than this, because the axis of rotation is not parallel to the mirror.

consisting of the weights and the weight pan, is added to the mass M_d on the disk arm of length l_d of the balance, and this total is balanced to give a scale reading S_o by the counterpoise of mass M_t acting with an arm l_t and by the effective mass M_c of the chain at an arm l_c. This effective mass is that borne by the balance when the reading is S_D. There may also be a force A_o acting upward on the disk at this time as a result of air currents. Equating moments about the central knife-edge leads to the equation

$$(M_r+M_d)gl_d-A_ol_d=M_tgl_t+M_cgl_c+P(S_o-S_D)/L \tag{3}$$

In the second operation M_r is removed, but the electric force F is acting on the disk, and the air force may have a new value A_v. The voltage applied to the instrument is alternating and the instantaneous electrostatic force pulsates sinusoidally, at double the frequency of the voltage, between zero and a maximum value and is proportional at each instant to the square of the instantaneous voltage. The mean value of the force over a cycle is therefore equal to the constant force which would be produced by a constant voltage, the value of which is equal to the effective (root-mean-square) value of the actual alternating voltage. The period of swing of the balance is so very great (several seconds) in comparison with the period (0.0083 sec) of the force produced by a 60-cycle voltage, that the amplitude of the forced oscillations is very small and the instrument may be taken as an indicator of the effective value of the applied voltage. Considering therefore only the constant mean force F, the equation with voltage applied is

$$(M_dg+F)l_d-A_vl_d=M_tgl_t+M_cgl_c+P(S_v-S_D)/L \tag{4}$$

Combining eq 3 and 4 gives for the attractive force

$$F=M_rg+(A_v-A_o)+P(S_v-S_o)/Ll_d \tag{5}$$

If the scale reading during the measurements with the coplanarity microscopes was S_m, and if these measurements showed the average rim of the disk to be h_m centimeters above the average rim of the guard ring, then at the time of weighing, the rim of the disk was

$$h=h_m-(S_v-S_m)l_d/L \tag{6}$$

centimeters above the rim of the guard ring.

Inserting this value and that for F_o (from eq 51 section IX 3) into the expression (eq 2) for the force and denoting by q the ratio L/l_d by which the motion of the disk is magnified at the scale, gives

$$F=\frac{V_s^2r_m^2}{8c^2}[1-fh_m+f(S_v-S_m)/q] \tag{7}$$

Here the factor outside the bracket is the force for the coplanar position and the bracket gives the correction factor which allows for the change in force with height of the disk relative to the guard ring. Equation 7 may be combined with eq 5 above; and the result solved for V_s. This gives

$$V_s=\frac{2c\sqrt{2M_rg}}{r_m}\left[\frac{1+\frac{A_v-A_o}{M_rg}+\frac{P(S_v-S_o)}{M_rgql_d^2}}{1-fh_m+f(S_v-S_m)q}\right]$$

When the instrument is operated at its normal undeflected position, the differences (S_v-S_o) and (S_v-S_m), as well as the air forces and the term fh_m, are relatively small and the polynomials containing them will give a rapid convergence when expanded by the binomial theorem. This procedure and the insertion for r_m of its value $(r_b+r_d)/2$ gives to a very close approximation

$$V_s=\frac{4c\sqrt{2M_rg}}{r_b+r_d}\left[1+\frac{A_v-A_0}{2M_rg}+\frac{fh_m}{2}-\frac{f(S_v-S_m)}{2q}+\frac{P(S_v-S_0)}{2ql_d^2M_rg}\right] \quad (8)$$

It follows from eq 7 that a lowering of the disk corresponding to an increase ΔS_v in reading causes a relative increase in the attractive force of $f\Delta S_v/q$. The corresponding increase in the restoring force is $P\Delta S_v/ql_d^2M_rg$. Unless the latter exceeds the former the balance will be unstable. The condition at which the balance is at the threshold of stability corresponds to

$$P=fl_d^2M_rg \quad (9)$$

and P must always be adjusted to a value somewhat greater than this.

It follows from eq 8 that the relative error in voltage $\Delta V_s/V_s$ resulting from an error ΔS_0 in reading the zero with no voltage applied, is

$$\frac{\Delta V_s}{V_s}=-\frac{P\Delta S_0}{2qM_rgl_d^2} \quad (10)$$

Since P cannot be less than the value giving stability, this sensitivity when reading the zero cannot be better than $\Delta V_s/V_s=f\Delta S_0/2q$. For $f=1$ cm^{-1} and $q=80$ an error of 1 mm in reading S_0 gives an error of 0.06 percent in the measurement of voltage.

On the other hand, the relative error in voltage resulting from an error ΔS_v in balancing the instrument while voltage is applied is, assuming f to be constant,

$$\frac{\Delta V_s}{V_s}=\frac{1}{2q}\left(\frac{P}{l_d^2M_rg}-f\right)\Delta S_v \quad (11)$$

and can be made as small as desired by adjusting P to be only very slightly greater than the critical value. Since the process for determining S_v is substantially the same as that for S_0, the only complication being unsteadiness caused by fluctuations in voltage, there is little to be gained by making P less than 1.1 times $fl_d^2M_rg$. The period of swing is then not excessively long and the error ΔV_s from a given ΔS_0 is only 10 percent worse than the unavoidable minimum.

The stability coefficient $P/2gql_d^2$ can be denoted by the single letter γ and can be measured experimentally by determining the sensitivity of the balance with no voltage applied. In terms of this quantity the criterion for stability becomes $2\gamma/M_r \geqq f/q$.

It is of interest to note that the tendency toward instability is so great that we are obliged to use values of the stiffness P which are from 7 to 50 times as great as that which would be feasible if the electrical action tending to instability did not exist. Hence a proportional and very large loss of sensitivity is incurred.

The steadiness of the a-c voltage and the period of the balance are such that by careful manipulation we can obtain experimental scale-

law curves even in the unstable region. Figure 5 gives a set of such curves in which voltage is plotted against scale reading. These curves were obtained by using different stabilizing weights, other conditions remaining unchanged. The sensitivity is seen to be low for curve *a*,

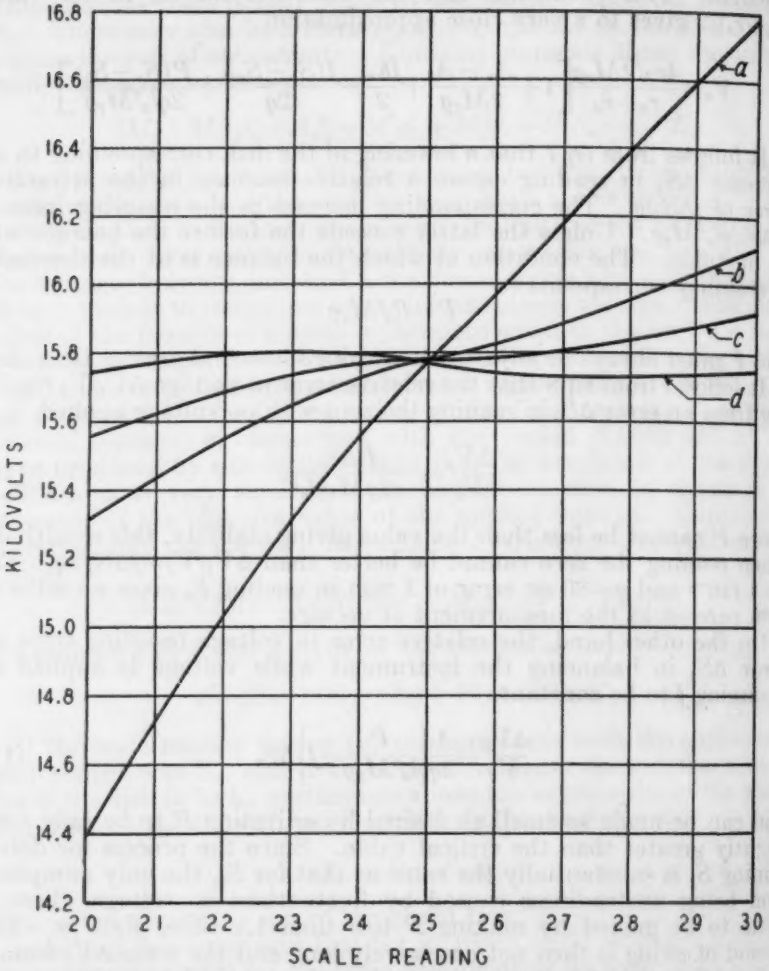

FIGURE 5.—*Scale law of electrometer for various stabilities.*

Disk and guard ring are coplanar at scale reading of 25. Curve *a* taken with excessive stabilizing weight so that $\gamma/M_F=0.0248$; curve *b* with normal stability $\gamma/M_F=0.0148$; curve *c* with low stability $\gamma/M_F=0.0121$; curve *d* with $\gamma/M_F=0.0098$, so that the movement is unstable between the 23- and the 27-cm positions but stable for greater displacements. Separation=6 cm, disk radius=5 cm, $M_F=250$ mg.

to become higher for *b* and *c*, and to be still high for *d* but with an unstable range near the coplanar position. In this unstable range an increase in reading corresponds to a decrease in voltage. It may be noted that the existence of such a region in which the instrument is unstable at small deflections but stable at larger ones, can be predicted from the purely theoretical treatment of Snow. (See eq 50, section IX–3, p. 310.)

IV. FORMULATION OF THE WORKING EQUATION

In addition to the factors considered in the derivation of eq 8 above, a number of other corrections must be introduced to obtain the final working equation which gives the applied voltage in terms of the dimensions, scale readings and auxiliary measured quantities.

If the guard hoops are not maintained at exactly the proper relative potentials, a correction for the departure of their potentials from the ideal distribution must be applied. As shown in section IX–1, this correction can be put in the form $\sum_{k=1}^{k=\infty} C_k G_k$, where G_k is a coefficient of the Fourier series which describes the departure of the actual potential distribution at the guard hoops from the ideal linear condition, and each C_k is a numerical coefficient which can be calculated from the dimensions of the electrometer.

As already indicated, any lack of flatness of the disk requires both the addition of h_d as a correction to the separation c and the application of the empirically determined correction $\phi_1(h_d/r_d)$ to the voltage.

At extremely wide separations the distortion of the electric field in the spaces between the guard hoops may produce an appreciable effect. The experimentally determined correction for this is represented by the term $\phi_2(s/r_h)$ in eq 12.

The dielectric constant ϵ, of the atmosphere in which the electric field exists is not exactly unity and the voltage required to produce a given force is less on this account by the factor $1/\sqrt{\epsilon}$, or approximately $1-(\epsilon-1)/2$. For dry air at 0° C and 760-mm Hg pressure the dielectric constant is 1.000585. The dielectric constant of moist air,[9] however, is appreciably larger than that of dry air at the same total pressure and temperature, and for moist air we have used a correction calculated on the basis of a simple mixture rule. The total correction for dielectric constant in the present work was usually about 0.031 percent.

To express the voltage indicated by the electrometer in absolute electromagnetic volts, V_M, the value in electrostatic units V_s must be multiplied by v, the ratio of the electrostatic unit to the electromagnetic unit. At present the factor 299.805 seems to be the best value. It results from the work of Rosa and Dorsey, combined with recent determinations of the ratio of the international and the absolute ohms.

By combining all of the various correction factors the following working equation of the instrument for small deflections results:

$$V_M=\frac{4v(c+h_d)\sqrt{2M_rg}}{(r_b+r_d)}\left[1+\frac{A_s-A_o}{2M_rg}+\frac{\gamma}{M_r}(S_s-S_o)\right.$$

$$\left.-\frac{f(S_s-S_m)}{2q}+\frac{fh_m}{2}-\sum_{k=1}^{k=\infty}C_kG_k-\frac{\epsilon-1}{2}+\phi_1\left(\frac{h_d}{r_d}\right)+\phi_2\left(\frac{s}{r_h}\right)\right] \quad (12)$$

[9] Dolcolier, Guinchant and Hirsch. Onde Electrique 5, 189 (1926).

In the use of the instrument, zero readings are always taken just before and just after the readings with voltage applied, and the unavoidable assumption is made that the air force A, while voltage is applied is the same as the mean, A_o, of the air forces during the zero readings. Although the second term in the bracket is therefore always taken to be zero, it has been retained throughout the derivation of eq 12 as a reminder that air forces are perhaps the largest uncontrolled source of error in the use of the instrument.

V. PRECISION AND ACCURACY

The usual process for obtaining an estimate of the accuracy of an instrument, namely, the comparison of its indications with those of a standard instrument known to be more accurate, could not be applied because no other standard of greater accuracy is available in this range.

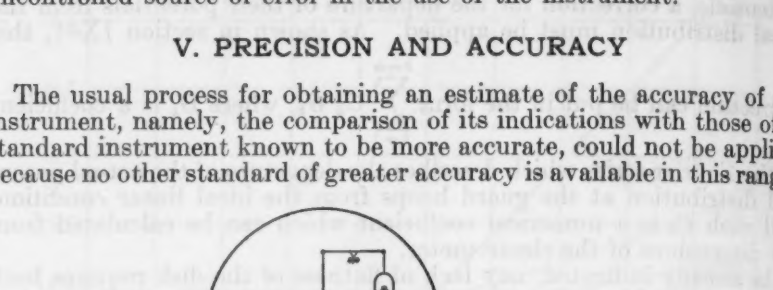

FIGURE 6.—*Schematic diagram of connections used in comparing electrometer with "voltmeter."*

The 230/100,000-volt step-up supply transformer is energized by a 60-cycle 15-kva alternator driven by a d-c motor supplied by storage batteries. The step-down transformer supplies the electrodynamic reflecting voltmeter Z which has a series resistor R. The potentiometer circuit P serves to calibrate the voltmeter.

The best comparison standard available consisted (as shown in fig. 6) of the combination of a step-down voltage transformer with a reflecting electrodynamic voltmeter Z of the suppressed-zero type [10] connected to its low-voltage winding W_2. The series resistor R of this voltmeter was adjusted to keep the deflection approximately the same for all values of applied voltage. Because of the long scale distance and delicate suspension of this voltmeter, its sensitivity (16 mm for 0.1 percent change in voltage) is nearly 10 times that of the electrometer. For brevity, the combination of transformer and reflecting voltmeter will be referred to simply as the "voltmeter."

Immediately before and after each set of weighings, the reflecting voltmeter is checked against the electromotive force of a standard cell by the use of a potentiometer circuit P. Careful checks made recently, as well as at intervals during the past 15 years, have shown that the ratio of the voltage transformer for a given set of operating conditions remains constant to at least 0.02 percent.

[10] F. K. Harris. *A suppressed-zero electrodynamic voltmeter.* BS J. Research 3, 445 (1929) RP105.

In the course of this work a series of 64 independent comparisons of the electrometer with the "voltmeter" were made at various voltages from 10,000 to 100,000. These comparisons were distributed over a variety of conditions which include: (a) The use of two disks of different radii; (b) five different separations between disk and lower plate; (c) six different combinations of series or parallel connection of the primary and the secondary windings of the step-down transformer; (d) seven different values of magnetic flux density at which the transformer was operated; and (e) many different values of resistance in the calibrating potentiometer circuit. This work, using the technique finally developed, extended over a period of about 8 months. The scattering of these observations, as shown by the average difference taken without regard to sign, between the results given by the two independent methods, is 0.010 percent. It is, of course, impossible to separate this resultant scattering into the portions contributed respectively by the two methods of measurement, but it is certain that this figure constitutes an upper limit to the scattering which could have originated in either method. If any small secular changes had occurred in the ratio of the transformer during the progress of the work they would also have contributed to this observed scattering. The ratio of the transformer for certain connections as measured after the comparisons differed by 0.008 percent from the value observed before the comparisons. This fact suggests that some secular changes probably did occur.

An estimate of the precision of the individual readings is had from a study of curves such as *E*, figure 26. Here differences between the two methods of measurement observed in random order but with voltage continuously applied at various scale readings, and hence with the disk at various heights above its guard ring, are plotted against scale reading. An examination of this and many similar curves shows that individual points seldom lie as much as 0.005 percent from a smooth curve.

If we consider the matter from the other point of view and deduce the probable accuracy of the whole by combining the accuracies of the parts, we find the situation to be as shown in table 1. Here the third column gives the observed or estimated values of the uncertainty of our measurements of the quantities listed in the first column. The observed values of uncertainty are deduced from data taken in the later part of the work, this uncertainty being expressed as the average, without regard to sign, of a number of differences between pairs of observations on supposedly the same quantity. In many cases the two observations of a pair were separated by a considerable lapse of time and hence the difference includes any secular drift during this time as well as the resultant errors of the two measurements themselves. In the three columns marked case 1, case 2, and case 3, for three assumed sets of operating conditions, is given the uncertainty in the measurement of voltage which would result from an uncertainty in each quantity equal to the value given in the third column. At the bottom of these columns is given the resultant uncertainty to be expected from a random combination of the errors contributed by the several quantities listed.

TABLE 1.—*Probable uncertainty in component measurement and in voltage*

Quantity	Symbol	Uncertainty observed or estimated	Resulting percentage uncertainty in voltage		
			Case 1	Case 2	Case 3
Weight	M_r	0.01 mg	0.000_3	0.000_3	0.000_3
Separation	c	3.4 μ	$.005_2$	$.002_8$	$.000_7$
Radius of disk and bushing	r_d+r_b	2.4 μ	$.001_5$	$.001_5$	$.001_5$
Zero setting (including air forces)	S_o	0.04 mm	$.003_4$	$.010_9$	$.005_7$
Voltage setting	S_v	0.04 mm	$.000_3$	$.008_9$	$.002_3$
Coplanar setting	S_m	0.06 mm	$.005_9$	$.005_9$	$.005_9$
Disk height	h_m	0.8 μ	$.005_2$	$.005_2$	$.005_2$
Disk concavity	h_d	2.2 μ	$.002_8$	$.003_6$	$.004_4$
Resistance arms of potential distribution bridge	R_1 or R_2	0.01 ohm			$.000_4$
Resultant uncertainty (square root of sum of squares)			.010	.014	.010

Case 1 is for $c=6$ cm, $V=30{,}000$ volts, $M_r=2{,}200$ mg, stability coefficient $\gamma=1.1$ times its value at the threshold of instability.

Case 2 is for $c=12$ cm, $V=60{,}000$ volts, $M_r=2{,}200$ mg, stability coefficient $\gamma=3.5$ times threshold value.

Case 3 is for $c=48$ cm, $V=120{,}000$ volts, $M_r=550$ mg, stability coefficient $\gamma=1.7$ times threshold value.

In the case of the quantity h_m the value given under the column headed "uncertainty" is the difference in the two values of h_m observed at the beginning and end of the set of weighings on the same day, the value, 0.8 μ, being the mean for 20 days. This measurement involves both the act of setting the vernier image to the scale reading S_m and the measurement of the resulting h_m with the coplanarity microscopes. The item 0.06 mm for the uncertainty in S_m is the same value expressed as a distance on the scale. Either uncertainty taken alone covers the entire operation and the two should therefore not be combined.

The value 0.04 mm for S_o is the mean of 20 pairs of observations, the members of each pair being obtained just before and just after a series of weighings, the time interval being on the average, ½ hour. As each "observation" is itself the mean of 30 readings, the true errors of reading have largely cancelled out and the result is rather an index of the changes in air force between beginning and end.

Similarly, the value for the uncertainty in S_v is deduced from the average deviation from their mean, without regard to sign, of the n individual readings (in most cases $n=10$) taken during a single weighing, by dividing this mean deviation by $(n-1)^{\frac{1}{2}}$. The value given, which is the mean of 10 such separate sets taken on different days, is largely a measure of variations in air currents combined with uncertainties resulting from unsteadiness in the applied voltage,[11] rather than a simple reading error.

An air force of 0.1 mg, which would produce an error of 0.01 percent in voltage under typical conditions, could be produced by a convection current having a velocity of about 1 cm/sec. It is therefore evident that such forces will materially reduce the precision otherwise attainable by a single reading with this instrument. On the other hand, the natural fluctuations in such air currents should cause their effects

[11] In the present work a 15-kva alternator of the revolving-field type was driven by a 230-volt d-c motor supplied by a 50-ampere storage battery, while the alternator field was supplied by a second battery. In spite of this arrangement and of the great pains taken to keep the bearings and brushes in prime condition, irregular fluctuations of the order of 0.01 percent were nearly always present.

to largely cancel each other when the mean of a fairly large number of readings is taken. The small scattering of the zero readings noted in table 1 is evidence for this.

It appears from an inspection of table 1 that the uncertainty in the measurement of weight, potential distribution, disk radius, separation (at large separations) and deflection setting (when working with a small margin of stability), could produce only negligible errors. On the other hand, errors of 0.005 percent may well be introduced by uncertainty in disk flatness, disk height, zero setting, separation (at small separations), and in deflection setting at high stability. If a random combination of their effects be assumed, the over-all uncertainty in any one complete determination of voltage may therefore be expected to have the value marked "resultant uncertainty" in table 1.

VI. EXPERIMENTAL TESTS

During the later stages of the development of the instrument a rather elaborate program of experimental work was carried out with it to determine its possibilities and limitations. Because of the small size of the high-voltage laboratory of the National Bureau of Standards, and the voltage rating of the available transformers, this experimental work was limited to 100,000 volts. However, it included measurements at potential gradients exceeding those which will normally be present in work at 275,000 volts, and also measurements at the full separation needed for this latter voltage.

Because of its intended use as an absolute instrument, independent of other methods of high-voltage measurement, it was essential that all necessary tests should be applied to insure that the construction and the functioning of the electrometer were in sufficiently close agreement with the ideal conditions for which its theoretical equation was derived. For this purpose various rather drastic departures from the ideal conditions were intentionally introduced and the corresponding effects determined by comparing the indications of the electrometer with those of the "voltmeter" described above, which was of course left unaffected [12] during each experiment.

In order that no disturbance should occur, other than the change in condition intentionally introduced in each experiment, the mass M_7 was left unchanged, and any resulting change in the voltage necessary to restore the balance of the instrument was derived from the readings of the "voltmeter."

Whenever feasible, runs with such changed operating conditions were immediately preceded and followed by check runs under normal conditions. This procedure tends to eliminate any secular drift in the calibration of either instrument. The constancy of the transformer allows us to place nearly as much confidence in observed differences for changed conditions on different days as when the runs under normal and changed conditions were made on the same day. For the purposes of this paper the absolute calibration of the transformer-electrodynamometer combination need not be considered. The results given below are expressed as a "relative difference" which is the percentage by which the indication of the electrometer exceeded that of the "voltmeter," both being reduced to the common basis of absolute

[12] Unfortunately, during the temperature runs, the transformer was necessarily exposed to the changes in room temperature.

electromagnetic volts. Practically all the measurements were made at a frequency of 60 cycles per second.

It is to be noted that a number of the measurements reported here were made early in the work before certain refinements of technique had been developed. The scattering in the early results should therefore not be taken as a measure of the precision attainable by the later procedures.

1. ELECTRICAL DISCHARGES

In addition to the many ways in which an electrometer may fail to satisfy the purely geometrical requirements of its theory, there is the further possibility, in an instrument operating at high voltage, that some brush discharge or other partial breakdown of the dielectric may produce abnormal conditions. The possibility of such a discharge appears evident when one considers that, if the disk has a sharp square edge, the electric gradient at that edge is theoretically infinite even if the disk is withdrawn into the aperture in the guard. Should a discharge be present there may well be mechanical forces set up by the resulting "electric wind," and in addition the distortion of the electric field by the resulting ionization and space charges may possibly be appreciable.

A considerable number of tests were therefore planned with a view to produce or to modify such a discharge, or to imitate to an exaggerated extent its effects so that the result might be observed. These tests were made with spacings of 12 cm or less so that the guard hoops and their potential divider were not needed. This permitted the use of average gradients running up to 5,300 volts (effective) per cm at which sparks would occasionally pass between the edge of the upper plate and the rather sharp edge of the lower plate. In no case did a spark pass to the disk itself. The results of this group of tests are summarized in table 2. The seventh column shows the change in the required applied voltage resulting from the change in conditions.

In set *A*, with the disk tilted about a diameter through an angle of 6 minutes, the edge protrudes at one side by 0.09 mm, this being nearly the extreme range measurable with the coplanarity microscopes. The force from any electric wind then present would be expected to vary materially with both the tilt and the applied voltage and thus reveal itself. The changes shown in the seventh column of table 2 are less than the precision at the time these experiments were made.

In set *B* the power supply was obtained from a 60-cycle and a 180-cycle generator connected in series, the latter delivering about 30 percent as much voltage as the former. By reversing or by opening the field circuit of the latter, the wave form could be markedly varied, although the effective value was kept adjusted to the constant value required to balance the mass M_F. To eliminate any effect of a change in transformer ratio with wave form, the step-down transformer was omitted and the electrodynamometer was used in series with a shielded resistor of about 400,000 ohms. It might be expected that with the peaked wave form, by reason of the greater crest value of voltage, there would be more discharge than under the other two conditions. It is seen from table 2 that no change was detected though the voltage was almost sufficient to cause sparkover.

TABLE 2.—*Effects of various abnormal conditions*

Set	Disk diameter	Gap	Separation	"Gradient" [a]	Voltage [b]	Change	Condition
	cm	cm	cm	v/cm	v	*Percent*	
A	10	0.0409	6	7,400	31,473.8 31,474.0	+0.00$_1$	Normal. Disk tilted 6.1 minutes.
A	10	.0931	6	7,400	31,953.0 31,945.0	−.02$_3$	Normal. Disk tilted 7.3 minutes.
B	10	.0085	6	4,220 3,670	15,775.6 15,774.8	−.00$_4$	Normal wave form. Crest factor 1.41. Dimpled wave form. Crest factor 1.24.
				7,430 9,150	31,556.0 31,556.0	.00$_0$	Normal wave form. Crest factor 1.41. Peaked wave form. Crest factor 1.74.
C	10	.0085	6	7,430	31,532.0 31,529.4 31,544.4	[c]−.00$_3$ [c]+.04$_0$	Normal. Disk edge rounded to r=.002 cm. Bushing edge also rounded to r=.007 cm.
D	16	.0108	12	2,940	24,979.4 24,977.7 24,982.4 24,980.7	−.00$_7$ +.01$_2$ +.00$_8$	Normal. Lint on lower plate. Lint on disk and lower plate.[d] Lower plate cleaned.
				5,900	49,991.8 50,001.0	−.01$_8$	Lint on disk and lower plate. Normal.
E	10	.0108	12	4,220	15,761.1 15,765.3 15,763.4 15,763.1	+.02$_2$ +.00$_9$ +.00$_8$	Normal. 1.5 volts d-c in series. 0.1 microfarad condenser in series with disk. 3×10^8 ohms resistance in series with disk.
F	10	.0055	6	7,450	31,691.8 31,690.2	−.00$_5$	Normal. Lower plate tilted 9 minutes.
G	16	.011	12	5,900	50,110.8 50,110.2	−.00$_1$	Normal, disk eccentricity 0.004 cm. Abnormal, disk eccentricity 0.025 cm.

[a] Discharge if present should depend upon the magnitude of this quantity, "gradient" = effective voltage × crest factor ÷ plate separation.
[b] This column gives the voltage as indicated by the "voltmeter."
[c] At the time of these observations the precision of measurement was no better than ±0.04 percent.
[d] Figure 7 shows distribution of cotton lint during this experiment.

The tests in set *C* were made by rounding off the lower edge, originally rectangular, of one disk to a radius of about 0.02 mm. Line *XX*, figure 4, p. 260, marks the center of the radius of rounding. This rounding should reduce the gradient, which is theoretically infinite for a rectangular corner, to a very moderate value. The slight difference observed in the readings may perhaps be the result of some general distortion of the disk produced by the rounding operation, in spite of the fineness of the stone and the gentleness of the grinding force used.

In normal operation the disk, guard, and lower plate were frequently wiped with soft leather soaked in benzol and were therefore reasonably free from dust particles. To see whether such particles as did elude our vigilance could make an appreciable error, a number of cotton fibers were caused to cling to the attracted disk. This was done by placing cotton lint on the lower plate and connecting an a-c and a d-c source in series between the plates. Figure 7 shows the resulting condition which obtained during this experiment. In spite of this very drastic treatment no consistent change in the performance of the electrometer appears in set *D*.

The tests of set E, in which either a source of direct voltage or a condenser was connected between the disk and its guard ring were intended to roughly simulate the effect of any possible electrical double layer on the surface such as might result from an electrical discharge or other cause. As shown in table 2, no effect was observed at 1.5 volts. At 4.5 volts the disk pulled over to the guard ring and adhered. Hence it may be assumed that there can be no rectifying action present which might cause an accumulation of charge.

2. TILT OF DISK AND OF LOWER PLATE

Departure from the ideal condition of parallelism between the disk and the upper and the lower plate was also studied. The data given in section A of table 2 for cases in which the disk is considerably tilted with respect to the guard ring and the lower plate show that no large error need be expected from the unavoidable slight tilt of the disk. Section F of table 2 gives similar data obtained when the lower plate was intentionally tilted at an angle of about 9′. These data indicate that the effect of tilt in normal operation must be very small, for the lower plate is always adjusted to have a tilt less than 1′.

3. ECCENTRICITY OF DISK IN APERTURE

Theoretically, one would expect that small horizontal displacements of the disk from its central position in the opening in the guard ring would have little or no effect on the attractive force for a given voltage, because such displacements do not alter the area of the gap. To test this point experimentally, weighings were made with the 16-cm disk and 12-cm separation. The results are given as set G of table 2. No guard hoops were used with this short separation. The greatest displacement used (0.025 cm) was such as to make the disk very nearly touch the guard ring at one side when no voltage was applied. It is natural to assume that the electrostatic forces tend to center the disk, so that the actual eccentricity when measuring an applied voltage may have been less than the values observed with no voltage applied. It is evident from the very small mean difference given in the seventh column of table 2 that the effect of an initial eccentricity is negligible.

4. WIDTH OF GAP

Of the purely geometrical factors to be considered the most obvious is the gap which must be left between the disk and its guard ring, if the former is to move without friction. The early work of Maxwell, and more particularly the recent paper of Snow,[13] indicate that the effect of this gap, of width a, can be properly allowed for, provided the disk and ring are coplanar, by adding half the radial width of the gap to the radius r_d of the disk itself. From the symmetry of the geometrical system treated by Snow, it is evident that his result can give no information as to terms of higher order in a/r_d, which might be appreciable in the case of disks of small radius and large gap. Such effects were therefore sought experimentally by a series of measurements in which a disk initially 10 cm in diameter having a radial clearance of 0.0055 cm was reduced in diameter by successive

[13] Chester Snow. *Effect of clearance and displacement of attracted disk, and also of a certain arrangement of conducting hoops upon the constant of an electrometer.* BS J. Research 1, 513 (1928). RP17.

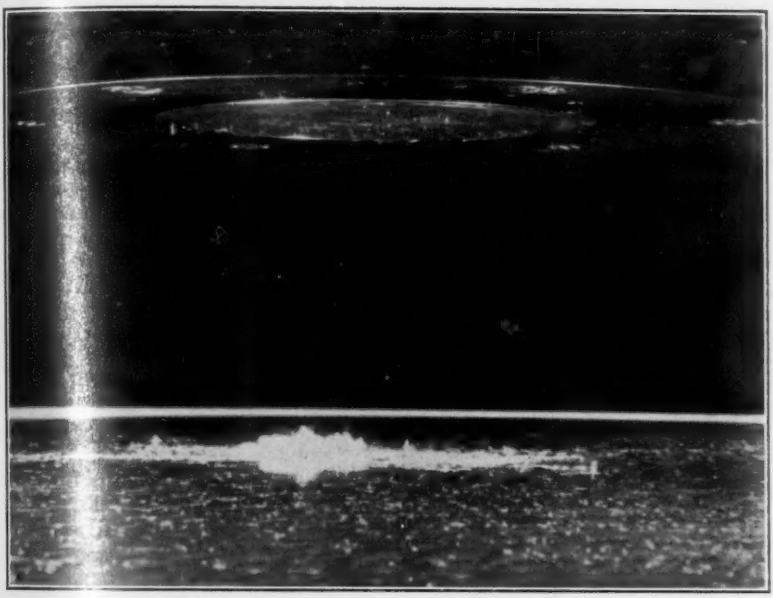

FIGURE 7.—*Condition of disk and guard ring after lint had been applied for measurements given in table 2, part D.*

The disk, guard ring, and gage-rod holes (all much foreshortened) are visible at the top and the pile of lint on the lower plate below.

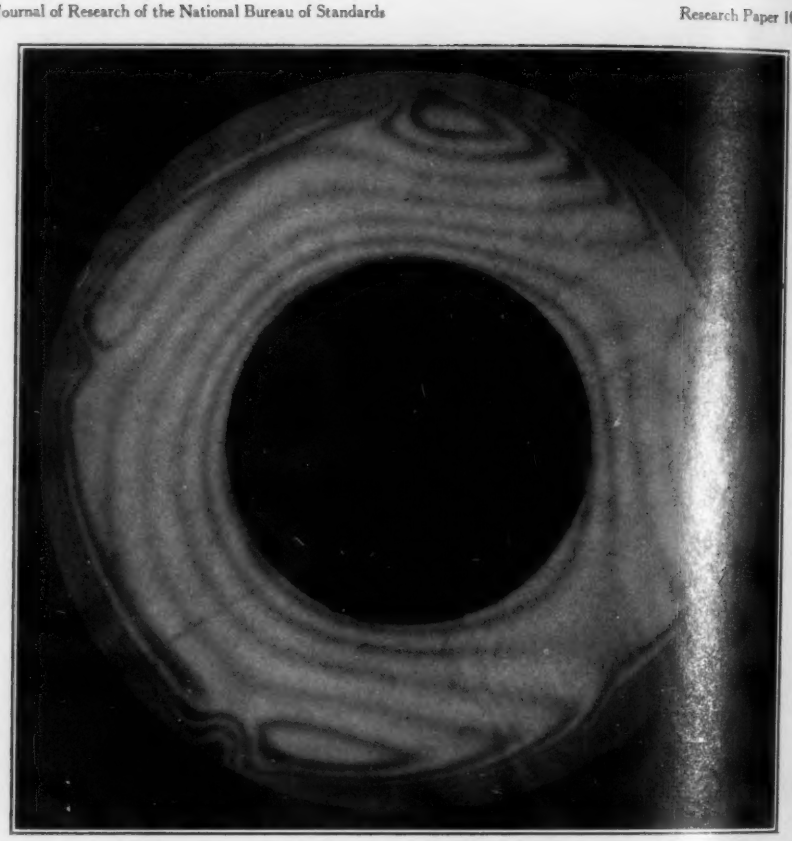

FIGURE 11.—*Optical interference pattern formed by active surface of 10-cm bushing insert and a glass flat.*

small amounts until the radial clearance was 0.26 cm. The results, shown in figure 8, shows that the voltage as deduced by eq 12, using the mean of the radius of the disk and that of the aperture, was not affected by more than 0.05 percent up to a gap of 0.26 cm or nearly 1.7 times the thickness of the disk. This somewhat remarkable result is consistent with a rough theoretical estimate based on Snow's work, which shows an astonishingly small penetration of lines of force into the gap even when it is wide. At the larger gaps the air damping of the moving system was greatly reduced and the operation of the instrument became very inconvenient. With a wide gap it is also necessary to slide the coplanarity microscopes through a greater range to sight on the disk and on the guard, and the possibility of error from irregularities in their supporting grooves is increased. For gaps of less than 0.005 cm the damping is excessive, mechanical center-

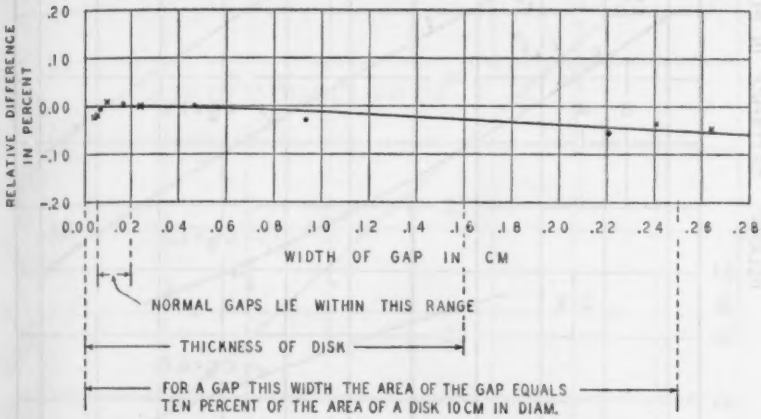
RELATIVE DIFFERENCE IN PERCENT
.20
.10
0.00
-.10
-.20
0.00 .02 .04 .06 .08 .10 .12 .14 .16 .18 .20 .22 .24 .26 .28
WIDTH OF GAP IN CM
NORMAL GAPS LIE WITHIN THIS RANGE
THICKNESS OF DISK
FOR A GAP THIS WIDTH THE AREA OF THE GAP EQUALS TEN PERCENT OF THE AREA OF A DISK 10 CM IN DIAM.

FIGURE 8.—*Effect of width of gap.*

Ordinates are the relative difference between the indication of the "voltmeter" and that of the electrometer as computed by adding half the width of the gap to the radius of the disk as required by eq 12. Dots correspond to a series of measurements in which a disk initially 10 cm in diameter was turned down in successive stages. Crosses correspond to a series in which the aperture in the guard ring was enlarged.

ing adjustment of the disk to provide clearance becomes tedious, and dust particles that lodge in the gap produce frictional trouble more readily. A gap in the range between 0.006 and 0.02 cm gives satisfactory performance. From figure 8 the effect of terms of higher order in a/r_d for gaps within this range is seen to be negligibly small.

5. FLATNESS OF DISK AND OF GUARD RING

Early in the work discrepancies between results obtained with different disks indicated that some previously unsuspected source of constant error was present. A considerable number of possible sources of error were investigated and the discrepancies were finally traced to the fact that the disks first used were not sufficiently plane. Figure 9 shows results obtained on a number of disks of varying degrees of flatness. Here the ordinates are the relative differences in the indications of the electrometer and the "voltmeter," while the abscissas are the values of h_d/r_d, i. e., the ratio of the mean height of the lower surface of the disk above its rim, to the radius of the disk. (If the curvature is constant this ratio is proportional to the ratio of the

radius of the disk to that of the spherical surface of which the lower surface of the disk forms a segment.) Positive abscissas correspond to concave disks. The radii of curvature R_c (in meters) of the spherical surfaces of several of the 10-cm disks are indicated along the axis at the corresponding values of h_d/r_d.

The shape of the active surface of most of the disks used approximated more or less closely to that of a segment of a sphere. Others,

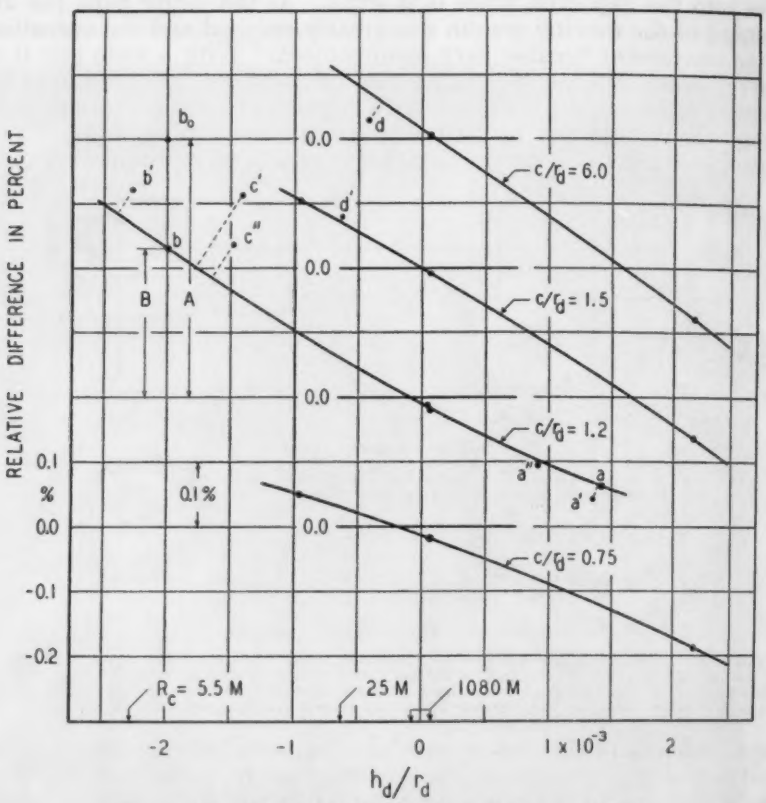

FIGURE 9.—*Residual effects of lack of flatness of disk.*

Abscissas are effective curvature expressed by the ratio of the mean height, h_d, of lower surface of the disk above the mean level of its rim, to its radius r_d. A plane disk has $h_d/r_d=0$. Positive values correspond to concave disks. The values indicated by R_c are the radii in meters of a spherical surface of which the lower surface of a disk at that abscissa would be a segment. The ordinates are the relative differences between the indications of the voltmeter and those of the electrometer after allowance has been made for h_d by using $c+h_d$ as the separation. Each curve corresponds to a different value of c/r_d. To avoid confusion each curve is drawn to a different axis of abscissas. Points a, a', and a'' show data obtained with an initially nearly spherical concave 10-cm disk before and after the surface had been reworked; b and b' show results before and after reworking a 10-cm convex disk. c' and c'', d and d' show data obtained on built-up disks which were not so nearly parts of spherical surfaces. Distance A to point b_o shows total effect of h_d in this case, no allowance being made for lack of flatness. Distance B to point b shows the residual effect after allowing for the direct effect of h_d on spacing.

such as those corresponding to points marked a', b', c', and d', were of somewhat different shape. The nearly linear relation between relative difference and h_d/r_d is perhaps fortuitous and may not apply to disks which depart markedly from the spherical shape. It is felt, however, that for the disks here used, the coefficients obtained from the slope of the plotted curves should suffice for computing the correction

to be applied to the nearly flat disks used in the best measurements. Irregularities of smaller scale than the general curvature and not near the edge would be expected merely to shift the charge from one part of the disk to another without much effect on the total force.

The relative importance of a given distortion h_d of the disk in its influence on the effective spacing and on the change in charge distribution is indicated by points b_o and b. The former was obtained by entirely ignoring h_d in the computation of the voltage as indicated by the electrometer, using eq 12, and this result differs from the ideal

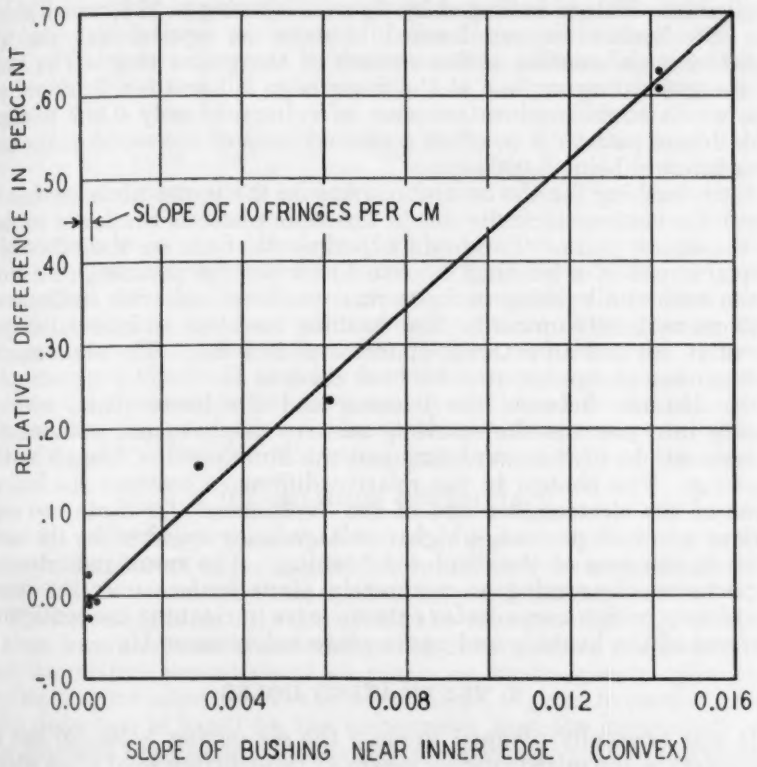

FIGURE 10.—*Effect of lack of flatness of guard ring.*

Abscissas are the slope of the surface at the edge of the aperture. Ordinates are relative difference between electrometer and "voltmeter."

result for a flat disk by the amount A. The same data when using $c+h_d$ for the spacing but still ignoring the correction term $\phi_1(h_d/r_d)$, yield point b, which still differs by the amount B from the ideal.

This remaining difference B from the value corresponding to a plane disk must be the result of some additional effect of the somewhat irregular convexity of the disk used and comes presumably from the tendency of the electric charge to crowd toward a convex and retreat from a concave part of the surface. It is this contribution which is represented by $\phi_1(h_d/r_d)$ in eq 12.

The slope of the curves in figure 9 shows that this additional effect is less at close separations ($c/r_d=0.75$) and increases with the separation.

For separations for which c/r_d exceeds 1.5 the effect becomes nearly independent of separation.

A corresponding effect is to be expected if the surface of the guard ring near the disk is conical. Figure 10 shows the results of a series of measurements in which the inner portion of the guard ring extending for a distance of 5 cm from the gap was initially made conical, and then made flatter in successive stages. A 10-cm disk was used in these experiments. The error in voltage is seen to be proportional to the slope of the conical surface. In the guard rings finally used this slope could readily be made small enough to make this source of error negligible. This is indicated by figure 11 (facing p. 273) which shows the interference pattern formed between an optical flat and the polished stainless-steel active surface of the guard ring. The slope of the guard-ring surface at the inner edge is less than 2 fringes per cm, which could produce an error in voltage of only 0.002 percent. This fringe pattern is in effect a contour map of the surface, the contour interval being 0.0003 mm.

Each bushing fits the central opening in the upper plate so that its lower flat surface normally lies in the same plane as the lower surface of the upper plate. To obtain experimental data on the effect of a displacement of a bushing relative to its normal position, runs were made with the bushing in its normal position and with it displaced 0.05 cm vertically upward. The bushing used had an internal diameter of 16 cm and an external diameter of 30.2 cm. The electrometer voltage was then computed for both cases in the usual way, using for c the distance between the bushing and the lower plate, without taking into account the resulting relative displacement between the outer portions of the guard ring and the inner portion formed by the bushing. The change in the relative difference between the indications of the electrometer and of the "voltmeter" for these two conditions was 0.38 percent, a higher voltage being required for the same force in the case of the displaced bushing. The result indicates the importance of securing an accurately plane surface over the entire guard ring, which necessitates extreme care in cleaning the contiguous surfaces of the bushing and upper plate before assembly.

6. VENTILATING HOLES

It was originally planned to close the six gaging holes (20 mm in diameter) in the guard ring by means of tight-fitting solid plugs whose lower ends were flush with the lower plane surface of the guard ring. Experience showed, however, that the closing of these holes in this manner increased the difficulties from air currents and made the damping excessive. Consequently, perforated plugs (9) figure 27 (see also fig. 16) are used which permit a rapid equalization of air pressure on the two sides of the disk. Because the centers of these plugs are only 13 cm from the center of the attracted disk, and the holes (4 mm in diameter) in the bottom of each plug break the continuity of the plane surface of the guard ring, it seemed desirable to obtain a satisfactory experimental check before considering their effect to be negligible. Such a check was made by removing three alternate plugs, stopping the holes in the upper side of the guard ring with corks, and then taking observations in the usual way. As customarily used with the plugs in place, the total area of the ventilating openings is

404 mm². With the three plugs removed this total area is increased to 1,106 mm². The mean of readings taken before removing and after replacing the plugs gives a value only 0.005 percent lower than the mean of readings taken with the plugs removed. This shows that the effect of the ventilating holes can be neglected.

7. TEMPERATURE

The primary effects of an increase in temperature on the indications of the electrometer arise from: (1) The expansion of the disk and of the aperture in the guard ring, both of which increase the effective area, and (2) vertical expansion of the silica pillars, of the invar rods supporting the lower plate, and of the lower plate itself, the net effect of which is a decrease in the separation. There is, therefore, a net increase in the force of attraction and a decrease in the voltage required for a given force. The temperature coefficient of voltage for a given force as calculated is -89×10^{-6} per °C at a separation of 6 cm and -24×10^{-6} per °C at 48 cm. The construction of the instrument is such as to minimize any other temperature effects, but as an experimental check to detect any large unsuspected temperature effects, observations were made in June 1933 at temperatures ranging from 25 to 34° C with a separation of 6 cm. These observations indicated that, after the calculated corrections mentioned above had been applied, there remained no residual temperature effect greater than the precision of the determinations. Because of the small range of temperature (only 9° C) and the fact that the voltage transformer as well as the electrometer was necessarily subjected to the change in temperature, the precision of these determinations was probably not better than 30×10^{-6} per °C in temperature coefficient of voltage.

8. GUARD-HOOP POTENTIALS

As the guard hoops constitute the most novel feature of the instrument, a number of experimental tests will now be described which were made to determine their applicability and limitations.

The derivation of an equation giving the voltage required to produce a given force on the disk, in terms of the dimensions of the instrument and the relative potentials of all points on an imaginary cylindrical surface tangent internally to the set of hoops, is given in section IX–1. This deduction is based on the assumption that the instrument and the potential distribution are axially symmetrical. It is convenient to express the potential $V_s(y)$ of a point on this cylindrical surface at a height y above the lower plate by the equation

$$V_s(y)=V_s\left[\frac{y}{b}+\sum_{k=1}^{k=\infty}G_k\sin\frac{k\pi y}{b}\right] \tag{13}$$

Herein V_s is the total applied voltage, b the separation between disk and lower plate, k is an integer, and the Fourier series in the second term describes the departure of the potential distribution from the ideal uniform gradient. Conversely, each coefficient G_k is connected with the potential distribution by the relation

$$G_k=\frac{2}{b}\int_0^b\left(\frac{V_s(y)}{V_s}-\frac{y}{b}\right)\sin\frac{k\pi y}{b}\,dy \tag{14}$$

It is proved in section IX–1 that to a first approximation the potential difference V_s required to produce a force F on a central disk of radius r_d is

$$V_s=\frac{2b\sqrt{2F}}{r_d}\left[1-\sum_{k=1}^{k=\infty}C_kG_k\right]\text{approximately,} \tag{15}$$

where the coefficients C_k are given by

$$C_k=(-1)^k\pi k\frac{2J_1\left(\frac{ik\pi r_d}{b}\right)}{\frac{ik\pi r_d}{b}\times J_0\left(\frac{ik\pi R}{b}\right)} \tag{16}$$

J_0 and J_1 being Bessel's functions with parameters 0 and 1, respectively.

Values of the coefficients C_k may readily be computed from the dimensions of the electrometer and are given in table 3 for an instrument of the present proportions.

TABLE 3.—*Typical values of the coefficients, C_k*

[r_d=8 cm, R=47.25 cm.]

C_k	b=6 cm n=2	b=12 cm n=5	b=24 cm n=11	b=48 cm n=23	b=110 cm n=54
C_1	-4.1×10^{-9}	-2.0×10^{-4}	-4.7×10^{-2}	−0.621	−2.094
C_2	$+4.8\times10^{-13}$	$+8.4\times10^{-9}$	$+4.1\times10^{-4}$	+.090	+1.678
C_3	-6.5×10^{-17}	-8.1×10^{-13}	-3.0×10^{-6}	-8.9×10^{-3}	−0.847
C_4					+.358
C_5					−.012
C_{23}				-3.9×10^{-27}	
C_{48}				$+7.4\times10^{-53}$	
C_{54}					$+4.2\times10^{-28}$
C_{110}					$+1.7\times10^{-62}$

Here n is the number of intermediate hoops which would be present when using the normal hoop spacing of 2 cm. It will be seen that the values of C_k are very small at small separations, which means that the hoops are then unnecessary. At larger separations the values are quite appreciable but decrease rather rapidly with increase in k, so that for values of k comparable with the number of hoops, C_k is vanishingly small.

Unfortunately, the correct values of G_k as defined by eq 14 cannot be determined because the potential $V_x(y)$ is not known at all points. However, for the particular values of y at which the hoops touch the imaginary cylindrical surface of radius R the values of $V_x(y)$ are necessarily the same as the potentials of the hoops. The potential of any hoop is fixed by the capacitances of the potential divider units combined with the stray capacitances between the various hoops and from the hoops to ground and also to metal parts at high potential. The ratio of the potential of a hoop above that of the lower plate to the total potential difference V_s is equal to the ratio of the effective capacitive reactance between the hoop and ground to the total capacitive reactance. This ratio is measured for each

hoop, as described in detail in section VIII–6, page 299, by using an audio-frequency bridge. It is assumed that when the electrometer is used with a high 60-cycle voltage, this ratio of reactances is the same as when measured with about 380 volts at 1,000 cycles per second.

The points plotted in figure 12 show the potentials of the hoops in terms of the total applied difference V_s, as thus observed for the full separation, 110 cm, when 54 intermediate hoops are used. The straight line A corresponds to a uniform potential gradient. It will be noted that the hoops are rather systematically at a lower potential than the ideal, the maximum distortion amounting to about 3 percent of V_s. The scale of the figure is too small to show the minor

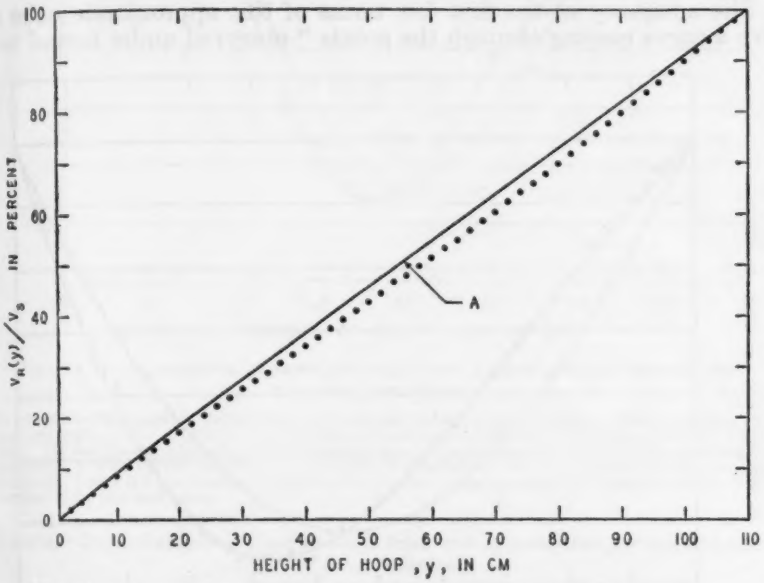

FIGURE 12.—*Typical potential distribution curve*

The plotted points show the potentials of the hoops with respect to the total applied voltage as deduced from measurements made with the audio-frequency bridge. The line A corresponds to the ideal uniform potential gradient. Abscissas are the heights of the hoops above the lower plate. Data were obtained with a separation of 110 cm and a hoop spacing of 2 cm.

irregularities which result from the slight inequalities in capacitance of the various units of the potential divider.

Although the appearance of figure 12 suggests that the potential varies according to a smooth curve through the plotted points, it must be remembered that no information can be obtained by direct experiment about the values of potential at intermediate points. In fact, it is not only possible but for theoretical reasons certain, that the curve of potential versus height must contain superposed ripples of wave length equal to the hoop spacing. The origins and possible effects of such ripples are discussed in section IX–2, page 305.

If the ripples are neglected, it is possible to compute, from the observations made with the audio-frequency bridge, a set of approximate Fourier coefficients, which we may denote by G_k'. The requirement that the curve defined by these n coefficients shall pass through

the n observed points gives n linear equations involving G_1', G_2' .... G_n'. The solution of these equations gives for the kth term

$$G_k' = \frac{2}{n+1} \sum_{m=1}^{m=n} \left(\frac{V_m}{V_s} - \frac{m}{n+1} \right) \sin \frac{km\pi}{n+1} \quad k = 1,2 \ldots . n \tag{17}$$

Table 4 gives values of G_k' which are typical of normal operation at separations of 48 and 110 cm, and shows the rapid decrease of G_k' with increase in k. This decrease makes the terms of higher order in $\Sigma C_k G_k'$ negligible even at the wide separations where the rate of decrease in C_k alone is slow.

The adequacy of the first few terms of this approximate series to give a curve passing through the points [14] observed under normal con-

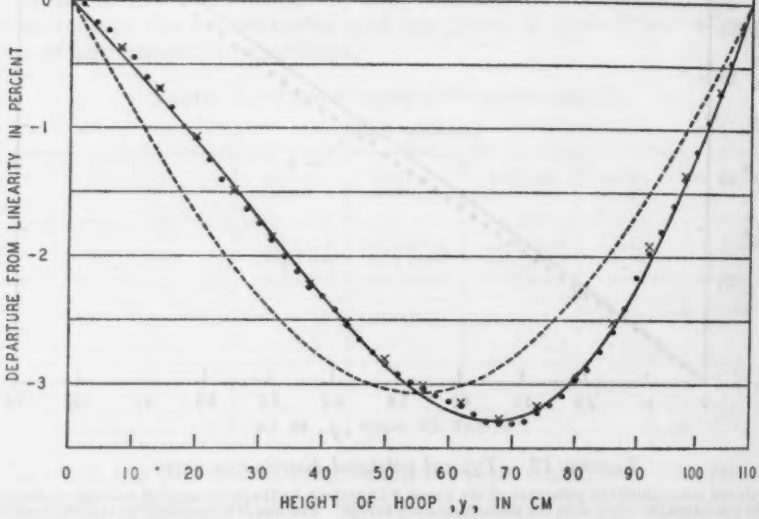

FIGURE 13.—*Departure of hoop potentials from linearity.*

Ordinates are the difference $(V_s(y)/V_s - y/b)$ between the relative potential at a height y above the lower plate and that corresponding to a linear variation. Abscissas are height above the lower plate. The dots correspond to the same data as those given in figure 12; the crosses to similar data obtained when two-thirds of the hoops were omitted so that the spacing was 6 cm. The dotted curve shows the values of potential corresponding to the first term only of the Fourier series. The solid curve is that given by the first two terms of the series.

ditions is indicated by figure 13 and curve A of figure 14. In figure 13 the points show the data of figure 12 for the full separation of 110 centimeters on a greatly magnified scale by using as ordinates the difference $(V_m/V_s - y/b)$ between the observed data and the ideal straight line. The curve shows the result of summing the first two terms only of the series. Similarly, curve A of figure 14 shows the resultant of the first two terms of the series using values of G_k' computed from data taken under normal conditions with a separation of 48 cm between the disk and the lower plate, the normal hoop spacing of 2 cm being used.

[14] The points shown as dots were observed when the hoop spacing was the usual 2 cm, and those indicated by crosses were observed on another occasion when two-thirds of the hoops had been removed, leaving a spacing of 6 cm between centers of adjacent hoops.

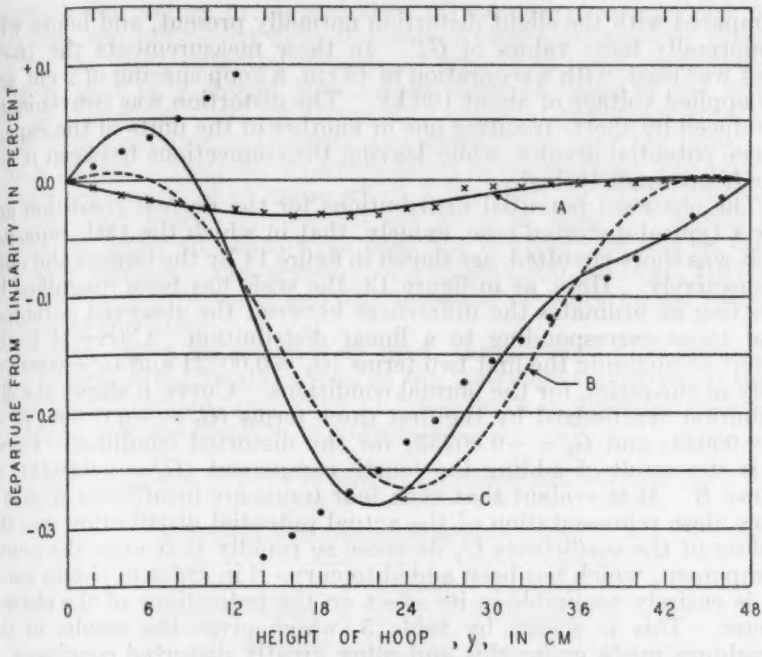

FIGURE 14.—*Departure of hoop potential from linearity under normal and abnormal conditions.*

The crosses show the observed departures from linearity under normal conditions; plate separation 48 cm and hoop spacing 2 cm. Curve *A* is the resultant of the first two terms of the Fourier series based on these data. The dots show the departures from linearity observed when the 6th and 7th hoops, counting from the bottom, were connected together (i. e., when the 18th capacitor unit counting from the top was short-circuited). Curve *B* is the resultant of the first three terms of the corresponding series and curve *C* is the resultant of the first four terms.

TABLE 4.—*Typical values of Fourier coefficients and of correction for nonuniformity of hoop potentials*

k	b=48 cm; n=23		b=110 cm; n=54	
	G_k'	C_kG_k'	G_k'	C_kG_k'
1	−0.00224	+0.00139	−0.03099	+0.06488
2	−.00128	−.00012	+.00655	+.01099
3	−.00006	+5×10^{-7}	−.00026	+.00022
4			−.00014	+.00005
5			+.00072	−.00001
48	−.00663	−4.9×10^{-53}		
110			−.00290	−4.9×10^{-53}
Sum		+0.00127		+0.07613
Δs^2		Negligible		+0.00291
Correction factor [b]		0.99873		0.93042

[a] Second order correction, as computed by eq 44.
[b] Factor in brackets in eq 43.

As an experimental test of the adequacy of the theoretical correction formula, and more particularly of the correctness of the coefficients C_k, a number of weighings were made with the potential distribution deliberately distorted by an amount which was very large

compared with the slight distortion normally present, and hence with abnormally large values of G_k'. In these measurements the 16-cm disk was used, with a separation of 48 cm, a hoop spacing of 2 cm, and an applied voltage of about 100 kv. The distortion was conveniently produced by short-circuiting one or another of the units of the capacitance potential divider, while leaving the connections between it and the hoops undisturbed.

The observed potential distributions for the normal condition and for a typical distorted case, namely, that in which the 18th capacitor unit was short-circuited, are shown in figure 14 by the crosses and dots, respectively. Here, as in figure 13, the scale has been magnified by plotting as ordinates the differences between the observed potentials and those corresponding to a linear distribution. Curve A is the result of summing the first two terms ($G_1'=0.00224$ and $G_2'=0.00128$) only of the series, for the normal conditions. Curve B shows the distribution synthesized by the first three terms ($G_1'=-0.01908$; $G_2'=+0.00035$; and $G_3'=+0.00755$) for the distorted condition. Curve C is the result of adding the fourth component ($G_4'=+0.00441$) to curve B. It is evident that even four terms are insufficient to give a very close representation of the actual potential distribution, yet the values of the coefficients C_k decrease so rapidly that even the fourth component, which has been added to curve B in order to obtain curve C, is entirely negligible in its effect on the indications of the electrometer. This is shown by table 5, which gives the results of the weighings made under this and other greatly distorted conditions.

TABLE 5.—*Adequacy of correction for nonuniformity of potential distribution*

Capacitor unit short-circuited	Observed difference between electrometer (uncorrected for hoops) and voltmeter	Correction for hoop potentials $-\Sigma C_k G_k$	Residual
	Percent	*Percent*	*Percent*
None	$+0.12_8$	-0.12_7	-0.00_1
1st	-1.58_7	$+1.60_3$	$+.01_6$
6th	-1.04_4	$+1.07_7$	$+.03_3$
11th	$-.06_9$	$+0.07_9$	$+.00_1$
18th	$+1.13_3$	-1.17_3	$-.03_4$
24th	$+1.56_8$	-1.61_5	$-.04_9$

In this table the first column indicates which one, counting from the top, of the 24 capacitor units in use was short-circuited. The second column gives the observed percentage difference between the voltage as deduced from the electrometer without applying any correction for the potentials of the hoops and that indicated by the "voltmeter." The third column gives the value of the theoretical correction $-\Sigma C_k G_k'$ for the same condition, the sets of values of G_k' being computed by eq 17 from sets of data obtained with the audio-frequency bridge under both the normal and the distorted conditions, using the first three terms only. The last column gives the residual difference between the two instruments after applying the correction for hoop potentials. Each residual discrepancy is less than one-thirtieth of the uncorrected discrepancy, and the greatest residual is less than 0.05 percent. If the underlying assumptions

on which the values of C_k and thus of the correction $\Sigma C_k G_k'$ are computed are sufficiently close to produce such a satisfactory correction for the large potential distortions present in these experiments, it seems that they should give a very accurate value of the much smaller correction (usually about 0.13 percent) resulting from the usual slight deviation of the potential distribution from the ideal.

As a matter of interest, a further series of experiments was carried out at a separation of 48 cm in which fewer than the normal number of hoops were used. The results are given in table 6. It will be noted that when no hoops were used the electrometer was in error by over 1 percent. The presence of a single hoop, midway, reduced this error to 0.5 percent, and the insertion of more hoops rapidly diminished this error.

Similarly, when no hoops were used, the presence of a grounded metal object in the neighborhood of the instrument affected its indication by 0.2 percent, but when 11 hoops were in place the effect of this object was too small to be detectable.

TABLE 6.—*Effectiveness of hoops in shaping the electric field and shielding it fro the effect of external objects*

[Data with a 16-cm disk at a fixed separation of 48 cm]

Hoop spacing	Number (n) of intermediate hoops used	Excess of electrometer indication over that of "voltmeter"	Increase in electrometer indication due to external object [1]
Centimeters		*Percent*	*Percent*
2	23	0.00	
4	11	.03	0.00
6	7	.13	+.01
8	5	.17	+.04
12	3	.26	+.05
16	2	.36	+.10
24	1	.48	+.12
48	0	1.06	+.18

[1] The "object" consisted of a grounded metal hemisphere 20 cm in diameter, mounted at the level of the lower plate at a distance of 38 cm from the hoops.

In the preceding discussion it has been assumed that the hoops were placed at exactly their proper heights and that only the potentials could be incorrect. This condition is fairly closely approached in the actual construction. Examination of a large number of measurements of height indicates that the hoops were on the average too high by 0.01_1 cm; the average deviation of these measurements, without regard to sign, being $\pm 0.02_7$ cm.

It can be deduced from eq 17 that an error $(\Delta y)_m$ in the height of the mth hoop produces an error in voltage given by

$$\frac{2s}{b^2}(\Delta y)_m \sum_{k=1}^{k=\infty} C_k \sin \frac{km\pi}{n+1}$$

where s is the hoop spacing (2 cm), n is the number of intermediate hoops in use, and b is the separation between disk and lower plate. From the values of C_k given in table 3, it appears that to produce an error of 0.01 percent, even under the worst conditions, one hoop would have to be as much as 1 mm out of place. However, a systematic

shift of all the hoops by 1 mm would produce an error of 0.02_5 percent at a separation of 24 cm, 0.16 percent at a separation of 48 cm, and 0.10 percent at 110 cm. Hence in the most careful work at these larger separations, corrections based on measurements of hoop height in which the accuracy of the mean is better than 0.1 mm are necessary.

It will be shown in section IX–2 that a further source of error exists in the possibility that the presence of external objects, and even of the floor and walls of the room, may cause the potential of a point in the space between the hoops to be appreciably different from the value it would have if the potential gradient external to the hoops was purely axial. Any such effect will be greatest when the plate separation is greatest, and will also increase rapidly with the spacing

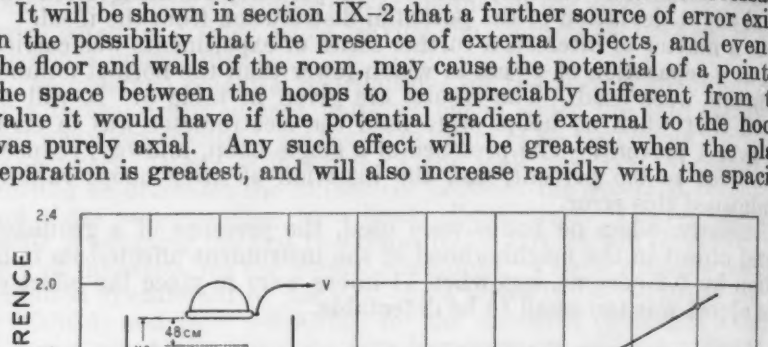

FIGURE 15.—*Effect of distortion of the electric field between the hoops*

Ordinates are the relative differences in the indications of the electrometer and of the "voltmeter." Abscissas are the squares of the center-to-center spacings of the hoops. The true indication should correspond to a spacing intermediate between the smallest, 2 cm, ($s^2=4$) at which observations were made and that, indicated by the line *TT*, at which the hoops touch. The insert shows to scale the electrometer and at each side the grounded metal of the walkways.

of the hoops. A rough estimate indicates that at the full separation of 110 cm this effect, if uncorrected, might introduce an error of 0.13 percent and that at a hoop spacing of 6 cm, instead of the normal 2 cm, this error would increase to 1.4 percent.

A series of experiments was made to test the correctness of these estimates by making measurements at a separation of 110 cm, first with the normal hoop spacing of 2 cm and then with part of the hoops removed to make the spacing 4 cm and later 6 cm. The results are shown in figure 15. Here each ordinate is the difference, expressed in percent, between the indications of the electrometer and of the "voltmeter," and the abscissa is the square of the hoop spacing. The insert shows in true proportion the relative distances between the plates and walkways.[15] It will be seen that the change in error with hoop spacing is in reasonable agreement with the estimated values.

[15] Two semicircular wooden walkways (faced with a grounded metallic mesh) are used, on which the observer stands while gaging and adjusting the balance mechanism. They are moved as far as possible away from the electrometer before voltage is applied but are then at a relative spacing indicated by the insert in figure 15. All other metal objects in the neighborhood of the electrometer are also grounded.

The lower curve in figure 15 gives corresponding data obtained with a plate separation of 48 cm. At this smaller separation the ratio of the radial component of the external potential gradient to the axial component is much smaller than at 110 cm, and the coefficients C_k are also much smaller, so that even if the same error in G_k' were present it would produce much less error in voltage. Consequently, the excess indication at 2-cm spacing and 110-cm separation over that at 48-cm separation may be taken as a correction, and applied in the later use of the instrument at 110 cm under the same geometrical condition, even at higher voltages than can be applied safely at the shorter spacing. This correction we have designated as $\phi_2(s/r_h)$ in eq 12. It is expected that as soon as greater space can be provided for the electrometer, enabling the walkways and other grounded objects to be removed to greater distances, this effect will be much reduced. By the addition of properly shaped conducting elements to the guard ring this effect can be further reduced to almost any desired extent. The criterion for the proper condition which gives a very small radial component of field will be the vanishing of the slope of lines such as those of figure 15, in which electrometer indication is plotted against the square of the hoop spacing.

It is interesting to note from figure 13 that the omission of two-thirds of the hoops to give a spacing of 6 cm did not appreciably change the potentials of the hoops which were retained, and therefore did not change the value of G_1' computed from the hoop potentials by more than 0.0004. The weighings, however, indicate that the true value, G_1, which includes the effects of the potential of points between the hoops, was probably changed by nearly 0.008, and hence that the ripple had an amplitude of approximately 0.8 percent. Ripples of this rather extreme magnitude are shown in case *II D* of figure 24.

In conclusion, the efficacy of the hoops may well be illustrated by an experiment made with a separation of 110 cm and with no intermediate guard hoops, which showed that the voltage required to produce a given force was then only 71 percent of that required when conditions were normal. The instrument without its hoops thus has an error of 41 percent of the true voltage being measured, as contrasted with a correction of about 0.1 percent when the hoops are used at this largest separation.

9. FLATNESS OF LOWER PLATE

When used at small separations the flatness of the lower plate is presumably of almost equal importance with that of the disk and of the guard ring in determining the density of charge and hence the force of attraction. As the separation is increased, however, the guard hoops become of greater and the lower plate of less importance in determining the electric field at the disk. At a separation of 110 cm, the removal of the guard hoops was found to change the calibration by 41 percent. A further indication of the lessened importance of the lower plate was obtained by an experiment at a separation of 48 cm with the hoops in the normal spacing and connection. A disk of metal, 1 cm thick and 11.2 cm in diameter, was placed on the center of the lower plate directly beneath the attracted disk. The voltage then required to produce a given force was found to be only 0.31 percent less than that required when the extraneous disk was absent, although the reduction in separation at the center was 2.1 percent.

10. VIBRATION

The pulsating character of the electrostatic force must cause a certain very small vertical oscillation in the disk of the order of 10^{-5} cm. The vibration of the balance mirror resulting from this is too small to be visible unless some resonant condition is approached. For one condition of loading for low stability, the mirror and stabilizing arm were found to exhibit a resonant vibration at 62 cycles per second, which produced a widening of the image at the scale. This widening was found experimentally not to alter the value of voltage determined by the electrometer, but since it reduced the ease of reading it was eliminated by loading the mirror mounting and thereby reducing the resonant frequency to about 55 cycles per second.

Because of the variation in instrument "constant" with height of the disk any appreciable vibration will tend to introduce a net contribution to the average force. Calculations indicate that such effects should not exceed a few thousandths percent unless the vibration is so large as to be easily visible.

Since it is assumed that the measured force is of electrostatic origin only, it was felt that a test should be made to determine the presence of any spurious aerodynamic force on the disk, such as the Bjerknes effect. The immediate concern was with continuous vibrations, either coming as sound from the 60-cycle supply transformers and electric heaters in the laboratory, or occurring in the disk itself because the electric force is pulsating. That such an effect is unimportant was determined by placing an improvised loud-speaker directly below the attracted disk and producing sound vibrations, over a wide range of audio frequencies, of several thousand times the amplitude usually present in the laboratory. Under this drastic condition only a small deflection was observed, and this was due largely to a translation of the balance beam resulting from its excessive vibration, the rotation being negligibly small.

The electrometer is not especially sensitive to the usual vibrations from nearby machinery and traffic.

VII. MECHANICAL DETAILS

1. MAIN STRUCTURE

The main framework of the electrometer, as shown in figures 2 and 27, consists of a circular base (43), an upper circular plate (4) with a central opening, and an intermediate ring (42), all about 1 meter in diameter. These parts are rigidly united by six hollow pillars (36) of fused silica 2.1 m long. The three metal parts were made of a particular cast iron chosen for its high machinability, stability, and freedom from warping, and were annealed before delivery to the Bureau. After the lower surface of the upper plate was machined,[16] it was "spotted" on a precision surface plate, then stored for a period of months and again checked against the surface plate. This repeat test showed that the casting had not warped an appreciable amount during the period of storage, and the lower surface was accordingly then scraped to a plane.

[16] This work was very carefully done by the U. S. Naval Gun Factory at Washington, the machine-tool equipment of the instrument shop of the National Bureau of Standards being inadequate to machine pieces of this size and weight.

The four cast-iron bushings (3) which make it possible to use any one of four attracted disks of various diameters, were machined to fit accurately into the circular central opening (30.2 cm diameter) in the upper plate. These bushings are of iron of the same quality as the main castings. Each bushing was accurately scraped while in the upper plate so that its lower surface would be in the same plane as the lower surface of the upper plate. The upper surface of each bushing was ground accurately plane and parallel to its scraped lower surface, in order that its definite thickness could be used in measuring the separation of the opposed surfaces of the lower plate and of the guard ring. Since the flatness and surface condition of that portion of the guard ring closely adjacent to the attracted disk are more important than those of the remainder of the guard ring, this portion was formed of a stainless-steel [17] insert (2) having a width of several centimeters. After being machined, the vertical side of the central opening of the insert and its lower surface were lapped and polished. The insert was held in position from above by retaining screws and stop screws which permitted precise vertical adjustment of the lower surface of the insert to make it coincide with the plane of the surrounding surface of the bushing.

The bushings were made hollow, primarily to avoid unnecessary weight, but the hollow interior proved to be of great convenience in the equalization of air pressure on the two sides of the disk. Six holes 20 mm in diameter extend completely through each bushing to accommodate the gage rods used when measuring the separation between guard ring and lower plate. These holes are ordinarily completely closed at the upper side and partially closed at the lower or working surface by means of brass plugs (9). The lower face of each plug was machined so as to lie in the plane of the lower surface of the bushing. The bottom and sides of these plugs are perforated so as to allow free passage of air between the lower side of the disk and the interior of the bushing.

The intermediate ring carries three micrometer screws (40), 120° apart, and between them three jackscrews (41) for raising or lowering the lower plate when it is to be set at a new level. At six equidistant points the cross section of the ring is enlarged to admit openings through which pass the silica pillars. The ring is rigidly fastened by screws to iron sleeves which in turn are secured to the pillars by casting melted tin in the small annular space between the sleeves and the pillars. Cast-iron machined sockets are attached to the ends of the pillars by the use of tin cast in place, and the sockets are secured by cap screws to the upper plate and to the lower plate.

Fused silica was chosen for the pillars for two principal reasons, namely, its very low expansivity and its high electrical resistivity. It retains its high surface resistivity very well under the condition of high relative humidity of the air. It has obvious minor drawbacks, such as the difficulty of obtaining it in regular geometric forms and of machining it. Its most serious shortcoming for the present purpose is its fragility. The upper plate of the electrometer, weighing about 600 pounds and bearing the intricate and expensive balance mechanism, is carried at a height of about 8 feet from the floor on six brittle pillars, one or more of which might easily be broken by

[17] This close-grained material (20 percent of Cr, 1 percent of Cu, and 0.30 percent of C) is capable of being worked by optical methods to a high precision.

an inadvertent blow. To safeguard personnel as well as the electrometer mechanism, each hollow silica pillar has an inner pillar of thick-walled Micarta tubing (see (36) and (37), fig. 27). Because of the relatively high expansivity of the Micarta as compared with that of the fused silica, this inner pillar was made a little shorter than the silica pillar so as to take none of the load under ordinary conditions. There is a clearance between the Micarta pillar and the silica pillar which avoids any reduction in the surface resistance between the hoops.

Three of the pillars, spaced 120° apart, have 55 small holes drilled in each, 2 cm apart, to receive pegs (32) for supporting the guard hoops (31). These holes were drilled by using a brass tube guided by a steel jig and kept charged with a mixture of water and carborundum.

2. LOWER PLATE

The lower plate (35) was cast of a special aluminum alloy [18] having a hardness about equal to that of cast iron. This alloy was used to make the plate light and easy to adjust when the distance between it and the upper plate is changed. To give maximum rigidity for a given mass of metal, the lower plate is heavily ribbed, after the manner of the precision surface plates used by machinists. Its upper surface was scraped to be accurately plane.

To protect the upper surface of the lower plate during gaging and when the instrument is not in use, an aluminum cover 6 mm thick is provided. This is formed of three interlocking pieces to permit its insertion between the pillars.

In use the lower plate rests on a set of three rods (38) (fig. 27) of nickel-steel alloy of low expansivity.[19] At their upper ends these rods are drilled and threaded to screw to studs set 120° apart in the under side of the lower plate, near its edge. The lower ends of these three legs are connected rigidly by a triangular aluminum frame (39) clamped to them by setscrews.

The ends of the three rods and of the micrometer screws on which they rest, were shaped in accordance with the classical "hole, slot, plane" arrangement. This permits the plate to be lowered to a definite position on the micrometer screws without introducing any strain or deformation. Unfortunately, the weight of the plate is so great that the resulting wedging of one screw in the slot and the friction of the other on the plane prevent the sliding required to relieve strain from differential thermal expansion. The relatively slender rods can bend sufficiently, however, to relieve such strain without developing any appreciable distortion in the lower plate itself.

The bearing surfaces of the rods and the adjusting screws (40) were chromium-plated to minimize wear. Each adjusting screw covers a range of somewhat more than 10 cm and the sets of supporting rods differ in length by a constant interval of 10 cm. The screws are of 1-mm pitch and their heads are graduated to read directly to 0.01 mm.

The three jackscrews (41) have coarse threads to permit relatively

[18] This plate was cast, machined, and scraped at the Naval Gun Factory. The alloy used had an expansivity of 21×10^{-6} per °C.

[19] About 2×10^{-6} per °C. Although nickel-steel alloy of still lower expansivity was obtainable, its much higher cost prevented its use.

rapid change of level of the lower plate. They also serve as a safety feature, for although they are lowered slightly after the plate reaches the desired level, to let the weight be carried on the micrometer screws, the ends of the jackscrews project deeply into recesses in the under side of the lower plate.

3. DISKS AND DAMPING CHAMBER

The attracted disks were made of sheet duralumin 1.5 mm thick. A central hub carrying a small conical chuck (see *a*, fig. 16) is attached to each disk by four screws which are so short as not to extend through the disk and mar its lower surface. This chuck grips the stem, which is made of thin-walled phosphor-bronze tubing, 2.5 mm in diameter and 30 cm long. At its upper end the stem has a conical fitting which engages a cone which in turn hangs on an annealed-copper suspension strip 0.6 mm by 0.03 mm by 4.0 cm long. The upper end of this strip is attached to the stirrup carried by the end agate bearing of the balance. The longer dimension of the cross section of the suspension strip is at right angles to the axis of the knife-edge so that the disk can hang as a pendulum without constraint in either direction, although any rotation about a vertical axis is checked by the torsion of the suspension. The rigid stem was made long to insure that the disk would hang nearly level even though the line from the center of the conical fitting perpendicular to the plane of the disk does not pass exactly through the center of gravity of the disk.

Disks of approximately the correct diameter were made to the required flatness or curvature as follows: A disk was clamped between two lapped and polished stainless-steel plates having the desired flatness or curvature and lubricated with graphite; this assembly with a thermocouple was packed in asbestos and held at approximately 400° C for 7 hours, then allowed to cool slowly. Both sides of the disk were lapped and polished with chromium oxide, the two sides being worked alternately. When necessary the disk was reannealed. Subsequently a light finishing cut was removed from the edge. The lower side of the disk was then ruled with a pattern of 25 extremely shallow radial lines 0.2 mm apart at the circumference and about 4 mm long, and other single lines at 60° intervals from the main group of lines. All burrs were then removed by honing with a fine abrasive stone. The main group of 25 lines is used in locating the disk in azimuth relative to a fiducial line on its bushing, when the disk is suspended in its working position in the electrometer. From the azimuth as thus located and the curve showing the height of the rim of the disk at various azimuths obtained when it was surveyed, its mean height can be correlated with the heights of the six positions on which the coplanarity microscopes are sighted.

Early experience with the electrometer showed that serious disturbances were produced even by very slow air currents, such as those resulting from temperature inequalities in the laboratory and within the electrometer dome, and even by wind outside the building. To minimize these effects, the air space just above the disk is separated as much as possible from the air in the dome by a metal cover *a*, figure 17. The stem of the disk passes through a hole in the center of this cover with only the necessary small clearance. The volume of the confined air space above the disk is reduced to a minimum by a wooden

filler (8), figure 27, and this space is vented to openings in the under surface of the guard ring. These openings are formed by small perforations (4 mm in diameter) in the lower ends of the brass plugs (9), figure 27, which normally close the six holes which are provided in each bushing for use in gaging. Because of the symmetrical location of these holes, the mean air pressure at them must be closely equal to the mean pressure at the disk. This mean pressure is transmitted through the plugs to the hollow interior of the bushing and thence through two connecting tubes *b*, figure 17, and (10), figure 27, to the air space behind the disk. A convenient adjustment of the damping is obtained by the use of a butterfly valve in one of these connecting tubes. This was usually so adjusted that the motion was slightly underdamped.

4. BALANCE

The balance beam and the stirrups used in the electrometer were taken from an assay balance. The beam is made of aluminum alloy and provided with agate knives. All three bearings are also of agate, the central one being plane and the end bearings of the V type. The load at either end is about 100 g. The distance between the end knife-edges is 128 mm. In the electrometer, the requirements to be met by the arrestment mechanism are so much more severe than those attending the ordinary use of a balance that an attempt to improve and adapt the control mechanism furnished by the balance maker was very soon abandoned, and a completely new design was developed. A view of this from the rear is shown in figure 18. Figure 19 shows a front view of part of the mechanism beneath the balance base; this latter view does not show the balance beam. Figure 20 shows a side view of the indicating and control mechanism.

The balance base (24), figure 27, is of annealed cast iron, and is supported from the upper plate by three legs (25). Micrometer adjustment provided at the upper ends permits the upper surface of the base to be brought into the desired plane. To minimize the vertical shift with temperature of the disk relative to the lower surface of the guard ring, the lower part of each leg is made of aluminum and the upper part of steel, as may be seen from figure 19; the proportionate lengths of the two parts are chosen with reference to the thickness of the cast-iron balance base and the height of the phosphor-bronze balance column from the upper surface of the base to the level of the central agate plane, so that the resultant expansivity of the structure supporting the balance beam shall be equal to the expansivity of the phosphor-bronze tubular stem and the suspension strip of the attracted disk.

Stop screws and clamping screws provide for locating and securing the balance base in approximately its correct position, namely, that in which the attracted disk hangs freely in the center of the opening in the guard ring. To allow the necessary horizontal adjustments the upper end of each leg fits into a hole in the underside of the balance base, with a relatively large clearance.

To provide the final, very precise horizontal adjustment of the position of the disk, the balance column is carried on a double V-slide arrangement with the two slides at right angles (fig. 17). The heads *c* of the screws controlling these slides are graduated in divisions, each corresponding to a movement of 0.01 mm of the balance column.

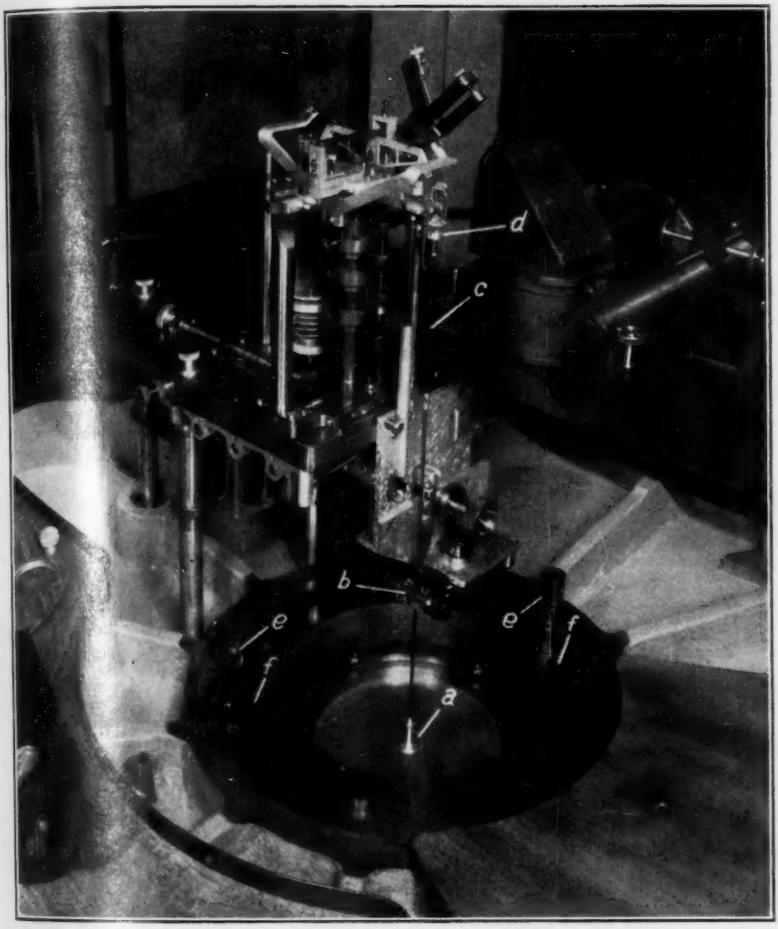

FIGURE 16.—*View looking down at upper side of disk, in position.*

Showing the hub, *a*; the stem and its clamp, *b*; the suspension strip, *c*; weights on the weight pan, *d*; and also the two types of perforated plugs, *e*, used in the gaging holes, *f*.

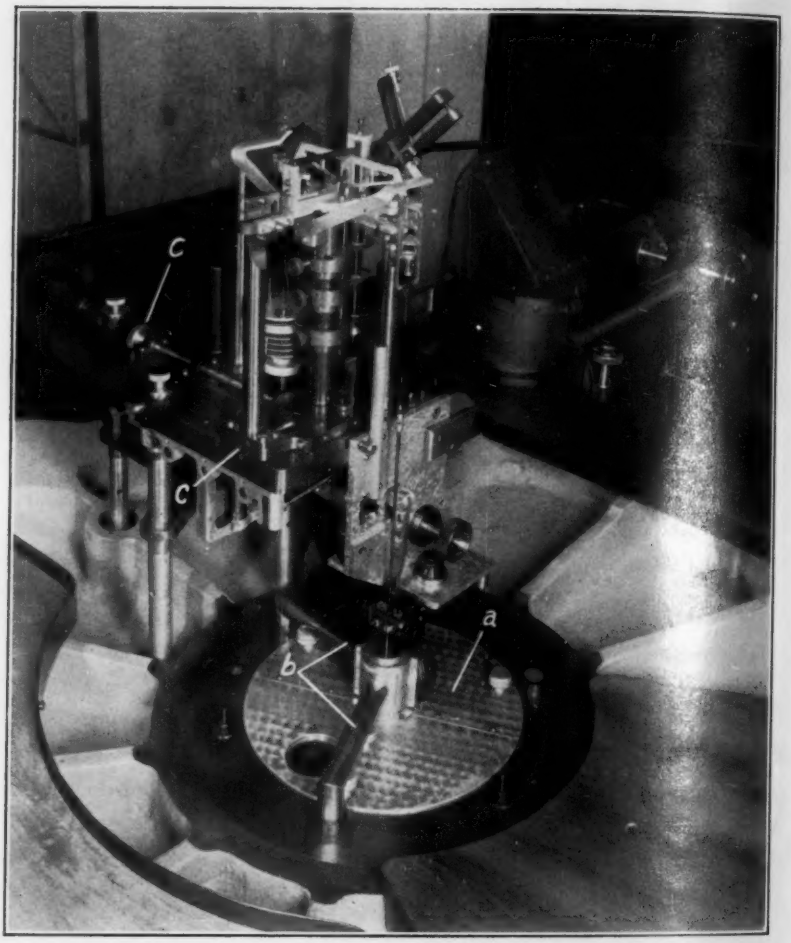

FIGURE 17.—*View of balance mechanism.*

Showing the metal cover, *a*, above the disk; the tubes, *b*, connecting air space above it to the gaging holes; and the heads, *c*, of the micrometer screws used to adjust the balance column in centering the disk.

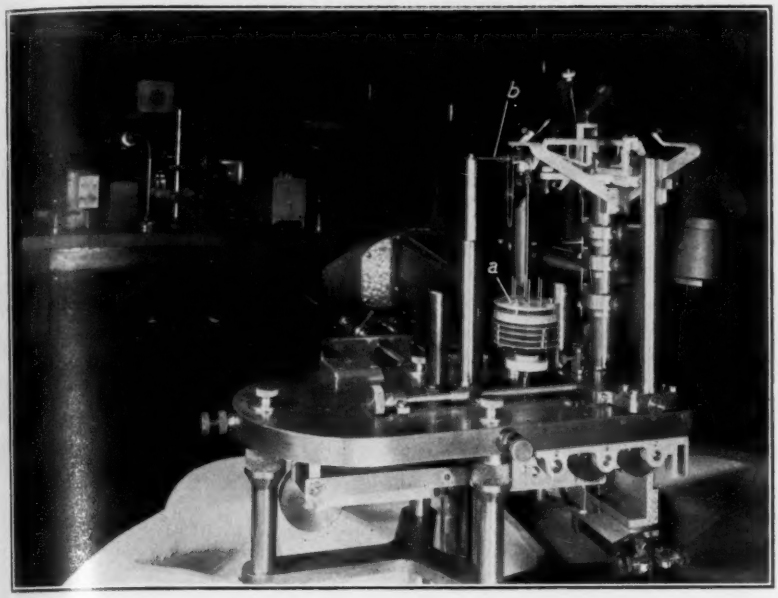

FIGURE 18.—*Balance mechanism as seen from the side opposite the observer's station.*

The counterpoise, *a*, with its multiple aluminum disks, and the chainomatic device, *b*, appear at the left of the balance pillar.

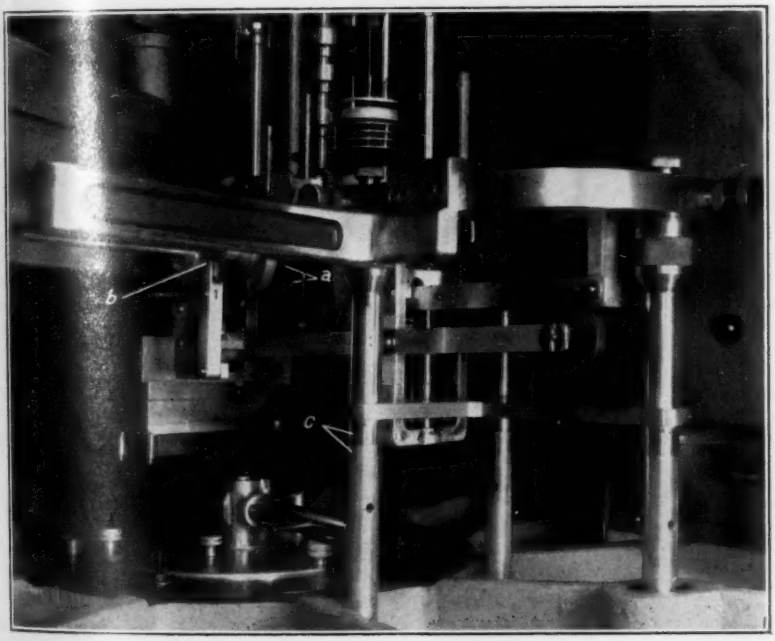

FIGURE 19.—*Lower part of balance control mechanism, showing cams, a; interlock, b; and bimetallic balance base legs, c.*

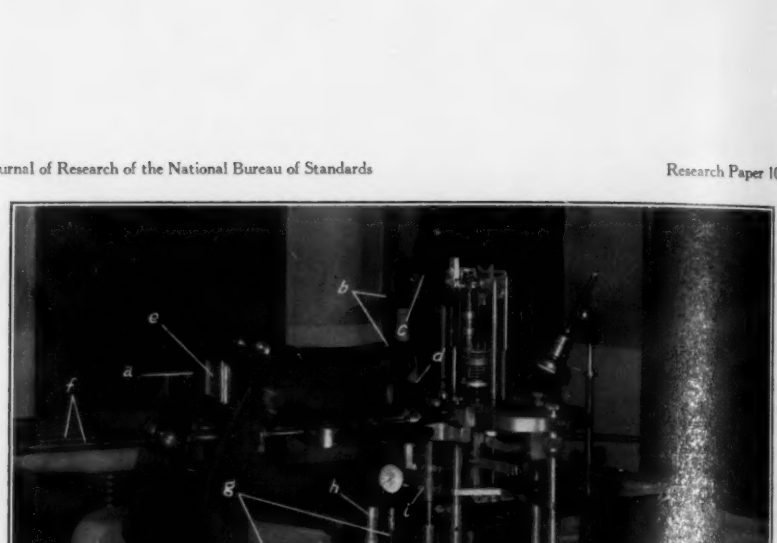

FIGURE 20.—*Side view of electrometer mechanism with dome lifted.*

Light from the source enters the light tube at *a* and is reflected by prisms, *b*, to the mirrors, *c*. Thence it is reflected by the prism, *d*, through the exit window, *e*, to the ground-glass scale at the observer's station. Control rods, *f*, at the left extend to the observer's station (not shown). Gage rod, *g*, block, *h*, and surface gage, *i*, are in position for measuring separation.

In the control mechanism for the balance a main arrestment is provided to remove the loads from the three knife-edges when the electrometer is not in use. This arrestment must also be operated between the determination of the disk height h_m and the actual weighing of the electrostatic force. In order that this operation of the mechanism shall not alter the previously determined correlation between disk height and scale reading, it is a fundamental requirement that each time the balance is released the disk shall return to the same position. For a precision of 0.01 percent the permissible tolerance in the vertical height of the disk is of the order of 1 μ, and a motion, even if horizontal, of one end of the beam exceeding this amount will also produce an angular motion of the mirror which will introduce an appreciable error in the scale indication.

The main arrestment utilizes the classical "hole, slot, plane" principle. The conical "hole" is located near that end of the beam which carries the disk, so as to return the disk always to the center of the aperture. The "slot" is at the other end of the beam, and the "plane" is formed on an extended part of the mirror mounting in line with the central knife-edge. Individual adjustments are provided for the two 60° lifting cones which engage the hole and the slot and for the spherical segment which engages the plane. The mechanism just described serves to lift the balance beam or to replace it on the central agate plane. Another lifter carrying two adjustable cones engages a hole and a slot in the upper part of the stirrup which carries the disk. In the fully arrested position this lifter separates the agate bearing from the knife-edge at this end of the beam. The load is taken off the third knife-edge in a more conventional manner by an adjustable plunger under the counterpoise which lifts it enough to take most of the weight. All three parts of the main arrestment are operated by turning a single control rod, and are so adjusted that the beam with its central knife-edge is lifted first and the end bearings immediately afterward. On release, these operations occur in the reverse order.

As a test of the precision with which the beam arrestments performed their function, six pairs of determinations of the zero of the instrument were made. Each determination consisted of 30 readings taken at intervals of about 3 seconds and averaged to eliminate the effect of variations in the ever-present air currents. After the first determination of each pair, the balance was arrested and released and the second determination of the pair was made. The six pairs of determinations were made on different days and the mean of the differences (taken without regard to sign) between the members of each pair was found to have the surprisingly small value 0.0011 cm on the scale. The balance sensitivity was such that this difference corresponds to a change in weight of less than 2 parts in 10,000,000 or to a shift in the effective length of the balance arm of only 0.01 μ.

However, the mass M_r, which is a measure of the attractive force, is at best only one-thirtieth of the total mass of the disk, stem, etc., so that an error in voltage of 0.01 percent will be produced by a change of only 2 parts in 1,000,000 in the effective length of either arm of the balance. Because the above very gratifying performance had not been anticipated, the possibility of errors from this source had been minimized by providing, in addition, a stem-clamping device [20] which serves to grip the stem of the disk while the mass M_r

[20] J. H. Poynting. *On a method of using the balance with great delicacy and on its employment to determine the mean density of the earth.* Trans. Roy. Soc. (London) **28**, 2 (1878).

or the voltage is being applied or removed. The purpose of this device (12), figure 27, is to ensure that the knife-edges remain in undisturbed contact with their bearings throughout the weighing process. The stem clamp consists of a pair of flexible jaws which are pressed together by a spring and moved apart by a cam. A very light pressure is sufficient because the weight to be changed never exceeds a few grams. The jaws are adjusted so that the unavoidable impulses of translation or rotation which they tend to impart to the stem as they release it are very small.

Two leaf-spring stops are located above the balance beam and adjusted to limit its motion to correspond to the length of the ground-glass scale at the observer's platform. By thus restricting the motion of the beam the relative shift of the balance knife-edges and bearings resulting from large deflections is minimized.

Interlocks are provided so that the main arrestment cannot be operated unless the stem clamp is in its released position, and the clamp cannot be operated unless the main arrestment is released. The same handle controls both the stem clamp and the lifter for the weight pan, so that the weights cannot be changed except while the stem is clamped.

For denominations of 20, 50, 100 . . . 1,000 mg the weights used are small cylinders of platinum-iridium alloy, which was chosen because of its high density and freedom from corrosion. The weights have rounded edges and a height 1.5 times the diameter. An electrical-instrument pivot, mounted in a pantograph engraving machine, was used as a marking tool to burnish the numerals 0.4 mm high on the top of each weight. This method of marking produces no grooves in which dirt may collect. The weight pan, of an aluminum alloy, contributes 100 mg to the total removable weight M_r.

A fine, continuous adjustment of the load on the counterweight arm of the beam is conveniently made from a distance by means of a mechanism which we have designated by its trade name, "chainomatic." It may be seen at the end of the balance beam in figure 18. One end of a gold chain of very small links weighing 0.029 g/cm is attached to a metal cup in which is mounted an inverted cupped sapphire jewel, which rests on the polished, rounded end of a steel pivot carried by an arm attached to the balance beam near its end. This arrangement allows the utmost flexibility of motion of the chain while maintaining a very definite length of arm at which the weight of the chain acts. The outer end of the chain is attached to a horizontal arm carried at the top of a vertical plunger which can be raised or lowered slowly by rotating a shaft at the observer's station. The convenient fine adjustment of the counterweight from a distance, made possible by this chainomatic device, would obviously involve great difficulty if it were attempted by the ordinary process of moving a rider.

Figure 21 shows the balance beam *c*, the beam mirror *a*, and alongside it the fiducial mirror *b* carried by a rigid support from the balance base and capable of fine adjustment by three screws. The light source at the observer's station consists of a brightly illuminated reticle, which is a photographic negative of a scale consisting of equally spaced lines. Light from this source enters the electrometer through a tube (*a*, fig. 20) which contains a lens adjustable by a rack and pinion for focusing. It is reflected upward and to the right

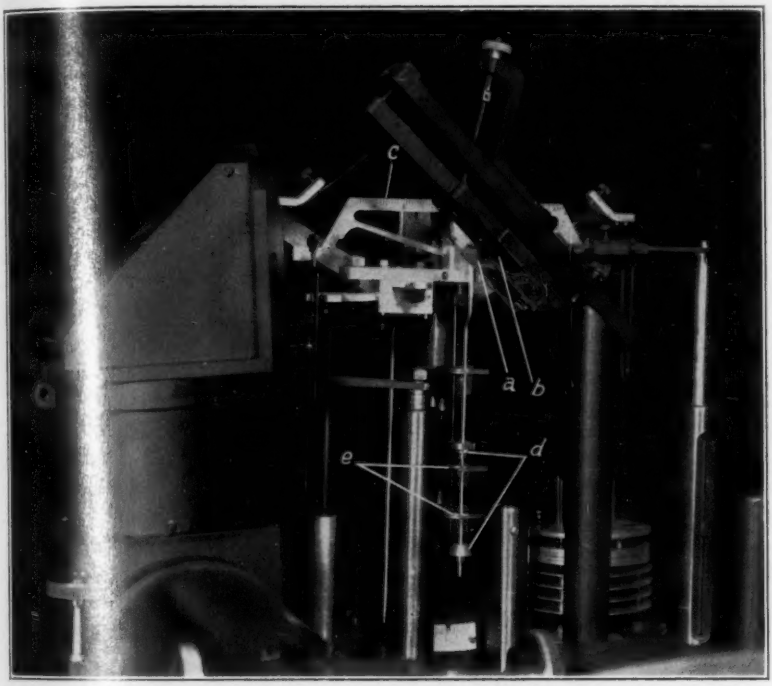

FIGURE 21.—*Balance mechanism from the front.*

At the left is the tube which contains lens and prisms for directing the beam of light onto the movable, *a*, and fiducial, *b*, mirrors, which are seen in the center. The balance beam, *c*, is seen behind the mirrors. The stabilizing arm, with its conical seats, *d*, and the stability weight lifters, *e*, is visible in front of the balance column.

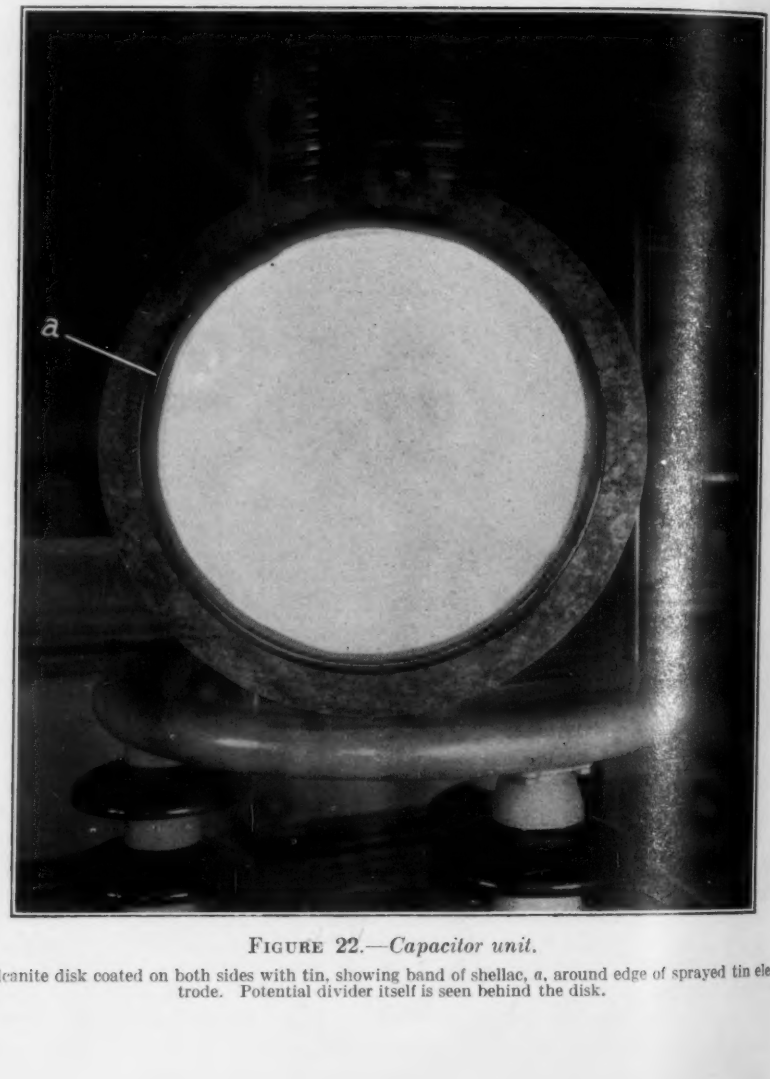

FIGURE 22.—*Capacitor unit.*

Micanite disk coated on both sides with tin, showing band of shellac, *a*, around edge of sprayed tin electrode. Potential divider itself is seen behind the disk.

by prisms in the tubular mounting and then strikes both the mirror mounted on the balance beam and the adjacent fiducial mirror. Each of these mirrors reflects its corresponding light beam downward to a prism (not shown in fig. 21 but visible at *d* in fig. 20) which in turn reflects the two beams back to the horizontal ground-glass scale at the observer's station. The spacing of the lines in the light source is such that each of its images on the screen forms a vernier when observed in connection with the millimeter divisions on the scale. A shift of one coincidence corresponds to 0.05 mm. By means of suitable adjustments of the light source and of the prisms and the scale, the central line of the image from the beam mirror may be brought to the central zero of the scale when the disk and guard ring are very nearly coplanar. The fiducial mirror is then adjusted so that its image also falls at the zero of the scale but lies vertically below and only partly overlaps the image from the beam mirror. The relative position of the two images is thus independent of any movement of the light source or the scale. This use of a fiducial image was described by A. Palm.[21] The optical magnification of the motion of the disk is approximately 80.

An aluminum rod extends downward from the center of the balance beam and carries three conical seats at distances of 4.1, 8.2, and 12.3 cm from the central knife-edge. Weights, ranging from 1 to 10 g, for increasing the stability of the balance may be placed on or removed from one or more of these seats by means of three weight lifters. These lifters are supported and guided by the central column of the balance so that weights can be applied or removed with a minimum disturbance of the balance.

The disk is balanced by a counterpoise carried by the stirrup at the other end of the beam. The counterpoise is of special design in order to avoid change in the equilibrium of the beam with variation in the barometric pressure. The disk, being of an aluminum alloy, has a large buoyancy effect, and if a brass counterpoise (for example) were used the zero position would change if the barometric pressure should change. The obvious remedy is to make the mean density of the counterpoise the same as that of the disk. In addition to this feature, however, it was felt to be expedient to take care of any possible difference in the tendency of metallic surfaces to take up moisture from the air and to give it out. Accordingly, the complex counterpoise shown at *a* in figure 18 was so constructed that it had the same exposed surface of each kind of metal as well as the same mean density and mass as the parts carried at the other end of the beam.

5. POTENTIAL DIVIDER AND HOOPS

The guard hoops and connectors are of thin-wall copper-nickel alloy tubing 8 mm in diameter, fitted together so as to avoid sharp edges and corners. They rest on maple pegs impregnated with paraffin which are inserted in holes in alternate silica pillars. Normally, the hoops are spaced 2 cm center-to-center.

The capacitor units, figure 22, are made of micanite disks 63.5 cm in diameter and 2 mm thick. The electrodes consist of coatings of tin, 53 cm in diameter, sprayed on both sides. To prevent the formation of corona near the edges of the electrodes, melted shellac was

[21] Z. tech. Physik 1, 137–146 (1920).

extruded to form a band about 3 mm thick and about 10 mm wide over the edge of the electrode and adjacent micanite surface. The presence of this band prevents the formation of a visible glow discharge at voltages below about 5,000 volts per unit, which is approximately twice the voltage at which corona would form in the absence of the band of shellac.

The capacitor units are assembled one above another, with aluminum spacers which serve to connect them in series and to hold them 2 cm apart. The spacers also support the tubular leads which connect each spacer to the appropriate hoop. When the electrometer is used at less than its maximum (110-cm) separation, the unused sections at the bottom of the potential divider are short-circuited. When the hoop spacing used is greater than 2 cm the appropriate intermediate tap leads and hoops are removed and the corresponding capacitor units are left connected in series between the remaining taps.

The assembly of micanite units and aluminum spacers is clamped together by bolts of insulating material, between a pair of thick aluminum end plates with rounded edges. The complete potential divider is shown at the left in figure 2.

The average capacitance of the units is about 6,500 $\mu\mu$f. Individual values unavoidably varied somewhat from this mean. In view of this fact, units were arranged in such an order [22] as to obtain the best approximation to the desired condition, in which the total capacitive reactance from the top to any spacer is exactly proportional to the number of units in circuit.

VIII. DETAILS OF OPERATION

1. WEIGHING

When everything has been made ready for a voltage measurement, as in a comparison of the electrometer with the "voltmeter," the balance arrestment and the stem clamp are released while the mass M, is on the stirrup and no voltage is applied. The vernier reticle at the lamp is adjusted to bring the image from the fiducial mirror into coincidence with the zero of the scale, the chainomatic control is then adjusted, if necessary, to bring the vernier image from the beam mirror also very close to this zero. Unless the air in the laboratory is unusually quiet, this image will not remain stationary and the "zero reading" is obtained by making 30 independent readings at equal time intervals (usually every 3 seconds) and taking the mean.

The stem is then clamped, the mass M, removed, and voltage is applied and adjusted to approximately the selected value. The stem clamp is then released. Because of the decreased stability of the balance the motion is now somewhat slower, and the amplitude is greater both by reason of the greater sensitivity and because of fluctuations in the applied voltage. By suitable manipulation of the applied voltage the spot of light can be kept very close to the fiducial mark for intervals of several seconds. When 10 satisfactory readings have been obtained in which both instruments have been reasonably steady for an interval as great as the period of the electrometer, the stem is clamped, the voltage removed, the mass M, replaced, and the stem again released. A second set of 30 readings

[22] W. A. Price. The Measurement of Electrical Resistance, Oxford, Clarendon Press, p. 83-84 (1894).

to obtain the balance zero is then made. If the zero readings differ only slightly, their average is taken as S_0 and the reading at which the settings were made with voltage applied is taken as S_v. It is then assumed that the respective air forces A_0 and A_v are equal and drop out of the final result. Just before and just after each group of weighings the barometer and the wet- and dry-bulb thermometers are read to give data needed for the calculation of the dielectric constant of the air. Temperatures are read from six other thermometers. Two of these are located in holes in the upper plate and the lower plate, respectively, one is clamped against one of the silica pillars, and the remaining three are clamped against the three invar legs which support the lower plate. The temperature of the upper plate is used in computing the radius of the disk, and the temperatures of the lower plate and of the invar legs are used in computing the separation from the previously determined values which for convenience had been reduced to a conventional standard temperature of 20° C.

To minimize errors arising from air forces it was found essential to maintain a thermostatic control of the air temperature. The indoor temperature was controlled at a value equal to the estimated maximum outdoor temperature. This is usually nearly constant for a period from 1 p. m. to 4 p. m. each day and hence during this time the indoor and outdoor temperatures are nearly equal and air currents resulting from temperature differences are a minimum. Also the air in the dome, having already come to thermal equilibrium with the air in the laboratory, shows no tendency to produce a steady air force on the disk by expansion or contraction. The air in the laboratory is stirred continuously except during each weighing and for an interval of about 10 minutes before the weighing is begun.

The thermostatic control and the stirring also serve to minimize errors in potential distribution among the hoops, which might result from the relative changes in capacitance of the end and the central sections of the potential divider, occasioned by the different rates at which these sections follow any change in room temperature.

2. MEASUREMENT OF COPLANARITY

The determinations of the height h_m of the disk relative to its guard ring are made at least twice daily, just before and just after each set of weighings. For this purpose there were constructed two special "coplanarity" microscopes. The essential features of one of these microscopes are shown in figure 27. Each consists of a 16-mm objective and a 12× eyepiece held about 70 cm apart. The eyepiece contains a ruled reticle which is used in measuring the width of the gap. Each objective was modified by the insertion of a right-angled prism between its lenses so that the central ray coming vertically downward from the disk through the front lens of the objective is reflected by the prism to pass horizontally through the back lens, intermediate lens and eyepiece. An intermediate lens (8-diopter) between the eyepiece and the objective can be moved through a range of 35 mm and serves to give a fine adjustment of focus and thus a measurement of object distance (over a range of 0.14 mm). The intermediate lens is mounted on a rack, the pinion of which is supported on the microscope tube and carries an indexed head and revolution counter to

show the position of the lens. Calibration curves for each indexed head and counter in terms of change in object distance were obtained experimentally by using a Zeiss Optimeter. A change of 1μ in object distance corresponds to about 1 mm on the micrometer head.

The two microscopes rest in a channel in an aluminum mounting. One-half of this is shown in longitudinal section at (29), figure 27. When in place this mounting extends completely through the instrument and can be clamped against the lower surface of the guard ring along any desired diameter. Two clamps, hinged near the ends of the channel, bear against the upper side of the guard ring, while two pairs of projections 20 cm from the ends bear against the lower side of the guard ring. Tightening the clamp screws bends the channel and moves the (inner) objective ends of the microscopes downward. This bending action is utilized to bring the microscopes within their focusing range. To prevent any change in this bending as a result of differential thermal expansion or of slipping at the points of contact after clamping, because of strain then set up, one pair of projections is mounted on two flexible strips which are mounted vertically to resist vertical thrust but permit the relief of horizontal strain. The other two projections are formed integral with the sides of the channel.

Each microscope can be moved horizontally in or out with respect to the channel to enable the observer to view either the disk or the guard ring at will. The outer end of the microscope tube at (29) is guided by four steel balls which limit shake and rotation but permit longitudinal motion. The inner end is guided by a groove accurately milled and scraped in the back of the objective housing. This groove rests on the top of an adjustable steel finger (30) mounted in the aluminum channel. By making observations on the almost optically flat surface of the stainless-steel insert, corrections were obtained for the slight vertical motion of the objectives resulting from unavoidable irregularities in their grooves. The magnification of the microscope is about 200 diameters.

Before the microscopes are used the position of the disk is made definite in the following manner. The mass M_r is removed from the stirrup and the stem clamp is released in the normal manner. The counterpoise end of the beam being heavier tilts down until it rests lightly against a small projection, carried on the chainomatic plunger. The observer at the scale then operates the chainomatic control to raise the counterpoise end of the beam until the vernier image from the beam mirror has the desired reading S_m. This is usually chosen to be in coincidence with the image reflected from the fiducial mirror. Under these conditions the disk hangs freely from its knife-edge in the same way as when voltage is being measured, and the stresses in the beam and at the knife edges differ from their normal values by only the small amount caused by a change $M_r g$ in the load.

Determinations are made at six equally spaced azimuths. Each determination is computed from 10 independent settings for sharpest focus on the disk near its edge and from 10 similar settings on the bushing. Each set of 10 readings is averaged and the vertical height in centimeters (from an arbitrary zero) corresponding to this average, is read off from the calibration curve of the microscope. The difference between these heights for each pair of sets is corrected for irregularities in the groove which guides the microscope objective and the corrected result is taken as the difference in height between the edge

of the disk and the guard ring at that azimuth. The six differences thus obtained are then averaged. The entire operation requires about 40 minutes.

3. GAGING

The gaging of the distance between the guard ring and the lower plate, both for the purpose of adjusting their opposed surfaces to parallelism and for accurately determining their separation c, is done as shown in figure 27. The long gage rod (33) rests on the segmental contact block (34) and protrudes through the gaging hole in the guard ring. A short gage block (6) is placed beside the rod and the difference in level of their upper ends is measured by the surface gage (5), which reads to 0.0001 inch. To protect the lower plate from damage it was covered during gaging by an aluminum plate, which had openings to receive and locate the segmental block (34) in the correct position. The separation c is computed from the readings of the dial indicator, the known thickness of the bushing, and the lengths of the blocks and the rod. The six thermometers attached to the instrument are read at the time of gaging to permit the result to be reduced to the standard 20° C basis.

The gage rods and blocks were made of nickel-iron alloy which had an expansivity of 2×10^{-6} per °C. Their ends were plated with chromium to minimize wear. The shorter ones were lapped to be correct to 2 μ and the longer to 0.001 percent. It was found much less expensive to make two complete sets of gages rather than a single set because the precise adjustment was thereby greatly facilitated. Each set comprises 15 rods, 1.9 cm in diameter and of lengths 12, 14, 16, 18, 20, 30, 40 . . . 120 cm; and 10 blocks, 3.2 cm in diameter and of length ranging from 4.8845 to 12.8845 cm by 2-cm intervals. These latter unusual lengths combined with the particular thickness of the guard ring facilitated the gaging.

4. MEASUREMENT OF DIAMETERS

The diameters of the duralumin disks and also of the apertures in the steel bushings are measured by comparing them with the lengths of a set of duralumin line standards 10, 12, 14, and 16 cm between lines. The measurements were made with two microscopes having micrometer eyepieces, for which one division of the indexed head of the screw corresponds to about 1 μ.

When a disk is to be measured, the microscopes are clamped firmly to a heavy steel bar which is supported above a turntable. The axes of the microscopes are vertical and at such a distance apart that the marks at the ends of the line standard are near the centers of their fields of view, when the standard lies along a diameter of the turntable. The focusing of the microscopes, after an initial adjustment, is done by vertical adjustment of the bar.

When the diameter of the aperture in a bushing is to be measured, the microscopes are mounted on studs which rise from a heavy cast-iron ring 30 cm in internal diameter, which is supported directly from the inverted bushing by three small brass levelling screws and is guided in its rotation by the external cylindrical surface of the bushing. The focusing of the microscopes after they are once aligned is done by the levelling screws which support the ring. In both cases measurements are made along 24 equally spaced diameters.

These diameter measurements involve in effect the notoriously difficult comparison of line standards with end standards. However, readings made under widely different types of illumination were so consistent as to indicate that the errors were probably well below the tolerance of 8 μ which corresponds to 0.01 percent in voltage. The fact that the ultimate object of the measurements is to determine the mean of the diameters of a solid disk and of an aperture doubtless tends to compensate the systematic error.

To reduce the results to the diameters at the standard temperature, 20° C, at which the length of the line standard is known, the values for the bushing aperture must be corrected for thermal expansion, using the difference in expansivity of stainless steel and duralumin. No correction is needed for the disks since their expansivity is the same as that of the standard.

5. SURVEY OF THE DISK

To obtain the data needed to locate the average height of the rim of the disk with respect to the six particular points viewed in the coplanarity microscopes, and also to determine the general shape of its lower surface and the corresponding value of h_d, it is necessary to make a precise survey of this surface.

Because of the softness of the aluminum alloy, it was not found feasible to produce a sufficiently high polish on the surface of the disk to permit the use of interference methods for this purpose. The survey is therefore made by reading an indicator, the contact finger of which is placed in succession at about 120 points uniformly distributed over the disk. The difference between the mean of these readings and the mean of 120 other readings made at points which lie along a circumference close to the edge, indicated by line YY, figure 4, is denoted by h_d and is used as indicated in the formulas. A graph of the readings at the edge, plotted against azimuth, serves to correlate the mean height of the rim with the height of the particular six points of the circumferential set at which observations are made with the coplanarity microscopes.

It was found that the pressures exerted by the contact fingers of the dial indicators available were excessive and would cause scratching of the disk. An optical indicator was therefore constructed embodying the principles of the Tuckerman strain gage.[23] In this indicator the motion of a contact finger, held against the disk by a very light force, tilts a prism, the angular motion of which, relative to a fiducial roof prism, is observed with an autocollimator. One division on the autocollimator scale corresponds to 0.0005 mm at the disk surface.

As an aid in surveying the disks and also in adjusting the stems and measuring the diameters of the disks, as described in the preceding section, a small precision lathe was mounted on a wall with its headstock down and its axis vertical. A stepped faceplate carried on the spindle of the headstock thus forms a turntable on which the disk can be laid, inverted, with its stem extending down through the hollow spindle. A bracket rigidly fastened to the lathe supports a surface plate on which the block carrying the optical indicator mentioned above is placed.

In carrying out the survey the effect of any tilt of the surface of the disk with respect to a plane at right angles to the axis of the lathe

[23] Proc. Am. Soc. Testing Materials 23, pt. 2, 602-610 (1923).

is eliminated by taking two sets of readings, the disk being rotated 180° between them. Irregularities and bending of the surface plate on which the indicator block slides are allowed for by suitable corrections. These are obtained by substituting an optical flat for the electrometer disk and making a pair of diametrical traverses across it. When the disk is hanging in the electrometer its shape will differ slightly from that which it assumes when it is supported near its rim upside down on the stepped faceplate. The magnitude of this change of shape, as calculated from observations of the deflection produced at the center of the disk when a known weight was hung from the stem, was found to be entirely negligible.

6. MEASUREMENT OF HOOP-POTENTIAL DISTRIBUTION

The ratio of the capacitive reactances above and below each of the tap points in the potential divider is measured by means of the bridge circuit shown at the left in figure 23. The two arms R_1 and R_2 are noninductive resistances; the other two arms are formed by the total

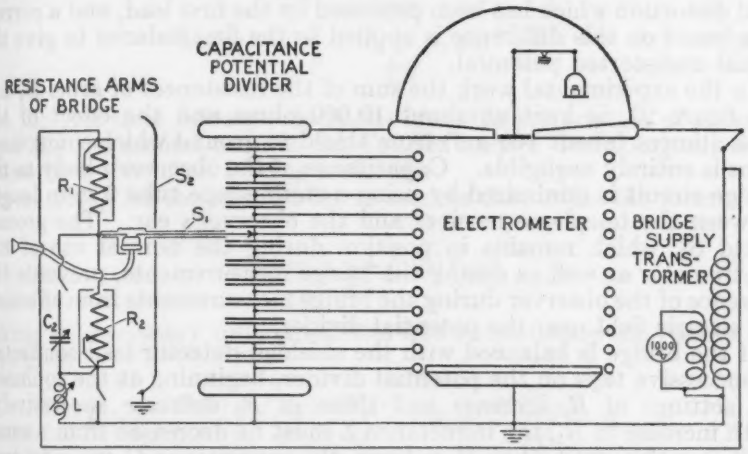

FIGURE 23.—*Schematic diagram of audio-frequency bridge used to measure potential distribution.*

capacitances effectively present between the tap under test and the electrometer plates. The bridge is supplied with 1,000-cycle current at about 350 volts.

As far as possible, during these bridge measurements, all leads and connected apparatus are located and connected as in the normal use of the electrometer, and thus introduce no disturbing capacitance. The connection from the spacer at the tap point to the telephone receiver, which constitutes the bridge detector, is, however, liable to distort the electric field and requires special consideration. This lead can be shielded, as is indicated in figure 23, up to a point a few millimeters from its junction with the spacer in the potential divider. If this shield, S_1 is connected to the junction of the two resistance arms of the bridge, no difference of potential will exist across the

capacitance between the shield and the lead within it; and the capacitances between the shield and external conductors will act merely as shunts around the resistance arms of the bridge, where they affect only the quadrature component of the impedances of these arms.

The mere presence of the shielded lead will, however, produce a distortion of the electric field and a consequent change in potential of the hoops, unless the lead should lie exactly in that surface which, prior to the insertion of the lead, was the equipotential which contained the spacer under test. By suitably mounting the telephone receiver, a considerable length of the lead at the end near the potential divider can be made to lie fairly close to this equipotential surface; and its departure from this ideal position at greater distances will only slightly distort the field. As a further precaution, however, it was found desirable to use two such shielded leads, symmetrically placed and electrically in parallel, but physically located at different azimuths so as to have but little mutual effect. The change in the bridge balance produced when the second lead is added is taken as a measure of the field distortion which has been produced by the first lead, and a correction based on this difference is applied to the first balance to give the initial undistorted potential.

In the experimental work the sum of the resistances of arms R_1 and R_2, figure 23, is kept at about 10,000 ohms and the effect of the capacitances (about 100 $\mu\mu$f) from shield to ground which shunt these arms is entirely negligible. Capacitance of the observer's body to the bridge circuit is minimized by using a stethoscope tube 2 m in length between the telephone receiver and the observer's ear. The ground shield S_2, which remains in position during the normal use of the electrometer as well as during the bridge measurements, prevents the presence of the observer during the bridge measurements from affecting the electric field near the potential divider.

If the bridge is balanced with the shielded detector lead connected to successive taps on the potential divider, beginning at the topmost, the settings of R_1 increase and those of R_2 decrease successively. With increase in R_1, the inductance L must be decreased from a small positive value until when R_1 is large, the capacitance C_2 must be connected in parallel with R_2. This is consistent with the effect to be expected from the capacitance between the shield S_1 and the divider. The slight shunting effect of this capacitance on the effective ratio of the resistances is therefore computed on the assumption that the voltages to ground of all the hoops are in the same phase, and that the small observed phase shifts are due only to the shield capacitance. Under normal conditions this shunting correction affects G'_k by only 10 parts in a million. The correction to the voltage deduced from the change in balance when the second shielded lead is attached is only about 0.03 percent, when the separation is 48 cm, but is about 0.25 percent when the separation is 110 cm.

IX. MATHEMATICAL DETAILS

1. CORRECTION FOR NONUNIFORMITY OF HOOP-POTENTIAL DISTRIBUTION

The electric potential $V(r, y)$ at any point within the space bounded by the plane, parallel electrometer plates at a separation b and by the

right cylinder of radius R tangent internally to the set of guard hoops, must satisfy Laplace's equation, which in cylindrical coordinates is

$$\frac{\partial^2 V}{\partial r^2}+\frac{1}{r}\frac{\partial V}{\partial r}+\frac{\partial^2 V}{\partial y^2}+\frac{1}{r^2}\frac{\partial^2 V}{\partial \theta^2}=0 \tag{18}$$

From the symmetry of the apparatus it is evident that $\frac{\partial^2 V}{\partial \theta^2}=0$. The problem is, therefore, to find V as a function of r and y which satisfies eq 18 and also meets the following boundary conditions (which assume the disk to be coplanar with the guard plate and the gap to be zero):

$$\left.\begin{array}{l}\text{For } y=0,\ V=0 \text{ for all values of } r\\ \text{For } y=b,\ V=V_S \text{ for all values of } r\\ \text{For } r=R,\ V=V_R\ (y)\end{array}\right\} \tag{19}$$

where $V_R(y)$ describes the distribution of potential at the cylindrical boundary. This function can be expressed in the form

$$V_R(y)=V_S\frac{y}{b}+V_S\sum_{k=1}^{k=\infty}G_k \sin\frac{k\pi y}{b} \tag{20}$$

Here the first term corresponds to the ideal linear variation of potential, while the second term is the Fourier's series describing the departure from this ideal, k being an integer.

In searching for the solution let us assume that it has the form

$$V=V_S\frac{y}{b}+F_1(y)F_2(r) \tag{21}$$

Making the necessary differentiations and substituting the results in eq 18 gives

$$F_1(y)\frac{\partial^2 F_2(r)}{\partial r^2}+\frac{F_1(y)}{r}\frac{\partial F_2(r)}{\partial r}+F_2(r)\frac{\partial^2 F_1(y)}{\partial y^2}=0, \tag{22}$$

or on rearranging terms to separate the variables

$$\frac{1}{F_2(r)}\times\frac{\partial^2 F_2(r)}{\partial r^2}+\frac{1}{rF_2(r)}\times\frac{\partial F_2(r)}{\partial r}=-\frac{1}{F_1(y)}\times\frac{\partial^2 F_1(y)}{\partial y^2} \tag{23}$$

Since the left-hand member of eq 23 is a function of r only, while the right-hand member is a function of y only, each member must be equal to a constant. Let this constant be designated by μ^2.

The equation involving r is then

$$\frac{\partial^2 F_2(r)}{\partial r^2}+\frac{1}{r}\frac{\partial F_2(r)}{\partial r}-\mu^2 F_2(r)=0 \tag{24}$$

a solution of which is

$$F_2(r)=J_0(i\mu r), \tag{25}$$

where J_0 is Bessel's function with parameter zero.

The equation involving y is

$$\frac{\partial^2 F_1(y)}{\partial y^2}+\mu^2 F_1(y)=0, \tag{26}$$

the solution of which can be written

$$F_1(y)=V_s A\cos \mu y+V_s B\sin \mu y \tag{27}$$

Since μ is entirely arbitrary the complete solution satisfying eq 18 is found by adding all possible solutions of the above forms and is

$$V=\frac{V_s y}{b}+V_s\sum_{k=1}^{k=\infty}\{A_k\cos(\mu_k y)+B_k\sin(\mu_k y)\}J_0(i\mu_k r) \tag{28}$$

To fit the boundary conditions given by eq 19, the series must vanish at $y=0$ and $y=b$ for any value of r. Hence the factor multiplying $J_0(i\mu_k r)$ must vanish for any value of k for these particular values of y. Hence

$$A_k=0 \text{ and } \mu_k b=k\pi \tag{29}$$

Inserting these relations in eq 28 gives

$$V=\frac{V_s y}{b}+V_s\sum_{k=1}^{k=\infty}B_k\sin\left(\frac{k\pi y}{b}\right)\times J_0\left(i\frac{k\pi r}{b}\right) \tag{30}$$

At the particular radius R this becomes

$$V_R=\frac{V_s y}{b}+V_s\sum_{k=1}^{k=\infty}B_k\sin\left(\frac{k\pi y}{b}\right)\times J_0\left(i\frac{k\pi R}{b}\right) \tag{31}$$

A comparison of eq 31 with eq 20 indicates that the boundary condition fixed by the latter will be satisfied if

$$B_k=\frac{G_k}{J_0\left(\frac{ik\pi R}{b}\right)} \tag{32}$$

and the final solution for the potential anywhere within the hoop-enclosed space becomes

$$V=\frac{V_s y}{b}+V_s\sum_{k=1}^{k=\infty}G_k\sin\left(\frac{k\pi y}{b}\right)\times\frac{J_0\left(\frac{ik\pi r}{b}\right)}{J_0\left(\frac{ik\pi R}{b}\right)} \tag{33}$$

To calculate the attractive force produced by such an electric field we have for the vertical component of potential gradient at any point

$$\frac{\partial V}{\partial y}=\frac{V_s}{b}\left[1+\sum_{k=1}^{k=\infty}k\pi G_k\cos\left(\frac{k\pi y}{b}\right)\times\frac{J_0\left(\frac{ik\pi r}{b}\right)}{J_0\left(\frac{ik\pi R}{b}\right)}\right] \tag{34}$$

The surface density of charge σ on the upper plate is related to the potential gradient adjacent to the surface by the equation

$$\sigma=\frac{1}{4\pi}\left(\frac{\partial V}{\partial y}\right)_{y=b} \tag{35}$$

Combining this relation with eq 34 gives for the charge density on the disk

$$\sigma=\frac{V_s}{4\pi b}\left[1+\sum_{k=1}^{k=\infty}(-1)^k k\pi G_k\frac{J_0\left(\frac{ik\pi r}{b}\right)}{J_0\left(\frac{ik\pi R}{b}\right)}\right] \tag{36}$$

For the present applications the summation corresponds to the relatively small departure from the ideal distribution and is small compared with unity. Neglecting the square of this summation therefore, we may write

$$\sigma^2=\frac{V_s^2}{16\pi^2b^2}\left[1+2\sum_{k=1}^{k=\infty}(-1)^k k\pi G_k\frac{J_0\left(\frac{ik\pi r}{b}\right)}{J_0\left(\frac{ik\pi R}{b}\right)}\right] \tag{37}$$

The attractive force is given by

$$F=2\pi\int_0^{r_d}\sigma^2\times 2\pi r dr \tag{38}$$

Substituting eq 37 in eq 38, noting that

$$\int_0^x xJ_0(x)dx=xJ_1(x),$$

where J_1 is Bessel's function with parameter 1, gives

$$F=\frac{V_s^2}{4b^2}\left[\frac{r_d^2}{2}+2\sum_{k=1}^{k=\infty}(-1)^k\frac{br_dG_kJ_1\left(\frac{ik\pi r_d}{b}\right)}{iJ_0\left(\frac{ik\pi R}{b}\right)}\right] \tag{39}$$

or on rearranging

$$F=\frac{V_s^2r_d^2}{8b^2}\left[1+4\sum_{k=1}^{k=\infty}(-1)^k\frac{b}{ir_d}G_k\frac{J_1\left(\frac{ik\pi r_d}{b}\right)}{J_0\left(\frac{ik\pi R}{b}\right)}\right] \tag{40}$$

and on solving for V_s, again neglecting higher powers of the summation,

$$V_s=\frac{2b\sqrt{2F}}{r_d}\left[1-\sum_{k=1}^{k=\infty}(-1)^k k\pi G_k\frac{2J_1\left(\frac{ik\pi r_d}{b}\right)}{\frac{ik\pi r_d}{b}}\times\frac{1}{J_0\left(\frac{ik\pi R}{b}\right)}\right]$$

which is in the form

$$V_s=\frac{2b\sqrt{2F}}{r_d}\left[1-\sum_{k=1}^{k=\infty}C_k G_k\right] \tag{41}$$

where

$$C_k=(-1)^k\pi k\cdot\frac{2J_1\left(\frac{ik\pi r_d}{b}\right)}{\frac{ik\pi r_d}{b}\times J_0\left(\frac{ik\pi R}{b}\right)} \tag{42}$$

In cases where the terms neglected in passing from eq 36 to eq 37 are appreciable, the voltage is given rigorously by

$$V_s=\frac{2b\sqrt{2F}}{r_d}\left[1+2\sum_{k=1}^{k=\infty}C_k G_k+\Delta_2\right]^{-\frac{1}{2}}, \tag{43}$$

where

$$\Delta_2=\sum_{k=1}^{k=\infty}\frac{\pi^2k^2\left[\left\{J_0\left(\frac{ik\pi r_d}{b}\right)\right\}^2+\left\{J_1\left(\frac{ik\pi r_d}{b}\right)\right\}^2\right]}{\left\{J_0\left(\frac{ik\pi R}{b}\right)\right\}^2}G_k^2+\left\{\sum_{k=1}^{k=\infty}\sum_{\substack{l=1,\\ l\neq k}}^{l=\infty}\right.$$

$$\left.\frac{(-1)^{k+l}2kl\pi^2b\left[ki J_1\left(\frac{ik\pi r_d}{b}\right)\times J_0\left(\frac{il\pi r_d}{b}\right)-lJ_0\left(\frac{ik\pi r_d}{b}\right)\times iJ_1\left(\frac{il\pi r_d}{b}\right)\right]}{\pi r_d(l^2-k^2)J_0\left(\frac{ik\pi R}{b}\right)J_0\left(\frac{il\pi R}{b}\right)}G_kG_l\right\} \tag{44}$$

It may be noted that for large values of the arguments, such as correspond to large values of k, the semiconvergent expansions for the Bessel's functions can be used to express C_k in the form

$$C_k=(-1)^k\frac{2b}{r_d}\left(\frac{R}{r}\right)^{\frac{1}{2}}\frac{\left(1+\frac{b}{8k\pi r_d}\cdots\right)}{\left(1-\frac{3b}{8k\pi R}\cdots\right)}e^{k\pi(r_d-R)/b} \tag{45}$$

Since R is considerably larger than r_d the exponential factor in this expression becomes exceedingly small for very moderate values of k. In particular, the ripple [24] in potential which results from the finite (2-cm) spacing of the hoops and which introduces terms of order $k=b$, will be affected by the factor $e^{\pi(r_d-R)}$, which for $R=50$ cm and

[24] This ripple has been treated by Snow (see footnote 7) from a somewhat different approach with similar results.

r_d=8 cm is about 10^{-50}. However, when b is sufficiently large compared with πR and πr_d, the values of C_k increase with successively increasing values of k, so that the summation will converge only if the successive values of G_k decrease at a sufficiently rapid rate.

2. SOURCES OF ERROR IN FOURIER COEFFICIENTS, G_k'

Although the experiments reported in table 5 indicate that the values of C_k are correct and that changes in potential distribution are adequately allowed for by the $\Sigma C_k G_k'$ correction term, there remains a further possible source of error if the values of G_k' computed from eq 17 differ from the true values of G_k, as defined by eq 14. The difference between these values may be written

$$G_k'-G_k=\frac{2}{b}\left[\sum_{m=1}^{m=n}\left\{s\left(\frac{V_m}{V_s}-\frac{m}{n+1}\right)\sin\frac{k\pi m}{n+1}-\int_{(m-1/2)s}^{(m+1/2)s}\left(\frac{V_R(y)}{V_s}-\frac{y}{b}\right)\sin\frac{k\pi y}{b}\,dy\right\}\right.$$

$$\left.-\int_0^{s/2}\left(\frac{V_R(y)}{V_s}-\frac{y}{b}\right)\sin\frac{k\pi y}{b}\,dy-\int_{b-s/2}^{b}\left(\frac{V_R(y)}{V_s}-\frac{y}{b}\right)\sin\frac{k\pi y}{b}\,dy\right], \quad (46)$$

where s is the spacing of the hoops, center to center. The significance of this expression can be seen best perhaps by the graphic interpretation shown in figure 24. Here in the upper-left corner is shown an assortment of assumed potential distribution curves similar to figure 12 and corresponding to different alternative hypothetical cases.

Line A illustrates the ideal linear potential distribution, curve B a smooth distribution such as would result if only the first few coefficients G_k had appreciable values. Curves C and D show other distributions in which the potential at points in the spaces between the hoops departs from the smooth gradient of curve B. To show the relations involved more clearly, the difference between each curve and the line A, i. e., the quantity $\frac{V_R(y)}{V_S}-\frac{y}{b}$, is plotted to a much enlarged scale in the central part of the figure. The end section I of curve B, containing the first three hoops, is shown at $I\,B'$, and a typical intermediate section II spanning two hoops and half of each space is shown magnified at $II\,B'$, $II\,C'$, and $II\,D'$ for the three types of distribution B, C, and D, respectively.

At S_I and S_{II} are shown (ordinate scale at the right) portions of a graph of the factor $\sin k\pi y/b$ (for the case $k=1$)[25] corresponding to sections I and II, respectively.

At the bottom of the figure $I\,B''$, $II\,B''$, $II\,C''$, and $II\,D''$, respectively, are shown portions of the corresponding graphs of the resultant quantity $\left(\frac{V_R(y)}{V_S}-\frac{y}{b}\right)\sin\frac{k\pi y}{b}$, $(k=1)$ which occurs in eq 46.

Now at the points P_1, P_2 . . P_m, where $y=\frac{1}{n+1}, \frac{2}{n+1}, \cdots \frac{m}{n+1}$,

[25] For convenience in drawing, the negative of this factor (i. e., $-\sin \pi\, y/b$) has been plotted in figure 24.

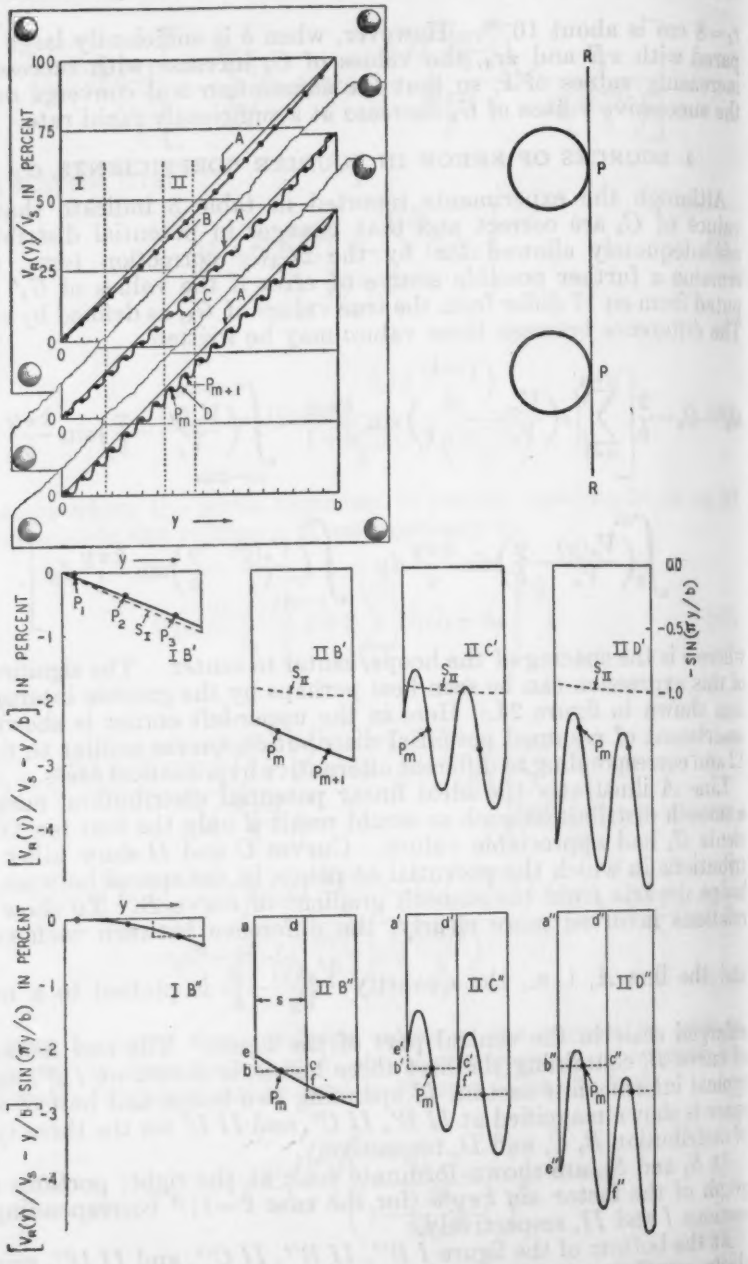

FIGURE 24.—*Graphic illustration of origin of error in Fourier coefficients G_1'.*

At *A*, *B*, *C*, and *D* are shown examples of the four following types of potential-distribution curves: *A*, the ideal linear distribution; *B*, a smooth curve similar to the resultant of the first few terms of the Fourier series, and passing nearly through the points $P_1, P_2, \ldots P_m$, which were observed with 6-cm spacing and 110-cm separation; *C*, a curve having a ripple of such magnitude as to satisfy the requirement that the potential be independent of height at points close to each hoop; and *D*, a curve having a ripple of the shape that is produced if the potential gradient has a radial as well as an axial component, and approximately of the magnitude present with a plate separation of 110 cm and the abnormal hoop spacing of 6 cm. Below are shown to a magnified scale for section *I* of curve *B* and section *II* of curves *C* and *D*, the departure $(V_R(y)/V_{s-y/b})$ from curve *A*. At the bottom are shown the product of the departure multiplied by the factor $\sin \pi y/b$ for the three cases, this product being the quantity which appears in eq 46 which gives the difference between the true coefficients G_1 and the approximate values G_1'.

respectively, $V_R(y)$ has the values V_1, V_2 . . . . V_m and hence the value of the contribution to the summation in eq 46 from the first term of each pair in the brace is equal to the area of a rectangle such as *abcd* (see *II B''*) of width s and of height equal to the height of the graph at point P_m. The second term of each pair contributes an amount equal to the area of a strip, also of width s, enclosed between the axis of y and the graph eP_mf of $\left(\frac{V_R(y)}{V_S}-\frac{y}{b}\right)\sin\frac{k\pi y}{b}$. The last two terms of eq 46 correspond to the areas of the first and last half-sections and are in practice entirely negligible, because both the factors of the integrand are zero at $y=0$ and at $y=b$.

The approximate coefficients G_k' will therefore equal the true coefficients G_k if the sum of the areas of the n rectangles is equal to the total area between the curve and the axis. If the curve is reasonably smooth, as drawn in *I B''* and *II B''*, the error arising from lack of equality between the two types of strip is very small. Because of the rapid decrease of C_k with increase in k, we are concerned only with the values of G_k' for small values of k. For these the factor $\sin k\pi y/b$ changes but little over the narrow range, s, of any one strip, and also y/b varies only by the small amount $1/(n+1)$. Therefore, a significant error in any of the first few values of G_k' is likely to arise only if the potential $V_R(y)$ changes so rapidly as to differ materially within each strip from its value V_m at the beginning of each interval. Such a rapid change in $V_R(y)$ may occur if a ripple of wave length $b/(n+1)$ is present, and a consideration of this possibility is now in order.

Each plotted point in the curves of potential distribution such as figure 13 and figure 14 and of points such as P_m of figure 24, corresponds to the potential of the circle along which each conducting hoop, of circular section, is tangent to the imaginary cylindrical surface of radius R considered in section IX–1. The insert at the upper right of figure 24 shows to scale for the normal 2-cm spacing a cross section of two adjacent hoops and the points P at which they are tangent to the surface RR. Therefore, in the immediate neighborhood of each point P, the potential must be nearly constant over a short distance and the curve of V versus y must have a horizontal tangent at each point. The actual shape of the curve is therefore similar to that shown in curve C of figure 24, and has a rippled appearance. Here line A shows again the ideal linear variation.

If we include in the Fourier series by which we attempt to represent $V_R(y)$, in addition to the n terms of which the coefficients are the values of G_k' already found, a term $G'_{2n+2}\sin 2(n+1)\frac{\pi y}{b}$ and set $G'_{2n+2}=-\frac{1}{2(n+1)\pi}$, this term will suffice to diminish the slope of the potential-distribution curve at each point of tangency by an amount equal to the mean slope V_S/b and thus to give the rippled appearance. Moreover, the term itself vanishes at each of the points of tangency so that its inclusion does not disturb the fit of the series already found.

In section *II C'* of figure 24 there is shown a ripple of this magnitude, and as shown at *II C''* its presence does not make the area $a'e'P_mf'd'$ materially different from the area $a'b'c'd'$.

An exact meeting of the requirement for a horizontal tangent at each hoop can be obtained by including also for each of the n terms of the original approximate series, such as the term $G_p' \sin \frac{p\pi y}{b}$, a pair of compensating terms. These are

$$-\frac{pG_p'}{4(n+1)} \sin (2n+2-p)\frac{\pi y}{b} \text{ and } -\frac{pG_p'}{4(n+1)} \sin (2n+2+p)\frac{\pi y}{b}.$$

The sum of such a pair of terms also vanishes at the points of tangency when $y=mb/(n+1)$, and therefore their inclusion does not affect the first n values of G_k'. Also the ripples which they introduce are in effect similar to those shown at $II\,C'$ in figure 24 and contribute on the whole substantially equal areas above and below the smooth curve $e'P_mf'$. Furthermore, the largest value of p is equal to n, so that these terms, which must be introduced to fit the curve to the required horizontal tangent at each observed point, will range in order from $n+2$ to $3n+2$. Table 3 shows that the values of C_k corresponding to these high orders are so exceedingly small as to make the contribution of these terms to the correction $\Sigma C_kG_k'$ entirely negligible.

Unfortunately, ripples of the type just discussed and in such a phase as to satisfy the condition of horizontal tangency are not the only type which may occur.

A ripple of the same wave length, $b/(n+1)$, but occurring in such a phase that the points of tangency lie at or near one set of its crests, as shown at D in figure 24, will cause a cumulative systematic difference between the area under the curve and that of the rectangle and thus an error in the value of G_k' even for $k=1$.

A ripple of this latter type is to be expected if in the region external to the hoops there exists a component of electric field acting radially outward in addition to the normal axial field. If the electrometer is used at its full separation of 110 cm in the confined space available in the Bureau's present high-voltage laboratory, the grounded metal shields on the walkways are on the average at a distance of only 120 cm from the hoops. Hence the radial gradient near the uppermost hoops is nearly equal to the axial gradient. Under such conditions the potential at any point in the open spaces between the hoops will be lower than it would be if the radial component of field were absent.

In figure 24 distribution curve D shows a ripple of this type and of about the magnitude probably present when the electrometer is used with the exaggerated hoop spacing of 6 cm (i. e., with two-thirds of the hoops removed). The area of the rectangular strip $a''b''c''d''$ is obviously not equal to the area $a''e''P_mf''d''$ between the curve and the axis and consequently by eq 46, G_1' is not equal to G_1.

A rough estimate of the magnitude of this shift in potential can be obtained from the treatment by Maxwell (Elec. and Mag. 1, sect. 203) for a plane grid of parallel wires, subjected to a field normal to the plane. This indicates that for an instrument of the present proportions this effect might introduce an error in voltage of 0.13 percent. It also indicates that the error would increase approximately as the square of the hoop spacing s, and for a spacing of 6 cm would amount to 1.4 percent. The experimental confirmation of the existence of these errors has already been discussed in section VI–8, page 284.

3. VARIATION OF FORCE WITH HEIGHT OF DISK

In the course of this work we have used as the best available basis for design and as a guide in reducing our observations, a theoretical expression for the attractive force based on the paper by Snow. [26] In this paper there is given a solution for the electric field existing between an infinite plane conductor, simulating the lower plate, and two semi-infinite conductors which simulate the disk and the guard ring. These latter are spaced at distances b and c, respectively, above the first conductor and have their lower surfaces plane and parallel to its upper surface. The two upper conductors are separated by a straight crevasse of width a and of infinite length, the sides of which extend for an infinite distance upward perpendicular to the upper surface of the lower conductor. This crevasse simulates the gap between the disk and the guard ring. Snow's eq 27, when expressed in the present notation, is

$$F_s=2\pi w\left(\frac{V_s}{4\pi c}\right)^2\left\{x-\frac{2h}{\pi}\log_e\frac{2c\left(e^{\frac{\pi x}{c}}-1\right)}{(a^2+h^2)^{\frac{1}{2}}}+\frac{a}{\pi}\tan^{-1}\left(\frac{a}{h}\right)\right\} \tag{47}$$

In this equation F_s is the downward force acting on a rectangular strip of width w, extending back from the edge of the crevasse for a distance x, and h is the height of the disk above the plane of the guard ring. This can be arranged to give

$$F_s=w\frac{V_s^2}{8\pi c^2}\left\{x\left(1-\frac{2h}{c}\right)-\frac{2h}{\pi}\log_e\frac{2c\left(1-e^{-\frac{\pi x}{c}}\right)}{(h^2+a^2)^{\frac{1}{2}}}+\frac{a}{\pi}\tan^{-1}\left(\frac{a}{-h}\right)\right\} \tag{48}$$

In this expression the first term in the brace contributes a force $\frac{V_s^2w}{8\pi c^2}\left(1-\frac{2h}{c}\right)x$, which is (neglecting terms in h^2/c^2 and higher) the same as $\frac{V_s^2wx}{8\pi b^2}$. This contribution is proportional to the area of the strip and represents the normal force which would be produced on an area wx by a uniform charge density $V_s/4\pi b$. The remainder of the right-hand member of eq 48 must therefore be taken to represent the small correction per unit length due to the nonuniformity of charge density along the edge of one conductor.

This result may now be applied approximately to the actual case of a circular disk of radius r_d, by substituting its area πr_d^2 for the area wx of the strip and its perimeter $2\pi r_d$ for the width w along the crevasse. By also substituting r_d for x in the exponential term of eq 48 we obtain the approximate relation

$$F=\frac{V_s^2}{8\pi c^2}\left[\pi r_d^2\left(1-\frac{2h}{c}\right)-2\pi r_d\left\{\frac{2h}{\pi}\log_e\frac{2c\left(1-e^{-\frac{\pi r_d}{c}}\right)}{(h^2+a^2)^{\frac{1}{2}}}-\frac{a}{\pi}\tan^{-1}\left(\frac{a}{-h}\right)\right\}\right]$$

[26] Chester Snow. *Effect of clearance and displacement of attracted disk, and also of a certain arrangement of conducting hoops, upon the constant of an electrometer.* BS J. Research **1**, 513 (1928) RP17. It may be noted that the method of applying this solution to the circular disk, which leads to his eq 29, is incorrect. The process given here, which leads to eq 50, has much greater justification but is still only an approximation.

This can be reduced to

$$F=\frac{V_s^2 r_d^2}{8c^2}\left[1+\frac{a}{r_d}-\frac{2h}{c}-\frac{4h}{\pi r_d}\log_e\frac{2c\left(1-e^{-\frac{\pi r_d}{c}}\right)}{(h^2+a^2)^{\frac{1}{2}}}+\frac{2a}{\pi r_d}\tan^{-1}\left(\frac{h}{a}\right)\right]$$

By introducing r_m, the mean of the radius of the disk and that of the aperture in the guard ring, that is

$$r_m=r_d+\frac{a}{2}$$

and neglecting terms in $\frac{a^2}{r_d^2}$, we have

$$r_m^2=r_d^2\left(1+\frac{a}{r_d}\cdot\cdot\cdot\cdot\right) \tag{49}$$

and

$$F=\frac{V_s^2 r_m^2}{8c^2}\left[1-h\left\{\frac{2}{c}+\frac{4}{\pi r_d}\log_e\frac{2c\left(1-e^{-\frac{\pi r_d}{c}}\right)}{(h^2+a^2)^{\frac{1}{2}}}-\frac{2a}{\pi r_d h}\tan^{-1}\left(\frac{h}{a}\right)\right\}\right] \tag{50}$$

which is in the form

$$F=\frac{V_s^2 r_m^2}{8c^2}\left[1-fh\right], \tag{51}$$

where the coefficient f varies only slightly with h, being in the form

$$f=f_0+\frac{1}{r_d}\phi_3\left(\frac{h}{a}\right), \tag{52}$$

where

$$f_0=\frac{2}{c}+\frac{2}{\pi r_d}\left\{2\log_e\left(\frac{2c(1-e^{-\frac{\pi r_d}{c}})}{a}\right)-1\right\} \tag{53}$$

and

$$\phi_3\left(\frac{h}{a}\right)=\frac{2}{\pi}\left\{\log_e\frac{1}{\left(1+\frac{h^2}{a^2}\right)}-\frac{a}{h}\tan^{-1}\left(\frac{h}{a}\right)+1\right\} \tag{54}$$

Figure 25 shows this quantity f plotted as a function of h for several different gap widths and spacings.

Equation 50 has proved to be of great utility in this work, but because of the approximations necessary in passing from the theoretical case, in which the field varies in two dimensions only, to the case of the actual electrometer, which is three-dimensional, it is not exact. The extent to which it correctly describes the variation of force with disk height is indicated in figure 26. This typical case is for the 16-cm disk with a separation of 12 cm, a clearance of 0.0106 cm, and a mass M_r of 2,550 mg. Here the abscissas are the scale readings of the electrometer. The disk and the guard ring are coplanar when the reading is 24.8 cm, and differ in height by about 0.0625 cm at scale readings of 20 cm and of 30 cm, the disk being high (h positive) for readings less than 24.8 cm.

If the electrometer is regarded as a deflection instrument, curve B, figure 26, gives its observed scale law, each ordinate being the voltage corresponding to the scale reading plotted as abscissa. If the electrostatic force for a given voltage were independent of disk height, the variation in voltage would on the contrary be such as to produce the force needed to tilt the balance against the moment of the stabilizing weights. This force corresponds to curve A, the slope of which is $2\gamma/M_p$. From curves A and B it is possible to compute for any scale reading what the electrostatic force at the corresponding disk height must be to give the scale law experimentally observed. This force is plotted in curve C, the force at the coplanar position being taken as unity. If the quantity $1-fh$ as calculated from eq 52 is subtracted

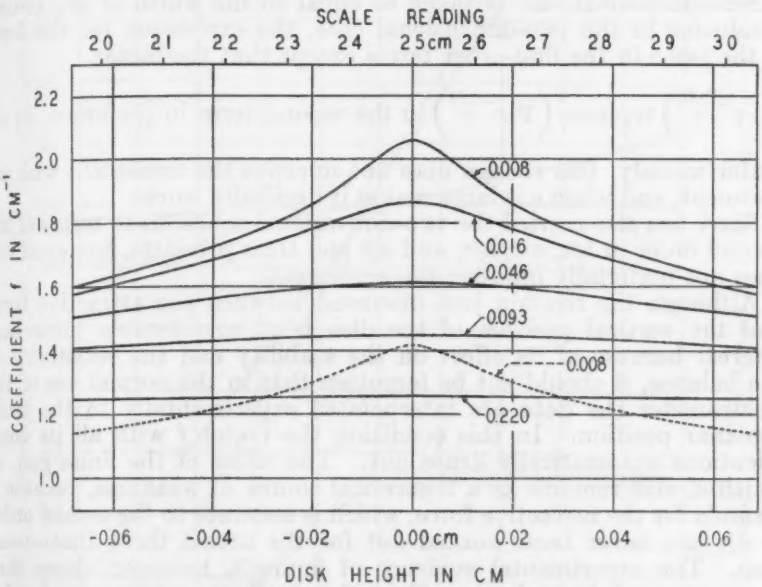

FIGURE 25.—*Graphs showing computed values of the coefficient f as a function of the height h of the disk relative to the plane of the guard ring.*

Solid-line curves are for 10-cm disk with different values of the width of gap (a in cm) indicated on each curve. The dotted-line curve is for a 16-cm disk having the same gap width (0.008 cm) as the uppermost curve. Spacing c=6 cm for all curves.

from curve C, the residuals are as shown in curve D. It is to be noted that because of the quadratic relation between force and voltage, the percentage discrepancies in terms of voltage here plotted to an enlarged scale in curve E are only one-half of the corresponding differences in force shown in curve D. It will be seen that the residual force, not accounted for theoretically, is very small. At the 30-cm point where the disk protrudes 0.0625 cm (six times the gap width) below the edge of the guard ring, the discrepancy is only 0.03 percent of the total force and only 0.4 percent of the actual change in force. At the 20-cm point, where the disk is withdrawn, the discrepancy is greater but the theory still accounts for 96 percent of the observed change in force. For wider separations the discrepancy becomes even less and is roughly inversely proportional to the separation.

The difference between theory and experiment, though very small, is however definitely greater than the precision of the measurements, as is indicated by the close fit of the experimental points to the smooth curve E. There must be, therefore, a real discrepancy and it is probably introduced in the arbitrary process of passing to the actual three-dimensional case from the two-dimensional case to which Snow's mathematical treatment of the field near the edge of the disk applies.

Later (unpublished) work by Snow has yielded a complete solution of another two-dimensional case in which the conductor which simulates the disk is bounded on two sides by infinitely long narrow crevasses which are bounded by the two semi-infinite conductors which simulate the guard ring. If the diameter of the disk in the three-dimensional case is taken as equal to the width of the central conductor in the two-dimensional case, the expression for the force is the same in the first-order terms except that the factor

$\left(1-e^{-\frac{2\pi r_d}{c}}\right)$ replaces $\left(1-e^{-\frac{\pi r_d}{c}}\right)$ in the second term in the brace, eq 50.

Unfortunately, this change does not improve the agreement with experiment, and when c is large makes it decidedly worse.

Snow has also carried the two-dimensional solutions to terms of the second order in h/c, a/c, h/r, and a/r and their products, but even this does not materially improve the agreement.

Although the relation just discussed between the attractive force and the vertical position of the disk is of considerable theoretical interest because of its effect on the stability and the sensitivity of the balance, it should not be forgotten that in the normal use of the electrometer the data are interpolated experimentally to the truly coplanar position. In this condition the factor f with all its complications automatically drops out. The effect of the finite gap, of width a, still remains as a theoretical source of weakness, because a formula for the attractive force, which is accurate to the second order in a/r has never been worked out for the actual three-dimensional case. The experimental evidence of figure 8, however, shows that the gaps used have been sufficiently small to make second-order terms in a/r negligible, and it is obvious that the first-order correction which we have used is that applying in the actual three-dimensional case.

X. CONCLUSIONS AND DISCUSSION

The absolute electrometer here described is intended for the accurate measurement of the effective value of alternating voltages up to 275,000 volts. It will be seen from the foregoing sections that for measurements up to 100,000 volts the accuracy approaches 0.01 percent.

The possibility of using the electrometer to make a new determination of the ratio, v, of the electrostatic to the electromagnetic unit of charge has been considered. For this purpose the spacing could be reduced to 12 cm, at which value the hoops become unnecessary and the voltage gradient can be raised to 5,000 v/cm. Using the 16-cm disk, the attractive force would be 2.2 g. Such a force could be weighed with sufficient accuracy if the optical magnification between the beam mirror and the scale were somewhat increased. It is

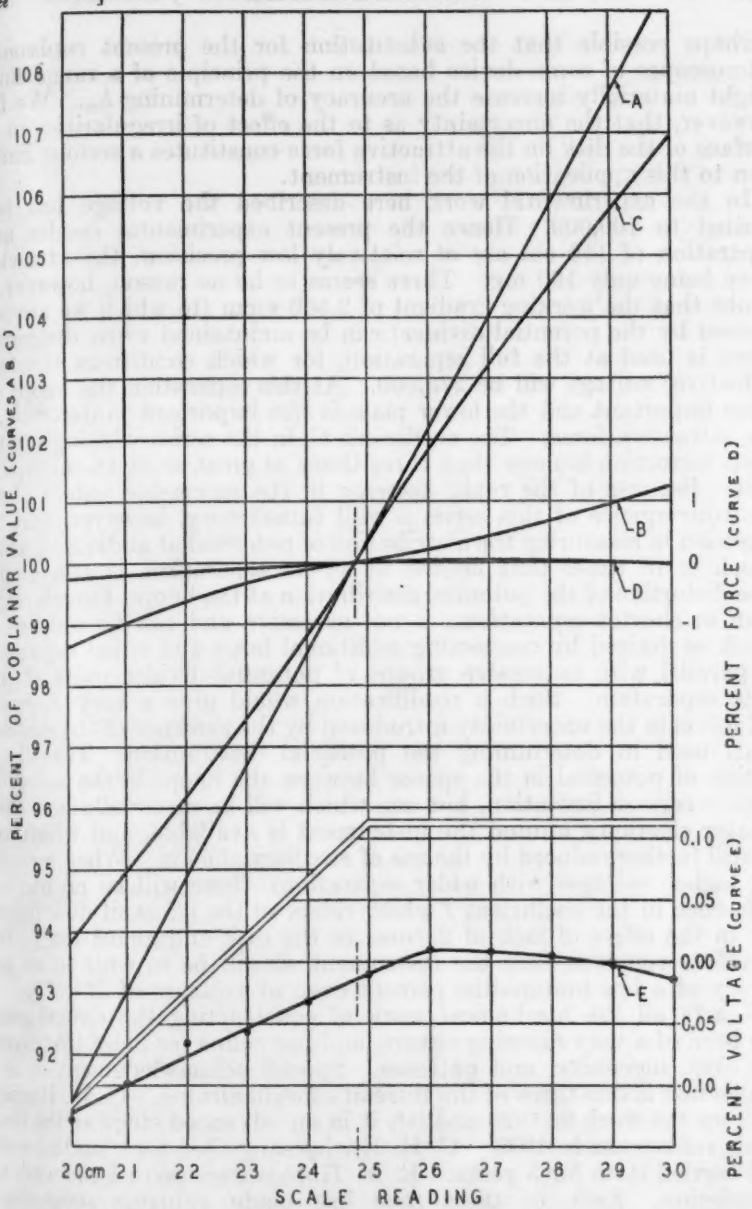

FIGURE 26.—*Comparison of theoretical with experimental scale law for a 16-cm disk at 12-cm separation.*

Abscissas are scale readings of the electrometer in centimeters and correspond to vertical displacements of the disk (protruding at 30 and receding at 20 cm) from the coplanar position indicated by the dot-dash line. The ordinates of each curve are expressed as a percentage of the ordinate at the coplanar position. Ordinates of curve *A* give the attractive force on the disk necessary to balance the resultant mechanical forces. For any given position of the disk this force is theoretically proportional to the square of the voltage. Ordinates of curve *B* show for all positions on the scale the voltage experimentally found necessary for balance. Ordinates of curve *C* were obtained by dividing the ordinates of curve *A* by the square of the ordinates of curve *B*. Ordinates of curve *D* were obtained by subtracting from the experimental curve *C* the theoretical values of $(1-fh)$ calculated from eq 50. The residual curve *D* has been replotted in curve *E* to a much larger scale and in terms of voltage rather than of force. The fit of the individual points on this curve gives an indication of the high precision of the experimental results.

perhaps possible that the substitution for the present coplanarity microscopes of some device based on the principle of a range finder might materially increase the accuracy of determining h_m. We feel, however, that the uncertainty as to the effect of irregularities in the surface of the disk on the attractive force constitutes a serious limitation to this application of the instrument.

In the experimental work here described the voltage has been limited to 100,000. Hence the present experimental results at a separation of 110 cm are of relatively low precision, the attractive force being only 100 mg. There seems to be no reason, however, to doubt that the working gradient of 2,500 v/cm (to which we are now limited by the potential divider) can be maintained when the instrument is used at the full separation, for which conditions the total (effective) voltage will be 275,000. At this separation the hoops are more important and the lower plate is less important in determining the attractive force. The coefficient C_1 in the series which gives the hoop correction is more than three times as great as at 48-cm separation. Because of the rapid decrease in the successive values of G_s, the convergence of this series is still satisfactory, however, and the precision in measuring the distribution of potential at audio frequency, which is 10 times that needed at 48-cm separation, is still ample. The distortion of the potential distribution at the hoops, though larger than at shorter separations, is not excessive and can be reduced as much as desired by connecting additional large and equal capacitors in parallel with successive groups of potential-divider units at this wide separation. Such a modification would give a very desirable reduction in the uncertainty introduced by the presence of the shielded leads used in determining the potential distribution. The distribution of potential in the spaces between the hoops is the source of a more serious limitation, but one which will be materially less when greater clearance around the instrument is available, and which can be still further reduced by the use of auxiliary shields. When measuring higher voltages with wider separations, there will be no marked difference in the coefficient f which refers to the effect of disk height nor in the effect of lack of flatness in the disk and guard ring. We therefore conclude that the instrument should be capable of an accuracy of a few hundredths percent even at voltages of 275,000.

Nearly all the mechanical work of constructing the electrometer has been of a very exacting nature, and has called for more than average skill, ingenuity, and patience. Special acknowledgment in this connection is due three of the Bureau's mechanicians. C. W. Buckey took up the work in 1923 and left it in an advanced stage at the time of his retirement in 1930. C. H. Hochgesang then took up the work and carried it on for 3 years. E. A. Tibbals then carried the work to completion. Each of these men has made valuable suggestions relating to the design of important details.

The authors also express their appreciation of the hearty cooperation of the U. S. Naval Gun Factory authorities, and in particular of the personal attention given by Messrs. Crown of the foundry, Strauss and Fawcett of the metallurgical laboratory, and Murray of the torpedo tube shop.

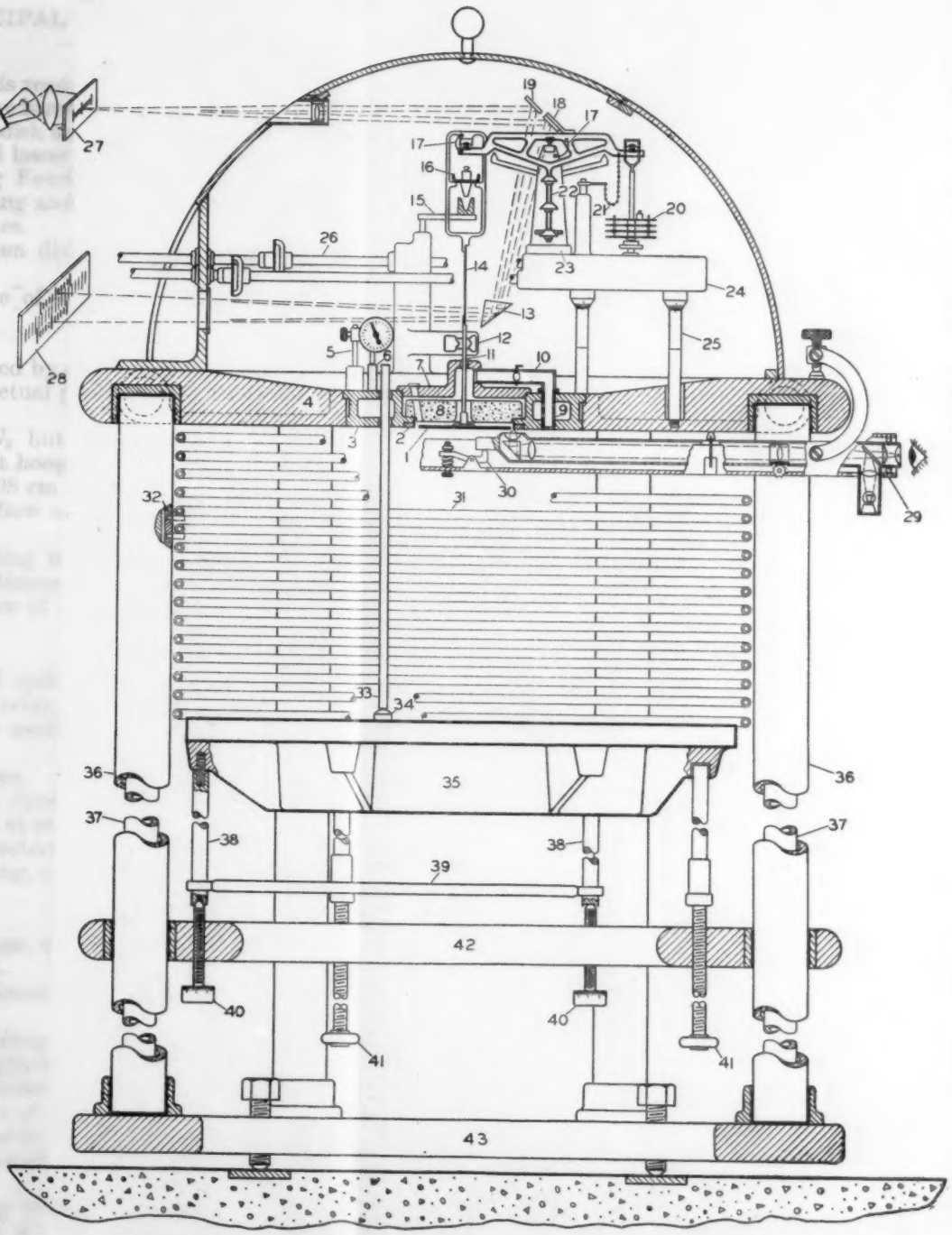

1. Disk.
2. Stainless-steel insert.
3. Bushing.
4. Upper plate.
5. Surface gage.
6. Gage block.
7. Cover above disk.
8. Balsa-wood filter.
9. Perforated ping in gage hole.
10. Air duct.
11. Disk stem.
12. Stem clamp.
13. Prism.*
14. Suspension strip.
15. Weight lifter.
16. Weight pan.
17. Gold ligaments.
18. Beam mirror.
19. Fiducial mirror.
20. Counterpoise.
21. Chainomatic chain.
22. Stabilizing rod.
23. Balance column.
24. Balance base.
25. Balance-base legs.
26. Control rods.*
27. Vernier reticle.*
28. Ground-glass electrometer scale.*
29. Coplanarity microscope and mounting.
30. Pin guiding microscope objective.
31. Guard hoops.
32. Maple pegs.
33. Gage rod.
34. Segmental gage block.
35. Lower plate.
36. Silica pillars.
37. Micarta inner pillars.
38. Invar rods.
39. Aluminum cross brace.
40. Micrometer screws.
41. Jackscrews.
42. Intermediate ring.
43. Base.

* In the actual instrument prism (13) is at 90° from the position here drawn so that the reflected rays to the scale (28) are at right angles to the plane of the figure. The path of the incoming beam of light and the location of the control rods (26) are also different from those shown.

FIGURE 27.—*Schematic cross section of electrometer and accessory equipment.*

44637—38 (Face D. 314)

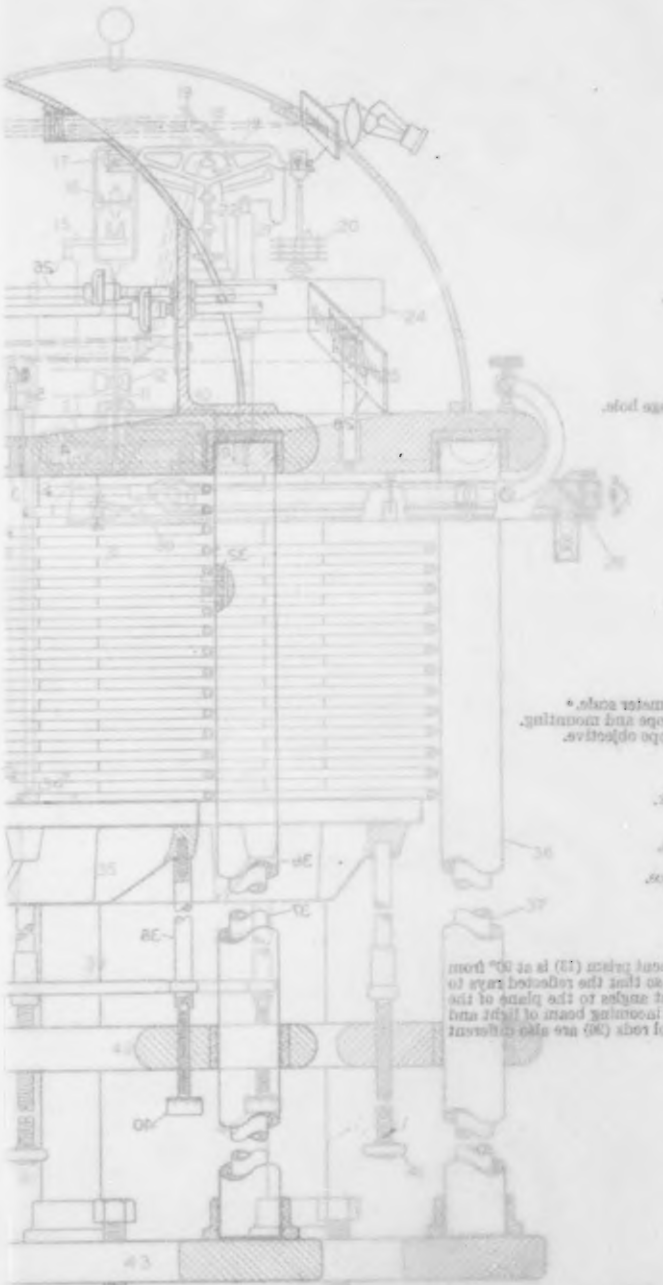

XI. LIST OF PRINCIPAL SYMBOLS

A=area of disk.
A_0=air force on disk when zero is read, dynes.
A_v=air force on disk when voltage is measured, dynes.
a=radial width of gap between disk and guard ring, centimeters.
b=separation between disk and lower plate, centimeters.
C_k=attenuation factor affecting Fourier coefficient of order k.
c=separation between guard ring and lower plate, centimeters.
F=attractive force on disk, dynes.
F_0=attractive force on disk when disk and guard ring are coplanar, dynes.
f=coefficient indicating change of force with height of disk, cm^{-1}.
f_0=value of f when $h=0$, cm^{-1}.
G_k=kth Fourier coefficient, defined by eq 14, in the series describing the departure of the actual potential distribution from the ideal linear one.
G_k'=coefficient approximating G_k but derived by eq 17 from potential measurements at hoops only.
g=acceleration of gravity, 980.08 cm sec^{-2}.
h=height, $(b-c)$, of lower surface of the disk above that of guard ring, centimeters.
h_m=value of h when scale reading is S_m, and the coplanarity microscopes are used, centimeters.
h_d=mean height of active surface of disk above the mean level of its rim, centimeters.
$i=\sqrt{-1}$.
L=equivalent pointer length of optical system, centimeters.
l_0, l_d, l_t=effective lengths of balance arms, centimeters.
M_r=mass of removable weights used on disk arm of balance, grams.
n=number of intermediate hoops.
P=effective stiffness of balance, dyne-centimeters per radian.
q=magnification of disk motion at scale, $=L/l_d$.
R=radius of guard hoops, centimeters.
r_b=radius of aperture in guard ring, centimeters.
r_d=radius of disk, centimeters.
r_m=mean of r_b and r_d.
r_h=radius of cross section of hoops, centimeters.
S=reading on scale, centimeters.
S_m=reading on scale when coplanarity microscopes are being used to determine h_m.
S_0=zero scale reading with no voltage applied, centimeters.
S_v=scale reading with voltage applied, centimeters.
s=spacing of hoops, center-to-center, centimeters.
V=potential with respect to that of the lower plate.
V_s=voltage applied to electrometer in electrostatic cgs units.
V_w=voltage applied to electrometer in electromagnetic volts (i. e., 10^8 cgs units).
V_m=voltage of mth hoop counting from the bottom.
v=ratio of the electrostatic unit to the electromagnetic volt,= 299.805.

y=height above lower plate, centimeters.
γ=stability coefficient, g cm^{-1}.
Δ_2=second-order correction defined by eq 44.
ϵ=dielectric constant of the air within the electrometer.
σ=electric-charge density, electrostatic units.
ϕ_1=correction determined experimentally for effect of disk shape.
ϕ_2=correction determined experimentally for field distortion between hoops.
ϕ_3=a function defined by eq 54.

WASHINGTON, November 4, 1937.

U. S. Department of Commerce National Bureau of Standards

RESEARCH PAPER RP1079

Part of Journal of Research of the National Bureau of Standards, Volume 20, March 1938

A TRANSFORMER METHOD FOR MEASURING HIGH ALTERNATING VOLTAGES AND ITS COMPARISON WITH AN ABSOLUTE ELECTROMETER

By Francis B. Silsbee and Francis M. Defandorf

ABSTRACT

Two entirely distinct methods available at the National Bureau of Standards for the measurement of the effective value of alternating voltages in the range from 10,000 to 100,000 volts are described. A comparison of these methods over a wide range of conditions involving 64 independent determinations has shown them to agree within 0.02 percent.

CONTENTS

	Page
I. Introduction	317
II. Electromagnetic method	318
III. Electrostatic method	329
IV. Results of comparisons	334
V. Conclusion	336

I. INTRODUCTION

Electrical measurements are universally made in terms of the practical electromagnetic system of units, including even the rare, though sometimes important, cases in which electrostatic instruments are used. The values of electrical units are maintained with high accuracy at the several national standardizing laboratories by means of standard cells and wire coils of 1-ohm resistance. In any type of measurement the attainable accuracy tends to become less as the magnitude of the quantity measured becomes very much larger or smaller than that of the quantity embodied in the primary standard. This decrease in accuracy may be more marked in some types of quantity than in others, and may be expected to be large when the nature of the quantity requires the use of radically different types of measuring apparatus in different ranges.

An example of this situation is found in the measurement of high alternating voltages, for the growth of engineering enterprise has brought a demand for the accurate measurement of voltages at least 300,000 times that of a standard cell. The inherent limitations of available insulating media, particularly the atmosphere, and other factors, have led to the use of a number of different types of measuring apparatus to cover different parts of this total range. In view of this situation it seemed desirable that some national laboratory should develop an alternative method of measurement, which should be simple and direct and at the same time as different as possible from

the conventional methods of the electrical engineer; and should compare the values obtained when the same voltage is measured by both methods. Any major discrepancy between the results would then be an indication of the probable existence of hitherto unrecognized errors in the conventional stepping-up method; and conversely a satisfactory agreement would add material assurance of freedom from such errors and cement a solid foundation for the future extension of the range of measurement along whichever line appeared to be the more feasible.

The alternative method selected as being applicable in the range from 10,000 to 275,000 volts and as giving promise of having adequate accuracy, was the use of the Brooks absolute attracted-disk electrometer. A brief discussion of this type of instrument is given in section IV (p. 329), and a more detailed account of its construction, operation, possibilities, and limitations will be found elsewhere.[1] Its advantage for the present purpose lies in the fact that it is completely different from the usual methods of measurement. The major differences are as follows: The full potential is applied directly to the instrument; its indications are primarily in absolute electrostatic units; and the transfer between alternating and direct quantities occurs in an electrostatic instead of in an electrodynamic system. The purpose of this paper is to describe the electromagnetic and electrostatic methods briefly and to state the results of the intercomparison of the two methods which has been carried up to 100,000 volts. Because some features of the electromagnetic process of measurement as regularly applied at this Bureau have not been published hitherto, this part of the procedure is described in somewhat more detail than is the electrostatic part, which has already been described.

In this work the two measuring equipments were supplied by the voltage developed at the secondary terminals of a 10-kva, 25-cycle, 400:1, oil-insulated, self-cooled, step-up transformer (designated as "10–B"). The primary of this transformer was supplied at about 250 volts, 60 cycles, from two line terminals of a 60-cycle, 3-phase, star-connected, 6-pole, 15-kva, revolving-field alternator, which, in turn, was driven by a direct-connected 30 hp, 230-volt d-c motor. The motor was supplied by a 48-ampere, 240-volt storage battery, and another similar battery supplied the alternator field circuits. By frequent attention to the brushes of both machines, the fluctuations in voltage could usually be kept within a few parts in 10,000, although abrupt changes of ten times this amount were occasionally noted. These fluctuations in voltage constitute the main limitation on the precision with which voltage measurements can be made by the electromagnetic method, and were of at least equal importance with the disturbances caused by air currents, which were a principal cause of uncertainty in the case of the electrometer measurements.

II. ELECTROMAGNETIC METHOD

Figure 1 shows the circuits used in the electromagnetic measuring process. The primary winding P of the voltage transformer T was connected directly across the terminals at which the voltage V_x to be measured was developed. The secondary voltage (about 120 volts)

[1] Herbert B. Brooks, Francis M. Defandorf, and Francis B. Silsbee. *An absolute electrometer for the measurement of high alternating voltages*, J. Research NBS **20**, 253 (1938) RP 1078.

of transformer T was applied to and measured by the special electrodynamic voltmeter Z of the suppressed-zero type, the series resistor of which is shown at R. This voltmeter in turn was calibrated at frequent intervals by comparing it by means of a specialized form of potentiometer D-S with a saturated standard cell C. This cell in turn was compared once a week with the reference group of standard cells maintained at this Bureau. The auxiliary current for the potentiometer circuit was supplied by the 200-volt battery B.

In most of the measurements reported herein the step-down transformer, indicated at T, figure 1, was a 25-cycle, 10-kva transformer designated as "10–A". Its primary winding was in 4 sections which

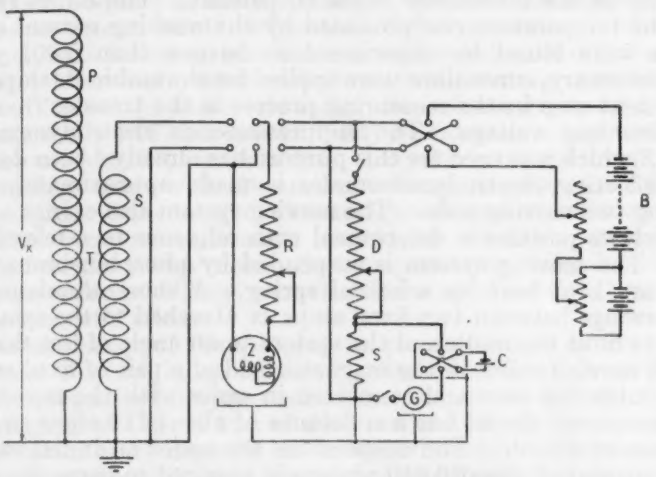

FIGURE 1.—*Circuits used in electromagnetic measurement.*

The primary P of the step-down transformer T is connected to the unknown voltage V_x. The secondary S supplies the reflecting electrodynamic voltmeter Z which has a series resistor R. This voltmeter is calibrated at frequent intervals using direct current from the battery B. The voltage then applied to the instrument is measured by the resistance voltage-divider D-S in terms of the electromotive force of the standard cell C.

by suitable series or parallel groupings gave voltage ratings of 100,000, 50,000, or 25,000 volts. Its secondary winding was in 2 sections and could be connected for ratings of 255 or 127.5 volts.

Studying now, in reverse order, the various steps in the measuring process, we may consider the probable accuracy of each step and the principle on which it is based. The comparison of the standard cell with the reference group can easily be made to 0.0001 percent. The cell was kept in a jacketed thermostatically controlled container and showed no changes exceeding 2 parts in 1,000,000 during the 6 months during which comparisons were in progress.

The first stage in the stepping-up process occurs in the potentiometer circuit. The ratio (about 100:1) of the d-c voltage applied to the voltmeter to the electromotive force of the standard cell is dependent upon the ratio of the resistances across which the respective voltages are applied. These resistances were measured at intervals of about 5 months and the accuracy with which the ratio of their values was determined was at least 0.001 percent. No secular drift as great as 0.001 percent was observed. The principle involved in obtaining

the ratio is that the resistance of several coils in series is equal to the sum of their separate resistances. This principle is valid except as imperfect insulation may shunt part of the current around one or more of the series coils. The resistance across which the galvanometer and standard cell were connected was 80 ohms. The total resistance of the potentiometer circuit ranged from 3,000 to 15,700 ohms, according to the voltage to be measured. For precision resistance boxes in this range, leakage errors should be negligible unless the insulation is seriously impaired as by exposure to an atmosphere of high humidity. To avoid this latter condition refrigerating equipment was employed to condense atmospheric moisture and thus to maintain the relative humidity in the laboratory below 60 percent. The errors resulting from the temperature rise produced by the working current of 0.012 ampere were found by experiment to be less than 0.001 percent. When necessary, corrections were applied for the ambient temperature.

The next step in the measuring process is the transfer from direct to alternating voltage. The suppressed-zero electrodynamic voltmeter Z which was used for this purpose has already [2] been described. This reflecting electrodynamometer is made approximately astatic by using two moving coils. The moving system also carries a mirror, by which its position is determined with reference to a telescope and scale. The moving system is suspended by phosphor-bronze strips, which are kept taut by a helical spring. A short aluminum boom which swings between two fixed stops is attached to the spindle and serves to limit the motion of the system to an angle of less than 3°.

Each moving coil is in the magnetic field of a pair of fixed coils also wound with fine wire and connected in series with the moving coils. The instrument circuit has a resistance of about 110 ohms and an inductance of 58 mh. The suspensions are under an initial torsion so that a current of about 0.040 ampere is required to cause the moving system to move away from the stop and deflect to the arbitrary zero point of the scale. A five-dial resistance box is in series with the instrument. The instrument is calibrated by applying a known direct voltage of about the same value as the alternating voltage to be measured and adjusting the series resistance until the instrument deflects to the desired point on the scale. To eliminate any residual effect of the terrestrial magnetic field, the applied voltage is reversed, and a second adjustment of the series resistance is made. The mean of the two values of series resistance is then used. The voltage is a linear function of the scale reading over a narrow range so that by calibration at two points 10 cm apart, an accuracy of 0.002 percent is obtained at intermediate points. The scale distance is 6 m. In the deflection position the axes of the moving coils are at right angles to those of the fixed coils so that the mutual inductance is nearly zero and the torque per unit current is near a maximum.

When an alternating voltage is being measured the series resistance is adjusted to bring the reading between the calibration points.

The effect of the self-inductance of the windings depends upon the value of the series resistance R. It usually amounts to about 0.004 percent and a suitable correction is applied. It is assumed that the construction of the instrument is such that errors from eddy currents, capacitance between the turns and layers of the winding, and residual capacitances shunting the coils of the series resistor are all negligible.

[2] F. K. Harris. *A suppressed-zero electrodynamic voltmeter.* BS J. Research **3**, 445 (1929) RP105.

As a check on the correctness of these assumptions the instrument was compared at frequencies of 600 and 1,200 cycles per second with two portable electrothermic indicating instruments. One of these was of the expanding hot-wire type and the other of the thermocouple type. When used with resistors to give a range from 90 to 150 volts, the net average discrepancy between the suppressed-zero voltmeter and the mean of the electrothermic instruments, after correcting for the self-inductance of the former, was only 0.12 percent at 1,200 cycles per second, and was one-fourth of this amount at 600 cycles per second, confirming the theoretical prediction that the residual frequency errors in the suppressed-zero voltmeter varied directly as the square of the frequency. On this basis these errors at 60 cycles per second would be less than 0.001 percent.

The suppressed-zero instrument was calibrated with direct current before and after each measurement with alternating current. The average difference in these two calibrations for a group of 50 pairs of calibrations is 0.002 percent and may be taken as a measure of the inherent precision of the instrument. In order to obtain this precision in the readings made with alternating voltage, in spite of the fluctuations then present, the mean of 10 readings was used at each determination. The frequent calibration served to eliminate temperature errors and rendered the nickel-wire compensating coils, described in RP105, superfluous. They were therefore removed to obviate any spurious magnetic effects.

The second stage of the stepping-up process occurs in the voltage transformer T which has a maximum nominal ratio of about 784 : 1. This is best separated for purposes of analysis, however, into two component factors of 196 : 1 and of 4 :1, respectively. The accuracy of the first factor rests directly on an experimental calibration of the transformer made while its high-voltage windings were connected in parallel, while that of the second depends primarily on the principle that when a number of windings are connected in series their voltages are additive.

The method used for the experimental calibration of the transformer was that originally suggested by Sharp and Crawford,[3] using the high-voltage shielded resistor and auxiliary circuits as described by Silsbee,[4] and is that regularly employed in testing voltage transformers at the Bureau.

The circuit used in this method is shown in figure 2. When switch T is closed to the left the voltage applied to the primary winding P of the transformer under test is also applied both to the "working" circuit which includes resistors W and R_2 and to the guard circuit connected in parallel with it, which includes resistors W' and R_2'. The voltage at the terminals of the secondary winding S of the transformer under test is opposed to the drop of potential in the adjustable section R_2 of the working circuit. When the vibration galvanometer G_1 indicates a balance, the ratio of the primary voltage to the secondary voltage is equal to the ratio of the total effective a-c resistance of W (together with that of the primary of M) to that of R_2. The mutual inductor M serves to balance any quadrature component of voltage resulting from the phase angle of the transformer.

[3] C. H. Sharp and W. W. Crawford. *Some recent developments in exact alternating-current measurements.* Trans. Am. Inst. Elec. Engrs. **29**, 1517 (1910).
[4] Francis B. Silsbee. *A shielded resistor for voltage transformer testing.* BS Sci. Pap. **20**, 489 (1924-1926) 516.

The shielded resistor is so constructed as to minimize errors from the capacitance currents which might flow from portions of the working resistor to ground. The resistor W (of manganin wound on micanite cards) is divided into 27 sections of about 20,000 ohms (16 cards) each, connected in series. Each section is enclosed in, but insulated from, an oil-filled brass box which serves as a shield which is connected to a tap from the guard circuit W'. Each tap is at a point such that the potential of the shield is the same as that at the midpoint of the resistor section enclosed by it. The capacitance currents flowing from the outer surfaces of the shields to ground flow in the

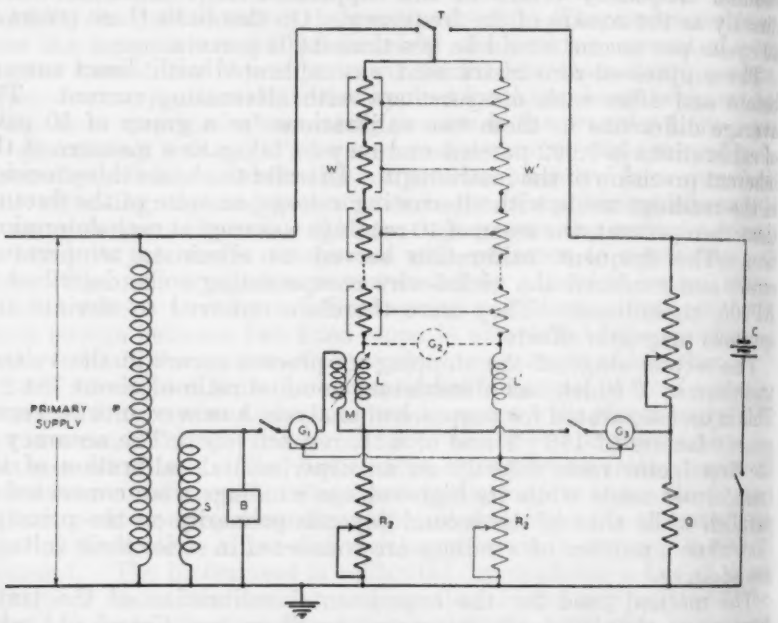

FIGURE 2.—*Circuit used in measuring the ratio and phase angle of voltage transformers.*

The shielded resistor W (in series with L and R_2) is connected in parallel with the primary winding P of the transformer under test. The voltage induced in the secondary winding S of the transformer is opposed to the sum of the voltage drop in the adjustable resistor R_2 and the voltage induced in the secondary of the mutual inductor M. When a balance has been obtained, as indicated by the a-c galvanometer G_1, switch T is thrown to the right and the ratio of W to R_2 is determined by direct current in terms of the known resistances of D and Q, using d-c galvanometer G_3.

guard circuit only and hence can produce only a second-order disturbance in the working circuit.

The capacitance between the parts of each section of the working resistor and its enclosing shield acts as a shunt in parallel with the section. As has been shown elsewhere,[5] the effective resistance and inductance of each section can be measured individually at a convenient voltage and with the shield at the potential of the midpoint of the resistor. This value will remain unchanged when the section is used in series with others, provided only that the potential of each shield remain equal to that of the midpoint of the resistor within it.

Because of the considerable heat developed (3 kw in the combined circuits) and of the resulting changes in temperature and resistance,

[5] See footnote 4.

the ratio of the resistance of W (including that of L) to that of R_2 is measured just after each a-c balance while the circuits are still at their operating temperature. This is readily done with switch T thrown to the right so that W, R_2, and the accurately known resistors D and Q, form a Wheatstone bridge supplied at about 30 volts by the battery C.

From this description of connections and procedure it is evident that the accuracy of the calibration of the step-down transformer depends on (1) the precision of the a-c balance; (2) the accuracy of the d-c bridge measurement; and (3) the accuracy with which the effective resistance which the working circuit of the shielded resistor offers to the alternating current is exactly the same as that which it offers to a much more feeble direct current. By using as the a-c detector a sensitive vibration galvanometer, an easily detectable deflection is developed by a lack of balance of only 0.002 percent. The accuracy of the d-c bridge is at least 0.01 percent. The shielded construction greatly reduces the voltage across possible leakage paths, and measurements with a 1,000-volt d-c source showed that all such leakage was entirely negligible Failure of the working circuit of the shielded resistor to have the same resistance to a large alternating as to a small direct current may arise as a result either of self-heating or of capacitance. The relatively large thermal storage capacity of the oil in which the resistance material is immersed, and the short time which elapses between the cutting off of the alternating supply and the attaining of the d-c balance, insure that the oil temperature is very closely the same for the a-c and the d-c balances. The alternating current of 0.05 ampere heats the resistance wire 3.3° C above the oil with a resulting change in its resistance of about 0.013 percent. However, by auxiliary measurements on a single section at larger currents this heating effect was definitely measured and appropriate corrections are regularly applied, with the result that the uncertainty introduced by temperature into the corrected ratio is less than 0.01 percent.

The possibility of a difference in resistance between direct current and alternating current as a result of capacitance effects may be studied on the basis of the theory of the high-voltage shielded resistor. This theory enables the effective resistance (and inductance) of the complete working circuit to be calculated from measurements made on the sections separately, provided the potentials of the shields are also known. The calculated relationships have been directly checked by experiments using two sections in series, and indirectly by a variety of experiments in which the observed changes in impedance resulting from known changes in the shield potentials were found to agree with the computed changes. The unavoidable capacitance from the shields to ground and the resulting effects on the shield potentials may however introduce a second-order error in the resistance, the magnitude of which can be estimated only roughly.

Because of such second-order effects, the use of a shielded resistor having a resistive [6] guard circuit is not practicable for precise work at voltages above about 30,000. The second-order errors produced by the stray capacitances are proportional to $\omega^2 R_w R_g C_w C_g$ where R_w and C_w are, respectively, the total resistance of the working circuit and the total capacitance between it and the shields, while R_g and C_g are,

[6] By using a set of autotransformers having a rating of 75 kva to supply the shield potentials, Weller (Trans Am. Inst. Elec. Engrs. 48, 790, (1929)) has successfully operated a shielded resistor up to 132,000 volts.

respectively, the total resistance of the guard circuit and the total effective capacitance between the shields and ground. If the voltage range of a shielded resistor is extended by adding more sections, each of the last four factors will increase in proportion to the voltage and the error will increase as the fourth power of the voltage. If the resistances are held constant and the voltage is increased, the resulting increase in heating will require the use of larger cooling surfaces in proportion to the square of the voltage so that the error, proportional to the product $C_w C_g$, is in this case also increased roughly as the fourth power of the voltage. Measurements of C_w and estimates of C_g indicate that in the equipment used, the second-order error may be 0.008 percent. Unfortunately, it is not feasible to measure C_g with sufficient definiteness to enable a correction to be applied. If this indeterminate error increases as the fourth power of the voltage it is evident that it will soon become excessive. The use of a third circuit to guard the guard circuit appears to be impracticably complex. It therefore appears that some different measuring process must be introduced to extend the measurement from the 30,000-volt limit of the shielded resistor to the 100,000-volt limit of transformer 10–A.

The additional measuring process which we have used is an application to the case of high-voltage step-down transformers of what may for brevity be called the "series-parallel principle." This well-known principle [7] is that an instrument transformer, the primary winding of which consists of a number of substantially equal sections, has the same ratio correction factor (i. e., quotient of true ratio divided by nominal ratio) and the same phase angle when used with any of the possible series or parallel groupings of these primary sections.

The measuring process therefore consists in using the shielded resistor to determine the ratio of transformer 10–A at voltages up to 30,000 with the four sections of its primary winding connected in parallel and then subsequently using the transformer with these sections connected in series. By the series-parallel principle, its ratio should then be exactly four times that under the former condition. Departures from this ideal factor of 4 may conceivably result from either of two causes: (1) Magnetic inequalities in the sections of the primary winding, and (2) currents flowing through the electrostatic capacitance which exists between various sections of the windings, and between the sections and the case.

For the first of these causes to be effective the mutual inductances between the secondary winding and the several primary sections must be different and also the exciting current must distribute unequally among the primary sections when they are connected in parallel. In any well designed transformer in which the same number of turns is used in each high-voltage winding, both of these disturbing conditions are necessarily extremely small; and the change in ratio correction factor with change in connections, depending as it does on the product of these two types of dissymmetry, will be of a still higher order of magnitude, vanishing if either of its two factors is zero. In the particular core-type transformer used (10–A) each of the two legs is encircled by four high-voltage coils placed end to end. Each of the four 25,000-volt sections of the primary winding consists of an end coil on one leg and an inner coil on the other leg. Each of the two

[7] This principle has also proved of great value in extending the range of current transformers. See BS J. Research 11, 98 (1933) RP580.

127.5-volt sections of the secondary winding consists of 38 turns on one leg and 37 turns on the other leg. The 38-turn coils are adjacent to and cover nearly the full length of the leg and the 37-turn coils are wound immediately over them.

The close magnetic equality of the primary sections is shown by the fact that the successive ratios observed when each section was used alone as a primary differed from their mean by less than 0.02 percent, and that the leakage impedances observed with the secondary short-circuited and each primary section in turn used alone as a primary, differed from their mean by less than 0.12 percent or 10 ohms in 8,900. These results show that this arrangement of coils gives an exceedingly close equalization of the magnetic effects of the several sections, but perhaps at the cost of somewhat increased capacitance effects.

The system of currents flowing in the various capacitances which exist both between the sections of the primary winding and between the primary winding and the secondary winding and ground is so complex that its effect on the ratio cannot be accurately evaluated, but rough approximations can be arrived at both by theoretical and by experimental methods. The total capacitance in the windings bushings, etc., of the particular transformer (10–A) used in this work, is so large that the leading current drawn by it more than offsets the lagging current required to magnetize the core, with the result that the no-load current of the transformer at 60 cycles per second leads the applied voltage. When the transformer is used, with its high-voltage winding as the secondary, the ratio is very materially affected by this leading current. At first sight, therefore, it might well be expected that such capacitance currents would have a very considerable effect on the step-down ratio of the transformer also. It appears, however, both from theory and from experiment that in this latter case such effects of capacitance on ratio are in reality surprisingly small. As a first step in considering the possible effects of capacitance on a step-down transformer it may be noted that: (1) A capacitance (as that of a bushing) which shunts the entire primary winding will have no effect on the ratio; (2) a capacitance which is connected between the midpoint and either terminal of the primary winding will have no effect on the ratio; (3) a capacitance which shunts more than half of the primary winding will have an effect which is greater than, and opposite in sign to, that of an equal capacitance which shunts less than half of the winding (hence the small capacitances spanning large sections tend to compensate for the effect of the larger capacitances between adjacent turns and layers); and (4) capacitance shunting any part of the primary winding will affect the ratio and phase angle only to the extent that the various parts of the primary winding are not sufficiently closely coupled to form an autotransformer of perfect (zero) regulation.

By making a number of simplifying assumptions the change ΔN in the ratio of a step-down transformer, produced by an assumed small capacitance C shunting a particular portion of the primary winding, can be estimated as $\Delta N=(1-\alpha)q\omega^2CL_1$, where α is the coefficient of coupling between the section of the primary winding which is shunted and the remainder of it, and L_1 is the total (open-circuit) self-inductance of the primary. The numerical coefficient q depends on what

fraction of the winding is assumed to be shunted and on the location of this particular fraction, and has as a maximum the value 0.09.

Measurements by the charge and discharge method indicated that the capacitance between the entire high-voltage winding and ground was about 1,700 $\mu\mu$f, and that the capacitance between the sides of adjacent sections was about 150 $\mu\mu$f. The coefficient of coupling ($\alpha=M/(L_1L_2)^{1/2}$) between the primary and the secondary windings departs from unity by only 0.0014 and the coupling between sections of the primary is presumably considerably closer than this.

Inserting these values into the expression for the change in ratio gives as an upper limit for the effect of shunting capacitance at 60 cycles per second the value 0.06 percent. Not only is this value very small compared to what might have been expected, but also it should be nearly independent of the flux density, and hence, for any one connection, independent of the voltage at which the transformer is operating. This follows because the factor $(1-\alpha)$, which is in effect the ratio of the leakage flux in the air space between the coils to the mutual flux in the iron core, varies inversely with the permeability, while the primary inductance L_1 is roughly proportional to the permeability.

Transformer 10–A is provided with two sections of low-voltage winding, which can be connected in series or in parallel to give rated secondary voltages of 255 or of 127.5 volts, respectively. By reason of the capacitance existing between the primary and the secondary windings there is, in normal operation, a certain capacitance current (of the order of 10 ma) flowing through portions, at least, of the secondary winding and returning to the primary circuit through the ground connections of the two circuits. This current affects the secondary terminal voltage by a few thousandths percent so that in general each of the six different combinations of connections of the primary and secondary windings yields a slightly different ratio correction factor.

The small magnitude of the capacitance effects predicted theoretically, led to the development of the following experimental procedure for extending the range of measurement by the step-down transformer beyond the limit set by the shielded resistor. The transformer is first tested with its four primary sections in parallel, using the shielded resistor up to its limit of 30,000 volts, which thus covers the full range of the transformer (up to 150 volts) with the secondary sections in parallel. These results may be plotted as in curve *AB* in the insert of figure 3 in which the ordinates are ratio correction factor (i. e., true ratio divided by nominal ratio) and the abscissas are secondary voltage (per coil). The primary sections are then connected in series-parallel and again tested up to the 30,000-volt limit of the resistor, which now corresponds to only 75 volts per coil on the secondary. These results will yield a curve such as *CD*. The primary connections are now changed to the series arrangement and again tested up to the 30,000-volt limit, which, in this case, corresponds to only 37.5 volts per coil on the secondary. These data will give a curve such as *EF*. For any given abscissa the flux density in the core is the same for all three curves and the difference in the ordinates is the result of capacitance currents. As mentioned above, it is to be expected that the differences in ratio correction factor will be nearly independent of voltage, and on this basis the upper curves may be extended at a constant distance above the lower as indicated by the dotted lines,

and the ratio correction factor at 60,000 volts may be taken as that given by point *G* and that at 120,000 volts as that given by point *H*.

When the experimental process just outlined is performed on transformer 10–A, results such as those plotted along the curve *KL* in figure 3 are obtained. Here, to avoid confusion, points for only three of the six possible combinations of connections have been included and a curve has been drawn only for the parallel-parallel connection. The striking feature of these data is that the differences in ratio correction factor between the several connections are exceedingly small and only slightly exceed the precision of the measurements. In other words, the performance of the transformer is almost independent of capacitance effects. Similar measurements on a large number of other voltage transformers (usually of somewhat lower

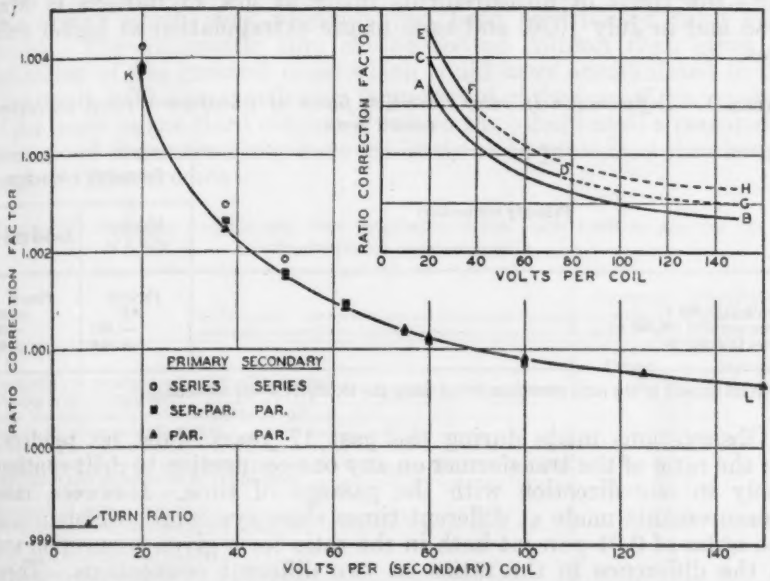

FIGURE 3.—*Ratio correction factor as a function of secondary voltage.*

Ordinates are the quotient obtained by dividing the true ratio of the transformer by the nominal ratio. Points shown by different symbols correspond to different connections of the primary or secondary windings as indicated. Insert shows the same variables plotted to an arbitrary scale in exaggerated form to illustrate the effects of capacitance and the process of "guided extrapolation."

range) have always shown only very small differences in ratio correction factor and phase angle when the primary windings were changed from parallel to series connection, and it appears that this process has very valuable possibilities as a means for extending the range of precision measurements at high voltages.

As a further confirmation experiments were carried out at 60 cycles with an additional capacitance of 1,900 $\mu\mu$f intentionally connected between the ¾ point and ground, and also, as a confirmation of the theory, between the ½ point and ground, on the primary of 10–A. These showed no change, when the capacitance was connected, exceeding the limits set by the sensitivity, which were 0.02 percent in ratio and 0.1 minute in phase angle.

From the foregoing discussion it would appear that the ratio of the transformer on the series connection can be relied upon to nearly the same accuracy as that to which it can be calibrated on the parallel connection.

The slight differences in ratio correction factor when the transformer is operating with different connections but at the same volts per coil and hence at the same flux density, are not as exactly constant as is suggested by the sketch inserted in figure 3 but show a tendency to decrease somewhat with increase in voltage for any one connection. For different connections table 1 lists the best mean values for the differences obtained by subtracting the ratio correction factors of transformer 10–A used in the parallel-parallel connection from those for the other five possible combinations of connections, as estimated from the trend of measurements made at low excitations in May 1935 and in July 1936, and used in the extrapolation at higher voltages.

TABLE 1.—*Differences* [a] *in ratio correction factor of transformer 10–A on various connections*

Primary connection	Secondary connection	
	Parallel (127.5 v)	Series (255 v)
	Percent	*Percent*
Parallel (25,000 v)	[a] 0	+0.003
Series-parallel (50,000 v)	−.005	−.005
Series (100,000 v)	±.000	±.000

[a] With respect to the ratio correction factor using the 25,000/127.5-volt connection.

Observations made during the past 17 years show no tendency for the ratio of the transformer on any one connection to drift continuously in one direction with the passage of time. However, ratio measurements made at different times show systematic differences of the order of 0.01 percent both in the ratio for a given connection and in the difference in the ratios on two different connections. These differences cannot be attributed to known effects of differences in temperature, for the effect of temperature on the resistance of the copper windings is easily computed and found to be negligible, and its effect on the magnetizing current was measured by observing this current at several temperatures and was also found to be negligible.

Tests have also been made before and immediately after the transformer core was magnetized by passing direct current through one winding. These also showed no permanent changes in performance. Nevertheless the differences in rato at different times though very small seem to be systematic and not attributable to the accidental errors of the measurement. Their origin is at present unknown.

In order to minimize the effect of these systematic differences on the comparison reported here, values of transformer ratio have been ·ed which are interpolated between values observed in May 1935 in July 1936, since most of the comparisons with the electro- nethod were made between December 1935 and June 1936.

ltage assigned to the standard cell was of course in terms of tional volt as maintained at the National Bureau of

Standards since 1910. To convert the final result into absolute electromagnetic units it is necessary to multiply the observed value by the ratio of the international volt to the absolute volt. The factor [8] 1.00035 has been taken as giving this ratio with sufficient accuracy for the present purpose.

While the accuracy of each step in the measuring process just outlined is fairly high, the great number of steps involved gives rise to the possibility of a considerable error resulting from the cumulative effect of many small ones. To summarize the situation there is given in the first column of table 2 a list of the various sources of error and in the second column an estimate of the maximum error which each source might have introduced under unusually bad conditions or by reason of unrecognized systematic errors. In the third column is given a less pessimistic estimate of the uncertainty (estimated probable error) which very probably has been contributed from each source. The arithmetic sum of the second column then gives an indication of the greatest error which could have accumulated in the final result. The geometric sum (square root of the sum of the squares) of the items in the third column gives, on the other hand, a reasonable estimate of the uncertainty believed likely to be present in the electromagnetic measurement.

TABLE 2.—*Probable uncertainty and maximum error from various sources in the electromagnetic measurements*

	Maximum error	Probable uncertainty
	Percent	*Percent*
Comparison of standard cell with reference cells	0.002	<0.001
Changes in cell during use	.020	.002
Ratio of resistances in potentiometer circuit	.010	.001
Leakage shunting potentiometer	.010	.001
Self-heating of potentiometer [a]	.002	.001
Reading error, of d-c galvanometer	.002	.001
Inductance and capacitance of voltmeter [a]	.005	.001
Reading error of voltmeter	.010	.002
Temperature drift of voltmeter	.005	.001
Balancing error on alternating current	.002	.001
D-c measurement of shielded resistor	.010	.005
Temperature of shielded resistor [a]	.010	.002
Capacitance of shielded resistor [a]	.010	.002
Magnetic inequalities in transformer	.002	<.001
Capacitance of transformer [a]	.020	.010
Secular drift of transformer since test [a]	.020	.005
Arithmetic sum	0.140	
Square root of sum of squares		0.013

[a] Values given are estimated possible residuals not accounted for by the correction normally applied for this effect.

III. ELECTROSTATIC METHOD

The absolute attracted-disk electrometer used in these measurements is shown in figure 4 and a schematic cross section is given in figure 5. The hemispherical metal "dome" E at the top of the instrument encloses a sensitive balance D which serves to measure the force of attraction between the movable aluminum disk A, which hangs from one of its arms, and the lower plate B of the electrometer. The disk hangs with a small clearance (0.01 cm) in a central opening in the large upper plate C which carries the dome, and which serves as a

[8] This factor also includes the ratio, as determined in 1937, of the international volt as maintained at the National Bureau of Standards to the mean international volt.

guard ring to minimize the concentration of charge at the periphery of the disk. Suitable bushings adapt the opening in the guard ring to suit the diameter of the disk used. At the wide spacings (110 cm) needed for an applied potential difference of 275,000 volts for which the electrometer is designed, the diameters (100 cm) of the upper and of the lower plate would not be sufficient to prevent an appreciable bulging of the lines of force and a corresponding distortion of the electric field at the disk. To obviate this effect and to approximate the ideal uniform electric field throughout the region between the plates without having recourse to plates of excessive diameter (i. e., 6 m), a series of guard hoops H are placed as seen in figure 4 at equal intervals (2 cm center-to-center) between the planes of the two plates. These hoops are supported mechanically by pins inserted in three of the six fused-silica pillars which support the upper plate. The hoops are connected electrically to suitable equally spaced taps on a potential divider G. This divider consists of a stack of equal micanite capacitors which are connected in series with each other, the whole stack being in parallel with the electrometer. With this construction the electric field just inside the guard hoops is very nearly vertical and uniform, except for slight ripples caused by the finite thickness and spacing of the hoops. The ripples become inappreciable a short distance in from the hoops.

A mirror fixed to the balance beam reflects the image of a vernier scale on to a ground-glass scale located at the control station about 2.5 m away from the electrometer, and serves to indicate the position of the beam and of the disk.

A measurement of voltage with this electrometer involves two operations. First, with no voltage applied but with a known mass M_r resting on the pan on the disk arm of the balance, the zero reading S_0 is observed. Second, by suitable manipulation of insulating control rods the disk stem is clamped, the mass M_r is removed, voltage is applied, and the stem is released. A second reading S_v is then taken, the voltage being adjusted to make the two readings nearly equal. The effective value of the applied voltage is then obtained in absolute electromagnetic volts by the following working formula:

$$V_m=\frac{4v\sqrt{2M_rg(c+h_d)}}{(r_b+r_d)}\left[1+\frac{A_v-A_o}{2M_rg}+\frac{\gamma(S_v-S_0)}{M_r}-\frac{f(S_v-S_m)}{2q}+\frac{fh_m}{2}\right.$$

$$\left.-\sum_{k=1}^{k=\infty}C_kG_k'-\frac{(\epsilon-1)}{2}+\phi_1(h_d/r_d)+\phi_2(s/r_b)\right] \quad (1)$$

Taking up in succession the various quantities appearing in this working eq 1, v is the ratio of the cgs electrostatic to the absolute practical electromagnetic unit of voltage. The work of Rosa and Dorsey [9] on this ratio gave a value 299.71 in terms of the international ohm as realized at the National Bureau of Standards in 1907. We have, however, used for v the value 299.805, which embodies a correction of their data for the effect of moisture in the air on the same basis as that used in the present work, and a correction for an adjustment, made subsequent to their publication, in the value of the ohm

[9] E. B. Rosa and N. E. Dorsey. *A new determination of the ratio of the electromagnetic to the electrostatic unit of electricity.* Bul. BS **3**, 533 (1907) S65.

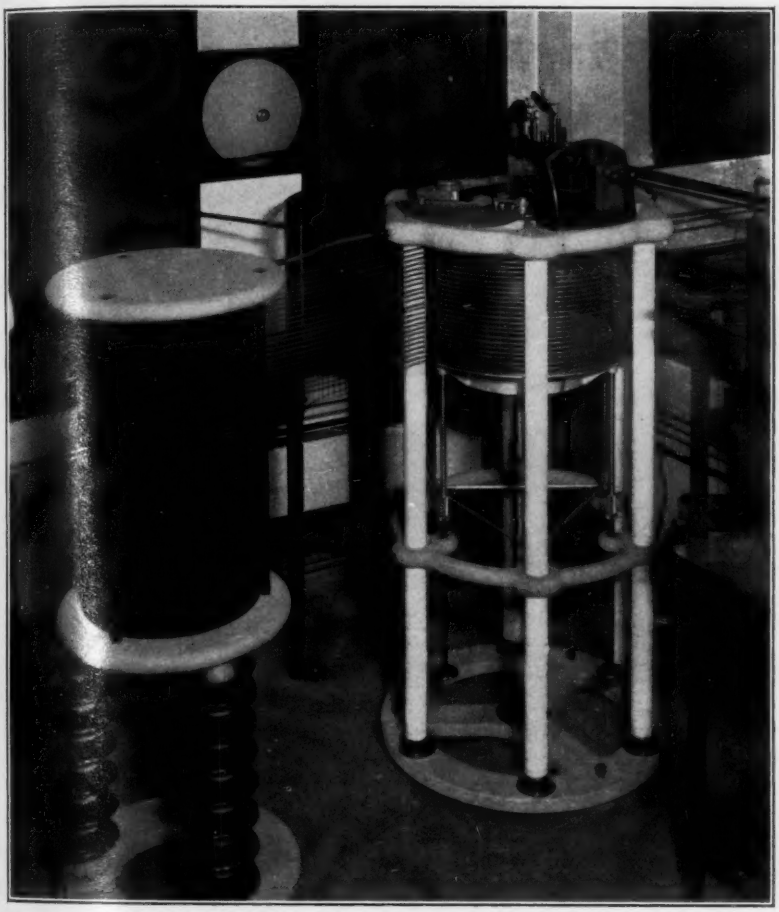

FIGURE 4.—*Brooks absolute electrometer.*

The electrometer proper is at the right; the balance mechanism visible above the upper plate is normally enclosed by a hemispherical metal cover. The capacitance potential divider is at the left.

as maintained at the Bureau, as well as for the ratio of the international ohm to the absolute ohm. For this latter ratio we have used 1.00048, which seems to be the best value from recent determinations.

The weight $M_r g$ of the mass removed from the disk arm when voltage was applied could be readily determined with ample accuracy (approaching 0.001 percent). The constant [10] of gravity g was taken as 980.08 cm/sec^2 and is probably accurate to 0.001 percent.

The separation c, as measured between the edge of the opening in the guard ring and the surface of the lower plate, is corrected by the

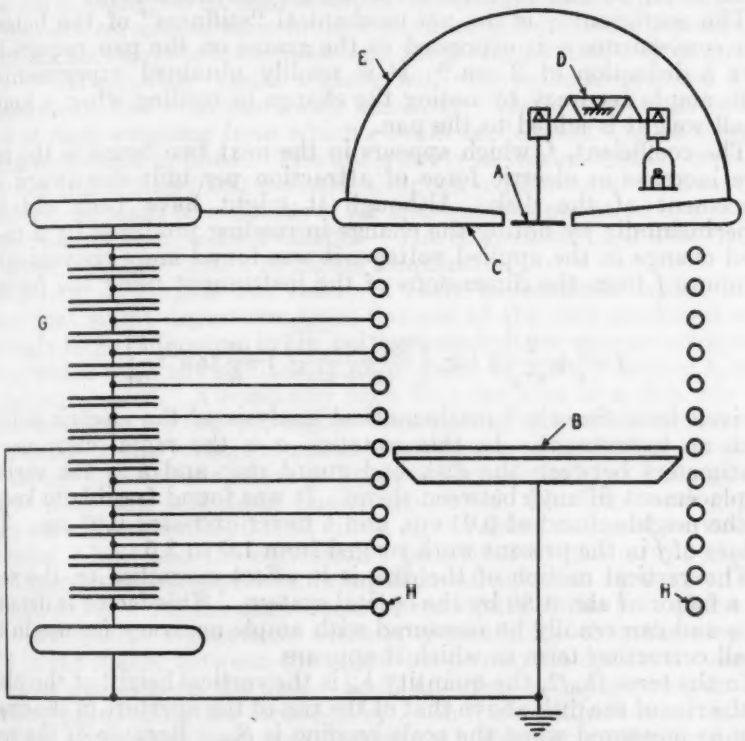

FIGURE 5.—*Schematic cross section of Brooks absolute electrometer.*

The attracted disk at *A* is suspended with its lower surface in the same plane as that of the guard ring *C* which is at the same potential. The electrostatic attraction is measured by the sensitive balance *D*. The horizontal hoops are each connected to a tap from the capacitance potential divider *G*. The two cross sections of each hoop appear as circles as at H–H. The capacitor units and hoops below the particular location at which the lower plate is used for a given voltage are short-circuited and grounded.

small difference h_d, which, as a first approximation, allows for the measured bulging upward of the average surface of the attracted disk above its rim.

The radii r_b and r_d of the aperture in the guard ring and of the disk, respectively, were measured to ± 0.0002 cm and were corrected by 0.0017 percent per degree C when the electrometer was used at temperatures other than that at which the radii were measured.

[10] Paul R. Heyl and Guy S. Cook. *The value of gravity at Washington.* J. Research NBS 17, 805 (1936) RP946.

Of the correction terms inside the brackets in the working eq 1, A_1 and A_0 symbolize the force (in dynes) exerted on the disk by air currents at the time the two readings with voltage on and with voltage off were made. These forces probably constitute the principal limitation on the accuracy of the instrument. Since they cannot be measured and allowed for, the standard procedure is to take a second zero reading immediately after the voltage had been removed. If the zero readings show that the air conditions are substantially constant, it is assumed that the mean of the values of A_0 before and after the run is equal to A_2, so that the term involving air currents is zero.

The coefficient γ is the net mechanical "stiffness" of the balance. For convenience γ is expressed as the grams on the pan required to give a deflection of 2 cm.[11] It is readily obtained experimentally with ample accuracy by noting the change in reading when a known small weight is added to the pan.

The coefficient, f, which appears in the next two terms is the relative increase in electric force of attraction per unit downward displacement of the disk. Although it might have been obtained experimentally by noting the change in reading produced by a measured change in the applied voltage, it was found more convenient to compute f from the dimensions of the instrument using the formula

$$f=\frac{2}{c}+\frac{2}{\pi r_d}\left\{2\log_e\left(\frac{2c(1-e^{\frac{-\pi r_d}{c}})}{(a^2+h^2)^{\frac{1}{2}}}\right)-\frac{a}{h}\tan^{-1}\frac{h}{a}\right\} \qquad (2)$$

derived from Snow's [12] mathematical analysis of the electric field in such an instrument. In this equation a is the radial clearance in centimeters between the disk and guard ring and h is the vertical displacement (if any) between them. It was found feasible to keep a in the neighborhood of 0.01 cm, and h never exceeded 0.07 cm. The values of f in the present work ranged from 1.0 to 2.5.

The vertical motion of the disk is in effect magnified on the scale by a factor of about 80 by the optical system. This factor is denoted by q and can readily be measured with ample accuracy for use in the small correction term in which it appears.

In the term $fh_m/2$, the quantity h_m is the vertical height of the plane of the rim of the disk above that of the rim of the aperture in the guard ring as measured when the scale reading is S_m. Because of the relatively large value of f it is necessary to know h_m with great accuracy. An error of 0.02 mm in h_m will produce 0.1-percent error in V_x and hence the determination of h_m by means of the coplanarity microscopes used for this purpose becomes a process of major importance in the measurement.

The correction term $\sum_{k=1}^{k=\infty} C_k G_k'$ is inserted in eq 1 to allow for the departures of the potentials of the individual guard hoops from their ideal values. The potential distribution as observed with a 1,000-cycle bridge is expressed as a Fourier series having coefficients G_k'. Each C_k is a factor, calculated theoretically, which connects the distortion of the potential at the outer boundary of the instrument with the attractive force at the disk. Except at very large spacings, the

[11] The factor 2 enters because of the quadratic relation between force and voltage.

[12] Chester Snow. *Effect of clearance and displacement of attracted disk, and also of a certain arrangement of conducting hoops, upon the constant of an electrometer.* BS J. Research **1**, 513 (1928) RP17.

values of C_k decrease rapidly with increase in k so that in practice it is never necessary to compute more than three terms of the series. The values of C_k are such that an accidental error of 1 percent in the experimental determination of the relative potential of a single hoop will change the values of G_k' enough to affect V_M by only 0.01 percent. A constant systematic error of this amount on all the hoops, however, would affect the values of G_k' cumulatively and make an error in V_M of ¼ percent. The errors actually present in the relative hoop-potential measurement probably did not exceed 0.02 percent and hence were quite negligible in their effect on the measurement of voltage.

The next correction term in eq 1 involves the dielectric constant ϵ of the air between the lower plate and the attracted disk and its guard ring. This quantity varies slightly with atmospheric pressure and temperature, and even more with humidity. Data were taken at the time of each weighing from which ϵ could be deduced and an appropriate correction applied. The uncertainty in this correction is probably not more than 0.001 percent, although experimental data on the dielectric constant of mixtures of air and water vapor at 60 cycles per second do not seem to be available. The corrections used were based on measurements [13] made at higher frequencies.

The term $\phi_1(h_d/r_d)$ is the result of early experiments which indicated that slight departures from flatness of the disk produced surprisingly large differences in the voltage required for a given attractive force, which were not sufficiently allowed for by merely adding h_d to c in the numerator. A concavity such that the area of a disk was on the average only 0.002 cm higher than its rim caused an increase of 0.1 percent in the voltage required to produce a given force. A similar though less serious effect is produced by conicality of the guard ring. With the technique finally developed the disks and guard rings were flat to within 0.0003 cm (i. e., the mean radius of curvature exceeded 1 km) and the correction represented by the term $\phi_1(h_d/r_d)$ and determined by experiments on disks of different curvature, was applied to allow for the slight residual curvature of the best disks.

At the widest separations there is a possibility that the electric field in the spaces between the guard hoops may be distorted enough to affect the force on the disk. Such an effect is represented in the working equation by the term $\phi_2(s/r_h)$. In the work here reported the greatest separation used was 48 cm. At this separation auxiliary tests were made with the spacing between hoops increased to 4 cm and to 6 cm. Under these conditions the term $\phi_2(s/r_h)$ is increased, respectively, to about 4 and 9 times its value at the normal spacing (2 cm). The observed changes in the indication of the electrometer in these auxiliary tests as compared with normal conditions, were +0.043 and +0.142 percent, respectively, from which it is to be inferred that the results obtained at normal spacing and 48-cm separation were 0.010 percent too high. A correction of this amount has been applied to the six points for which this separation was used.

In the last two columns of table 3 there are summarized, respectively, for each of the quantities concerned in the electrostatic method the maximum error, which could have occurred under unusually bad conditions, and the uncertainty (estimated probable error) which may reasonably be expected to be present.

[13] Delcellier, Quinchant, and Hirsch. *Inductive capacity of gases and humid air.* Onde Electrique 5, 189 (1926).

A comparison of table 3 with table 2 shows that the accuracy of the electrostatic measurements here reported is limited primarily only by the air forces and the uncertainty in determining coplanarity, while the electromagnetic measurement is subject to a large number of sources of much smaller errors, and in addition involves the uncertainty which results because the series-parallel principle is here applied to a transformer having considerable capacitance.

TABLE 3.—*Probable uncertainty and maximum error from various sources in the electrostatic measurements*

	Maximum error	Probable uncertainty
	Percent	*Percent*
Ratio of units, r	0.010	0.003
Mass of weight[a], M_P	.008	.001
Gravity, g	<.001	<.001
Separation, c	.005	.003
Radius, $(r_3+r_4)/2$	.005	.002
Air forces	.050	.005
Reading error, S_c	.010	.002
Reading error, S_v	.010	.001
Stiffness coefficient, γ	<.001	<.001
Force coefficient, f	.001	<.001
Coplanarity[a], h_m	.020	.005
Potential distribution[a], G_4'	.010	.002
Dielectric constant[a], ϵ	.005	.001
Flatness of disk[a], $\phi_1(h_4/r_4)$	.010	.003
Distortion of field between hoops[a], $\phi_2(s/r_4)$	.015	.002
Arithmetic sum	0.160	
Square root of sum of squares		0.010

[a] Values given are estimated possible residuals not accounted for by the correction normally applied for this effect.

IV. RESULTS OF COMPARISONS

The two methods of measurement outlined above were compared by using them simultaneously to measure the voltage developed at the secondary terminals of a step-up transformer. These comparisons were made under a variety of different conditions. The voltage measured ranged from 10,000 to 100,000 volts. The electrometer was used at separations (between disk and lower plate) of 6, 12, 24, and 48 cm. The system of guard hoops is unnecessary and was not used at the two smaller of these separations. Most of the measurements were made with the best 16-cm attracted disk, because this gives the greatest force for a given voltage and because the edge effects are less in proportion than with the disks of smaller diameter. However, three comparisons made while using the 10-cm disk are included.

The step-down transformer, 10–A, has two secondary windings, rated at 127.5 volts each, which can be used connected in series or in parallel. For each set of conditions comparisons were made using each of these two connections with a corresponding change in the ratio of the potentiometer circuit used to calibrate the electrodynamic voltmeter. The three possible connections of the sections of the primary, high-voltage winding, namely, in series for 100,000 volts, in series-parallel for 50,000 volts, and in parallel for 25,000 volts, were each used over the range corresponding to from 10,000 to 25,000 volts per section. Observations were made with both the series and the parallel connection of the secondary circuit over most of these ranges.

In all, 64 comparisons were made. The results of these are shown graphicly in figure 6, in which the relative differences between the values of voltage as determined by the two methods are plotted as ordinates. The points are arranged in the order in which the determinations were carried out, but the abscissas are not proportional to the time intervals between measurements. The separation between disk and lower plate in centimeters is indicated at the top of the figure and the connection of the transformer is indicated by the shape of the plotted symbol. An unweighted algebraic average of the differences between the two methods was found to be +0.006 percent, the plus sign indicating that the electrostatic method gave the higher result. The average taking the differences without regard to sign comes out ±0.010 percent. It may therefore be concluded that the two methods of high-voltage measurement are in agreement to within a few hundredths of one percent up to voltages of 100,000. The scattering is seen to be slightly less than the value 0.016 percent to be expected from combining the estimates in tables 2 and 3.

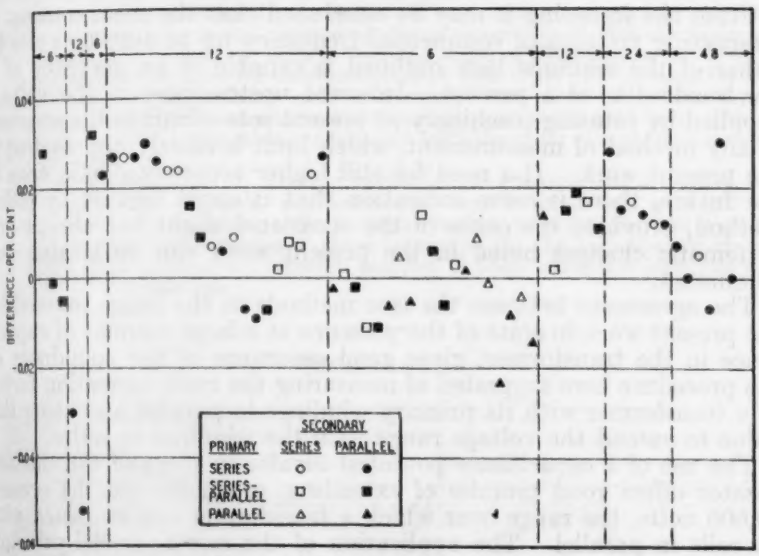

FIGURE 6.—*Graphic summary of results.*

Ordinates are the differences, expressed in percent, obtained by subtracting the value indicated for a given voltage by the electromagnetic method from the value indicated for the same voltage by the electrostatic method. The 64 independent comparisons are arranged in the order in which they were made. The first three points were obtained with a 10-cm disk in the electrometer, the remainder with a 16-cm disk. The separation between the electrometer plates is indicated at the top of the figure, and the manner of grouping the coils of the step-down transformer is indicated by the shape of the plotted symbol.

A more detailed study of the individual differences shows no systematic correlation between them and any one of the following variables: (a) Magnitude of voltage measured; (b) magnetic flux density in the core of the step-down transformer; (c) resistance of the d-c potentiometer; (d) separation of electrometer plates; or (e) diameter of electrometer disk. However, the differences depart somewhat from following a simple Gaussian distribution and give some indication of the occasional occurrence of abrupt changes of 0.01 or 0.02 percent in some factor entering the measurements. The origin of these changes

has not yet been located, and they are so small as to be of negligible importance in the present state of the art of high-voltage measurement.

The agreement between the two methods is as good at the higher voltages, for which the values of transformer ratio were extrapolated, as at the lower voltages at which it could be measured directly. This fact is convincing evidence for the soundness of applying the series-parallel principle to transformers of the type here used.

It may be noted incidentally that if these measurements are regarded as a determination of the ratio of the electrostatic unit of electromotive force to the absolute volt, the mean of the results corresponds to the value 299.783 for this ratio. This value happens to be a trifle closer to the values which correspond to the more recently published results [14] for the velocity of light than is the value 299.805 derived from the work of Rosa and Dorsey.

V. CONCLUSION

From the foregoing it may be concluded that the measurement of alternating voltages of commercial frequency up to 100,000 volts by either of the methods here outlined is capable of an accuracy of a few hundredths of a percent. Inherent unsteadiness in the voltage supplied by rotating machinery at present sets a limit to the accuracy of any method of measurement, which limit is closely approached in the present work. If a need for still higher accuracy should arise in the future, there is some indication that it could be met by either method, provided the cause of the occasional slight but abrupt and systematic changes noted in the present work can be located and eliminated.

The agreement between the two methods in the range covered by the present work in spite of the presence of a large amount of capacitance in the transformer, gives good assurance of the soundness of the procedure here suggested of measuring the ratio correction factor of a transformer with its primary windings in parallel and using this value to extend the voltage range with the windings in series.

The use of a capacitance potential divider in place of the shielded resistor offers good promise of extending, much beyond the present 30,000 volts, the range over which a transformer can be tested with its coils in parallel. The application of the series-parallel principle to step-down transformers of still higher voltage rating therefore seems to offer almost unlimited possibilities for the precise measurement of the effective value of high voltage.

There is every expectation that the absolute electrometer, when installed in a laboratory affording sufficient clearances, will be capable of measurement with an accuracy of at least 0.1 percent up to the voltage, 275,000, for which it has been designed. Hence, if the series-parallel principle is found in future to be valid up to this voltage, it should be permissible to extend the application of this principle to still higher voltages without needing further checks by another electrometer of still higher range.

WASHINGTON, November 4, 1937.

[14] Michelson. Astrophys. J. 65, 1 (1927) 299.798
Karolus and Mittelstaedt. Physik. Z. 29, 698 (1929) 299.778
Michelson, Pease, and Pearson. Astrophys. J. 82, 26 (1935) 299.774
Anderson. Rev. Sci. Instr. 8, 239 (1937) 299.794

U. S. DEPARTMENT OF COMMERCE NATIONAL BUREAU OF STANDARDS

RESEARCH PAPER RP1080

Part of Journal of Research of the National Bureau of Standards, Volume 20, March 1938

REFERENCE TABLES FOR IRON-CONSTANTAN AND COPPER-CONSTANTAN THERMOCOUPLES [1]

By Wm. F. Roeser and Andrew I. Dahl

ABSTRACT

Tables have been prepared giving corresponding values of temperature and thermal electromotive force at various temperatures from −200 to 1,000° C (−300 to 1,800° F) for iron-constantan thermocouples. Similar tables from −200 to 400° C (−300 to 750° F) for copper-constantan thermocouples, although not new, have been included for completeness. The temperature-emf relations embodied in these tables are such that (1) each can be reproduced with materials generally and readily available; (2) each is the same (within ±¾ percent) as the temperature-emf relation of a large percentage of such thermocouples of that type now in use; (3) each is near the mean of the extreme limits of the temperature-emf relations for thermocouples of that type; (4) the table for iron-constantan is near the existing table most widely used, while the one for copper-constantan is the one most widely used; and (5) the constantan used with one element to reproduce one table can be used with the other element to reproduce the other table.

This paper also gives (1) average values of the thermal emf of copper, iron which is generally available, and constantan against platinum, as a guide in selecting materials to yield any specified relation between thermal emf and temperature for thermocouples of these types and (2) the variations in thermal emf that might be expected between samples of these materials from the same lot and from different lots.

CONTENTS

		Page
I.	Introduction	337
II.	Purpose and scope of the present work	340
III.	Experimental procedure	342
IV.	Copper-platinum	342
V.	Copper-constantan	344
VI.	Constantan-platinum	345
VII.	Iron-platinum	347
VIII.	Iron-constantan	349

I. INTRODUCTION

The foundations of pyrometry as an industrial art were laid more than 30 years ago with the development [2] of a relatively rugged indicator which was suitable for use in industrial plants. The relatively low sensitivity of the indicator necessitated the use of a thermocouple which developed a relatively high thermal emf. It had been known for some time [3] that thermocouples of iron or copper in combination with an alloy of approximately equal parts of copper and nickel, de-

[1] The tables given in this paper are intended primarily for use above 0° C. Values at lower temperatures have been included for the convenience of those who might find use for a table that extends both above and below 0° C.

[2] Wm. H. Bristol. Trans. Am. Soc. Mech. Engrs. 27, 552 (1906).

[3] Stephan Lindeck. Rep. Brit. Assn. Adv. Sci. p. 130 (1892).

veloped a high thermal emf, and it had been demonstrated [4] that such thermocouples were suitable for fairly accurate temperature measurements. These thermocouples fulfilled other requirements (stability, reproducibility, low cost, etc.) of commercial thermocouples as well as any other combination of materials available at that time. There was already on the market a copper-nickel alloy known as "Constantan," so named because its electrical resistivity remained practically constant as its temperature was changed. This alloy was being produced with fairly well controlled electrical properties and its thermoelectric power against either iron or copper was substantially the maximum obtainable with any copper-nickel alloy; hence it was readily adopted as one of the elements of industrial thermocouples.

Accounts of the development and some early investigations of copper-nickel alloys are given by K. Feussner,[5] [6] S. Lindeck,[7] E. Weston,[8] and Fuessner and Lindeck.[9] The name "Constantan" apparently originated at the firm of Basse and Selve. According to Feussner,[5] "Konstanten" was the name given by Basse and Selve to the copper-nickel alloy with zero temperature coefficient of resistance and again, according to Feussner,[6] "Konstantan" was the name given the 60 copper–40 nickel alloy. According to Feussner and Lindeck,[9] "Constantan" was the name given to the 60 copper–40 nickel alloy by Basse and Selve and, according to Lindeck (see footnote 3), "Constantan" was the name of the 50 copper–50 nickel alloy. In any event, the name constantan has become a general name which covers a group of alloys containing[10] 60 to 45 percent of copper and 40 to 55 percent of nickel (with or without small percentages of manganese, iron, and carbon) because all the alloys in this range of composition have a more or less negligible temperature coefficient of resistance. Constantan thus includes the alloys made in this country under such trade names as Advance (Ideal), Copel, Copnic, Cupron, etc., most of which contain approximately 55 percent of copper and 45 percent of nickel.

With the introduction of pyrometers into general industrial use, one of the first requirements was that the scales of the instruments should be graduated to read temperature directly. It is not practicable to calibrate the scale of an instrument in accordance with the temperature-emf relation of a particular thermocouple and to change the scale each time the thermocouple is replaced. Consequently, the scales of such instruments are calibrated in accordance with a particular temperature-emf relation which was considered representative of the materials of this class at the time the relation was determined. New thermocouple materials are purchased or selected to approximate the particular temperature-emf relation which had been previously adopted.

Before the amount of constantan used in thermocouples became an important item, the composition of constantan was controlled to insure a negligible temperature coefficient of electrical resistivity, but this control did not prevent rather large differences in thermoelectric

[4] A. de Forest Palmer, Jr. Phys. Rev. **21**, 65 (1905).
[5] K. Feussner. Verhandl. physik. Ges. Berlin **10**, 109 (1892).
[6] K. Feussner. Elektrotech. Z. **13**, 99 (1892).
[7] S. Lindeck. Proc. Int. Elec. Cong. Chicago, p. 165 (1893) [Pub. by Am. Inst. Elec. Eng.]
[8] E. Weston. In the discussion of Lindeck's paper, p. 176 of reference 7.
[9] Feussner and Lindeck. Wiss. Abhandl. Physik.-Tech. Reichsanstalt **2**, 514 (1895).
[10] Woldman and Dornblatt. Engineering Alloys (Am. Soc. Metals, 1936).

properties. At the present time, the amount of constantan used in thermocouples is large enough to interest the manufacturers in controlling the composition of certain grades of the alloy to give predetermined thermoelectric properties. Although the differences in thermoelectric power between various samples of constantan made today may be as much as 1.8 μv/°F. (about 6 percent of the thermoelectric power of an iron-constantan thermocouple), these differences are not due to poor control of composition, but to the fact that the manufacturers are purposely reproducing materials made years ago and still in demand. In general, the thermal emf between any two samples of constantan is approximately proportional to the difference between the temperatures of the junctions. (See fig. 2.)

On the other hand, the amount of iron wire used in thermocouples is an extremely small percentage of the total amount of iron wire produced. Consequently, the large producers of iron wire have not been particularly interested in controlling the composition of commercial iron to give predetermined thermoelectric properties. The differences between various samples of commercially pure iron are about one-fifth as large as those in the case of constantan and are due, no doubt, to differences in chemical composition. However, in the case of iron, the thermal emf between any two samples (when plotted against the temperature) may depart considerably from a straight line. (See samples 10 and 21 in fig. 3.) Two samples of iron may give exactly the same thermal emf at 1,400° F, and yet differ by as much as 0.3 mv at 400° F (equivalent to about 10° F on an iron-constantan thermocouple). Twenty or more years ago, the differences between various samples of commercially pure iron used for thermocouples were greater and more irregular than at the present time, because iron wire, in general, was less pure and the composition was not as well controlled.

In comparison with other commercial materials, copper is and has been remarkably uniform in its thermoelectric properties, primarily because electrolytic copper of comparatively high purity has been generally available for years. A difference in thermoelectric power greater than 0.05 μv/° F (about 0.2 percent of the thermoelectric power of a copper-constantan thermocouple) between two samples of annealed copper is seldom encountered.

Owing to the differences in composition and thermoelectric properties between various lots of constantan and of iron, a number of different tables and curves have been published which give corresponding values of temperature and thermal emf for copper- and iron-constantan thermocouples. The origin of all the different curves is not known to the writers but the differences (as large as 7 percent) can easily be explained, as the various curves were determined at different times and by different investigators, using materials of the same general name but differing in thermoelectric properties.

In order to obtain thermocouples which will give the temperature-emf relation of any table or curve for thermocouples of either type, it is necessary to use materials which have the same characteristics as those used in determining that curve. This may be seen from a study of figures 2 and 3. If iron such as sample 21 and iron such as sample 10 are combined with the same constantan to form two thermocouples, the thermal electromotive forces developed by these two thermocouples will be practically identical in the range 700 to 800° C (1,292 to 1,472° F), but they will differ appreciably at other temperatures. In other

words, the curves showing the emf as a function of temperature for these two thermocouples do not have the same shape. Therefore, if a reference curve be derived for thermocouples consisting of iron like No. 21 and any sample of constantan, no sample of constantan can be found which can be combined with a sample of iron like No. 10 to yield temperature-emf values which are in agreement with those of the derived curve except over short ranges of temperature.

Most of the tables and curves now being used for iron-constantan thermocouples were prepared 15 or more years ago. Owing primarily to changes in the process of manufacturing commercially pure iron, iron wire now generally available is not the same as that in use at the time the curves were developed. Consequently, it is now necessary to obtain a more or less special iron in order to reproduce these temperature-emf relations over wide temperature ranges. However, as the variations in constantan are much greater than those in iron, it has always been possible to select materials which will match any of these curves in a limited temperature range.

II. PURPOSE AND SCOPE OF THE PRESENT WORK

The National Bureau of Standards has been frequently requested by other Government agencies and some industrial organizations to provide the data necessary for the preparation of specifications for copper-constantan and iron-constantan thermocouples. The important feature of such a specification for each type of thermocouple is a table of corresponding values of temperature and thermal emf that can be reproduced over a large temperature range by the proper selection of materials generally available at the present time. A number of such tables might be prepared, inasmuch as constantan and commercially pure iron, each with different compositions and thermoelectric properties, are still generally available. However, the choice becomes very limited if it is restricted to tables which meet the requirements given below.

It is essential that the temperature-emf relation for each type of thermocouple fulfill the following two conditions or requirements:

1. It should be such that it can be reproduced over a large temperature range with materials readily available at this time (and presumably in the future).
2. It should be the same (within reasonable limits) as the temperature-emf relation of a large percentage of such thermocouples now in use.

It would be desirable if each table could also be made to fulfill the following three conditions, but these may be inconsistent with the two essential ones above.

3. It should be near the mean of the extreme limits of the temperature-emf relation for thermocouples of that type.
4. It should agree with the existing table most widely used.
5. The constantan selected for use with copper to reproduce the relation for copper-constantan should be such that it can be used with a particular iron to reproduce the relation for iron-constantan as well.

After a study of the temperature-emf relations of a large number of thermocouples from different sources it was found (a) that Adams'

table [11] for copper-constantan thermocouples meets the first four conditions given above, and (b) that none of the tables being used for iron-constantan thermocouples prior to this investigation would meet the first requirement within the limits specified by some Government agencies and some industrial organizations. Furthermore, it happens that any two tables which will meet requirements 1 and 2 for these two types of thermocouples will meet condition 3 and come so close to meeting condition 5 that this last condition can also be met with no sacrifice of any of the other advantages. Obviously, any table prepared to meet requirement 2 for iron-constantan thermocouples will also come close to meeting condition 4.

The situation then may be summarized as follows: (a) Adams' table meets the requirements for copper-constantan thermocouples; (b) constantan selected for use with copper to reproduce Adams' table has thermoelectric properties near the mean of available constantan; (c) if this mean constantan is combined with iron near the mean of generally available commercial iron, a table is obtained for iron-constantan thermocouples which comes as near meeting all the conditions as appears possible at this time.

The fact that Adams' table covers a large temperature range (−200 to +385° C) makes it more suitable for the present purpose than other published tables [12] [13] [14] which cover ranges only below room temperature.

The particular steps in the procedure followed are then: (1) The thermal emf of copper with respect to platinum was determined; (2) these values were combined with Adams' relation for copper-constantan to obtain the thermal emf of constantan against platinum; (3) the thermal emf of generally available iron against platinum was determined; and (4) these iron-platinum and constantan-platinum values were combined to obtain values for iron-constantan. This was done for the temperature range covered by Adams' table (−200 to 385° C), but it was necessary to make additional observations on constantan to extend the iron-constantan values to higher temperatures.

The thermal emf of each sample studied was determined against the Platinum Thermoelectric Standard Pt 27 of this Bureau. In this way the thermoelectric properties of each thermocouple material could be studied independently of the others and the thermal emf of any two samples against each other could be obtained by combining the values of thermal emf of each against platinum. Thus, in obtaining the data necessary for determining the temperature-emf relation of copper or iron against constantan, representative temperature-emf relations for each material against platinum were determined and some information was obtained on the differences in thermal emf to be expected between samples of wire from the same lot and from different lots.

The results of similar investigations on platinum to platinum-rhodium [15] and on Chromel-Alumel [16] thermocouples have been published recently in this journal.

[11] L. H. Adams, Pyrometry, p. 165 (Symposium published by Am. Inst. Mining Met. Engrs. 1920). Int. Crit. Tables 1, 58 (1926).
[12] Gianque, Buffington, and Schulze, J. Am. Chem. Soc. **49**, 2343 (1927).
[13] Southard and Andrews. J. Franklin Inst. **207**, 323 (1929).
[14] Aston, Willihnganz, and Messerly. J. Am. Chem. Soc. **57**, 1642 (1935).
[15] BS J. Research **10**, 275 (1933) RP530.
[16] J. Research NBS **14**, 239 (1935) RP767.

III. EXPERIMENTAL PROCEDURE

Samples of iron, copper, and constantan were obtained from a number of sources. Most of the samples were supplied by or purchased from pyrometer or wire manufacturers. The other samples were prepared at this Bureau. In addition to the data obtained on the samples included in this particular investigation, data on a number of samples of wires from various sources were already available in the records of this Bureau.

The thermal emf of each sample against platinum was determined in air with no protection from oxidation, in the same way and with the same apparatus as used at this Bureau in the calibration of high temperature thermocouples.[17] From one to five samples of wire are welded together with a platinum working standard. These wires are insulated and placed in a tube furnace with the junction of a calibrated platinum to platinum-rhodium thermocouple inserted in a hole drilled into the composite junction formed by welding the wires being tested to the platinum wire. The standard thermocouple and platinum wire are sealed into porcelain tubes with a Pyrex glass, leaving a very short length of wire exposed at the measuring junction. When possible the reference junctions are maintained at 0° C. In other cases, the temperature of this junction is measured with a mercury-in-glass thermometer. Simultaneous readings of the temperature and the thermal emf of the samples against platinum are made at various temperatures. It is estimated that the accuracy of the measurements and the intervals between observation points were such that the uncertainty in the determination of the corresponding values of temperature and emf of each material against platinum did not exceed $\pm 5\,\mu$v up to 5 mv. and ± 0.1 percent up to the emf corresponding to 900° C (1,652° F). This estimate of the uncertainty includes the effect of changes in the wire during the determination. No claim is made for the accuracy of the temperature-emf relations above 900° C because the thermal emf of some of the samples of iron and constantan changed with time as the temperature was maintained constant.

The thermal emf of only a few selected samples was determined at temperatures below 0° C. These observations[18] were made using a stirred liquid bath[19] cooled by liquid air. A platinum resistance thermometer was used as a standard for determining the temperature.

All the temperature measurements were in terms of the International Temperature Scale[20] of 1927.

IV. COPPER-PLATINUM

Although it is generally accepted that commercial copper is exceptionally uniform as far as its thermoelectric properties are concerned, the thermal emf between a number of samples of copper was measured to determine the differences that might be expected between samples of copper of different sizes and from different sources, before determining the thermal emf of representative copper against platinum. The thermal emf of copper, as with most metals, depends

[17] J. Research NBS **14**, 247 (1935) RP768.
[18] Acknowledgment is made to D. O. Burger and R. B. Scott for the observations at low temperatures.
[19] BS J. Research **6**, 401 (1931) RP284.
[20] BS J. Research **1**, 635 (1928) RP22.

to some extent upon its physical condition, cold-worked copper being thermoelectrically positive to the same material annealed. The magnitude of the thermal emf between the cold-worked and annealed material depends upon the amount of cold working. Differences as large as 24 μv between cold-rolled and annealed samples (junctions at 0° and 300° C) have been brought to our attention.

The thermal emf between a number of samples of copper is given in table 1. In all these measurements a sample of No. 12 gage copper was used as a reference material and the junctions were maintained at 350 and 0° C. Excluding one sample of No. 34 gage wire of unknown origin and the two samples of tubing, the maximum thermal emf between the samples is 29 μv. The authors do not have a satisfactory explanation for the fact that, in general, the smaller wires are thermoelectrically positive to the larger ones. The differences in thermal emf may be caused by differences in the crystal structure or in the amount of dissolved oxygen or oxide.

For determining the thermal emf of copper against platinum, nine samples were selected from those listed in table 1, and the thermal emf of each measured against platinum from 0 to 1,000° C at intervals of 50° C. These nine samples included six samples of No. 8 gage wire and one sample each of Nos. 12, 18, and 22 gage wire. A test made on three sizes of wire (Nos. 12, 18, and 22) showed no detectable drift in thermal emf during 30 hours of heating at 500° C. The values at the higher temperatures are of very little importance. Only one sample, the No. 28 gage wire, was used in determining the thermal emf of copper against platinum at temperatures below 0° C.

TABLE 1.—*Thermal electromotive force between samples of copper wire* [1]

[Temperature of junctions 350 and 0° C]

Samples as received from manufacturer				Wire drawn from the same 0.5-in. rod		
Size (gage)	Electromotive force	Size (gage)	Electromotive force	Size (gage)	Cold-worked	Annealed at 450° C in air
	μv		μv		μv	μv
8	−18	28	0	8	−2	−11
8	−12	28	0			
8	−2	30	−2	12	−2	−11
8	−10	30	−5			
8	−3	32	+11	18	+9	+1
8	−10	32	+11	22		+7
10	−3	32	−7			
12	+2	32	−6			
14	−1	34	−3			
16	−7	34	−110			
18	0	36	+7			
20	0	36	+6			
22	−1	38	+3			
22	−4	40	+6			
22	−1					
24	0	5/64-in. tubing	−93			
26	+6	5/32-in. tubing	−61			

[1] The electrical conductivity of the No. 8 gage wire drawn from ½-inch copper rod and annealed was 102.64 percent of that of the International Copper Standard (1.7241 microhm-cm at 20° C). The samples of No. 8 gage wire listed in the first column were from 4 different manufacturers and ranged in electrical conductivity from 100.65 to 101.20 percent.

The samples of wire, No. 10 gage and smaller, were taken from the storeroom and laboratories of this Bureau and are from various manufacturers.

Corresponding values of emf and temperature of copper against platinum as derived from these observations are given in tables 5 and 6.

V. COPPER-CONSTANTAN

Primarily because of differences in the thermoelectric properties of constantan, the temperature-emf relations of available copper-constantan thermocouples differ as much as 8 percent. However, a study of the temperature-emf relations of a large number of copper-constantan thermocouples determined at this Bureau shows that the relation given by Adams is very near the mean of the extreme limits of these relations and that it can be easily reproduced by materials now available. Any temperature-emf relation which we might develop as representative of copper-constantan thermocouples at the present time would not differ significantly from the relation given

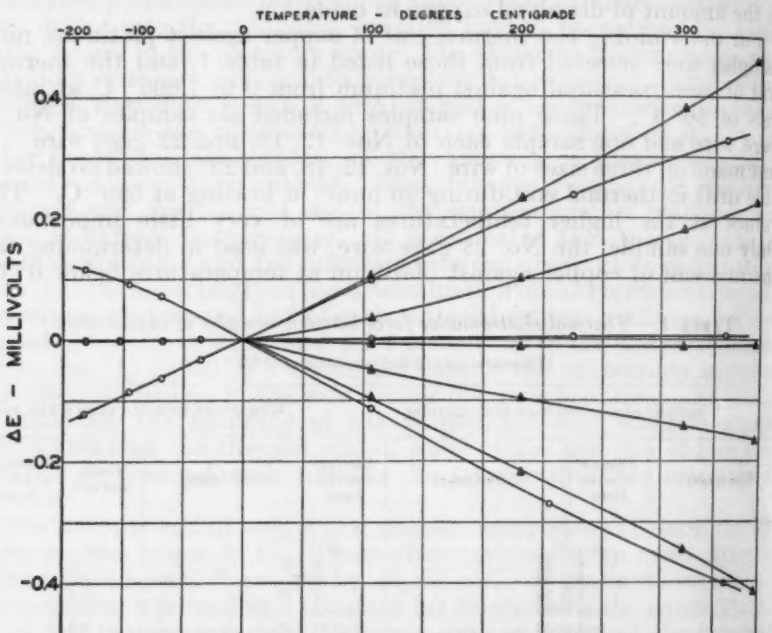

FIGURE 1.—*Differences between the calibrations of some copper-constantan thermocouples and the values in tables 7 and 8.*

by Adams. Corresponding values of temperature and emf as derived from Adams' table are given in tables 7 and 8.

Figure 1 shows the deviations of the temperature-emf relations of several different thermocouples from Adams' table. In general, these difference curves approximate straight lines.

Although copper-constantan thermocouples are not recommended for the accurate measurement of temperatures above 350° C (662° F), they may be used at higher temperatures for less accurate measurements. However, the life of such a thermocouple is very short in an oxidizing atmosphere at high temperatures. There is a slight drift

in the thermal emf of this type of thermocouple as oxidation proceeds, but it is not large (the order of 0.2 percent up to the time the copper wire is practically oxidized through). Tables 7 and 8 may be extended to higher temperatures by combining the copper-platinum and constantan-platinum values in tables 5 and 6.

VI. CONSTANTAN-PLATINUM

The thermal emf, relative to platinum, of samples of constantan from 27 different lots was determined at intervals of 50° C from 0 to 800° C. Observations on 17 of these samples were made up to 1,000° C. All of the samples were from lots of No. 8 gage wire which had been selected by pyrometer instrument manufacturers as suitable for use with iron in iron-constantan thermocouples. As most of the iron and constantan used for thermocouples is selected to give a particular temperature-emf relation and as the thermal emf between samples of commercially available iron seldom exceeds 0.3 mv, the temperature-thermal emf curves of most of the samples of constantan against platinum fell within a very narrow band.

Corresponding values of temperature and emf, relative to platinum, of the constantan used by Adams in obtaining the copper-constantan values in tables 7 and 8, were obtained by combining the copper-platinum values in tables 5 and 6 with Adams' values for copper-constantan. However, these values extended only over the range of Adams' table, −200 to 385° C. The thermoelectric characteristics of the constantan which, when combined with iron, approximates the curve most widely used for iron-constantan thermocouples are very similar to those of the constantan which, when combined with copper, yields the values in Adams' table. The values of thermal emf of 18 of the constantan samples against platinum agreed with the derived values for Adams' constantan to ± 100 μv at 350° C (662° F) (slightly less than the equivalent of 2° C on either an iron- or copper-constantan thermocouple). The two extreme samples differed from Adams' constantan by +515 and −490 μv at 350° C. Only a small amount of constantan differing appreciably from the mean values (or from Adams' constantan) is being used for thermocouples.

If the temperature-emf values of the 18 samples which fell within a narrow band are averaged, a curve is obtained which gives the thermoelectric characteristics, within narrow limits of most of the constantan now being used for iron-constantan thermocouples. Such an average curve agreed with the derived curve for Adams' constantan against platinum in the range 0 to 350° C, well within the limits of the experimental error. Consequently, there appears to be no objection to modifying this average curve to agree exactly with that of Adams' constantan in the range 0 to 350° C and modifying it correspondingly at higher temperatures. This might be done in a number of ways, all of which give substantially the same result because so many of the samples of constantan were practically the same thermoelectrically as Adams' constantan. It was apparent from the curves that the thermal emf between any two samples of constantan was approximately proportional to the temperature but more nearly proportional to the emf of the samples against platinum. The emf of Adams' constantan against platinum is 13.93 mv at 350° C (662° F). Consequently, if the emf, E_t, of each sample of constantan against plati-

num at any temperature is multiplied by $13.93/E_{350}$, the modified curves will all coincide at 350° C (662° F) and will agree within very small limits at other temperatures. Excluding 4 of the 27 samples, the maximum difference between the modified curves was about 100 μv at 700° C (1,292° F). The modified curves for 17 of the samples agreed with the mean to ±30 μv up to 700° C (the equivalent of about 0.5° C on an iron-constantan thermocouple).

The corresponding values of temperature and thermal emf for constantan-platinum above 350° C (662° F) in tables 5 and 6, were obtained by taking the mean of the modified curves. These mean values agreed with the values for Adams' constantan in the range 0 to 350° C to within 7 μv. Figure 2 shows the differences between

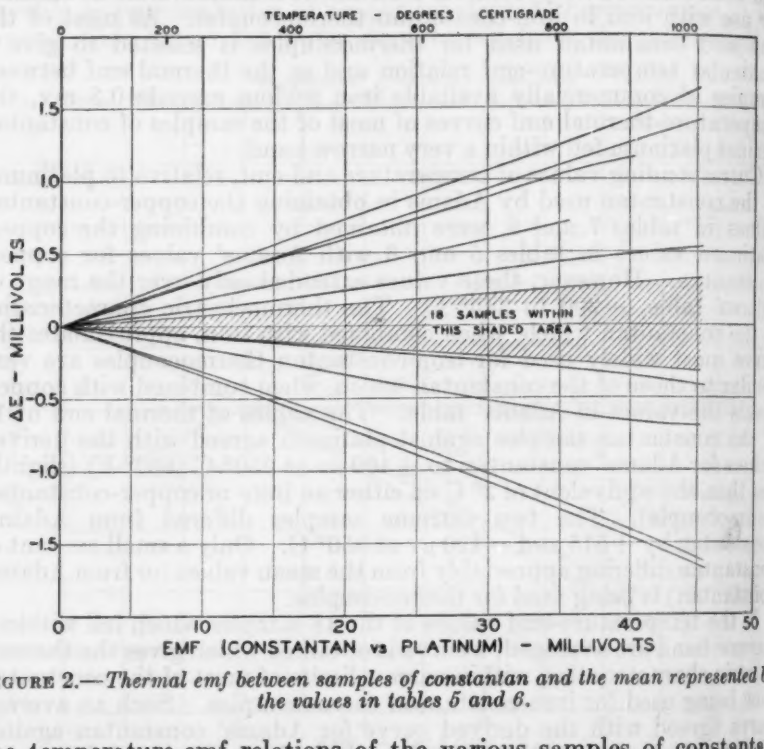

FIGURE 2.—*Thermal emf between samples of constantan and the mean represented by the values in tables 5 and 6.*

the temperature-emf relations of the various samples of constantan against platinum and the mean values in tables 5 and 6. The curves within the shaded area were also practically linear.

A few measurements were made to obtain some idea of the magnitude of the differences that might be expected between samples of wire from the same coil as produced by the manufacturer and between samples from different coils of the same heat.[21]

The thermal emf between two samples of No. 8 gage wire from the same coil was a maximum, 21 μv, at 400° C in one case and a maximum, 36 μv, at 800° C, in another. Table 2 gives the thermal emf of platinum against each of three different sizes of contantan wire drawn from the same 100-lb coil.

[21] A coil, 50 to 100 lb contains 1,000 to 2,000 ft of No. 8 gage wire. A heat is a melt of metal containing several thousand pounds.

TABLE 2.—*Thermal electromotive force of different sizes of constantan wire drawn from the same coil*

[Reference material NBS Pt 27]

Temperature	Electromotive force (reference junctions at 0° C)		
	No. 8	No. 14	No. 20
°C	mv	mv	mv
0	0	0	0
100	3.51	3.51	3.50
200	7.43	7.44	7.43
300	11.69	11.70	11.68
400	16.17	16.19	16.16
500	20.77	20.80	20.77
600	25.46	23.49	25.46
700	30.18	30.22	30.19
800	34.89	34.92	34.89

The maximum thermal emf between two samples of No. 8 gage wire from different coils was 9 μv at 800° C in the case of one heat, 2 in another, and 72 in the third.

VII. IRON-PLATINUM

The results of measurements on samples of iron wire are shown in figure 3. These curves give the differences between the thermal emf

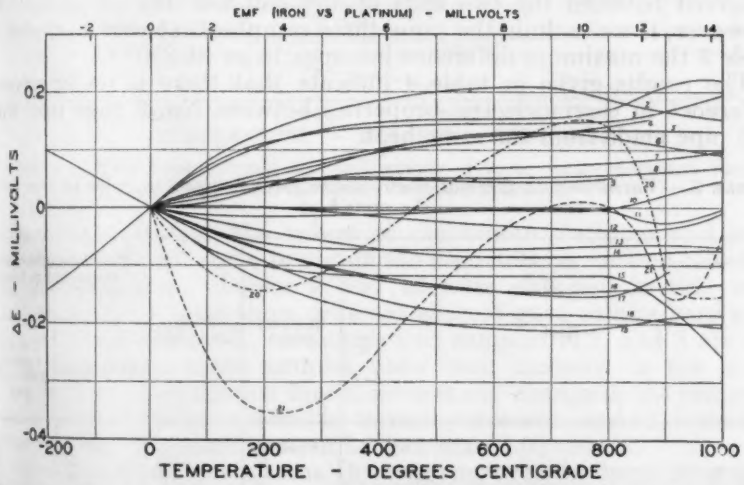

FIGURE 3.—*Thermal emf between samples of iron and the mean of samples 1 to 19.*

of the various samples against platinum and the mean thermal emf of samples 1 to 19. The results on a number of the samples were checked by running duplicates. All the samples but four were obtained from pyrometer manufacturers in this country. Samples 1, 2, and 3 are irons of higher purity than commercial irons and were drawn at this Bureau from materials obtained from metallurgical research laboratories.

The curves for samples 20 and 21 are of particular interest because their shape (markedly different from that of sample 1 to 19) is of the type required to give the temperature-emf relations embodied in the existing tables in the temperature range 0 to 870° C (1,600 ° F). The most significant difference found between the analyses of samples 20 and 21 and the other samples was the manganese content. Sample 20 contained 0.33 percent of manganese and sample 21 contained 0.36 percent of manganese, whereas the maximum in any of the other samples was 0.11 percent. Sample 21 also contained 0.099 percent of phosphorus compared with a maximum of 0.013 percent in any of the other samples.

It appears that commercially pure iron generally available at the present time has the thermoelectric characteristics shown by the curves for samples 1 to 19, as all the samples reported to have come directly or indirectly from a number of large producers of iron wire are included in this group. The corresponding values of emf and temperature given in tables 5 and 6 for iron against platinum represent the mean of samples 1 to 19.

Table 3 gives the results of a few measurements made to determine the differences in thermal emf that might be expected between samples of iron from the same heat. Each of the first three heats investigated included one sample which differed markedly from all the others of that heat as shown by the last column.

Samples of wire were taken from 40 coils of iron wire (from 7 heats) to determine the differences within a coil. The maximum difference observed between the two ends of any coil was 141 μv at 800° C. However, if we exclude the same three samples that were excluded in table 3 the maximum difference becomes 18 μv at 800° C.

The results given in table 4 indicate that there is no significant difference in thermoelectric properties between No. 8 gage iron wire and pipe made from the same heat.

TABLE 3.—*Variations in thermal electromotive force between samples of iron from the same heat*

Heat	Samples tested	Coils sampled	Maximum difference in electromotive force at 800° C	
			All samples	Excluding 1 sample from each heat
	Number	*Number*	μv	μv
1	26	13	34	12
2	17	10	108	25
3	12	6	115	70
4	22	11	18	

TABLE 4.—*Thermal electromotive force of iron wire and pipe from the same heat*

[Reference material NBS Pt 27]

Temperature	Electromotive force (reference junctions at 0° C)	
	No. 8 wire (mean of 13 samples)	Pipe (mean of 3 samples)
°C	μv	μv
0	0	0
100	1,912	1,919
200	3,583	3,590
300	4,898	4,904
400	5,925	5,928
500	6,836	6,834
600	7,847	7,845
700	9,163	9,161
800	10,905	10,905

VIII. IRON-CONSTANTAN

If the mean of iron samples 1 to 19 in figure 3 is accepted as representative of iron generally available at the present time, it is only

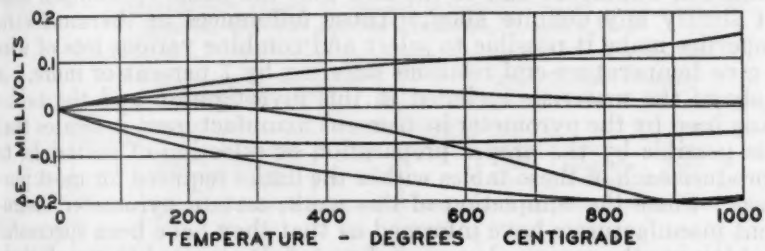

FIGURE 4.—*Differences between the calibrations of some iron-constantan thermocouples and the values in tables 9 and 10.*

necessary to combine the values of constantan-platinum and iron-platinum in tables 5 and 6 to obtain the desired table for iron-constantan thermocouples. Tables 9 and 10 were obtained in this way. Samples received from three different sources gave results very near the mean thus obtained. Although iron samples 1, 2, and 3 are not commercial irons, these samples have been included in the mean because (1) it is our opinion that if there is any change in the composition of commercial irons it will be toward purer iron, and (2) including these samples changes the mean by less than 0.03 mv.

For the past few years some Government agencies have been purchasing thermocouples to give essentially the same temperature-emf relation as that given in tables 9 and 10. As far as we know there has been no difficulty in obtaining wire which will give this relation to ±¼ percent. Most of the iron-constantan thermocouples calibrated at this Bureau during the past 5 years give this relation to ±¾ percent up to 1,400° F (760° C). Figure 4 shows the differences between the temperature-emf relations of some iron-constantan thermocouples from different sources and the values in tables 9 and 10.

Although the tables give corresponding values of emf and temperature up to 1,800° F, iron-constantan thermocouples are not recommended for continuous or accurate measurements at temperatures above 1,400° F (760° C) in an oxidizing atmosphere. A few observations indicate that both elements of a No. 8 gage thermocouple of this type will oxidize through in approximately 1,000 hours in an oxidizing atmosphere at 1,400° F. In these tests the emf of the thermocouples changed by the equivalent of about 8° F in 800 hours at 1,400° F and by about 30° F just before oxidizing through at 1,000 hours.

The difference between the temperature-emf relation in tables 9 and 10 for iron-constantan thermocouples and the one most widely used[22] by pyrometer instrument manufacturers at the present time is about 2 percent at 400° F and ⅛ percent at 1,200° F. The fact that this new relation for iron-constantan thermocouples does not agree exactly with any of the tables used by pyrometer instrument manufacturers prior to this investigation obviously does not in any way affect the accuracy with which wire supplied by the manufacturers will conform with the temperature-emf relations which they have been using. Different lots of iron and constantan may have very different thermoelectric properties owing to the fact that commercial iron contains a number of impurities and to the fact that the name constantan does not signify any definite alloy. Those differences in thermoelectric properties make it possible to select and combine various lots of wire to give temperature-emf relations differing by 7 percent or more. A study of the materials included in this investigation and the tables being used by the pyrometer instrument manufacturers, indicates that it is possible by the proper preparation or selection of materials, to reproduce each of these tables within the limits required for most purposes. Since the completion of this work, certain pyrometer instrument manufacturers have informed us that they have been successful in obtaining the more or less special materials required to match their curve over the entire range.

The table for iron-constantan thermocouples given in this paper can be approximated only by selecting materials on the basis of tests at two or more temperatures. It does not differ, however, in this respect from any other such table that is now in use or that can be devised at this time.

The accuracy with which any of these relations can be reproduced depends to a large extent upon the accuracy obtained in the testing and combining of materials into thermocouples. The important advantage of the proposed table over existing ones is that it can be reproduced more accurately, over the entire range, with materials which are readily available.

[22] Tech. Pap. BS 14, 306 (1920-21) T170. Int. Crit. Tables 1, 59 (1926).

TABLE 5.—*Representative values of the thermal electromotive force of copper, constantan, and iron against Platinum Standard Pt 27*

Temperature	Electromotive force (reference junctions at 0° C)			Temperature	Electromotive force (reference junctions at 0° C)		
	Copper-platinum	Constantan-platinum	Iron-platinum		Copper-platinum	Constantan-platinum	Iron-platinum
°C	mv	mv	mv	°C	mv	mv	mv
−200	−0.19	+5.35	−2.92				
−150	−.35	+4.25	−2.55				
−100	−.37	+2.98	−1.84				
−50	−.24	+1.56	−0.96				
0	.00	0.00	.00				
50	+.34	−1.69	+.97	550	7.35	−23.12	7.27
100	.76	−3.51	1.89	600	8.34	−25.47	7.80
150	1.26	−5.44	2.75	650	9.39	−27.83	8.41
200	1.83	−7.45	3.54	700	10.49	−30.18	9.12
250	2.46	−9.55	4.24	750	11.64	−32.53	9.95
300	3.15	−11.71	4.85	800	12.84	−34.86	10.86
350	3.89	−13.93	5.39	850	14.10	−37.17	11.83
400	4.68	−16.19	5.88	900	15.41	−39.45	12.84
450	5.52	−18.48	6.34	950	16.78	−41.70	13.55
500	6.41	−20.79	6.79	1,000	18.20	−43.92	14.30

TABLE 6.—*Representative values of the thermal electromotive force of copper, constantan, and iron against Platinum Standard Pt 27*

Temperature	Electromotive force (reference junctions at 32° F)			Temperature	Electromotive force (reference junctions at 32° F)		
	Copper-platinum	Constantan-platinum	Iron-platinum		Copper-platinum	Constantan-platinum	Iron-platinum
° F	mv	mv	mv	° F	mv	mv	mv
−300	−0.26	+5.02	−2.85				
−200	−.38	+3.73	−2.28				
−100	−.32	+2.24	−1.39				
0	−.10	+0.57	−0.35	1,000	7.12	−22.55	7.15
100	+.25	−1.27	+.73	1,100	8.21	−25.15	7.73
200	.70	−3.26	1.77	1,200	9.37	−27.77	8.40
300	1.25	−5.39	2.73	1,300	10.59	−30.39	9.19
400	1.88	−7.64	3.60	1,400	11.88	−32.99	10.13
500	2.59	−9.98	4.37	1,500	13.23	−35.58	11.16
600	3.37	−12.40	5.03	1,600	14.65	−38.14	12.25
700	4.21	−14.88	5.60	1,700	16.14	−40.66	13.21
800	5.12	−17.41	6.12	1,800	17.69	−43.13	14.03
900	6.09	−19.97	6.62				

TABLE 7.—*Corresponding values of temperature and electromotive force of copper-constantan thermocouples as derived from Adams' table*

[Reference junctions at 0° C.]

Temperature	Electromotive force	Temperature	Electromotive force	Temperature	Electromotive force
°C	mv	°C	mv	°C	mv
−200	−5. 539	0	0. 000	200	9. 285
−190	−5. 378	10	. 389	210	9. 820
−180	−5. 204	20	. 787	220	10. 360
−170	−5. 016	30	1. 194	230	10. 905
−160	−4. 815	40	1. 610	240	11. 455
−150	−4. 602	50	2. 034	250	12. 010
−140	−4. 376	60	2. 467	260	12. 571
−130	−4. 137	70	2. 908	270	13. 136
−120	−3. 886	80	3. 356	280	13. 706
−110	−3. 623	90	3. 812	290	14. 280
−100	−3. 349	100	4. 276	300	14. 859
−90	−3. 063	110	4. 747	310	15. 443
−80	−2. 765	120	5. 225	320	16. 030
−70	−2. 456	130	5. 710	330	16. 621
−60	−2. 137	140	6. 202	340	17. 216
−50	−1. 807	150	6. 700	350	17. 815
−40	−1. 466	160	7. 205	360	18. 418
−30	−1. 114	170	7. 716	370	19. 025
−20	−0. 752	180	8. 233	380	19. 635
−10	−0. 381	190	8. 756	390	20. 248
0	. 000	200	9. 285	400	20. 865

TABLE 8.—*Corresponding values of temperature and electromotive force for copper-constantan thermocouples, as derived from Adams' table*

[Reference junctions at 32° F]

Temperature	Electromotive force	Temperature	Electromotive force	Temperature	Electromotive force	Temperature	Electromotive force
°F	mv	°F	mv	°F	mv	°F	mv
−300	−5. 283	0	−0. 671	300	6. 644	600	15. 769
−290	−5. 184	10	−. 464	310	6. 924	610	16. 096
−280	−5. 081	20	−. 255	320	7. 206	620	16. 424
−270	−4. 973	30	−. 043	330	7. 489	630	16. 753
−260	−4. 861	40	+. 172	340	7. 774	640	17. 084
−250	−4. 745	50	. 390	350	8. 061	650	17. 416
−240	−4. 626	60	. 610	360	8. 350	660	17. 749
−230	−4. 503	70	. 832	370	8. 640	670	18. 083
−220	−4. 376	80	1. 057	380	8. 932	680	18. 418
−210	−4. 245	90	1. 285	390	9. 226	690	18. 754
−200	−4. 110	100	1. 516	400	9. 521	700	19. 091
−190	−3. 971	110	1. 750	410	9. 819	710	19. 430
−180	−3. 829	120	1. 987	420	10. 119	720	19. 770
−170	−3. 683	130	2. 226	430	10. 420	730	20. 111
−160	−3. 533	140	2. 467	440	10. 722	740	20. 453
−150	−3. 380	150	2. 711	450	11. 026	750	20. 796
−140	−3. 223	160	2. 957	460	11. 332		
−130	−3. 062	170	3. 206	470	11. 639		
−120	−2. 898	180	3. 457	480	11. 948		
−110	−2. 731	190	3. 710	490	12. 259		
−100	−2. 560	200	3. 966	500	12. 571		
−90	−2. 386	210	4. 224	510	12. 885		
−80	−2. 209	220	4. 484	520	13. 200		
−70	−2. 028	230	4. 747	530	13. 516		
−60	−1. 844	240	5. 012	540	13. 833		
−50	−1. 656	250	5. 279	550	14. 152		
−40	−1. 465	260	5. 548	560	14–472		
−30	−1. 271	270	5. 819	570	14. 794		
−20	−1. 074	280	6. 092	580	15. 118		
−10	−0. 874	290	6. 367	590	15. 443		
0	−. 671	300	6. 644	600	15. 769		

TABLE 9.—*Corresponding values of temperature and electromotive force for iron-constantan thermocouples*

[Reference junctions at 0° C]

Temperature	Electromotive force	Temperature	Electromotive force	Temperature	Electromotive force	Temperature	Electromotive force
°C	mv	°C	mv	°C	mv	°C	mv
		0	0.00	400	22.07	800	45.72
		10	.52	410	22.62	810	46.37
		20	1.05	420	23.17	820	47.03
		30	1.58	430	23.72	830	47.69
		40	2.12	440	24.27	840	48.34
		50	2.66	450	24.82	850	49.00
		60	3.20	460	25.37	860	49.66
		70	3.75	470	25.92	870	50.32
		80	4.30	480	26.47	880	50.97
		90	4.85	490	27.03	890	51.63
		100	5.40	500	27.58	900	52.29
		110	5.95	510	28.14	910	52.88
		120	6.51	520	28.70	920	53.47
		130	7.07	530	29.26	930	54.06
		140	7.63	540	29.82	940	54.65
		150	8.19	550	30.39	950	55.25
		160	8.75	560	30.96	960	55.84
		170	9.31	570	31.53	970	56.43
		180	9.87	580	32.11	980	57.03
		190	10.43	590	32.69	990	57.63
−200	−8.27	200	10.99	600	33.27	1,000	58.22
−190	−8.02	210	11.56	610	33.86		
−180	−7.75	220	12.12	620	34.45		
−170	−7.46	230	12.68	630	35.04		
−160	−7.14	240	13.23	640	35.64		
−150	−6.80	250	13.79	650	36.24		
−140	−6.44	260	14.35	660	36.84		
−130	−6.06	270	14.90	670	37.45		
−120	−5.66	280	15.46	680	38.06		
−110	−5.25	290	16.01	690	38.68		
−100	−4.82	300	16.56	700	39.30		
−90	−4.38	310	17.12	710	39.93		
−80	−3.93	320	17.67	720	40.56		
−70	−3.47	330	18.22	730	41.19		
−60	−3.00	340	18.77	740	41.83		
−50	−2.52	350	19.32	750	42.48		
−40	−2.03	360	19.87	760	43.12		
−30	−1.53	370	20.42	770	43.77		
−20	−1.03	380	20.97	780	44.42		
−10	−0.52	390	21.52	790	45.07		
0	0.00	400	22.07	800	45.72		

TABLE 10.—*Corresponding values of temperature and electromotive force for iron-constantan thermocouples*

[Reference junctions at 32° F.]

Temperature	Electromotive force	Temperature	Electromotive force	Temperature	Electromotive force	Temperature	Electromotive force	Temperature	Electromotive force
°F	mv	°F	mv	°F	mv	°F	mv	°F	mv
		0	−0. 92	500	14. 35	1, 000	29. 70	1, 500	46. 74
		10	−. 63	510	14. 65	1, 010	30. 01	1, 510	47. 10
		20	−. 35	520	14. 96	1, 020	30. 33	1, 520	47. 47
		30	−. 06	530	15. 27	1, 030	30. 64	1, 530	47. 83
		40	+. 23	540	15. 58	1, 040	30. 96	1, 540	48. 20
		50	. 52	550	15. 89	1, 050	31. 28	1, 550	48. 56
		60	. 82	560	16. 20	1, 060	31. 60	1, 560	48. 93
		70	1. 11	570	16. 50	1, 070	31. 92	1, 570	49. 29
		80	1. 41	580	16. 81	1, 080	32. 24	1, 580	49. 66
		90	1. 70	590	17. 12	1, 090	32. 56	1, 590	50. 02
		100	2. 00	600	17. 43	1, 100	32. 88	1, 600	50. 39
		110	2. 30	610	17. 73	1, 110	33. 20	1, 610	50. 75
		120	2. 60	620	18. 04	1, 120	33. 53	1, 620	51. 12
		130	2. 90	630	18. 34	1, 130	33. 86	1, 630	51. 49
		140	3. 20	640	18. 65	1, 140	34. 18	1, 640	51. 85
		150	3. 50	650	18. 95	1, 150	34. 51	1, 650	52. 22
		160	3. 81	660	19. 26	1, 160	34. 84	1, 660	52. 55
		170	4. 11	670	19. 56	1, 170	35. 17	1, 670	52. 88
		180	4. 42	680	19. 87	1, 180	35. 50	1, 680	53. 21
		190	4. 72	690	20. 18	1, 190	35. 84	1, 690	53. 54
−300	−7. 87	200	5. 03	700	20. 48	1, 200	36. 17	1, 700	53. 87
−290	−7. 72	210	5. 34	710	20. 79	1, 210	36. 50	1, 710	54. 20
−280	−7. 55	220	5. 64	720	21. 09	1, 220	36. 84	1, 720	54. 52
−270	−7. 38	230	5. 95	730	21. 40	1, 230	37. 18	1, 730	54. 85
−260	−7. 20	240	6. 26	740	21. 70	1, 240	37. 52	1, 740	55. 18
−250	−7. 02	250	6. 57	750	22. 01	1, 250	37. 86	1, 750	55. 51
−240	−6. 83	260	6. 88	760	22. 31	1, 260	38. 20	1, 760	55. 84
−230	−6. 63	270	7. 19	770	22. 62	1, 270	38. 54	1, 770	56. 17
−220	−6. 43	280	7. 50	780	22. 92	1, 280	38. 88	1, 780	56. 50
−210	−6. 22	290	7. 81	790	23. 23	1, 290	39. 23	1, 790	56. 83
−200	−6. 01	300	8. 12	800	23. 53	1, 300	39. 58	1, 800	57. 16
−190	−5. 79	310	8. 43	810	23. 84	1, 310	39. 93		
−180	−5. 57	320	8. 75	820	24. 14	1, 320	40. 28		
−170	−5. 34	330	9. 06	830	24. 45	1, 330	40. 63		
−160	−5. 11	340	9. 37	840	24. 75	1, 340	40. 98		
−150	−4. 87	350	9. 68	850	25. 06	1, 350	41. 34		
−140	−4. 63	360	10. 00	860	25. 37	1, 360	41. 69		
−130	−4. 38	370	10. 31	870	25. 67	1, 370	42. 05		
−120	−4. 13	380	10. 62	880	25. 98	1, 380	42. 40		
−110	−3. 88	390	10. 93	890	26. 29	1, 390	42. 76		
−100	−3. 63	400	11. 24	900	26. 59	1, 400	43. 12		
−90	−3. 37	410	11. 56	910	26. 90	1, 410	43. 48		
−80	−3. 11	420	11. 87	920	27. 21	1, 420	43. 84		
−70	−2. 85	430	12. 18	930	27. 52	1, 430	44. 20		
−60	−2. 58	440	12. 49	940	27. 83	1, 440	44. 56		
−50	−2. 31	450	12. 80	950	28. 14	1, 450	44. 92		
−40	−2. 04	460	13. 11	960	28. 45	1, 460	45. 28		
−30	−1. 76	470	13. 42	970	28. 76	1, 470	45. 65		
−20	−1. 48	480	13. 73	980	29. 07	1, 480	46. 01		
−10	−1. 20	490	14. 04	990	29. 39	1, 490	46. 37		
0	−0. 92	500	14. 35	1, 000	29. 70	1, 500	46. 74		

WASHINGTON, July 15, 1937.

U. S. Department of Commerce National Bureau of Standards

RESEARCH PAPER RP1081

Part of Journal of Research of the National Bureau of Standards, Volume 20, March 1938

MAGNETIC METHOD FOR MEASURING THE THICKNESS OF NONMAGNETIC COATINGS ON IRON AND STEEL

By Abner Brenner

ABSTRACT

A nondestructive, magnetic method is described for measuring the thickness of nonmagnetic coatings on steel. The instrument used is similar to that previously described for measuring nickel coatings on nonmagnetic base metals. The present method depends on the decrease in the attraction of a permanent magnet for steel when the two are separated by a nonmagnetic coating.

Measurements on commercial coatings of which the actual thicknesses were determined by standard methods yielded results that were accurate to ±10 percent for most coatings. The results were about 25 percent low for hot-dipped tin coatings, which are only about 0.0001 in. thick.

Because nickel is less magnetic than steel, the thickness of nickel coatings on steel can be measured by this method, using a suitable calibration curve.

CONTENTS

	Page
I. Introduction	357
II. Principles involved	358
III. Types of instruments	358
IV. Spring balance	359
1. Design	359
2. Magnet	360
3. Procedure	361
4. Calibration	361
V. Factors affecting precision and accuracy	361
1. Smoothness of surface	362
2. Curvature of surface	363
3. Thickness of base metal	363
4. Magnetic properties of base metal	363
5. Magnetic properties of coatings	365
VI. Typical results	366
VII. Conclusions	368

I. INTRODUCTION

During recent years, the interest in tests for the thickness of metallic coatings has been increased by the adoption of specifications for plated coatings. Most methods of testing destroy the coating and sometimes the whole specimen. It is desirable to have nondestructive methods which will permit the testing of a larger number of specimens without increased cost. Such methods will be useful especially for plant control.

In a previous publication,[1] a nondestructive magnetic method was described for measuring the thickness of nickel coatings on nonmagnetic base metals, such as copper or brass. The present work is

[1] J. Research NBS 18, 565 (1937) RP994.

an extension of magnetic methods to the testing of nonmagnetic coatings upon steel.

Methods for the latter purpose have received attention during the last few years, and several papers on this subject appeared while this research was in progress. The purpose of this paper is to describe a simple, compact, magnetic instrument for such measurements and to discuss the accuracy of the method.

II. PRINCIPLES INVOLVED

The method for measuring the thickness of nickel plating on brass depends on the magnitude of the attractive force between a magnet and the nickel coating. The method to be described for the measurement of nonmagnetic coatings on steel depends on the decrease in magnetic attraction caused by the presence of a nonmagnetic coating between a magnet and the steel base metal.

The maximum attractive force between a magnet and steel is obtained when the two are in contact. Any nonmagnetic material, such as zinc, copper, enamel, paint, or an air gap, placed between the magnet and the steel, decreases the magnetic attraction to an extent that depends upon the thickness of the intervening layer. If a device with a permanent bar magnet is calibrated with nonmagnetic coatings of known thickness on steel, it can be used to determine the thicknesses of other nonmagnetic coatings. The measurement consists in bringing the end of the magnet into contact with the coating on the steel and determining the force necessary to detach the magnet. The thickness is read off from the appropriate calibration curve, on which the decrease in the detaching force is plotted against the thickness.

III. TYPES OF INSTRUMENTS

For measuring the attractive forces involved, any instrument can be used which will measure a force of several grams with an error of not more than 1 percent. An ordinary analytical balance may be used. Recently, W. E. Hoare and B. C. Chalmers [2] described a device in which a permanent magnet is attached to one arm of an improvised lever balance. The detaching force is measured in terms of the weight (or volume) of water which is introduced into a graduated cylinder attached to the other arm. This instrument was used for measuring the thickness of coatings on tin plate.

For similar measurements, I. V. Radtchenko and F. K. Shestakovsky [3] used a magnet suspended from a galvanometer needle, the attractive force being measued in terms of the current through the galvanometer that was required to detach the magnet from the coating.

The General Electric Co.[4] manufactures an electric gage with which the thickness of a coating is measured by the reluctance of a magnetic circuit passing from a coil in the gage head, to the steel base, through the coating. This instrument measures thickness in terms of an electric current instead of an attractive force. It is useful chiefly for measuring coatings at least several thousandths of an inch thick, such as vitreous enamels, and has not been adapted to plated coatings,

[2] J. Sci. Instr. 14, 248 (1937).
[3] J. Tech. Phys. U. S. S. R. 5, 1372 (1935).
[4] Instruments 8, 341 (1935); Enamelist, p. 9 (Nov. 1936).

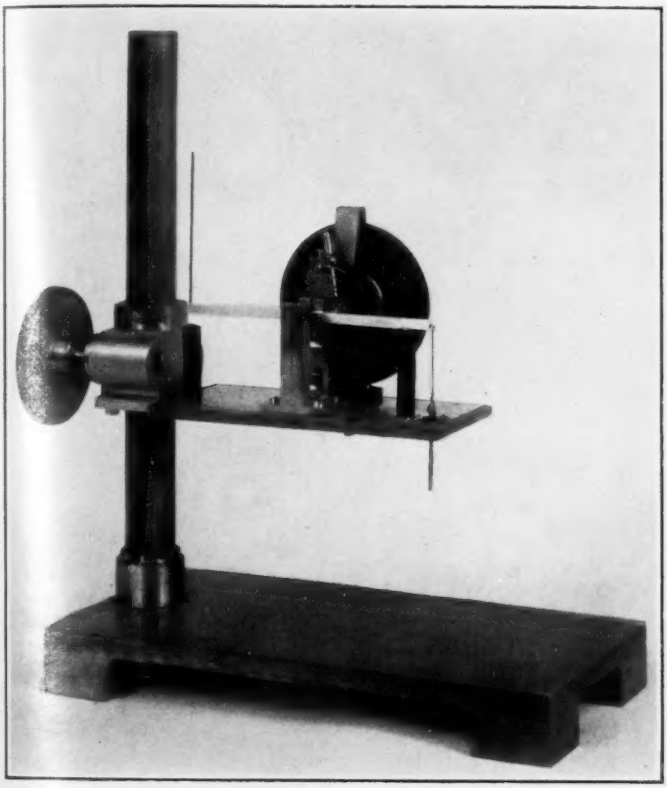

FIGURE 1.—*Spring balance with cover and false bottom removed.*

which are usually less than one thousandth of an inch thick. One disadvantage of this gage, as designed, is that it can be used only on plane surfaces. Recently, W. H. Tait [5] described an instrument that is similar in principle to the General Electric gage, and used it for measuring the thickness of thin coatings, such as those on tin plate.

IV. SPRING BALANCE

1. DESIGN

A spring balance, figure 1, may be used for measuring the thickness of nonmagnetic coatings on steel. The instrument is of the same

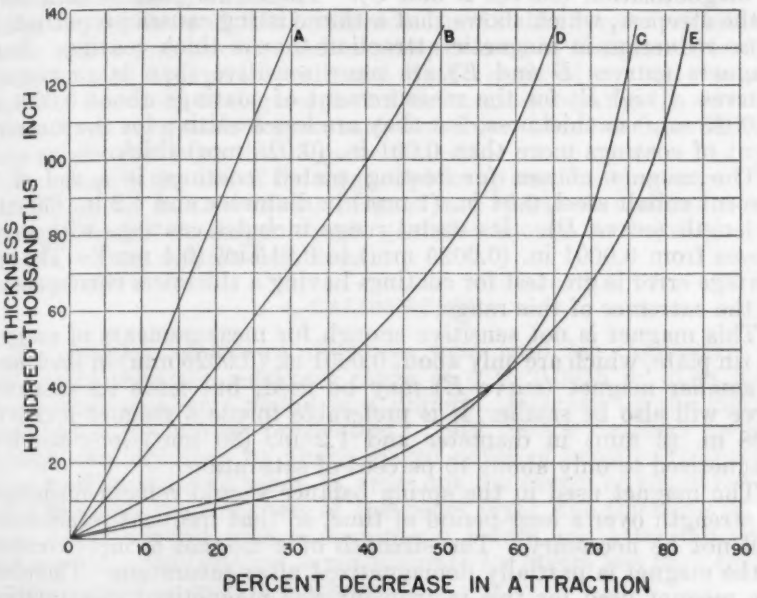

FIGURE 2.—*Percentage decrease in the attraction of various magnets for mild steel, caused by the interposition of nonmagnetic coatings*

Curve	Magnet				Magnetic saturation	Attractive force for uncoated steel
	Diameter		Length			
	in.	mm	in.	mm	*Percent*	g
A	0.2	5	6	150	100	270
B	.08	2	1.2	30	100	41
C	.08	2	1.2	30	15	6
D	.04	1	1.2	30	80	6
E	.03	.75	1.2	30	100	2.5

type as that described for measuring the thickness of nickel coatings on nonmagnetic base metals.[6] The principal differences are that in the present instrument the magnet is smaller and the spring stronger.

[5] J. Sci. Instr. 14, 341 (Oct. 1937).
[6] J. Research NBS 18, 565 (1937) RP994.

The magnet is freely suspended from one end of a horizontal Duralumin lever arm, which carries a vertical brass needle for indicating the position of the magnet. The magnet slides through a glass bead which prevents sidewise movement. The end of the magnet is hemispherical and polished.

2. MAGNET

The choice of a magnet is somewhat arbitrary and depends on the range of thicknesses to be measured. Curves for the decrease in attractive force against thickness of coating for magnets of various sizes are shown in figure 2. The shape of the curve depends on both the dimensions of the magnet (curves *A*, *B*, *D*, and *E*) and its degree of magnetization (curves *B* and *C*). The initial part of each curve is the steepest, which shows that a thin coating causes proportionally more reduction in magnetic attraction than a thick coating. Small magnets (curves *D* and *E*) are more sensitive than large magnets (curves *A* and *B*) for the measurement of coatings about 0.0001 in. (0.0025 mm) in thickness, but they are less sensitive for the measurement of coatings more than 0.001 in. (0.025 mm) thick.

The magnet chosen for testing plated coatings is a rod of 36 percent cobalt steel, 0.04 in. (1 mm) in diameter and 1.2 in. (30 mm) in length (curve *D*). Its useful range includes coatings with thicknesses from 0.0001 in. (0.0025 mm) to 0.015 in. (0.4 mm). The percentage error is greatest for coatings having a thickness corresponding to the extremes of this range.

This magnet is not sensitive enough for measurements of coatings on tin plate, which are only about 0.0001 in. (0.0025 mm) in thickness.[7] A smaller magnet (curve *E*) may be used, but since its attractive force will also be smaller, it is preferable to use a magnet (curve *C*) 0.08 in. (2 mm) in diameter and 1.2 in. (30 mm) long which is magnetized to only about 15 percent of saturation.

The magnet used in the spring balance should remain unchanged in strength over a long period of time, so that frequent recalibration will not be necessary. The strength of a magnet is more constant if the magnet is partially demagnetized after saturation. Therefore, the magnet used for this instrument was magnetized to saturation, and then demagnetized to about 80 percent of saturation, by bringing a larger magnet near it. A magnet so treated retains its strength indefinitely provided that only the end comes into contact with steel. However, if the magnet is stroked from the center towards the end, or vice versa, with a piece of steel, its strength is decreased. By continued stroking, the strength of small magnets may be reduced to 40 percent of saturation. Loss of magnetism by accidental contact of the shaft of the magnet with steel is prevented by encasing the magnet in a glass tube with thin walls (0.02 in. or 0.5 mm thick) so that the end projects only a very short distance beyond the end of the tube.

The instrument, as developed, has several advantages over the types previously described. The advantages of an instrument employing a permanent magnet over the electrical devices are that (1) measurements with the former are scarcely influenced by the curvature of a surface, and (2) it measures the thickness of coating at a

[7] Much of the commercial tin plate has about 2 lb of tin per base box. Each "pound per base box" corresponds to a thickness of about 0.00006 in. (0.0015 mm) of tin.

point rather than over an area. The present design of instrument is simpler, more compact and more rugged than those previously described that also employed a permanent magnet.

3. PROCEDURE

Measurements with the instrument are made by bringing the end of the magnet into contact with the coating and then turning the dial until the magnet is detached. The first reading is approximate and several more readings should be taken and averaged. The dial should be turned quite slowly in the neighborhood of the point of detachment of the magnet. Dial readings are converted to thicknesses by means of a calibration curve, or the dial may be graduated to read thicknesses directly.

The test specimen should be placed normal to the magnet. Measurements with a freely suspended magnet, as used in the present instrument, are not appreciably affected if the angle of contact varies a degree or two from 90 degrees; but if the magnet were rigidly attached to the lever arm, each degree variation from the normal would produce an error of more than 3 percent.

Occasionally the end of the magnet picks up small magnetic particles which prevent contact of the magnet and specimen and cause low, nonreproducible readings. Such particles should be brushed from the end with a camel's-hair brush.

4. CALIBRATION

Zinc coatings of known thickness were used for calibrating the instrument over the thickness range of 0 to 0.0015 in (0.04 mm). These specimens were plated to a uniform thickness by the method described in a previous publication.[8] Still thicker coatings for calibration were obtained by gluing glazed paper of known thickness to sheet steel, care being taken to press out the excess of adhesive. In order to check the thickness of the paper layer, the thickness of the sheet was measured with a micrometer before and after the paper was applied. This method is not accurate for layers less than several thousandths of an inch in thickness.

The calibration is best represented by a curve such as shown in figure 4. The dial of the instrument, which is graduated into 100 divisions, is set to read 100 when the instrument is balanced in the absence of any magnetic material. The spring is so selected that the dial reads close to 0 when the magnet is detached from bare steel. By this method of setting the dial, low scale readings correspond to thin coatings and high readings to thick coatings.

V. FACTORS AFFECTING PRECISION AND ACCURACY

The factors that affect the precision and accuracy of the method are:

1. The smoothness of the surface.
2. Curvature of the surface.
3. Thickness of the base metal.
4. Magnetic properties of the base metal.
5. Magnetic properties of the coatings.

[8] J. Research NBS 18, 565 (1937) RP994.

1. SMOOTHNESS OF THE SURFACE

Lack of smoothness of the steel base metal or coating is one of the chief sources of inaccuracy with this method, and is more likely to cause errors than are differences in the magnetic properties of the steels. Occasionally it is necessary to test bare steel for the purpose of comparing it with the standard steel. Reproducible readings on bare steel can be obtained only if the surface is smooth and free from imperfections. Some cold-rolled steel has a sufficiently smooth surface, but, in general, the surface of steel must be polished before testing, either by buffing or, if the surface is too rough, by use of successively finer polishing papers. Polished steel surfaces give readings reproducible to about 1 percent, while readings on rough surfaces are erratic.

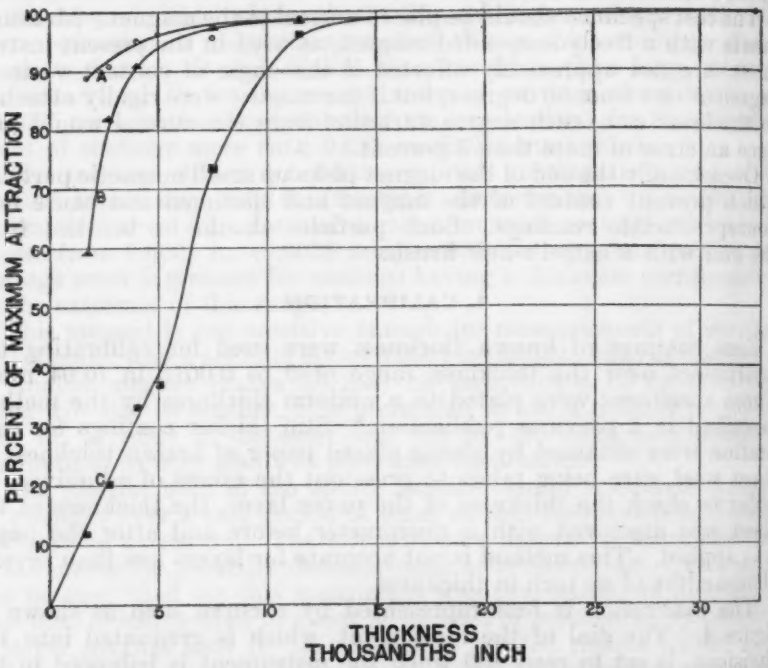

FIGURE 3.—*Attractive force of magnets for various thicknesses of sheet steel, expressed as percentage of the maximum force obtainable on steel*

Curve	Magnet			
	Diameter		Length	
	in.	mm	in.	mm
A	0.04	1	1.2	30
B	.08	2	1.2	30
C	.20	5	6.0	150

The effect of roughness of the base metal or coatings on the accuracy is most pronounced with coatings less than 0.001 in. (0.025 mm) thick. The smoothness of the coating is even more important than

that of the base metal; in fact the reproducibility of readings is fairly good on smooth coatings even though they are produced on a rough base metal. For example, fairly reliable readings are obtained on galvanized zinc surfaces (which are wiped smooth in the manufacturing process), even though the base metal may have been severely etched prior to galvanizing.

It was found that more reproducible and accurate measurements on rough coatings can be obtained if the coating is burnished at the point to be tested, just enough to produce a smooth area about 0.1 in. (3 mm) in diameter. A suitable tool for the purpose consists of a 0.5 in. (1.3 cm) ball bearing soldered to a rod. A drop of oil is applied before burnishing. It is necessary to use burnishing only if the readings on a surface are not reproducible. It may be used with advantage on rough or coarsely crystalline coatings of zinc, cadmium, or copper, but is unnecessary on galvanized sheet, terne plate, or tin plate, or on any coatings more than 0.001 in. (0.025 mm) thick.

2. CURVATURE OF THE SURFACE

Magnetic measurements with a magnet 0.04 in. (1 mm) in diameter are not affected very much by curvature. No appreciable error is involved in measurements on cylindrical rods more than 0.125 in. (3 mm), or on spheres more than 0.5 in. (13 mm) in diameter. Measurements are not affected by the proximity of an edge, if the magnet is at least 0.08 in. (2 mm) from it.

3. THICKNESS OF THE BASE METAL

The curves in figure 3 show that the thickness of the base metal does not affect the accuracy of measurements made with a 0.04-in. (1-mm) magnet if the base metal is more than 0.01 in. (0.25 mm) thick. The attractive force between very thin sheet steel (less than 0.005 in. thick) and the largest magnet used (curve C) is almost proportional to the thickness of the sheet (which relation also exists with thin layers of nickel).

4. MAGNETIC PROPERTIES OF THE BASE METAL

The nature of the ferrous base metal affects magnetic measurements, and separate calibrations should be made for metals which vary by more than about 5 percent in magnetic properties (as measured by their magnetic attraction). The attractive forces between a small magnet and many different specimens of mild steel, such as are used in stamping and forming operations, were determined and found not to vary more than a few percent. Hence, with one calibration, measurements can be made on the majority of plated iron or steel products. Figure 4 illustrates calibration curves for several ferrous metals. Curve *A* was drawn through points for zinc coatings on various steels. All these points are within ± 4 percent of the average curve. Coatings on malleable cast iron would also be represented by this curve.

Certain high-carbon steels, and also gray cast iron, require separate calibrations. Gray cast iron (curve *B*) is attracted by the magnet with only about 90 percent of the force exerted by mild steel. How-

ever, the curve approaches that for mild steels (curve A) at about 0.001 in. (0.025 mm). Hence, for coatings thicker than 0.001 in., the calibration curve for mild steels will serve for practically any ferrous metal. Curve C is an extension (on a different scale) of curve A to thicker coatings. From 0.001 in. on, it agrees with the curve for cast iron within about one-half scale division.

Whether or not coatings on a given ferrous metal will fit a certain calibration curve can be determined by taking a reading on the uncoated metal (suitably polished). If the attractive force of a particular metal does not vary by more than two scale divisions

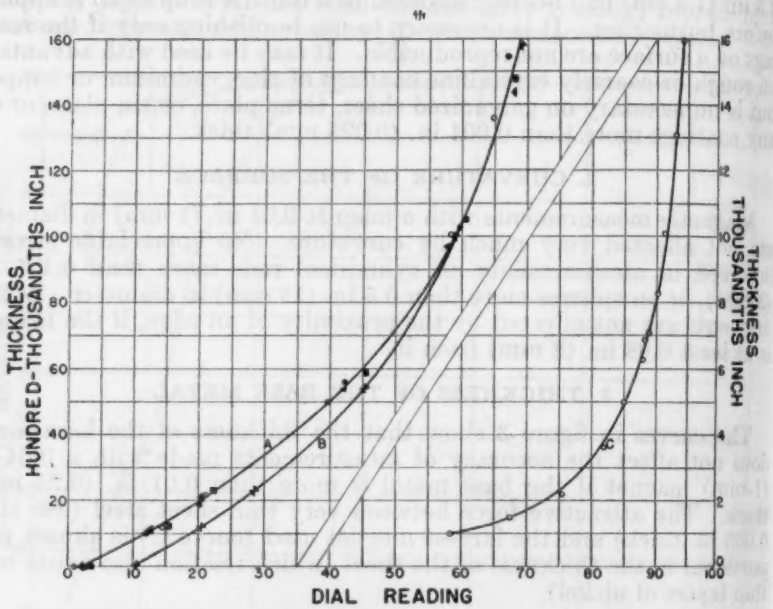

FIGURE 4.—*Calibration curves for various ferrous base metals*

Curve A is an average curve for the following steel base metals:
○=Cold-rolled steel, 0.033 inch thick.
▼=Sheet steel, 0.012 inch thick.
■=Spring steel, 0.15 inch thick.
●=Drill rod, 0.25 inch in diameter.
Curve C is an extension of curve A (on a different scale) to thicker coatings.
Curve B is the calibration curve for gray cast iron, 0.15 inch thick.

from that of the steel used for calibration, the error involved in the measurement of coatings thicker than 0.0001 in. (0.0025 mm) will not be significant. However, if the reading on the base metal varies by more than this amount, a correction should be applied to the dial readings obtained on coatings that are thinner than about 0.0005 in. (0.013 mm). This correction is made by adding to or subtracting from the dial reading F, a quantity equal to $D(1-T)$, where D is the difference (in scale divisions) between the initial reading on the standard steel and on the uncoated specimen, and T is the thickness of coating in 1/1000 in. For example, if a sample of iron gave an initial reading of plus 4 divisions (D), while that on the standard steel was 0, and, with a coating approximately 0.0003 in. thick, the dial reading, F, was 35, the latter should be corrected as follows:

$$F_1=F-D(1-T)=35-4(1-0.3)=32.2$$

The thickness should then be read from the standard calibration curve at the point corresponding to 32.2 divisions and not 35 divisions. It will be noted that when $T=1$, i. e., 0.001 in., the correction becomes 0.

If a metal differs by more than 5 divisions (or about 5 percent) from the standard steel, it is preferable to make a separate calibration curve for coatings on that metal, rather than to apply a correction for thin coatings.

5. MAGNETIC PROPERTIES OF COATINGS

Thus far, the discussion has been confined to measurements of nonmagnetic coatings. Measurements can be made also of magnetic nickel coatings on steel because with the magnets used the nickel exerts only about one-half as much attraction as does the steel. A separate calibration is required for nickel coatings. The curves given in figure 5 (to be compared with fig. 4) show that the interposition of nickel coatings does not decrease the attraction of the magnet for the steel as much as do corresponding nonmagnetic coatings. Hence, measurements of nickel coatings on steel may be expected to be less accurate than measurements of nonmagnetic coatings. There is a compensating factor, however. Most nickel coatings are deposited over a smooth steel surface and are themselves polished, so that more reproducible readings are obtained. Nickel coatings much over 0.001 in. (0.025 mm) in thickness cannot be measured magnetically because beyond that range of thickness the attractive force changes too slowly with the thickness. The calibration curve for nickel should be checked more frequently than the one for nonmagnetic coatings, because a small error in the dial reading produces a larger error in determining the thickness of nickel than of nonmagnetic coatings.

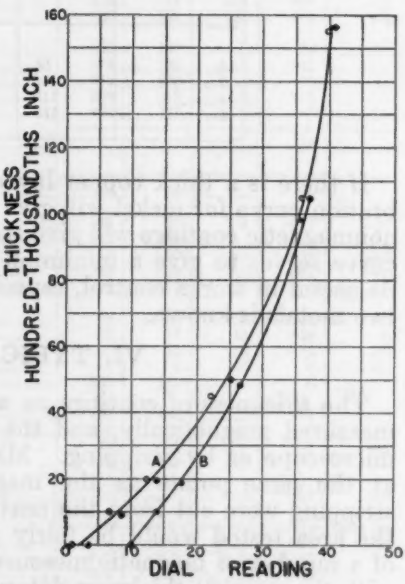

FIGURE 5.—*Calibration curves for nickel coatings on ferrous base metals.*

Curve *A* is an average curve for the following steels:
○ = Cold-rolled steel, 0.033 inch thick.
■ = Spring steel, 0.15 inch thick.
Curve *B* is for gray cast iron, 0.15 inch thick.

The variation in the magnetic properties of nickel coatings will not have much effect on the accuracy of measurement. Nickel deposited from a "single salt" bath operated at a high pH (5.9) is only 40 percent as magnetic (according to its attractive force for a small magnet) as nickel deposited under ordinary conditions. Magnetic tests of coatings 0.0005 and 0.001 in. thick, deposited under the above conditions on steel, gave results about 10 and 25 percent too high, respectively. In commercial plating, the variation in the magnetic prop-

erties of nickel is less than half of that represented by the above specimens and hence should not cause errors greater than about 10 percent in the magnetic measurement of thickness.

Composite coatings of nickel and copper can be measured magnetically only if the copper layer is less than 10 percent of the total. The accuracy of measurements on nickel coatings plated over a copper flash is shown in table 1.

TABLE 1.—*Thickness of composite copper-nickel coatings*

[Thickness of coating in hundred-thousandths in.]

Copper	Nickel	Total	Total by magnetic method	Error
				Percent
3	54	57	60	+5
7	54	61	69	+13
4	115	119	126	+6
8	113	121	144	+16

If there is a thick copper layer in the composite coating, the calibration curve for nickel will give too high a result, and the curve for nonmagnetic coatings will give too low a result. However, the latter curve serves to give a minimum thickness for the deposit, and may be useful in works control, especially if the approximate ratio of the two metals is known.

VI. TYPICAL RESULTS

The thickness of coatings on a number of commercial articles was measured magnetically, and the results were checked either with a microscope or by stripping. Microscopic measurements were made at the same points as the magnetic measurements. Samples for stripping were cut from the central portion of the specimen, so that the area tested would be fairly uniform in thickness. The average of a number of magnetic measurements on the sample was compared with the average thickness determined by stripping the same sample.

Table 2 summarizes the results of measurements on about 50 commercially plated articles. Those coatings that were not smooth were measured both before and after burnishing. In nearly all cases the burnishing gave more accurate results in addition to improving the reproducibility of the readings. The average error of the method is about ± 10 percent for coatings thicker than 0.0002 in. (0.005 mm). Measurements of electrodeposited coatings of good quality and of smooth painted or enameled surfaces are generally satisfactory. Measurements on galvanized sheet were about 10 percent low, perhaps because of the presence of zinc-iron alloys. Results on tin plate are about 25 percent low, but all the coatings tested were very thin, for example, only 0.0001 in. (0.0025 mm) in thickness. If measurements on tin plate are consistently low, an appropriate curve can be based on calibration with similar coatings. The low results may be due to the formation of an alloy layer.[9]

[9] E. F. Kohman and N. H. Sanborn. Ind. Eng. Chem. 19, 514 (1927).

TABLE 2.—*Thickness of commercial coatings*

Coating		Article	Average thickness in hundred-thousandths inch			Error of magnetic method	
				Magnetic			
Metal	Process		Stripping	Unburnished	Burnished	Unburnished	Burnished
						Percent	*Percent*
Zinc	Hot galvanized	Sheet	116	105		−10	
Do	do	do	132	120		−9	
Do	do	do	104	85		−18	
Do	do	do	139	121		−13	
Do	do	do	114	115	111	+1	−3
Do	do	do	129	127	124	−2	−4
Do	do	do	720	630		−13	
Do	do	Pipes	174	155		−11	
Do	do	do	312	250		−20	
Do	do	Conduit boxes	338	310		−8	
Do	do	do	465	443		−5	
Average error.						−10	
Do	Sherardized	do	56	58		+4	
Do	Electroplated	Lock-arm	18	21	16	+17	−11
Do	do	Wire, 0.09 inch diameter	222	230		+4	
Do	do	BX cable	42	50	45	+19	+7
Do	do	do	43	48	45	+12	+5
Do	do	Stamping	13	14	14	+7	+7
Do	do	do	15	16	14	−7	−7
Do	do	do	15	18	15	+20	0
Do	do	Bolt	17	15	12	−12	−29
Do	do	Washer	9	9	7	0	−19
Do	do	Conduit	152	152		0	
Do	do	do	167	165		−1	
Do	do	do	115	122		+6	
Do	do	do	77	71	74	+8	+4
Do	do	do	115	122	122	+6	+6
Average error.						±9	±9
Cadmium	do	Machine part	16	21.5	19.2	+34	+20
Do	do	do	8.2	9.0	8.0	+10	−3
Do	do	Stamping	8.2	7.0		−15	
Do	do	do	7.2	7.6		+6	
Do	do	do	24	27	25	+13	+5
Average error.						±16	±9
Chromium	do	AES specimens	24	24		0	
Copper	do	do	47	52	48.5	+10	+3
Terne plate	Hot-dipped	Sheet, thick. 0.009 in	6.5	6.5		+2	
Do	do	Sheet, thick. .015 in	93	94		+1	
Do	do	Sheet, thick. .011 in	70	64	58	−9	−17
Do	do	Sheet, thick. .016 in	63	62	64	−2	+2
Average error.						±4	
Tin	do	Tinplate sheet, 0.010 thick.	11.2	8		−29	
Do	do	do	12.3	8		−35	
Do	do	do	7.5	5.6		−25	
Do	do	do	11.0	9.0		−18	
Do	do	do	7.1	6.3		−11	
Average error.						−24	

TABLE 2.—*Thickness of commercial coatings*—Continued

Coating		Article	Average thickness in hundred-thousandths inch			Error of magnetic method	
				Magnetic			
Metal	Process		Stripping	Unburnished	Burnished	Unburnished	Burnished
						Percent	*Percent*
Paint	Spray	Refrigerator	[a] 88	95		+8	
Do	do	do	199	193		−3	
Porcelain enamel	Vitreous	do	[b] 1,600	1,530		−4	
			Local thickness, microscopic				
Nickel	Electroplated	Electric-iron cover, outs	105	100		−5	
Do	do	Electric-iron cover, ins	19	22.5	18.5	+18	−3
Do	do	Electric-iron base, cast iron.	60	58		−3	
Do	do	Bumper bar	37	42		+14	
Do	do	AES specimens, buffed	59	56		−5	
Do	do	do	51	48		−6	
Do	do	do	47	45		−4	
Do	do	do	44	43		−2	
Do	do	do	40	42		+5	
Do	do	AES specimens, unbuffed	61	68	62	+11	+2
Do	do	do	55	64	56	+16	+2
Average error.						±8	

[a] Thickness by chord method.
[b] Thickness by micrometer.

VII. CONCLUSIONS

The magnetic method has been shown to be accurate enough for most commercial requirements. In most cases the method is nondestructive because it is not often necessary to test the base metal. The steel base metal of articles that have been through forming operations usually need not be tested, as they are very probably made of mild steel. If the coating is thicker than 0.001 in. (0.025 mm) the base metal need not be tested, since the calibration curves for thick coatings on many ferrous metals tend to approach each other. Therefore, a single calibration curve for nonmagnetic coatings on mild steel will fill the majority of needs. In plant control the magnetic properties of the base metal should be determined before plating.

Polished nickel coatings up to 0.001 in. in thickness can be measured (with an appropriate calibration curve) with about the same degree of accuracy as nonmagnetic coatings. On rough coatings, lack of reproducibility of measurements is serious for coatings thinner than 0.001 in. (0.025 mm). This difficulty can usually be removed by burnishing the coating before testing.

The author acknowledges the advice and assistance received from R. L. Sanford and W. Blum in this investigation.

WASHINGTON, January 18, 1938.

U. S. Department of Commerce National Bureau of Standards

RESEARCH PAPER RP1082

Part of Journal of Research of the National Bureau of Standards, Volume 20, March 1938

A METHOD FOR THE INVESTIGATION OF UPPER-AIR PHENOMENA AND ITS APPLICATION TO RADIO METEOROGRAPHY

By Harry Diamond, Wilbur S. Hinman, Jr., and Francis W. Dunmore

ABSTRACT

Experimental work conducted for the U. S. Navy Department on the development of a radio meteorograph for sending down from unmanned balloons information on upper-air pressures, temperatures, and humidities, has led to radio methods applicable to the study of a large class of upper-air phenomena. The miniature transmitter sent aloft on the small balloon employs an ultrahigh-frequency oscillator and a modulating oscillator; the frequency of the latter is controlled by resistors connected in its grid circuit. These may be ordinary resistors mechanically varied by instruments responding to the phenomena being investigated, or special devices the electrical resistances of which vary with the phenomena. The modulation frequency is thus a measure of the phenomenon studied. Several phenomena may be measured successively, the corresponding resistors being switched into circuit in sequence by an air-pressure-driven switching unit. This unit also serves for indicating the balloon altitude. At the ground receiving station, a graphic frequency recorder, connected in the receiving set output, provides an automatic chart of the variation of the phenomena with altitude. The availability of a modulated carrier wave during the complete ascent allows of tracking the balloon for determining its azimuthal direction and distance from the receiving station—data required in measuring the direction and velocity of winds in the upper air.

CONTENTS

	Page
I. Introduction	370
II. Classification of prior and contemporary developments	370
III. Basis of our method	371
IV. Transmitting-circuit arrangement	372
V. Ground-station receiving equipment	373
VI. Applications of our method in simplified forms	374
VII. Measurement of cloud height and thickness	375
VIII. Altitude determination	376
1. Pressure switching	377
IX. Navy radio meteorograph	379
1. Pressure-switching circuit arrangement	379
2. Temperature capillary tube	381
3. Meteorograph unit	383
4. Complete radio-meteorograph assembly	384
5. Sample record of an ascension	384
6. Calibrating procedure	387
X. Electrical hygrometer	389
XI. Other applications of the general method	389
XII. References and notes	391

I. INTRODUCTION

The use of special radio equipment carried aloft in unmanned balloons for the investigation of upper-air phenomena has attracted the attention of a number of scientific workers during recent years. A large class of phenomena may be conveniently studied by such methods at relatively low cost. Examples of such phenomena include meteorological elements, such as barometric pressure, air temperature, humidity, wind velocity, cloud height, and vertical thickness; radio-wave propagation; light intensity in various parts of the light spectrum; electrical conductivity and voltage gradient; cosmic-ray intensities, etc. Measurements of these phenomena may be carried out at predetermined fixed altitudes or as a function of altitude. In general, besides providing means for translating the variation of the phenomenon to be measured into radio signals which may be interpreted on the ground, the apparatus carried aloft must also transmit information on the altitude of the balloon. In several of the applications, such as the determination of upper-air wind velocities and radio-propagation studies, it is also necessary to know the distance to the balloon, which may be determined by radio direction-finding methods. It is thus desirable that the type of radio emission employed on the balloon be continuous in order to facilitate direction finding.

This paper describes a radio method which fulfills the three requirements just outlined and appears particularly adaptable for the study of certain of the phenomena enumerated. The principal objective of our experiments has been the development of a radio-meteorograph system for use in the aerological service of the U. S. Navy Department, at the request of that Department. However, as will appear from a description of the method and apparatus evolved, its properties permit of a considerably broader field of application.

II. CLASSIFICATION OF PRIOR AND CONTEMPORARY DEVELOPMENTS

In general, most upper-air phenomena may be measured in terms of the deflection of mechanical instruments or of changes in the properties of electrical devices. For transmitting these measurements by radio to a receiving station on the ground it is necessary to convert the mechanical deflection or the change in electrical properties into an interpretable characteristic of the radio emission. Means for accomplishing this conversion may be divided into three general classifications according to their operation. In one class, the angular deflections from fixed references of the pointers of one or more mechanical instruments are interpreted in terms of time intervals. The various arrangements of the Olland type radio meteorograph developed in this country and abroad [1] [1] are representative of this class. A rotating contactor, propelled by a clock or other drive, makes contact as it passes pointers which are controlled by changes in pressure, temperature, and humidity, and thereby keys the radio transmitter. The time intervals between these contacts and others which the rotating contactor makes regularly with fixed points may be interpreted as definite values of pressure, temperature, and humidity. A special case of this class consists in converting electrical impulses into the

[1] Figures in brackets throughout this paper relate to references given on pages 391–392.

operation of a relay for keying the balloon transmitter, the frequency of keying being a measure of the intensity of the phenomenon producing the impulses. This method has been applied to the study of cosmic rays [2].

In a second class, the deflections of the pointers are interpreted in terms of some measuring scale independent of time. The radio meteorographs developed by Moltchanoff [3] and Bureau [4] and the pressure indications employed by Duckert [5] are representative of this class. In the Moltchanoff arrangement, the pointer deflections are interpreted in terms of coded signals repeated in distinctive groupings. In Bureau's arrangement, the pointers are grouped, as in the Olland method; however, the rotating contactor carries with it a means for mechanically modulating the transmitter, so that the angular deflection of a given pointer from its zero reference is interpreted in terms of the number of cycles of the modulation occurring between the corresponding contacts rather than in terms of the intervening time. In the Duckert instrument, the barometer serves to interrupt the transmitter at fixed pressure levels. By keeping track of the number of interruptions occurring from the beginning of an ascension, the pressure level corresponding to a given interruption may be determined.

In the third class, the deflections of mechanical instruments or the changes in properties of electrical devices are caused to vary either the carrier frequency or the modulating frequency of the balloon transmitter, and the values of the effects studied are interpreted in terms of the frequency. In the radio meteorograph developed by Väisällä [6], three condensers, controlled respectively by mechanical instruments responsive to pressure, temperature, and humidity, and two additional calibrating condensers are successively switched into the carrier oscillator circuit. The values of pressure, temperature, and humidity are interpreted in terms of the carrier frequency. Similarly, in the Duckert radio meteorograph, a bimetallic thermometer controls a condenser which varies the carrier frequency. Feige [7] devised a modification of the Duckert radio meteorograph for measuring cloud height and vertical thickness. He substituted a photoelectric cell for the bimetallic thermometer and employed a special milliammeter, carrying a variable condenser, for controlling the carrier frequency as a function of the current through the photocell, and, hence, as a function of light brightness.

Consideration of the several means described for translating variations in the phenomena under investigation into interpretable characteristics of the emitted signals reveals that they are more suited to the use of mechanical instruments than to electrical devices. In the two cases [2, 7] discussed in this section where electrical devices are employed, their variations are first converted into mechanical deflections before they are caused to control a characteristic of the radio emission.

III. BASIS OF OUR METHOD

In our experimental work, a method was sought which would not be restricted to the use of mechanical devices. The basis for this search is the fact that a number of the upper-air phenomena which it was desired to study are best measured by means of electrical devices. In particular, there appeared to be possibilities in such a

method for eliminating the operational difficulties involved in the use of the several radio meteorographs described in the previous section. A study of such devices revealed that a considerable number of them were characterized by changes in electrical resistance as a function of the phenomena to which they were responsive. For example, the temperature coefficient of resistance of certain electrolytes is quite high, so that their variation in resistance may be used as a measure of temperature; the surface leakage resistance of certain glasses may be used as a measure of humidity; the resistance of an air gap ionized by a radioactive substance varies as a function of the barometric pressure; the equivalent resistance of a photoelectric cell varies as a function of light intensity or brightness; etc. Accordingly, a translating means was desired wherein the variation of electrical resistance was caused to vary a characteristic of the radio emission from the balloon, namely, the modulating frequency.

The negative transconductance circuit described by Herold [8] (of the voltage-controlled type), was adapted to this purpose since it provided a light-weight audio-frequency oscillator in which the generated frequency is approximately inversely proportional to the grid-circuit resistance. With this translating means, electrical devices having inherent resistance variation as a function of some phenomenon may be connected directly in the grid circuit, while the deflection of a mechanical instrument responsive to some phenomenon is readily converted into the variation of a grid-circuit resistor.

An added advantage of the negative-transconductance circuit is that the generated audio frequency is also a function of the bias voltage on the control grid so that electrical devices producing a variable current through a constant grid-circuit resistor may also be made to vary the modulating frequency of the emitted radio wave. For example, a Geiger counter may be connected in a suitable resistance-capacitance network to supply a variable current to the grid-circuit resistor, the average value of this current being directly proportional to the frequency of the counter breakdown. The generated audio frequency, varying in accordance with the resultant variations in the grid-bias voltage, will then be a measure of the cosmic-ray intensity. Similarly, the variation in electrical charge on collecting conductors may be used to produce a proportional variation in the grid-bias voltage, and, hence, the generated audio frequency of the modulating oscillator may be made a function of atmospheric potential gradient or conductivity.

A particular advantage of the translating means just described is that the continuous emission from the balloon on a constant carrier frequency facilitates the application of direction-finding methods at the ground station.

IV. TRANSMITTING-CIRCUIT ARRANGEMENT

A circuit diagram of the radio transmitting equipment used on the balloon is given in figure 1. The transmitter employs a type-1A6 tube for the audio oscillator, a type-32 tube as an audio amplifier, and a type-30 tube as a radio-frequency oscillator. The audio oscillator operates on the negative characteristic produced between grids 2 and 4 of the 1A6 tube. Its frequency-determining circuit consists primarily of the charging condenser C and of the total resistance of the

control-grid circuit. In this circuit, V is the device whose electrical resistance varies as a function of the phenomenon to be measured and R and R_2 are limiting resistors to fix, respectively, the lower and upper limits of the frequency range covered. (A range of from 20 to 200 c/s has been employed in practically all of our experiments). The generated frequency is, however, also dependent to considerable extent upon the value of the charging resistor, R_3, upon the plate-battery voltage, the internal-battery resistance (which adds to the charging resistance), and, to lesser degree, upon the filament-battery voltage. The frequency is also affected by radio-frequency feedback into the grid circuit which operates to change the effective control-grid bias. The voltage-regulating neon tube in figure 1 is employed to minimize the effect of variations in the plate-battery voltage and in its internal resistance. The audio amplifier serves to reduce the radio-frequency

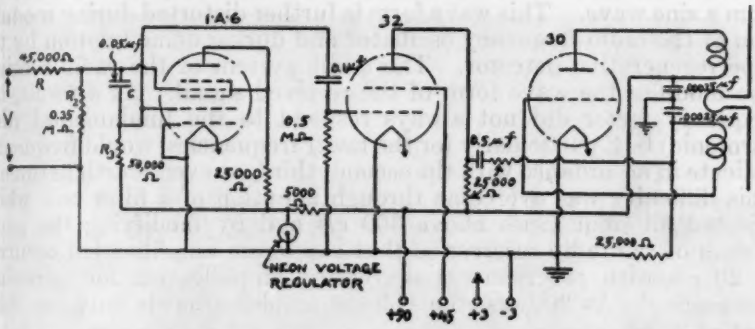

FIGURE 1.—*Electric-circuit arrangement of the radio transmitter used on the balloon.*

feedback and at the same time presents a high impedance load to the output circuit of the audio oscillator.

Grid modulation of the radio-frequency oscillator is employed, nearly complete modulation of the emitted carrier being obtained. In our experiments we have used carrier frequencies ranging from 50 to 200 Mc/s, the upper frequencies in this range being generated by means of a special type 955 acorn tube having low filament power consumption, furnished by the Radio Corporation of America.

With the various precautions used for increasing the frequency stability of the audio oscillator, as indicated, the generated frequency corresponding to a given grid-circuit resistance remains constant within ± 3 percent for changes in the filament-battery voltage of from 3 to 2 v., for changes in the plate-battery voltage of from 90 to 65 v., in the plate-battery resistance of from 100 to 1,500 ohms, in the transmitter temperature of from $+35$ to $-20°$ C., and in the antenna load of from 100 to 20 percent. These variations represent the extreme limits encountered in the usual upper-air studies.

V. GROUND-STATION RECEIVING EQUIPMENT

Figure 2 shows the ground-station receiving and recording equipment used with this method. The superregenerative receiving set, A, feeds an electronic frequency meter, B, through a suitable amplifier and electric filter unit, C. The electronic frequency meter operates to deliver a series of direct-current pulses to its indicating meter, the

average value of which ranges from 0 to 500 $\mu\alpha$ as the frequency varies from 0 to 200 c/s. This current is filtered to an average value and the voltage drop obtained by passing it through a resistor is applied to the input terminals of a high-speed recording millivoltmeter, *D*. The complete setup is essentially a recorder which converts the audio-frequency notes received in the radio-receiver output into a graphic chart. The abscissa scale of the chart may obviously be calibrated directly in terms of the phenomenon measured, provided the generated audio frequency in the balloon transmitter is a known function of the phenomenon.

In the first use of the receiving setup, considerable difficulty was experienced due to varying wave form of the received audio-frequency note. The frequency meter responds to the predominant harmonic of the voltage applied to its input terminals. The wave form produced by the audio oscillator in the balloon transmitter departs considerably from a sine wave. This wave form is further distorted during modulation of the radio-frequency oscillator and during demodulation by the superregenerative detector. The audio system of the radio receiver also modifies the wave form of the received signal. As a result, the frequency meter did not always respond to the fundamental (first harmonic) but, particularly for the lower frequencies, would frequently indicate in accordance with the second, third, or even fourth harmonic. This difficulty was overcome through adoption of a filter unit which rejected all frequencies above 300 c/s and by modifying the audio system of the radio receiver so that maximum amplification occurred at 20 c/s with progressively decreasing amplification for increasing frequencies. At 200 c/s, the voltage amplification is only one-third that at 20 c/s.

The limited frequency response of the audio circuits coupled with the operation of the frequency meter to respond only to the predominant note of a signal renders the receiving system quite free from interference. An interfering signal must have a single note below 300 c/s which is of greater intensity than the desired signal before it can take over the operation of the frequency meter and recorder.

The receiving setup is practically automatic in its operation. There is little need for retuning, except just after the transmitter has left the ground. Two separate automatic volume-control features take care of the large variation in received voltage as the distance of the balloon transmitter from the receiving station increases. The first is inherent in the operation of the superregenerative detector, while the second is provided by the frequency meter which operates accurately for a range of input voltages of from 2 to 150 v.

VI. APPLICATIONS OF OUR METHOD IN SIMPLIFIED FORMS

The operation of our method is best illustrated by means of several simplified applications. In figures 3 and 4 are shown experimental models of electrical devices designed to respond to temperature and humidity, respectively. The temperature device consists of a glass capillary tube filled with an electrolyte having a high temperature coefficient of resistance, so that its resistance is a function of temperature. The humidity device consists of a bifilar winding on the etched surface of a glass tube, the surface leakage resistance as meas-

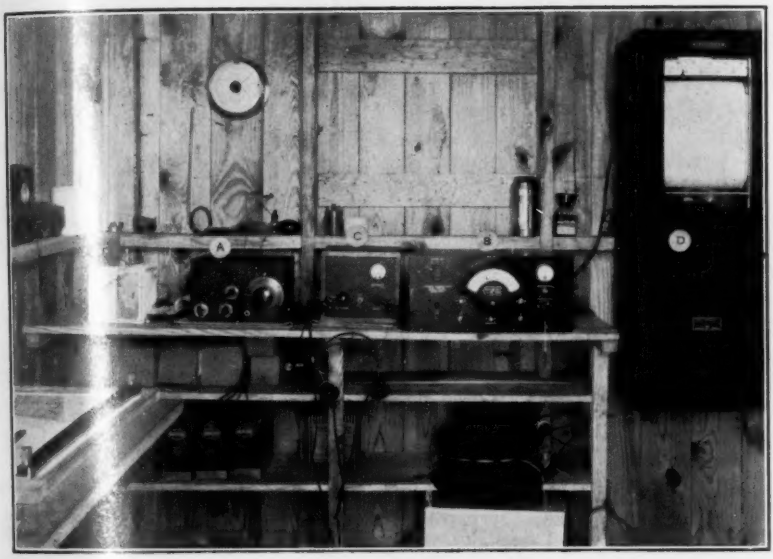

FIGURE 2.—*Ground-station receiving and recording equipment.*

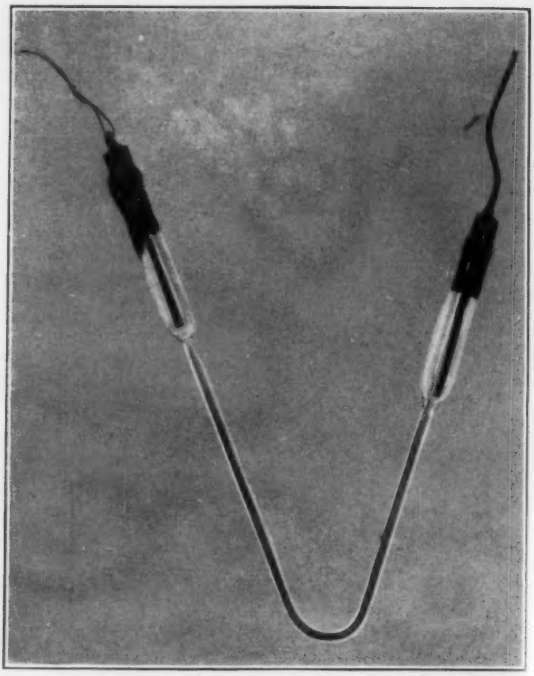

FIGURE 3.—*Capillary electrolytic thermometer.*

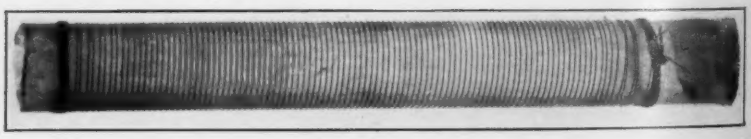

FIGURE 4.—*Electrical hygrometer.*

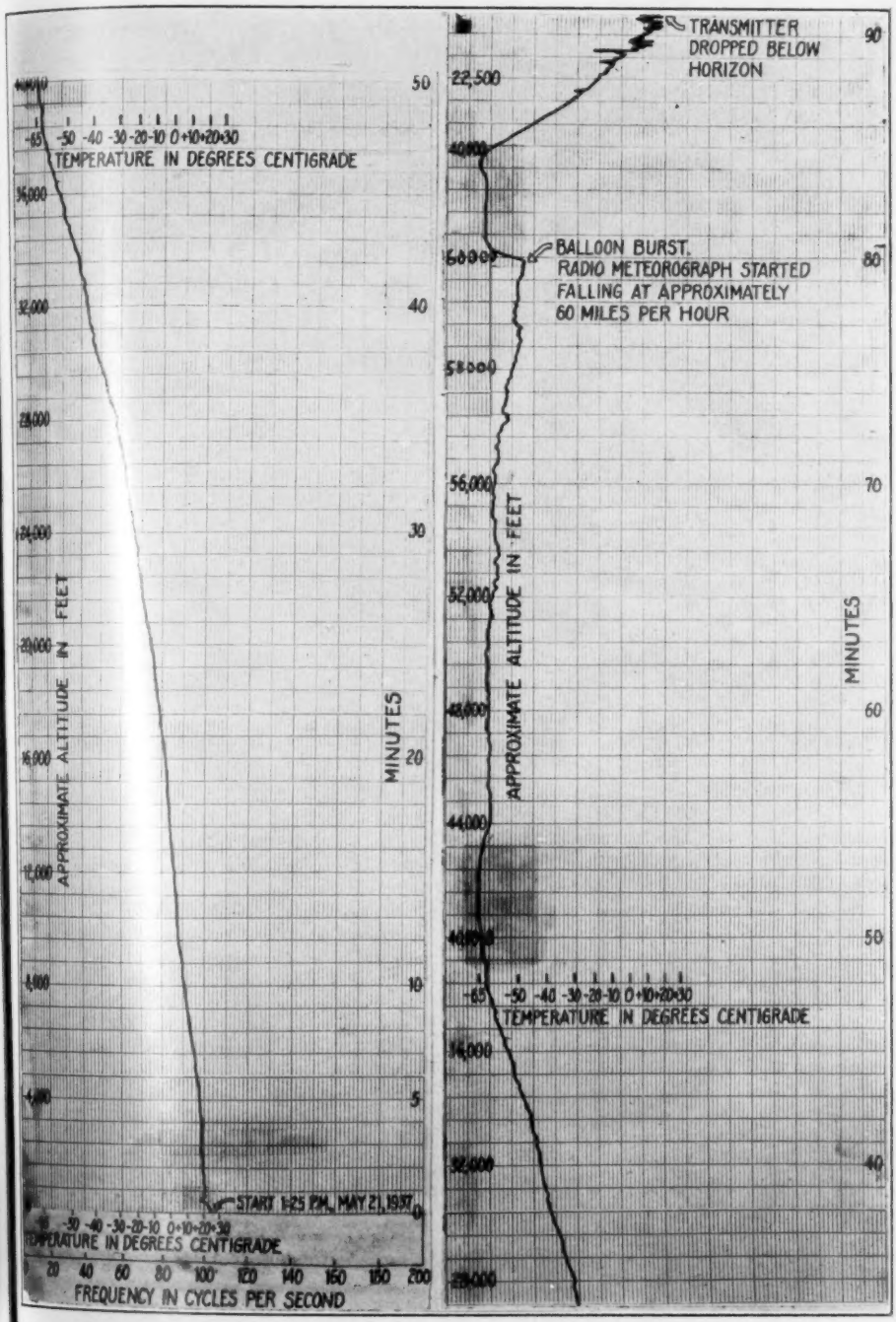
TRANSMITTER DROPPED BELOW HORIZON
BALLOON BURST. RADIO METEOROGRAPH STARTED FALLING AT APPROXIMATELY 60 MILES PER HOUR
TEMPERATURE IN DEGREES CENTIGRADE
-50 -40 -30 -20 -10 0 +10 +20 +30
APPROXIMATE ALTITUDE IN FEET
MINUTES
START 1:25 P.M. MAY 21, 1937
FREQUENCY IN CYCLES PER SECOND
20 40 60 80 100 120 140 150 200

FIGURE 5.—*Ascension record illustrating operation of electrolytic thermometer.*

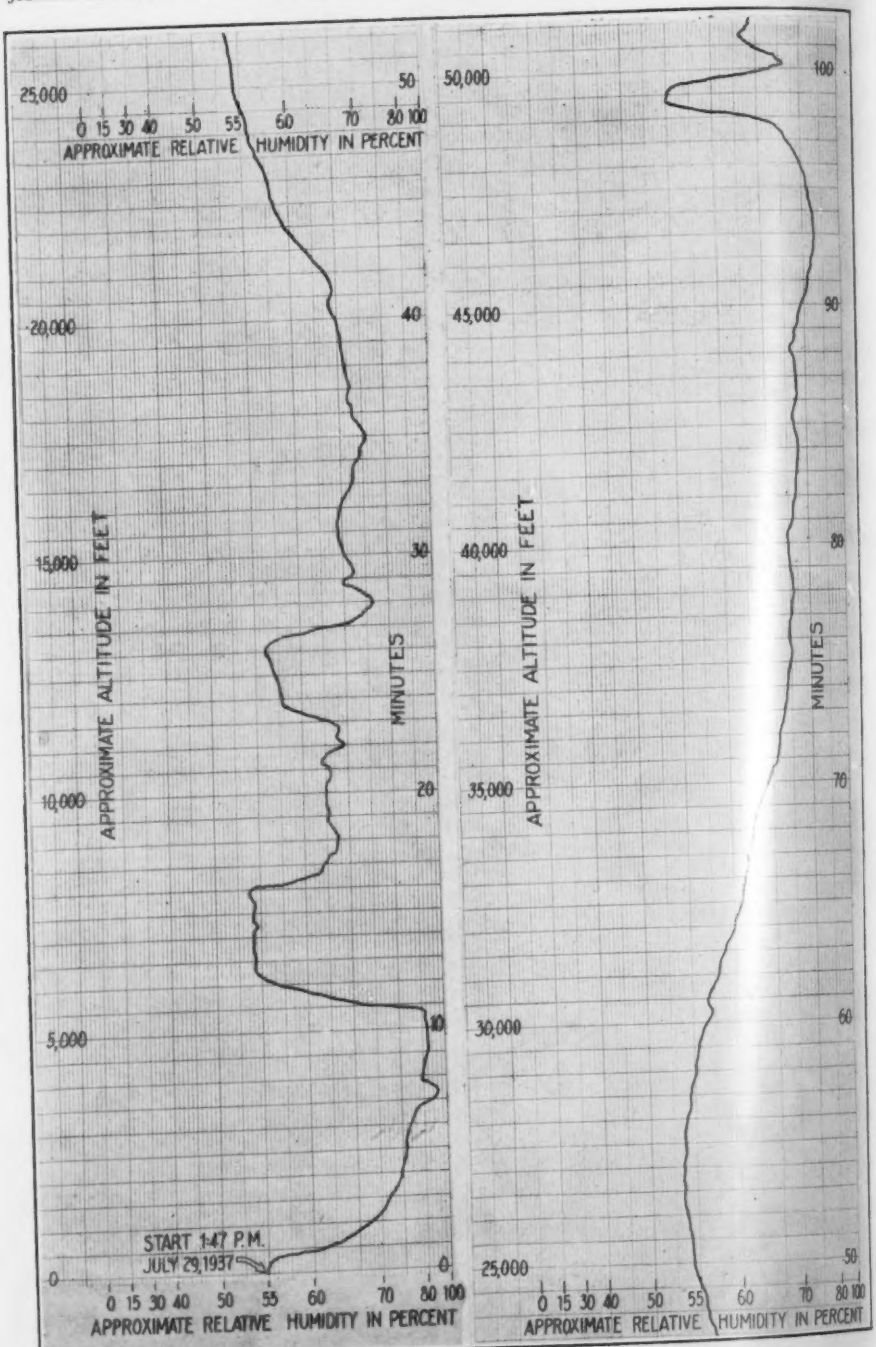

FIGURE 6.—*Ascension record illustrating operation of electrical hygrometer.*

ured between the two wires being a function of humidity. Further description of the two devices will be given in later sections. Figures 5 and 6 show typical charts obtained at the ground receiving station from ascension tests in which the temperature and humidity tubes, previously calibrated, were respectively connected in the grid circuit of the audio oscillator. The abscissas give the values of the received audio frequency and also the corresponding values of the functions measured. The ordinates show the estimated altitude of the balloon based on the amount of balloon inflation at the surface altitude. The balloon rate of ascent is approximately constant (except when the balloon is close to its bursting point) and, hence, the altitude is directly proportional to the elapsed time from the beginning of the ascent.

VII. MEASUREMENT OF CLOUD HEIGHT AND THICKNESS

A record obtained from an ascension test in which a photoelectric cell was connected in the grid circuit of the audio oscillator to give information on the variation of light brightness with altitude is shown in figure 7. Such data give a direct measure of the height to the tops of existing clouds and the visibility conditions above each cloud. The window of the photoelectric cell was pointed downward to eliminate the effect of direct sunlight upon emergence from the clouds. Heavy overcast with intermittent rain occurred on the day of the test.

Referring to the record, the abscissas represent brightness, the reference mark "dark" corresponding to complete absence of light. The ordinates represent altitude or elapsed time. As the balloon ascended it will be noted that the brightness was quite low and steady except for minor fluctuations, until the balloon reached approximately 3,800 ft. In the altitude range of from 3,800 to 5,200 ft, the increase in brightness with height indicates the presence of a cloud layer some 1,400 ft thick. The balloon, penetrating the light-absorbing layer, is moving toward the region of higher brightness.

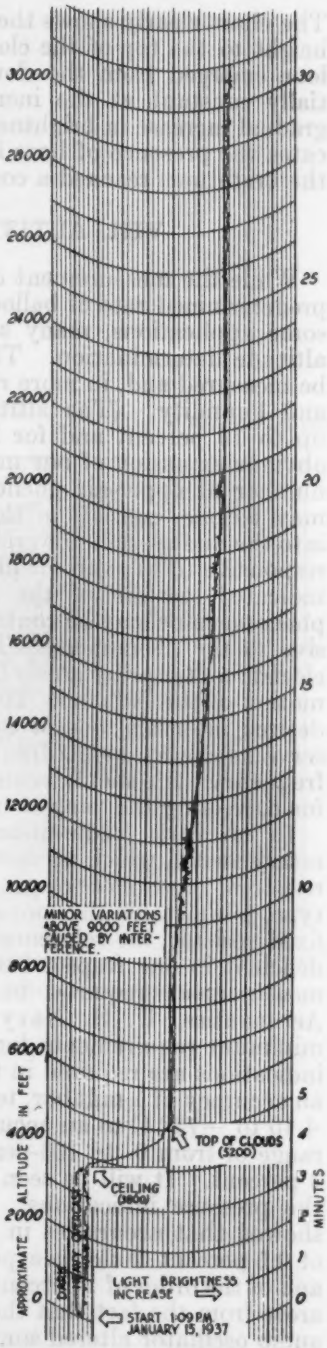

FIGURE 7.—*Ascension record illustrating use of photoelectric cell in measuring ceiling and height of top of clouds.*

The chart clearly shows the height of the "ceiling" (3,800 ft) and the height to the top of the cloud layer (5,200 ft). At 5,200 ft the balloon emerged from the cloud and the brightness remained substantially constant at the increased value until about 9,000 ft. The gradual increase in brightness from 9,000 to 20,000 ft probably indicates the presence of haze in this altitude region. Above 20,000 ft the brightness reached a constant value.

VIII. ALTITUDE DETERMINATION

While the measurement of altitude in terms of elapsed time and a predetermined rate of balloon ascent may be sufficiently accurate for some applications, many studies require considerably more precise altitude determination. This requires that the barometric pressure be measured and, in more rigorous applications, also the temperature and humidity. (The altitude correction for temperature may be up to 10 percent and for humidity up to about 0.5 percent.) An obvious extension of our method to include the measurement of any number of upper-air phenomena, of which the barometric pressure may be one, consists in the use of a rotary switch which connects into the audio-oscillator grid circuit, in any desired succession, resistors responsive to the various phenomena to be measured. As previously indicated, certain of the resistors may vary inherently with the phenomena or may be controlled mechanically by instruments responsive to the phenomena. The switch may be driven by a spring or electric motor or by an air fan which operates by virtue of the upward motion of the balloon. The switch may also connect into circuit, at desired intervals, one or more fixed calibrating resistors which may serve as checks on the frequency stability of the audio oscillator. If frequency drift should occur, the reference frequencies provide means for correcting the various measurements on a proportional basis.

In an early radio-meteorograph model, we used a fan-driven rotary switch which successively connected into circuit three variable resistors, controlled respectively by a barometer of the diaphragm type, a bimetallic thermometer, and a hair hygrometer, and a fourth, fixed resistor, for reference purposes. This arrangement was found deficient in one respect because of the unusual precision of pressure measurement required in radio meteorography. The Bureau of Aeronautics, U. S. Navy Department, formulated the following minimum requirements for radio meteorograph operation: Pressure indications are required in the range of from 1,050 to 150 millibars to an accuracy of 1 millibar, temperature indications in the range of from $+40$ to $-75°$ C to an accuracy of 1°, and humidity indications in the range of from 0- to 100-percent relative humidity accurate to within 3 percent. It will be seen that the required accuracy is greatest for the pressure indications. Experiments with the method described showed that accuracies in the frequency measurements of the order of 0.5 percent could be expected under carefully controlled conditions and of the order of 1 percent in routine operation. The chief difficulty arose from the fact that the frequency-resistance characteristic of the audio oscillator altered somewhat under operating conditions so that, even after correction for drift on the basis of the reference frequency, a residual error of about 0.5 percent remained. While this error was

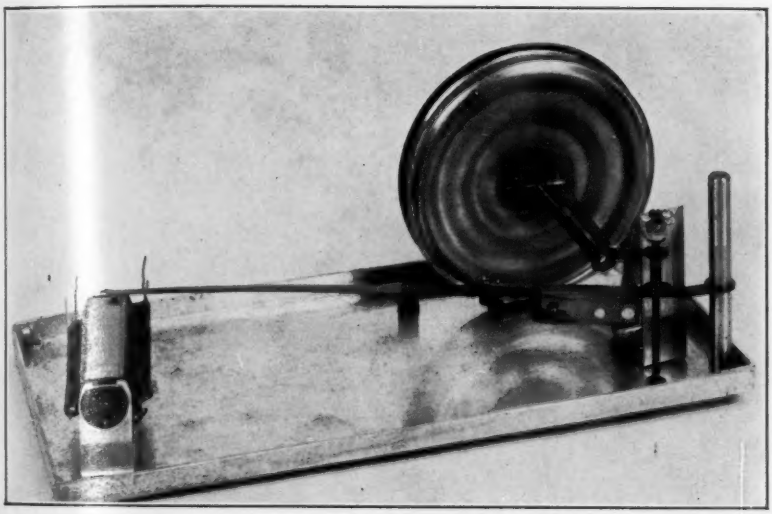

FIGURE 8.—*Experimental model of one form of the pressure-switching unit.*

not sufficient to affect the required accuracy of temperature and humidity indication, it was much too large for the pressure measurements.

To increase the accuracy of pressure measurement, we adopted a novel method [2] of indication which at the same time introduced several additional operating improvements. This method makes use of the fact that the pressure element deflects continuously in one direction as the balloon ascends, and employs this motion for carrying out the switching operation in the balloon transmitter. The sequence of switching operations serves for absolute indication of the barometric pressure in discrete steps, thereby obviating the need for interpreting pressure in terms of either time or frequency. A greater accuracy of indication is inherent in this arrangement. At the same time, the need for any other form of motive power for carrying out the switching operations is eliminated. Other advantages of this type of pressure indication will be considered in the following section.

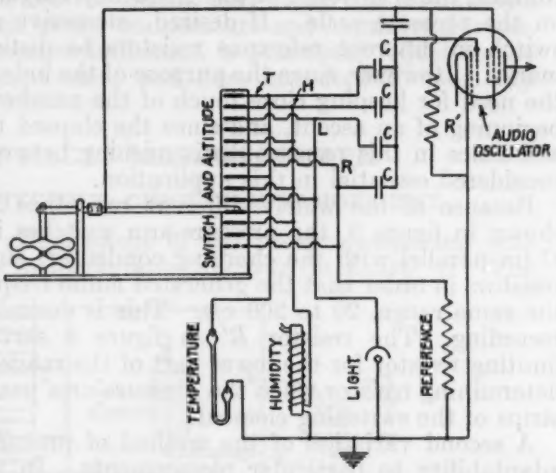

FIGURE 9.—*Schematic drawing of pressure-switching circuit arrangement as employed in the measurement of three properties of the atmosphere in addition to altitude (barometric pressure).*

1. PRESSURE SWITCHING

An experimental model of one form of pressure-switching with which we experimented is shown in figure 8, and the corresponding electrical circuit arrangement in figure 9. The pressure diaphragm operates a pointer which moves over a simple switching element consisting of electrical-conducting strips separated by insulating strips. The face of the switching element is polished so that friction opposing the arm movement is negligible. Contact of the pressure arm with a given conducting strip is therefore a direct measure of the barometric pressure to which the diaphragm is subjected. It is necessary only to provide means for identifying the particular conducting strip being contacted to secure an absolute-pressure scale. This is accomplished by the sequence of switching into circuit the several devices employed and by the regular spacing of the conducting strips to which the reference resistor is connected. In figure 9 are shown elements responsive to temperature, humidity, and brightness, and the reference resistor. The symbols T, H, L, and R refer to the

[2] Some months ago there came to the attention of the authors a description of a temperature-switching arrangement (see reference [9]) applied to the switching of lights for use of meteorographs at night, somewhat similar to the pressure-switching method which we have developed.

conducting strips on the switching element to which these are connected. The pressure arm moving over the conducting strips of the switching element successively connects into circuit the three devices in the order named and then repeats the sequence. After each two groups, the reference resistor is switched into circuit. Since it produces a substantially fixed frequency which occurs every seventh contact, the occurrence of this frequency may serve as an index mark on the pressure scale. If desired, successive seventh contacts may switch in different reference resistors to distinguish between index marks. However, since the purpose of the index marks is to eliminate the need for keeping close touch of the number of contacts from the beginning of an ascent, and since the elapsed time is of considerable assistance in this respect, distinguishing between index marks is not considered essential in this application.

Because of the widely different resistance ranges of the devices shown in figure 9, the pressure-arm switches in suitable condensers C (in parallel with the charging condenser) simultaneously with the resistors in order that the generated audio frequencies may remain in the same range, 20 to 200 c/s. This is desirable for convenience in recording. The resistor R' in figure 9 serves as the frequency-limiting resistor for the lower part of the range. It is the frequency-determining resistor when the pressure arm passes over the insulating strips of the switching element.

A second variation of the method of pressure-switching shows its adaptability to particular requirements. In routine radio-meteorograph operation, it is desirable that the balloon equipment be as simple as possible in order to reduce weight and to keep the unit price within the cost of the present airplane ascensions made for upper-air soundings. Also, the readings of temperature and humidity should be made at as many altitude levels as possible in order to obtain a nearly continuous picture of their variations. Accordingly, the radio meteorograph designed for use by the Navy Department [10] does not include the photoelectric cell; also, the electrical circuit of the pressure-switching unit is arranged so that temperature readings are obtained when the pressure arm is on an insulating segment and humidity readings when the pressure arm is on a conducting segment (exclusive of the index contacts).

A description of this instrument will form the chief subject matter of the remaining portions of this paper. However, before entering into this description, a brief outline will be given of the advantages of pressure-switching in combination with the frequency scale for measuring the upper-air phenomena investigated. The advantages are:

1. The method provides for great flexibility in the measurement of upper-air phenomena, a large class of mechanical and electrical devices being readily employed.

2. Readings of the phenomena being measured are obtained directly as a function of pressure, which may be readily converted into height. The record obtained at the ground station is plotted in this form and is easy to interpret.

3. Observations are obtained at predetermined pressure levels, independent of the rate of ascent of the balloon. This permits of using any practicable rate of ascent, thereby reducing the time required for a given set of observations. The use of electrical devices is of par-

ticular value in this respect since they are inherently faster in response than mechanical instruments.

4. The possibility of higher rates of ascent provides other important advantages: (*a*) Since the balloon will not drift so far, there is a greater chance for recovery of the instruments, particularly in near-coastal regions; (*b*) the shorter range permits taking check observations during the descent of the equipment; (*c*) battery requirements may be reduced appreciably; (*d*) better ventilation may be had of instruments requiring ventilation, such as the temperature and humidity devices.

5. The accuracy of pressure indication is practically equal to the accuracy of the instrument itself and does not depend upon any translatory means.

IX. NAVY RADIO METEOROGRAPH

1. PRESSURE-SWITCHING CIRCUIT ARRANGEMENT

The electrical circuit arrangement of the pressure-switching unit used in the Navy radio meteorograph is shown in figure 10. The

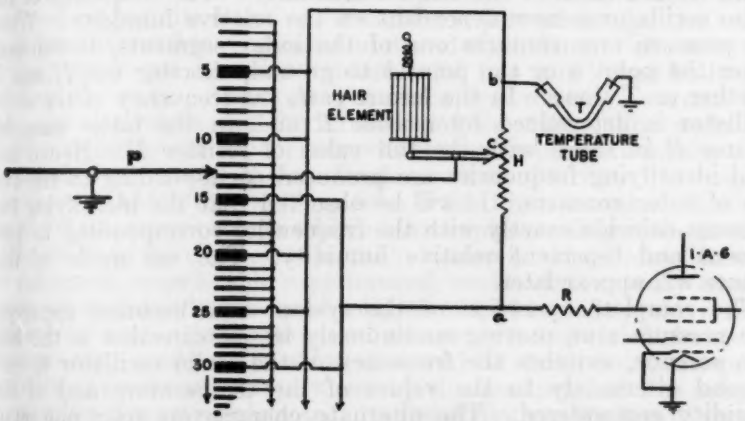

FIGURE 10.—*Electric-circuit arrangement of the pressure-switching unit employed in the Navy radio meteorograph*

grid circuit of the audio oscillator includes three resistors, *R*, *H*, and *T*, in series. Resistor *R* is of fixed value. *H* is a special resistor which is controlled by a hair hygrometer, so that the position of the contact point *c* varies in accordance with the relative humidity, being at the point *a* for 100-percent value, at the point *b* for 0 percent, and at intermediate positions for intermediate values of the relative humidity. *T* is a special resistor which varies inherently with the temperature. (*See* fig. 3.) The switching element consists of 75 conducting strips separated by insulating strips. The conducting strips are arranged in groups of four adjacent intermediate contacts, the adjacent groups being separated by wider index contacts. The intermediate conducting strips are all connected together, while the index contacts are connected in two sets. Referring back to figure

10, the three resistors are electrically connected to the switching element as shown. The point a is connected to one set of index contacts, (numbers 15, 30, 45, etc.); the point b is connected to the second set of index contacts, (numbers 5, 10, 20, 25, etc.); and the variable-contact point c is connected to the intermediate conducting strips of the switching element. Pressure arm, P, which moves over the switching element, is electrically connected to ground as is also the lower end of resistor T.

It will be seen that so long as the pressure arm rests on one of the insulating strips of the switching element, the series circuit formed by R, T, and H is undisturbed. Since R is fixed and the full value of H is in circuit, the frequency of the audio oscillator is controlled by the value of resistor T and hence by the temperature. Assume now that the pressure arm contacts one of the intermediate conducting strips. The contact c is thereby connected to ground, shorting out a portion of resistor H (c to b) together with the variable resistor T. The value of resistance remaining in circuit consists of R and a variable portion of H depending upon the position of point c and hence on the value of the relative humidity. The frequency of the audio oscillator is now dependent on the relative humidity. When the pressure arm contacts one of the index segments, it connects either the point a or the point b to ground, shorting out H and T together or T alone. In the former case, the frequency of the audio oscillator is determined by resistor R and, in the latter case, by resistor R in series with the full value of resistor H. Hence two fixed identifying frequencies are produced corresponding to the two sets of index contacts. It will be observed that the identifying frequencies coincide exactly with the frequencies corresponding to 100-percent and 0-percent relative humidity. The use made of this feature will appear later.

The complete operation of the system now becomes apparent. The pressure arm, moving continuously in one direction as the balloon ascends, switches the frequency of the audio oscillator to correspond alternately to the values of the temperature and of the humidity encountered. The alternate changeovers from one set of frequencies to the other indicate that the pressure arm is just reaching or is just leaving one of the intermediate contacts and has attained definite deflection positions which may be determined. When the pressure arm reaches successive fifth conducting segments, the frequency of the audio oscillator attains predetermined fixed values which positively identify these contacts so that they may serve as index marks for the absolute-pressure scale. The two identifying frequencies used serve an additional purpose in that they provide periodic checks during the progress of a flight on the degree of frequency stability of the audio oscillator. If any accidental variation should occur, for example, due to varying battery conditions, the recorded value of temperature may be corrected for the indicated variations. Corrections to the humidity readings need not be applied even in such event. Upon completion of a record, two lines may be drawn in on the chart to connect the recorded values of the two sets of identifying frequencies. These two lines frame the scale of humidity indications, thereby automatically transferring the plot of humidity indications to a corrected frequency scale.

2. TEMPERATURE CAPILLARY TUBE

A description of the temperature capillary tube is of interest at this point. A photograph of a practical form of this device was shown in figure 3. The glass capillary tube has an over-all length of 8 cm, a bore diameter of 0.75 mm, and a wall thickness of 0.4 mm. The dimensions were chosen on the basis of the following practical considerations: (a) The capillary bore and wall thickness had to be as small as practicable to insure rapidity of response of the electrolyte to ambient temperature changes; (b) the capillary length was required to be as short as possible to afford a maximum of mechanical sturdiness; (c) the bore diameter and wall thickness had to be large enough to permit commercial production to the required tolerance at low cost; (d) finally, the range of electrical resistance obtained, using a given electrolyte, was required to be of an order such as to produce a substantially uniform scale of frequency vs. temperature in the circuit of figure 10. Full compliance with these requirements is realized in the design shown in figure 3. Capillary lengths of the required bore are purchased to a tolerance of 10 percent. Measurement under a microscope permits selecting from these a percentage (of the order of 25 percent) within 1 percent of the desired bore. The selected capillary tubes are bent into U-form and two small glass bulbs are fused on its ends. The wells provide a low-resistance contact between the electrolyte and the terminals of the tube. The wells are sealed with miniature rubber stoppers through which extend the copper terminals. One of the terminals consists of a very fine copper tube through which the capillary tube is filled in a vacuum chamber. The end of this copper tube is soldered to complete sealing of the device.

The choice of an electrolyte suitable for use in this application was the subject of considerable experimental work. In our early experiments, we used a sulphuric acid solution of 1.30 specific gravity, and, with special care in calibration and use, many successful flight measurements were made. The solution served for determining the practicability of measuring temperature by this method, but was subject to a number of practical defects. Its resistivity was too low to permit the use of the capillary dimensions indicated. The solution froze at −70° C, whereas readings are sometimes required to lower temperatures. The process of electrolysis gave a resistance which, for a given temperature, varied with the current passing through it, hence a given capillary tube had to be calibrated in combination with the particular audio oscillator with which it was to be used. The attendant polarizing action produced a serious lag in indication of the true temperature due to the charging required of the equivalent battery each time the tube was switched into circuit by the pressure-switching unit.

We are indebted to D. N. Craig of the National Bureau of Standards for experimental work which eliminated these difficulties. First experiments showed that the addition of as much copper sulphate as could be taken into solution, in combination with the use of copper terminals, caused an electroplating action to take place which tended to eliminate the production of gases at the terminals and hence the polarizing action. Consideration was given to the addition of alcohol to the mixture to secure an effectively higher resistivity; however, this further limited the amount of copper sulphate which could be taken into solution.

Finally, a different electrolyte was adopted consisting of hydrochloric acid, cuprous chloride, and alcohol. Use of predetermined ratios of these ingredients permits obtaining a wide range of resistivities so that the required resistance may be had with a capillary tube of the specified dimensions. Tests showed that the solutions do not freeze at temperatures above −78° C. Ample cuprous chloride is taken up by both the hydrochloric acid and the alcohol to practically eliminate the polarizing action. As a result, the capillary tube resistance corresponding to a given temperature remains constant for a wide range of current passing through it and may therefore be calibrated independently of the audio oscillator with

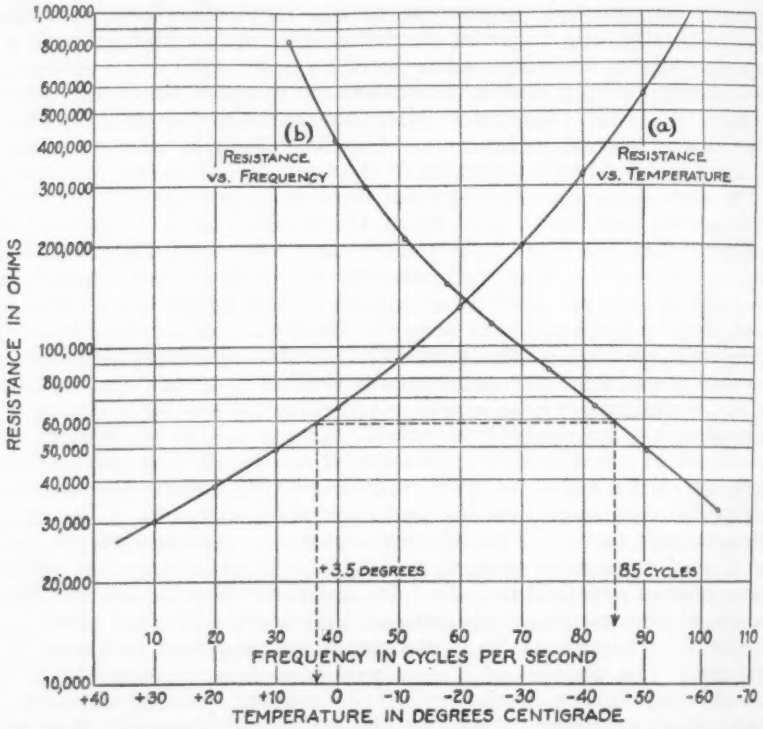

FIGURE 11.—*Graphs showing the variation of electrical resistance with temperature of the electrolytic thermometer and the variation of the generated audio frequency with resistance for a sample audio oscillator.*

Together they determine the temperature-frequency scale of the radio meteorograph.

which it is to be used. Some choice of temperature coefficient is also possible with this electrolyte. A detailed account of its properties is given in a separate paper by Craig [11].

The solution employed in our experiments, chosen to give a resistance of 30,000 ohms at +30° C, consists of 24 percent (by volume) concentrated hydrochloric acid, 76 percent of ethyl alcohol, and 2.7 g of cuprous chloride for each 100 cm^3 of the resultant combination. The variation of resistance with temperature for a typical capillary tube is given by curve *a* of figure 11, while curve *b* shows the resistance-frequency characteristic of a typical audio oscillator. The corresponding variation of modulation frequency with temperature when

Journal of Research of the National Bureau of Standards

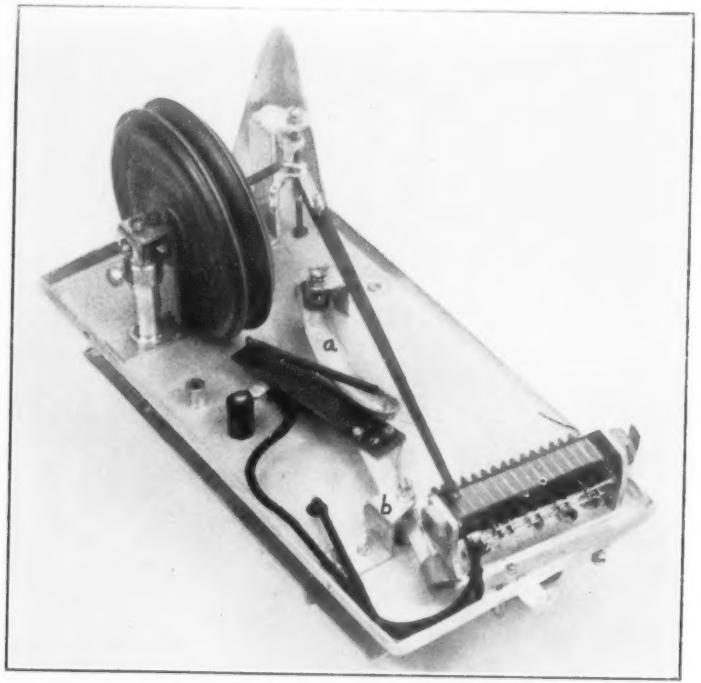

FIGURE 12.—*Meteorograph unit.*
Front view.

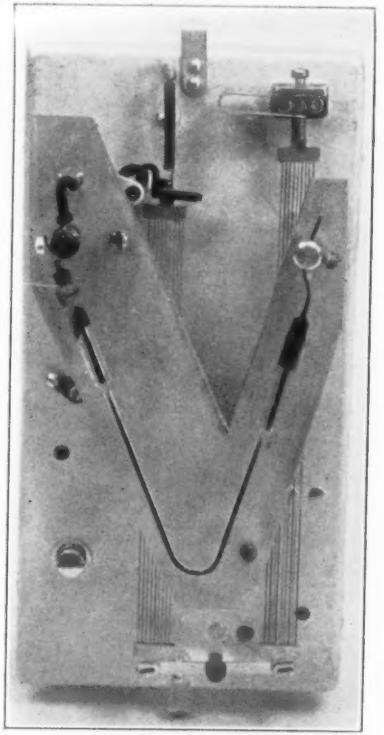

FIGURE 13.—*Meteorograph unit.*
Rear view, with radiation shield removed.

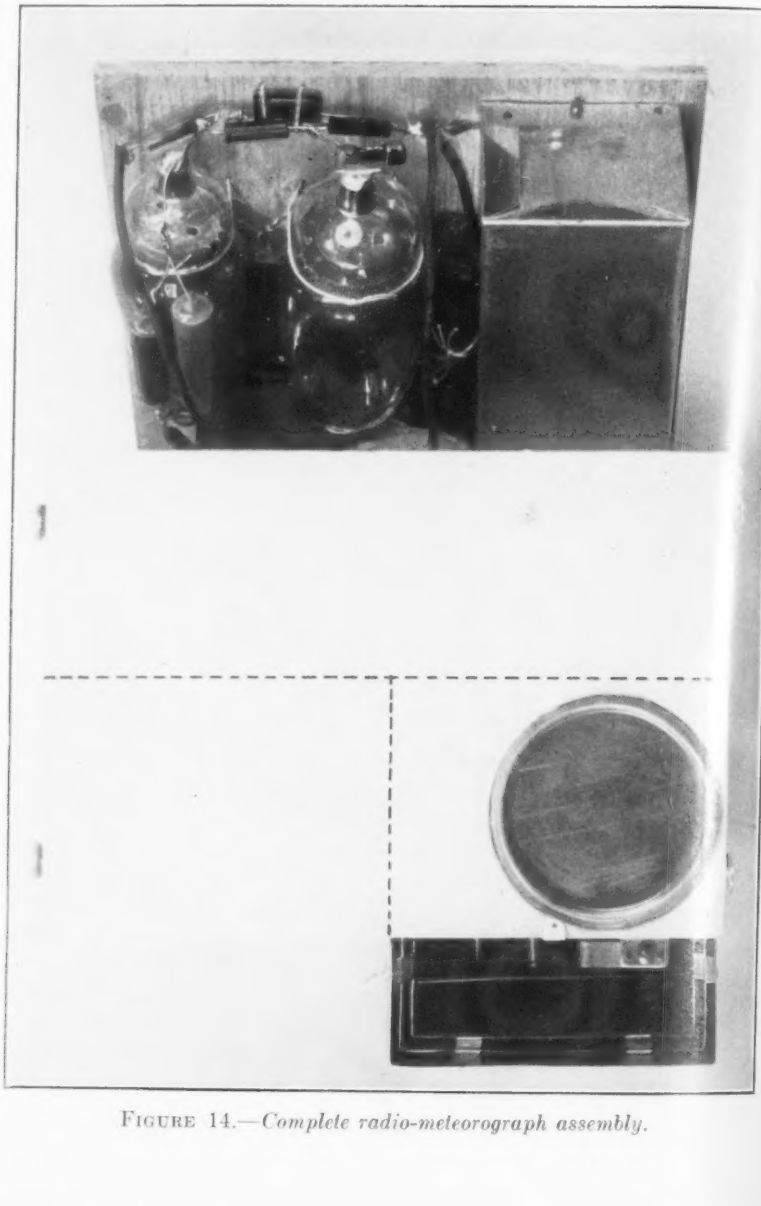

FIGURE 14.—*Complete radio-meteorograph assembly.*

the capillary thermometer is connected in the grid circuit of the audio oscillator may be evaluated from these two curves, as indicated in figure 11.

Aside from the advantage of eliminating mechanical parts, the capillary thermometer offers several other advantages over the bimetallic thermometer usually employed in radio meteorographs.

One advantage is its property of responding very rapidly to temperature changes. The time-lag constant of the tube in an air stream of 10 mph is 2 sec compared with 5 sec for the fastest bimetallic thermometer. The high rate of response of the temperature device is of particular value in the method of pressure-switching. Since readings are obtained corresponding to fixed pressure values, the total number of readings obtained during an ascension does not depend upon the rate of balloon ascent. Hence, a high rate of ascent would be desirable in order to reduce the total time required for securing a complete set of observations. The response of the temperature device is believed sufficient for any practical rate of ascent. At the present time, the hair hygrometer appears to be the limiting factor of the radio meteorograph in this respect.

Another advantage of the capillary temperature device lies in the simplicity of its connection to the body of the meteorograph; only two small connecting leads are required. This and the length and small diameter of the capillary tube contribute considerably to the avoidance of heat transfer from the meteorograph.

3. METEOROGRAPH UNIT

Figures 12 and 13 are two views of the meteorograph which incorporates the pressure-switching unit, the temperature tube, and the hair-controlled hygrometer. In fig. 12 the pressure diaphragm, linkage, and arm are clearly shown. The end of the pressure arm carries a platinum tip which slides over the polished surface of the switching element. The conducting segments of the switching element stand out in the photograph as white lines, particularly the index contacts, which are of greater thickness. The conducting segments are of coin silver 0.005 in. thick and the insulating segments of Bakelite 0.015 in. thick. Double or triple segments are used for the index contacts, as desired. For convenience in manufacture and assembly the segments are punched out to the desired shape from material of the required thickness. Holes in the center provide for their assembly on a rod having a threaded end. The assembly is made with a jig so that the connecting tabs forming an integral part of the conducting segments may be properly aligned. After assembly, the segments are pressed together by a nut on the threaded end of the rod. The face of the unit is then polished.

At *a* in figure 12 is shown a small metal cam which is swung about its shaft by two hair elements operating in series (on the other side of the base plate). A wire-wound resistor mounted to pivot at the point *b* is held in contact with the cam by a spring. As the cam moves under the action of the hair hygrometer, the resistor is forced to follow it due to the spring. A rolling contact is thereby obtained between the metal cam and the resistor. This contact moves from one end of the resistor to the other as the relative humidity varies from 0 to 100 percent. The arrangement is therefore ideally suited

to serve for resistor *H* shown in figure 10. This satisfactory arrangement was developed for us by Julien P. Friez & Sons, Inc.

Figure 13 shows the other side of the meteorograph unit with the radiation shields removed. The hair-drive for the metal cam and the temperature capillary tube are seen in this view. The thin metal plate normally mounted between the hair elements and the temperature tube is cut away to permit a view of the hair elements. This plate serves as a shield against the radiation of heat from the base plate to the temperature tube. The ventilated outer radiation shield protects the temperature tube from direct solar radiation.

4. COMPLETE RADIO-METEOROGRAPH ASSEMBLY

The complete radio meteorograph consists of a radio-transmitting unit, a battery unit, and a meteorograph. The entire assembly of the three units is contained in a balsa-wood box, 6 by 6 by 4½ in. The total weight is 2 lb. in the current design and is capable of considerable reduction through refinement of the component units. In its present design, the transmitter is capable of over 4 hr. of efficient operation under ground conditions.

Figure 14 is a top view of the complete instrument. The balsa-wood box is divided into three individual compartments: for the radio transmitter, the batteries, and the meteorograph. Separate access is possible to each compartment for convenience in adjusting and calibrating. A small cover plate at the top of the meteorograph compartment permits ready access to the switching element for checking the instrument just prior to its ascent. The electric-circuit arrangement of the radio transmitter was described in connection with figures 1 and 10. The carrier frequency of the transmitter is 65 Mc/s.

The battery unit consists of two 45-v batteries for the plate supply and a 3-v dry-battery unit for the filament supply. The plate batteries weigh slightly over 4 oz each and have a capacity of 65 ma-hr. The filament battery weighs 2 oz and has a capacity of 750 ma-hr. The total plate current required by the transmitter is 15 ma and the filament current is 180 ma. The battery unit is packed in rock-wool insulation in order that it may retain its original heat as long as possible during an ascent. In the course of an ascent, the ambient temperature may drop to −75° C, while the batteries cease to operate when they drop to −20° C. Because of the effect of the low ambient temperatures upon the battery capacity, the operation of the transmitter during an actual ascent is limited to an average of 2 hr.

5. SAMPLE RECORD OF AN ASCENSION

Some 75 ascensions have been made using the radio meteorograph described. These have shown the system to be practicable and have provided gratifying records. Fifty of these ascents were made at the U. S. Naval Air Station, Anacostia, D. C., under service conditions, and the records obtained were compared with aerograph observations obtained simultaneously in a Navy airplane. The results of these comparisons are described in a separate paper [12]. The excellent agreement obtained indicates that the accuracy of indication of pressure, temperature, and humidity, while not quite within the require-

ments set forth in section VIII, is sufficient to warrant the use of the instrument to replace the present airplane soundings.

A sample record, obtained on September 2, 1937, is shown in figure 15. The speed of the graph paper through the recorder was ½ in./min, the distance between successive horizontal lines on the graph paper representing 1-min intervals. The scale of abscissas on the chart is on a frequency basis, 0 to 200 c/s (left to right). For ease in interpretation, the corresponding temperature and humidity scales are also marked on the chart. The start of the run, corresponding to the release of the balloon, is at *A* at the bottom of the chart.

It is convenient to consider the recorder pen as producing a temperature plot which is a function of time and hence of the ascent of the balloon. This plot, represented by the lower-frequency traces at the left of the record, is not continuous, being interrupted at predetermined altitude levels of the balloon by contact of the pressure arm with the conducting strips of the switching element. The modulating frequency of the emitted wave then changes to either the humidity or the reference values. At each interruption, the recorder pen sweeps laterally to the right to record these values, returning again to the left when the pressure arm leaves the corresponding conducting strip and the modulating frequency is again proportional to temperature. A line drawn through the frequency traces (at the right of the chart) which relate to the intermediate or humidity contacts will, therefore, represent the variation of humidity as the balloon ascends. Similarly, vertical lines through the two sets of reference frequency traces represent the 0- and 100-percent points of the scale of humidity values. The horizontal traces of the record made by the recorder pen in sweeping from the temperature traces to the humidity (and index) traces, and vice versa, show that the pressure arm has reached definite points of deflection and may be evaluated in terms of pressure, based on previous calibration. Note that the humidity readings occur in groups of four, while the index traces define the 5th, 10th, 15th, 20th, etc., contacts. On the record, the values of the barometric pressure corresponding to the beginning of contact of the pressure arm with the index conducting strips are shown, forming an ordinate scale of pressure values. The balloon altitude at these points, corrected for the indicated temperature and humidity, are also shown. Similar data are not inserted for the other contacts for the sake of clarity of the record.

At the time of releasing the balloon, the barometric pressure at the ground surface was 1,018 millibars, the temperature 24.8° C, and the relative humidity 100 percent. The pressure arm was on the third intermediate contact and gave a reading of 100-percent relative humidity. When the balloon reached an altitude of about 570 ft., the pressure arm left this contact and the first reading of temperature was obtained. From this point on the reader can trace for himself the motion of the recorder pen under the influence of the received signal frequency as the balloon ascended.

When the balloon reached an altitude of 34,000 ft., the pressure arm being then just above the 65th contact, a special pressure-operated releasing device opened the string connection between the balloon and a small parachute to which the radio meteorograph was attached. The parachute then opened and the equipment descended back to the earth's surface. This releasing device was employed in certain of our

tests to prevent the equipment from reaching the normal ceiling heights of 65,000 to 75,000 ft, since it was desired to obtain check temperature readings during the descent of the equipment while the batteries were still in good condition and the balloon not too far away from the receiving station. Referring to figure 15, check readings were obtained down to the 5th contact, the equipment being then within 1,200 ft. of the ground.

The temperature readings during the descent agreed with the corresponding readings during the ascent within less than 1° C, testifying to the accuracy of the frequency-translating means and the independence of the temperature tube of rate of motion through the air. The

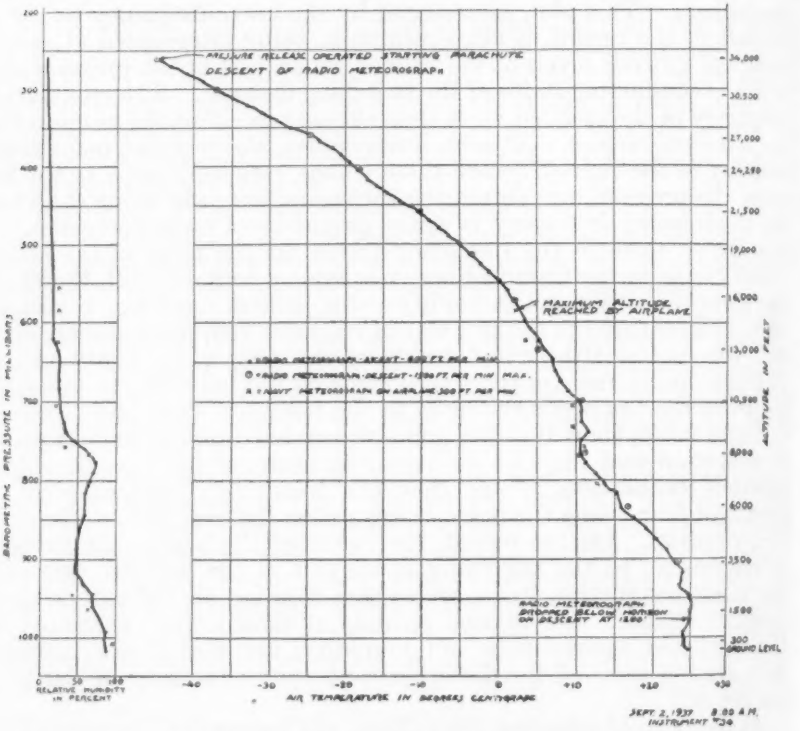
MAXIMUM ALTITUDE REACHED BY AIRPLANE
RADIO METEOROGRAPH STOPPED BELOW MOTION ON DESCENT AT 1200
BAROMETRIC PRESSURE IN MILLIBARS
ALTITUDE IN FEET
RELATIVE HUMIDITY IN PERCENT
AIR TEMPERATURE IN DEGREES CENTIGRADE
SEPT. 2, 1937 8:00 A.M.
INSTRUMENT #34

FIGURE 16.—*Chart showing agreement of radio-meteorograph and aerograph observations.*

humidity readings, while indicating changes at the same altitude levels, did not check the ascending values because of the inherent lag in the hairs after exposure to low temperatures. Several contacts were missing during the final portion of the descent, probably because of the deposit of moisture upon the cold surface of the switching element as the radio meteorograph entered the warmer air masses of higher water-vapor content. It is unlikely for this to happen during an ascent, because the air is then breathing outward from the partially sealed compartment housing the switching element.

The meteorologist examining the record of figure 15 would be interested chiefly in the points where the temperature variation with increasing altitude departs from a normal cooling rate and either

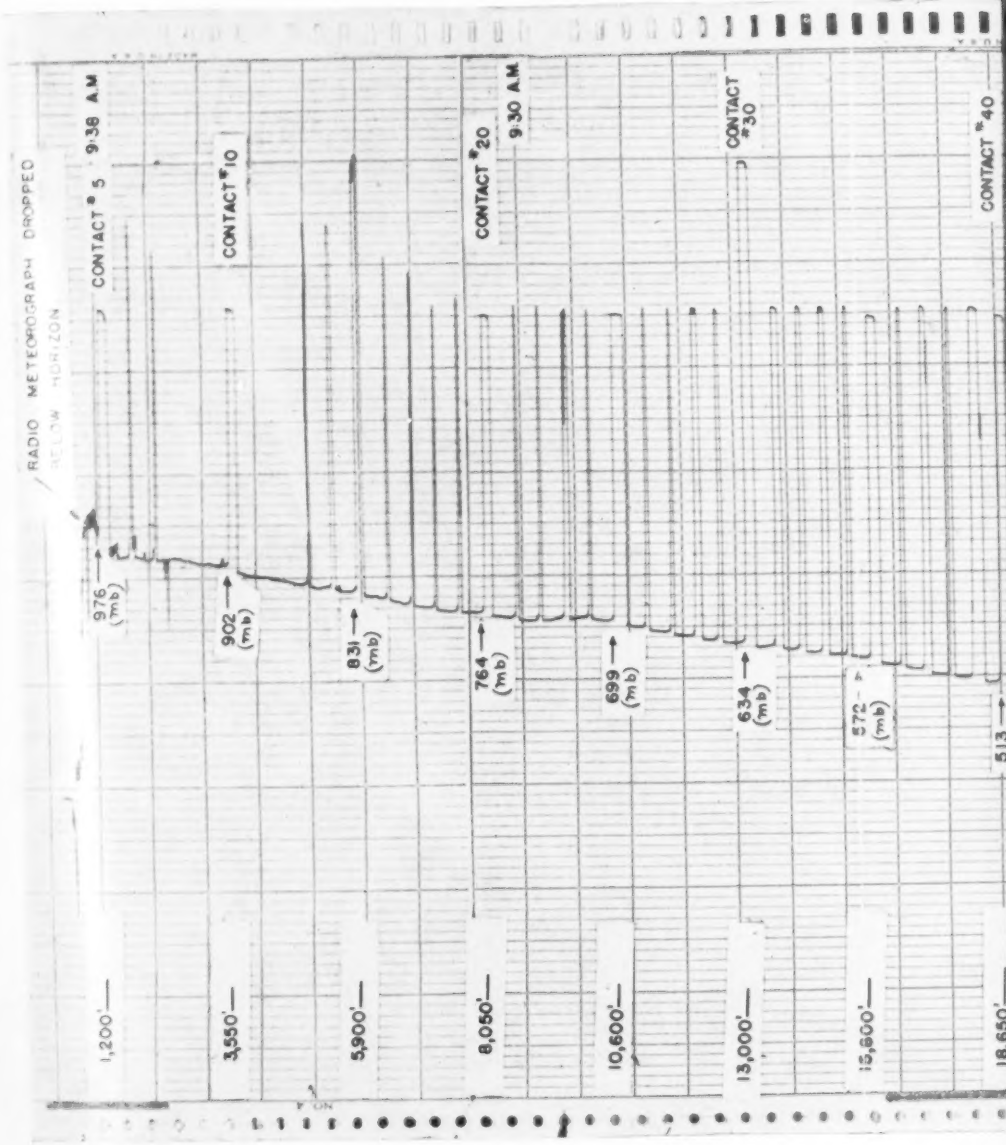
RADIO METEOROGRAPH DROPPED
BELOW HORIZON
CONTACT # 5 9:38 A.M.
CONTACT #10
CONTACT #20 9:30 A.M.
CONTACT #30
CONTACT #40
976 (mb)
902 (mb)
831 (mb)
764 (mb)
699 (mb)
634 (mb)
572 (mb)
513
1,200'
3,550'
5,900'
8,050'
10,600'
13,000'
15,600'
18,650'

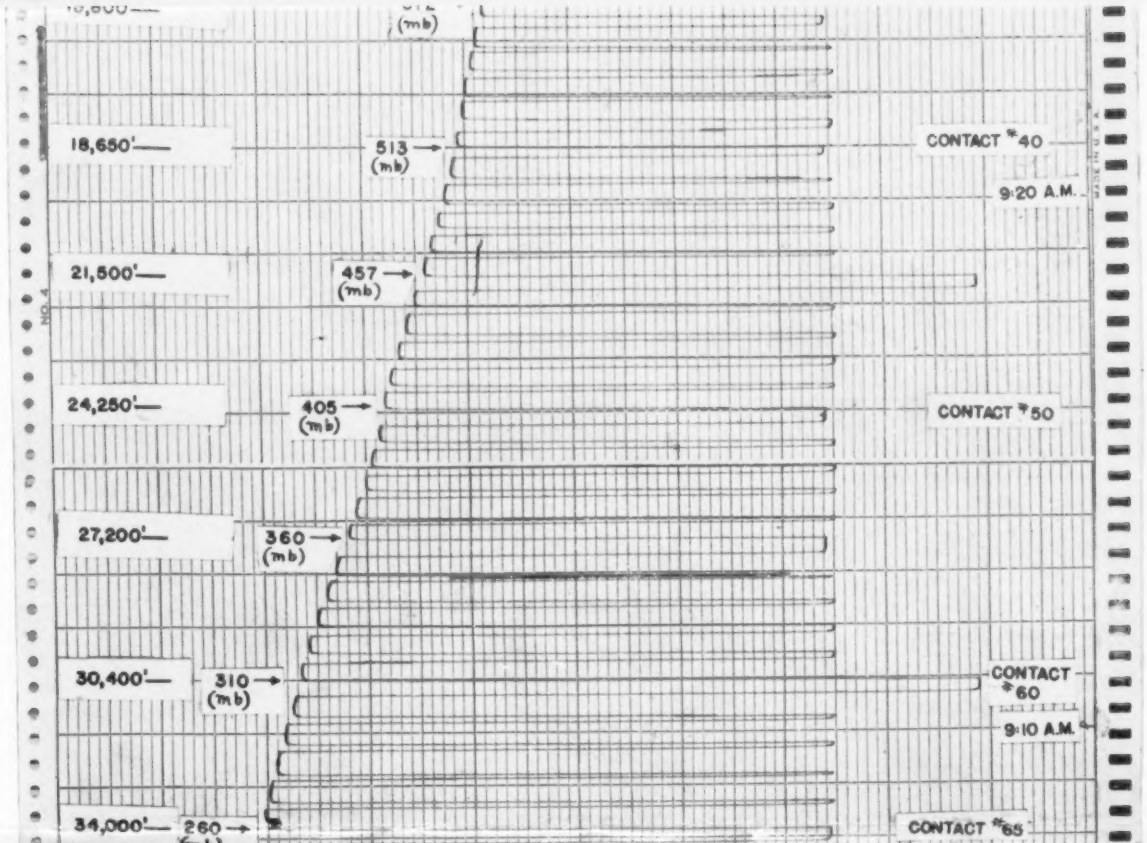
18,650'
513 (mb)
CONTACT #40
9:20 A.M.
21,500'
457 (mb)
24,250'
405 (mb)
CONTACT #50
27,200'
360 (mb)
30,400'
310 (mb)
CONTACT #60
9:10 A.M.
34,000'
260
CONTACT #65

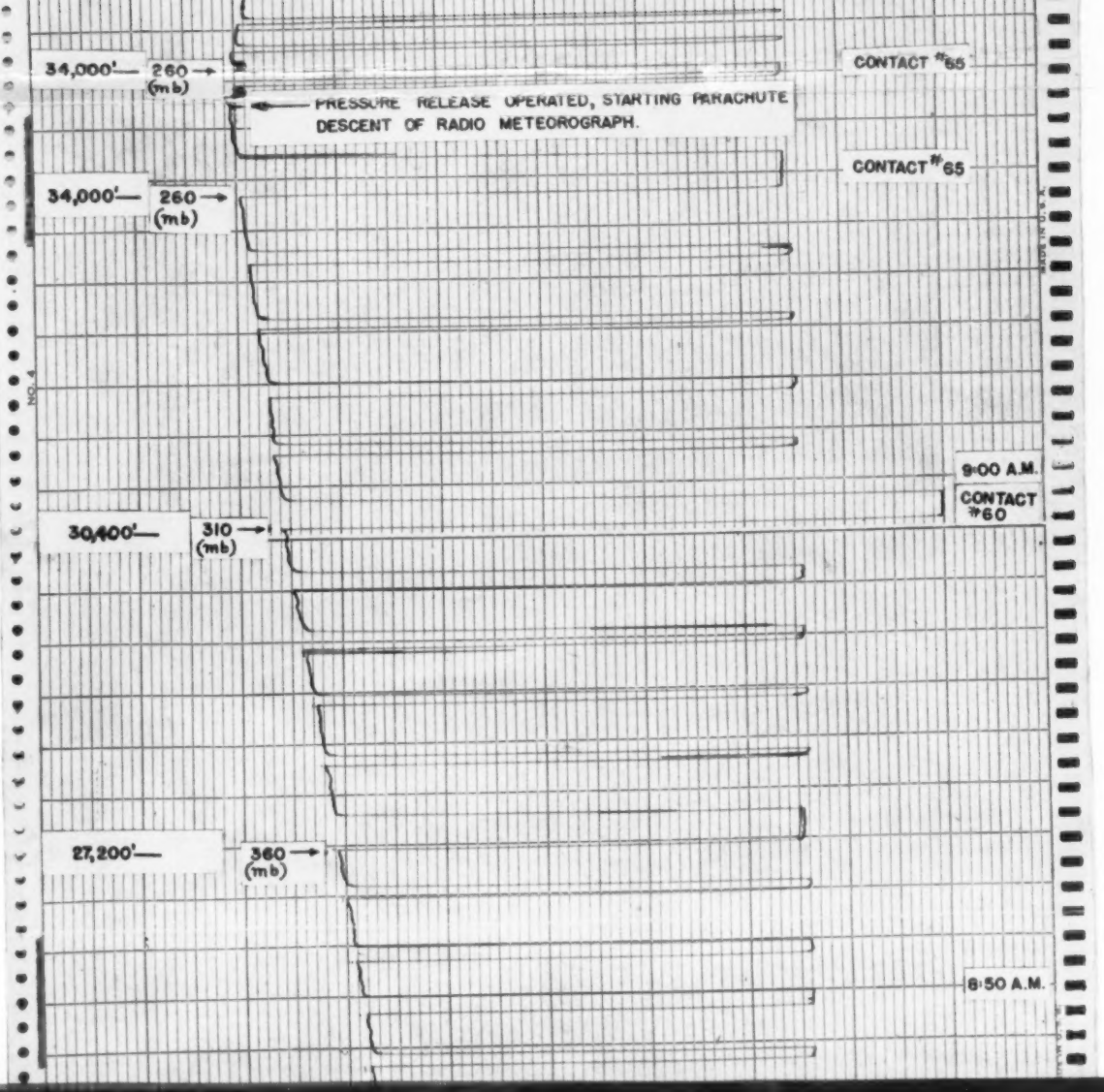

FIGURE 15.—*Sample*

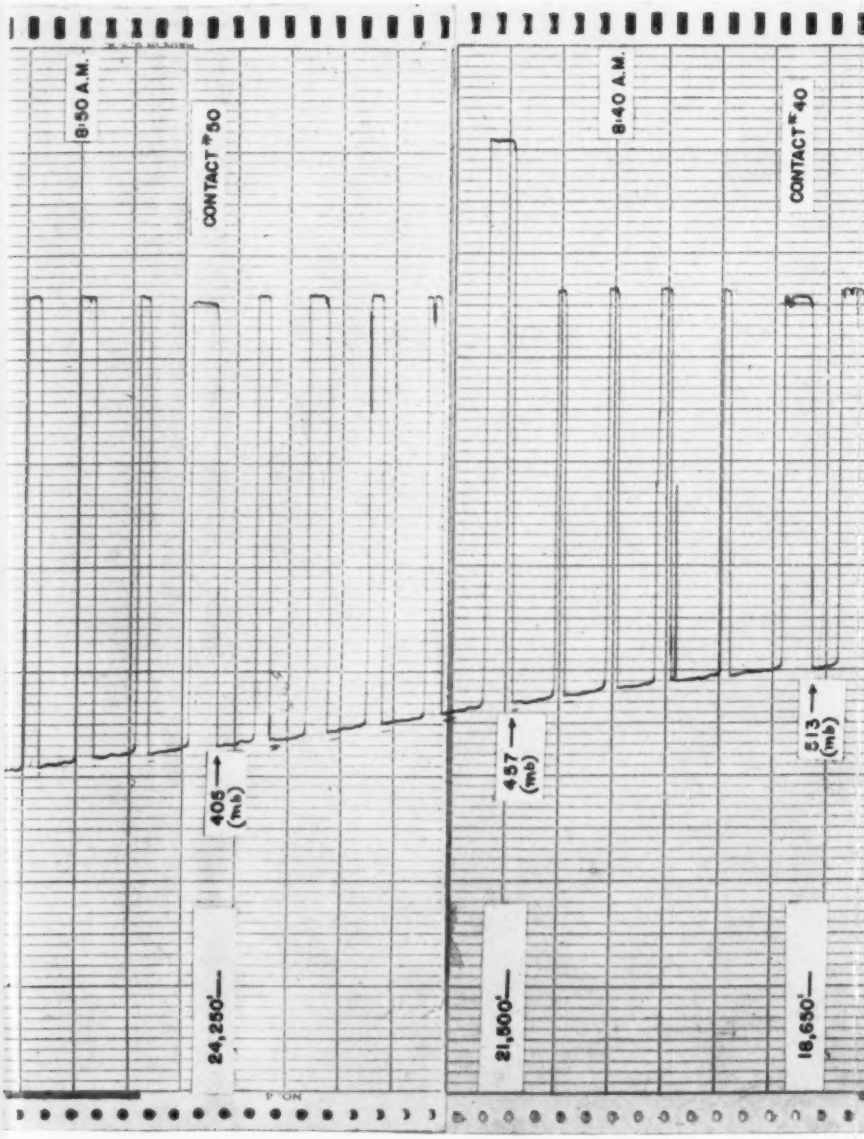

RE 15.—*Sample radio-meteorograph ascension record.*

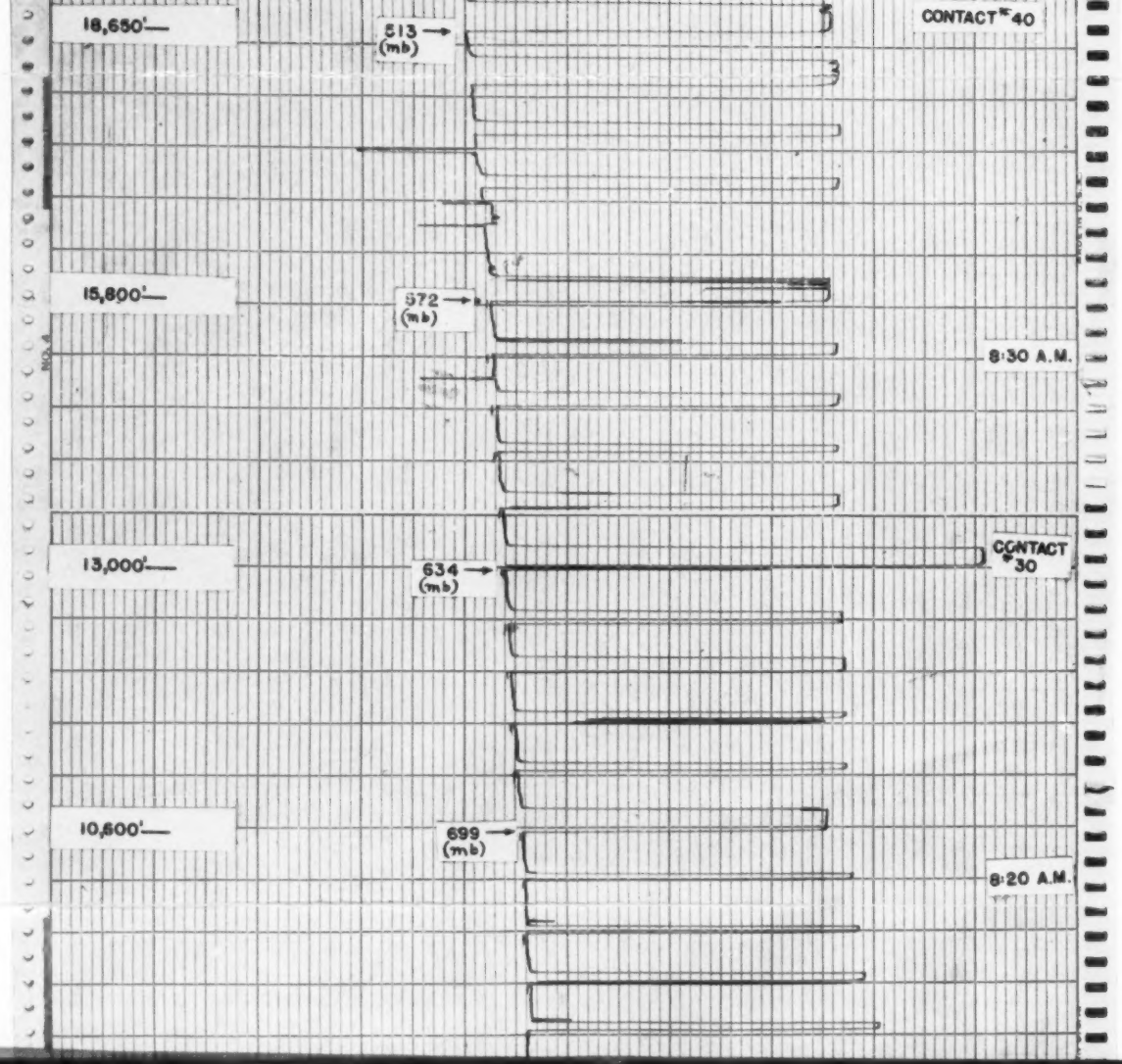
18,650'
513 (mb)
CONTACT #40
15,800'
572 (mb)
8:30 A.M.
13,000'
634 (mb)
CONTACT #30
10,600'
699 (mb)
8:20 A.M.

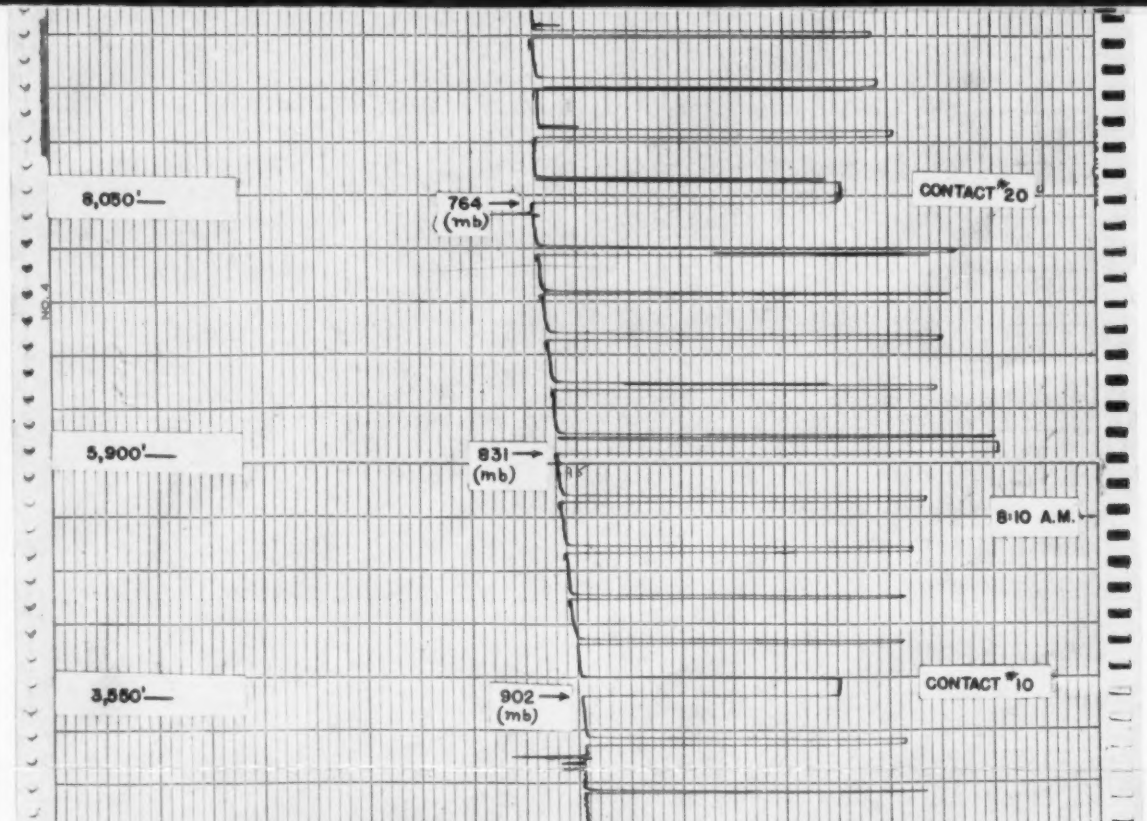
8,050'
764 (mb)
CONTACT #20
5,900'
831 (mb)
8:10 A.M.
3,550'
902 (mb)
CONTACT #10

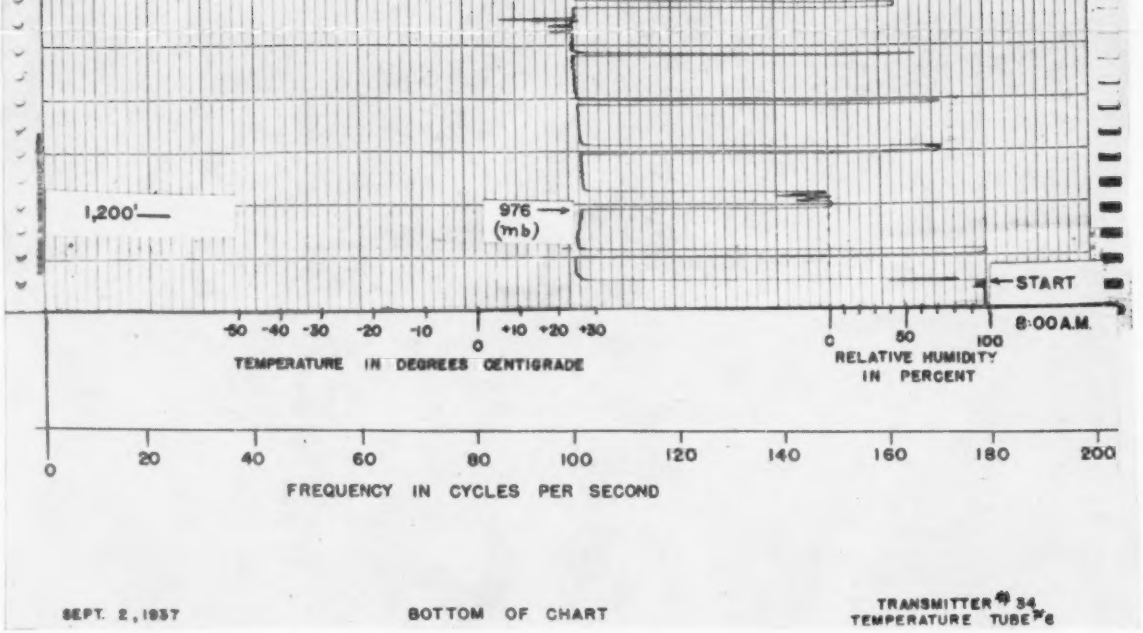

Research Paper 1082

UNIV. OF MICH.

ceases to decrease or actually increases. These are termed temperature-inversion points. Information is required on the extent of the inversions, the altitudes at which they occur, and of the corresponding values of relative humidity. These data are plotted on an adiabatic chart for further computation. An advantage of the type of record shown in figure 15 is that the significant data required may be used without consideration of the remaining data.

An indication of the order of agreement obtained between the radio-meteorograph and aerograph observations may be had from the chart shown in figure 16. In this chart the ordinates represent values of the barometric pressure in millibars and the abscissas values of the temperature in degrees centigrade and of relative humidity in percent. The full lines represent the radio-meteorograph data corresponding to the record of figure 15. The crosses represent the aerograph data obtained simultaneously. It will be seen that the temperature readings agreed within 1° C and the humidity readings within 5-percent relative humidity except at abrupt changes. The close agreement of the temperature and humidity plots testifies to the agreement of the pressure readings.

6. CALIBRATING PROCEDURE

The procedure of calibrating the complete radio meteorograph in preparation for a flight test is of interest. The procedure has been simplified to the point where it is carried out completely in terms of resistance measurements.

The meteorograph unit is placed in a pressure chamber and an ohmmeter is connected between the upper end of the humidity resistor and ground. See figure 10. Evacuation of the pressure chamber at the rate of about 75 millibars per minute is then begun. As the pressure arm passes over the index contacts, the ohmmeter will read either zero resistance corresponding to one set of index contacts or the total value of the humidity resistor corresponding to the second set. For intermediate contacts, the ohmmeter will read the value of a portion of the humidity resistor depending on the humidity conditions in the pressure chamber. Between contacts the ohmmeter will show the value of the humidity resistor in series with the temperature tube (or with a fixed resistor substituted for the temperature tube, if more convenient). For each contact, the value of the pressure is recorded corresponding to the instant of making the contact. A complete calibration of the pressure unit can be carried out in 10 to 15 min. The data may be tabulated in any convenient form. Using a special graph paper for plotting the data, in which the ordinates are spaced proportionally to the spacing of the conducting strips in the switching element, we have found it feasible to restrict the calibration to the index contacts only, thereby further reducing the time for a calibration. Repeated calibrations of a number of instruments over a period of a month, several of which were from recovered radio meteorographs, showed that readings are repeated to within an accuracy of one millibar.

The temperature correction for the pressure unit is next determined. To reduce cost, no attempt to compensate for temperature during manufacture is made, other than that the diaphragm is evacuated as completely as possible. This automatically provides for temperature

compensation at the lowest pressure level. However, there is an appreciable change in pressure indication with temperature at ground pressure. The difference per degree centigrade change in temperature may be readily determined by observation of the position of the pressure pointer at room temperature and in a cold temperature chamber; it is of the order of 0.3 millibar per degree centigrade. This correction factor tapers off linearly to zero as the pressure to which the pressure diaphragm is subjected is reduced to the lowest value. The temperature correction is applied at the ground pressure level on the basis of the temperature obtaining at the time of ascent and at lower pressure levels on the basis of estimated temperatures within the compartment housing the diaphragm. When the higher expense justifies, there is no primary difficulty in compensating the pressure element for the effect of temperature at all pressures.

Calibration of the temperature device has been simplified so that but a single temperature tube of a batch filled with the same solution need be calibrated over the complete temperature range. The ratio of the resistance of this tube at any temperature to its resistance at +30° C is determined. For all of the other tubes, only the resistance at +30° C is measured. Since the same electrolyte is employed in all of the tubes, the same variation of resistance with temperature will obtain. In practice it has been found that the use of the same proportion of ingredients will produce an electrolyte having the same temperature coefficient of resistance. Hence, the same calibration will hold for temperature tubes filled in different batches. Repeated calibrations of a number of tubes, several after recovery, showed that they maintain their calibration within 1° C over a period of a month.

Calibration of the humidity device is obtained by placing the meteorograph unit in a humidity chamber and measuring the resistance between points *a* and *c*, figure 10, corresponding to various values of humidity. Since the resistance-humidity relationship is quite linear, two readings corresponding to, say, 10- and 90-percent relative humidity are usually sufficient.

Calibration of the audio oscillator of a given transmitter is accomplished by inserting a series of 10 standard resistors successively in its grid circuit and measuring the corresponding value of the modulating frequency on the frequency meter of the receiving set-up shown in figure 2. To facilitate conversion of the frequency traces on the record received at the ground station into corresponding values of temperature and humidity independently of the combination of temperature tube, humidity resistor, and audio oscillator employed, the frequency-resistance characteristic of the oscillator is plotted on special graph paper, and special auxiliary sliding temperature and humidity scales are employed. The operation of these scales is described in a separate paper [12].

With the calibrating procedure outlined, a radio meteorograph may be taken off the shelf, completely calibrated, and prepared for an ascent within 90 min. If the instrument has been previously calibrated by the manufacturer, the check calibrations necessary to insure its accurate operation, together with the preparation of the instrument, balloon, parachute, etc., for ascent, take about 45 min. With the aid of the special graph paper, sliding scales, etc., the record can be evaluated and plotted on the standard adiabatic chart used by meteorologists within a few minutes of the time the signals corre-

sponding to the highest altitude of the interest have been recorded. In our service tests the 400-millibar pressure level (approximately 23,500 ft) has been arbitrarily taken as that altitude.

X. ELECTRICAL HYGROMETER

In section VI, a brief description is given of a resistance device which varied inherently with the moisture content of the air. A photograph of the device is shown in figure 4 and a record obtained in an ascension flight in figure 6. The development of an electrical hygrometer was undertaken to find a substitute for the hair hygrometer universally employed in upper-air soundings. Complete details of this development are given in a separate paper [13]. A serious defect of the hair-type hygrometer is its inability to respond to abrupt change in humidities encountered by rapidly ascending balloons. This lag in response increases rapidly with decreasing temperature. Hence the hair hygrometer gives only a qualitative measurement of the variation of humidity with altitude. It was believed that an electrical device for measuring humidity would provide much more rapid response to humidity variations, especially at the low temperatures.

The development of the unit shown in figure 4 was based on an observation that the resistance between the two wires of a bifilar winding on a glass tube was influenced quite markedly by humidity. An extensive investigation of this phenomenon was undertaken, the work including the study of the effect of different types of glass, roughness of the glass surface, coatings over the glass, binders over the coatings, spacing of the wires, and wire size and composition. Over 150 samples were made up and tested. All of the units were found to vary in electrical resistance with relative humidity, and, in lesser degree, with temperature. The temperature effect was different for different samples and the amount of temperature correction required for a given sample was found to be a function of the relative humidity to which it is exposed, increasing with increasing humidity. A simple graphical arrangement permits applying the appropriate correction factor on the basis of the observed temperatures and relative humidities obtained during an ascent.

The record of figure 6 shows the rapidity of response obtained with the electrical hygrometer. In comparative laboratory tests at room temperatures in an air stream of 10 mph, the time lag constant for this device was found to be 3 sec compared with 40 sec for the hair hygrometer. The indicated variations in humidity at the higher altitudes in the record of figure 6 shows the operation of this device when exposed to low temperatures at which the hair hygrometer could not possibly respond. As previously indicated, the altitude scale of figure 6 is only approximate.

XI. OTHER APPLICATIONS OF THE GENERAL METHOD

In the foregoing text, we have limited our description to arrangements wherein the device for pressure indication is also utilized to carry out all of the switching operations of the balloon transmitter. In certain applications it is convenient to employ auxiliary means for accomplishing the switching. An example of this class is the investi-

gation of Stair and Coblentz [14] on the measurement of ultraviolet solar intensities in the stratosphere. In this application, based on our method, the variation in resistance of a photoelectric cell equipped with several light filters is converted into a variable modulation of the emitted carrier. At predetermined altitudes, the pressure-switching unit introduces fixed resistors in the grid circuit of the audio oscillator for the purpose of altitude determination. Between the altitude measurements, a motor-driven wheel successively interposes several filters over the photocell to determine the spectral quality of untraviolet in the solar radiation.

A second example in which auxiliary switching is employed is shown in figure 17. In this arrangement, a miniature motor-driven switch

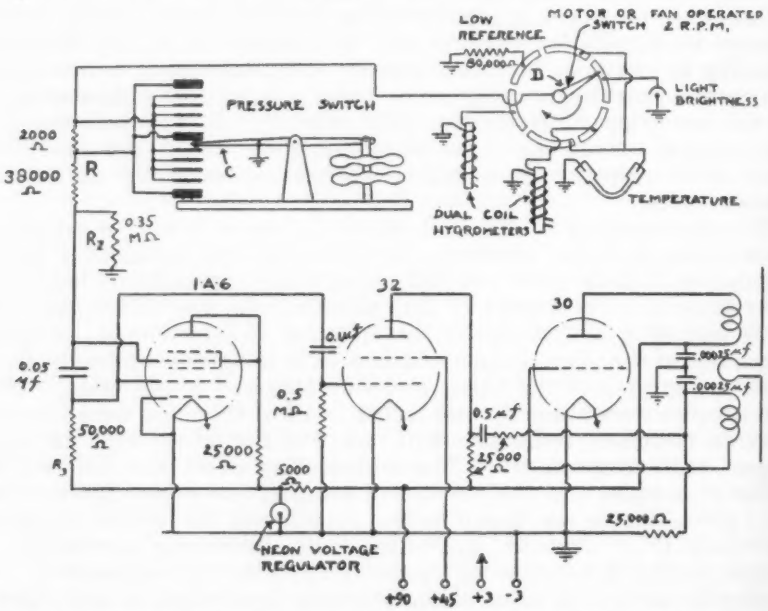

FIGURE 17.—*Electric-circuit arrangement illustrating the use of the method of pressure indication in combination with an auxiliary switching device.*

connects into the grid circuit of the audio oscillator a number of devices. In the illustration are shown a capillary thermometer, a photoelectric cell, two electrical hygrometers (covering different portions of the humidity scale), and a fixed calibrating resistor. These may be connected into circuit as rapidly as the response of the recording equipment will permit, of the order of a few seconds. The arm of the pressure-switching unit, upon reaching a conducting strip, short-circuits whatever device happens to be in circuit, giving a fixed frequency. The latter represents a point on the altitude scale. For the purpose of providing index marks on the altitude scale, only a portion of resistor R is left in the grid circuit when the pressure arm reaches the index contacts. An advantage of this arrangement over the one shown in figure 8 is the possibility of its extension to the measurement of a large number of phenomena without requiring an unduly complicated pressure-switching element.

The writers express their appreciation to L. L. Hughes of the Bureau's radio section for his skillful construction and contributions to the mechanical design of numerous experimental models; to D. N. Craig of the battery section for cooperation in the design of the temperature capillary thermometer; to J. P. Schrodt and C. L. Snyder of the battery section for assistance in determining battery requirements; and to W. G. Brombacher of the aeronautic instruments section for advice and data on meteorological instruments and calibration procedure and equipment. Special acknowledgment is made to Commanders J. B. Anderson and W. M. Lockhart, of the Bureau of Aeronautics, U. S. Navy Department, for advice on the meteorological aspects involved in the development of the radio meteorograph, and to Julien P. Friez & Sons, Inc., for cooperation in the mechanical design of the instruments.

XII. REFERENCES AND NOTES

[1] P. Moltchanoff, *Zur Technik der Erforschung der Atmosphäre*, Beitr. Physik freien Atm. **14,** 45–77 (1928).

In this paper Moltchanoff proposed adoption of the telemeteorographic principle of Olland to radio meteorography. His first working model was however based on a different principle.

L. Heck and G. Sudeck. *Neue Meteorographen für drahtlose Fernübertragung*, Gerlands Beitr. **31,** 291–314 (1931). *The modern radio meteorograph*, Nature (London) **130,** 1006–1007 (1932).

These papers give descriptions of the first radio meteorograph utilizing the Olland principle; this instrument was developed by Moltchanoff and manufactured by the Askania Werke, Germany.

W. Wenstrom. *Radiometeorography as applied to unmanned balloons*, Proc. Inst. Radio Engrs. **23,** 1345–1355 (1935). K. O. Lange, *Radio-meteorographs*, Bul. Am. Meteorol. Soc. **16,** 233–236, 267–271, 297–300 (1935).

These papers represent reviews of the prior art.

L. F. Curtiss and A. V. Astin. *A practical system for radio meteorography*, Aero. Sci. **3,** 35–39 (1935).

An Olland type radio meteorograph similar to the Askania Werke model, but employing ultrashort waves.

K. O. Lange. *The 1935 radio meteorograph of Blue Hill Observatory*, Bul. Am. Meteorol. Soc. **17,** 136–147 (1936).

An Olland type radio meteorograph employing ultrashort waves and having an expanded scale to reduce errors due to the pulsating motion of the clock arm.

O. C. Maier and L. E. Wood. *The Galcit radio meteorograph*, Aero. Sci. **4,** 417 (1937).

An Olland type radio meteorograph on 200 Mc/s.

L. F. Curtiss and A. V. Astin. *An electric motor for radio meteorographs*, Rev. Sci. Instr. **7,** 358 (1936).

[2] L. F. Curtiss, A. V. Astin, L. L. Stockman, B. W. Brown, S. A. Korff. *Cosmic ray observations in the stratosphere.*

To appear in a forthcoming issue of the Physical Review.

[3] P. Moltchanoff. *On the accuracy of the atmosphere investigations by means of radio meteorographs.* [In Russian; title in English.] Meteorol. Hydrologia **2,** Nr. 2, 30–41 (1936).

[4] R. Bureau. *Les Radiosondages météorologiques*, Onde Electrique **14,** 10–26, 87–96 (1935).

[5] P. Duckert. *Das Radiosondemodell Telefunken und seine Anwendung*, Beitr. Physik freien Atm. **20,** 303–311 (1933).

[6] Vilho Väisälä. *Eine Neue Radiosonde*, Mitt. Meteorol. Inst. Univ. Helsingfors **29** 1012 (1935). *The Finnish radio-sound*, Mitt. Meteorol. Inst. Univ. Helsingfors **35,** 1–28 (1937).

[7] R. Feige. *Zur Messung der oberen Wolken-und Nebelgrenze auf drahtlichem und drahtlosem Wege*, Z. Instrumentenk. **54,** 23–26 (1934).

[8] E. W. Herold. *Negative resistances and devices for obtaining it*, Proc. Inst. Radio Engrs. **23,** 1201–1224 (1935).

[9] J. Patterson. *A visual signalling meteorograph*, Trans. Roy. Soc. Canada **25,** section 3, 115–120 (1931).

[10] H. Diamond, W. S. Hinman, Jr., and F. W. Dunmore. *Development of a radio-meteorograph system for the Navy Department*, Bul. Am. Meteorol. Soc. **18,** 73–99 (1937). *A radio-meteorograph system with special aeronautical applications*, J. Inst. Aero. Sci. **4,** 241–248 (1937).

[11] D. N. Craig. *An electrolytic resistor.*
To appear in a forthcoming issue of the J. Research NBS.

[12] H. Diamond, W. S. Hinman, Jr., and E. G. Lapham. *Radio-meteorograph operation and performance.*
To appear in a forthcoming issue of the J. Research NBS.

[13] F. W. Dunmore. *An electric hygrometer and its application to radio meteorography.*
To appear in a forthcoming issue of the J. Research NBS.

[14] W. W. Coblentz and R. Stair. *A radiometric method of measuring ultraviolet solar radiation intensities in the stratosphere*, Radiologica **1,** 12 (1937).

R. Stair and W. W. Coblentz. *Radiometric measurements of ultraviolet solar intensities in the stratosphere*, J. Research NBS **20,** 185 (1938) RP1075.

WASHINGTON, December 6, 1937.

U. S. DEPARTMENT OF COMMERCE NATIONAL BUREAU OF STANDARDS

RESEARCH PAPER RP1083

Part of Journal of Research of the National Bureau of Standards, Volume 20, March 1938

PHOTOELASTIC DETERMINATION OF STRESSES AROUND A CIRCULAR INCLUSION IN RUBBER

By Wilfred E. Thibodeau and Lawrence A. Wood

ABSTRACT

Analysis is made of the stresses around a rigid circular inclusion with cemented boundary in a rubber sheet which is under simple tension at a distance from the inclusion. The analysis is performed by the photoelastic method, in which data are obtained from observations of the changes produced in a beam of polarized light passing through the transparent model. The fundamental principles of the method and a detailed account of their application are given. The possibilities of the use of rubber as a model material are demonstrated. The stress-optical coefficient of a certain soft vulcanized rubber compound is found to be 2,030 brewsters. This is in agreement with the results of previous work. The maximum stresses near the boundary of the disk are found to be about 50 percent greater than the average applied stress. The experimental results are compared with those given by a theoretical treatment of this problem, and quite satisfactory agreement is obtained.

CONTENTS

	Page
I. Introduction	393
II. Theory of stresses	394
1. Principal stresses	394
2. Isoclinic lines	395
3. Isostatic lines	395
4. Maxwell's equation of equilibrium	396
III. Photoelastic theory	398
1. Stress-optical coefficient	398
2. Location of isoclinic lines	399
IV. Experimental arrangement	399
1. Apparatus	399
2. Model	400
V. Procedure	400
1. Determination of stress-optical coefficient	400
2. Location of isoclinic lines	402
3. Location of isostatic lines	402
4. Evaluation of stresses	402
VI. Theoretical solution	407
VII. Discussion of results	408
VIII. Conclusions	409

I. INTRODUCTION

The problem of the stress distribution around a rigid inclusion in a body under tension is of considerable interest in a number of different fields, and yet there has been comparatively little work done on it. The related problem of the stresses around a hole has received much more attention. In the case of rubber, the problem of the rigid inclusion is particularly important not only with respect to inclusions of appreciable size, but also with respect to the microscopic and sub-

microscopic filler particles, which must give rise to some rather complex stress distributions. The present investigation of the stresses around a circular inclusion in rubber was originally undertaken with the aim of solving the much more complicated problem of the distribution of stress in rubber containing filler particles. Some preliminary work was done, on the mutual effect of the stresses arising from the presence of more than one inclusion, but the investigation was not completed.

For the experimental solution of such stress problems the extremely useful method of photoelastic analysis has come into prominence in recent years, especially since the publication by Coker and Filon of a comprehensive treatise [1] on the subject. The necessary data are obtained by observing in polarized light the patterns obtained when a transparent model is stressed.

Many years ago Maxwell [2] outlined the theory underlying the general methods of such analysis, but it remained for Mesnager,[3] Coker,[4] and others to develop practical procedure [5 6] and the materials [7] for the models. Extensive use of the method has been made in the study of engineering materials with models constructed of glass, Celluloid, Bakelite, and other substances, especially the organic plastics.

Since the results of a previous investigation [8] of the photoelastic properties of soft vulcanized rubber have indicated that some rubber compounds fulfill many of the requirements for a desirable model material, it was decided to study the problem of the stresses around a rigid circular inclusion with a cemented boundary in a rectangular model consisting of a sheet of transparent, soft vulcanized rubber under tension in one direction. In this manner, therefore, contrary to the usual practice, the problem could be studied with a model of the very material for which the solution was desired. Furthermore, by a definite illustration, it was desired to give a demonstration of the possibilities of the use of rubber as a model material in photoelastic work, and to present in convenient form for those unfamiliar with this field a detailed outline and illustration of the exact experimental procedure used for the solution of problems by this method.

II. THEORY OF STRESSES

1. PRINCIPAL STRESSES

Through every point in a plane section under stress there is a pair of mutually perpendicular lines across which the stresses are normal, the shearing stresses being zero in this case alone. These normal stresses are known as the principal stresses at this point. Across all other lines through the point, in general, shearing stresses exist. The directions of the principal stresses, if joined in continuous curves throughout the body, form a system of mutually orthogonal lines.

[1] E. G. Coker and L. N. G. Filon. A Treatise on Photoelasticity (Cambridge Univ. Press, 1931).
[2] J. C. Maxwell. *On the equilibrium of elastic solids.* Trans. Roy. Soc. Edinburgh **20**, 87 (1853); Reprinted in Scientific Papers **1**, 30 (Cambridge Univ. Press, 1890).
[3] A. Mesnager. *Contribution to the study of the elastic deformation of solids.* Ann. Ponts et Chaussées **4**, 128 (1901); *Determination of stresses in a glass model.* **16**, 133 (1913).
[4] E. G. Coker. *Photoelasticity for engineers.* Gen. Elec. Rev. **23**, 870 (1920); **23**, 966 (1920); **24**, 82 (1921); **24**, 222 (1921); **24**, 455 (1921).
[5] A. L. Kimball. *Optical determination of stress in a transparent material.* J. Opt. Soc. Am. **5**, 279 (1921)
[6] H. B. Maris. *Photoelastic investigations.* J. Opt. Soc. Am. **15**, 203 (1927).
[7] R. B. Carleton. *Suitability of materials for photoelastic investigations.* Rev. Sci. Instr. **5**, 30 (1934).
[8] Wilfred E. Thibodeau and Archibald T. McPherson. *Photoelastic properties of soft, vulcanized rubber* J. Research NBS **13**, 887 (1934) RP751. Reprinted in Rubber Chem. Tech. **8**, 183 (1935).

Knowledge of the magnitude and direction of the principal stresses at every point in the body furnishes a complete solution of the stress problem, both the normal and shearing stresses in any other direction being derivable by means of simple equations.

The symbols P and Q will be used to represent the maximum and minimum principal stresses, respectively, at a point in the plane of stress. Since neither normal nor shearing stresses can exist on a free boundary, the value of one of the principal stresses at a free boundary is zero. Tensile stresses will be represented by positive values for P or Q, while compressive stresses will be represented by negative values.

2. ISOCLINIC LINES

As an aid to the expression of the directions of the principal stresses at all points in a plane section under stress, it is convenient to define a family of curves, called isoclinic lines, along each of which the direction of the principal stress P makes a constant angle with the direction of applied stress. This constant angle, the parameter of the isoclinic, here denoted by ϕ, is the same as that between the normal to the direction of the applied stress and the direction of the Q stress. The family of isoclinic lines, then, serves to specify completely the directions of the principal stresses at all points in the plane section. It will be shown later that the isoclinics in a transparent medium under stress may become visible in polarized light under the proper conditions, and can be traced from direct observation.

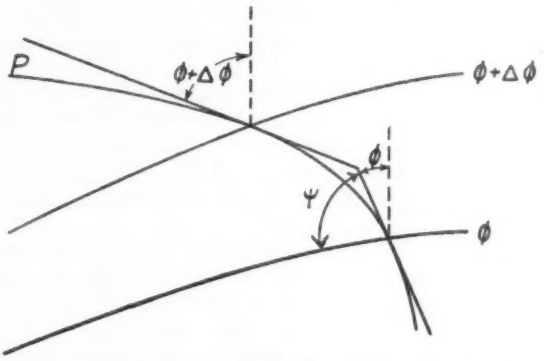

FIGURE 1.—*Method of plotting isostatic lines from the isoclinic lines.*

3. ISOSTATIC LINES

Another family of curves, called isostatic lines or simply lines of stress, can be drawn so as to indicate by their direction at any point, the direction of one of the principal stresses. In other words, for example, the direction of the Q stress at any point is given by the tangent to the Q isostatic at that point.

This manner of plotting the isostatics from the isoclinics is shown in figure 1. Let ϕ and $\phi+\Delta\phi$ be adjacent isoclinics. ϕ then is the locus of all points at which the principal stress line makes an angle ϕ with the zero position, and at the points along $\phi+\Delta\phi$ the principal stresses are inclined at the angle $\phi+\Delta\phi$. If now at certain intervals along ϕ, lines are drawn making the angle ϕ with the zero position, these will be tangent to the principal stress lines. These lines are continued to a point midway between the two isoclinics, and from there are continued through $\phi+\Delta\phi$ at an angle $\phi+\Delta\phi$. A continuation of

this process will furnish an envelope to which the principal stress lines can be drawn. After one set of principal stress lines has been completed in this manner, the other family of stress lines can be drawn in at right angles to the first or it can be obtained from the isoclinics in the same manner as the first.

The isoclinics and one set of isostatics, the Q lines, for the present case are shown in figure 2. These lines in themselves are not sufficient for a complete solution of the stress problem, since this requires the magnitudes of P and Q as well as their directions.

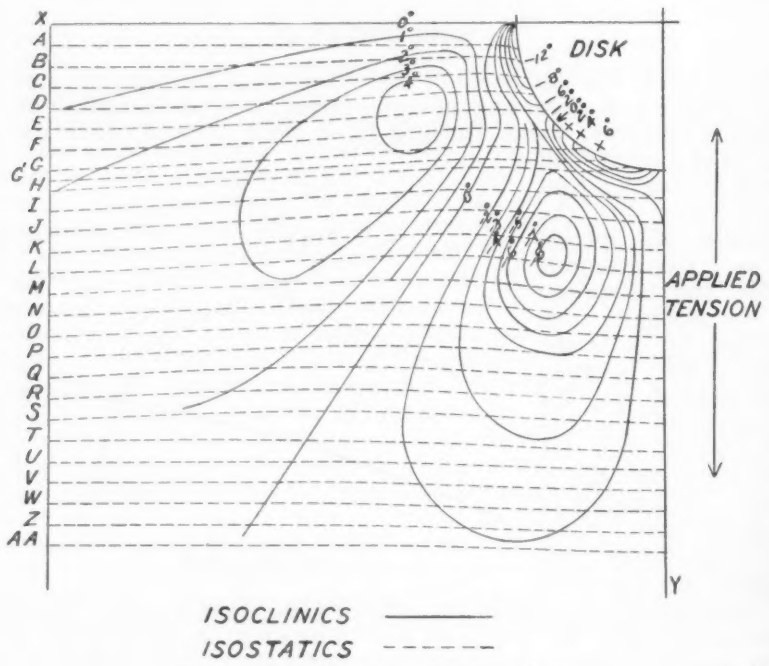

FIGURE 2.—*Isoclinic and O-isostatic lines.*

4. MAXWELL'S EQUATION OF EQUILIBRIUM

Maxwell, in his fundamental work, presented a pair of simplified equations of equilibrium:[9]

$$\frac{P-Q}{r_Q}+\frac{\partial P}{\partial s_P}=0 \tag{1a}$$

$$\frac{P-Q}{r_P}-\frac{\partial Q}{\partial s_Q}=0 \tag{1b}$$

On integration eq 1a yields:

$$P=P_0-\int_0^{s_P}\frac{P-Q}{r_Q}ds_P \tag{2}$$

[9] J. C. Maxwell. *On the equilibrium of elastic solids.* Trans. Roy. Soc. Edinburgh **20**, 87 (1853); Reprinted in Scientific Papers **I**, 30 (Cambridge Univ. Press, 1890). For a derivation of these equations, see page 129 of S. Timoshenko, Theory of Elasticity (McGraw-Hill Book Co., New York, N. Y., 1934).

in which P and Q are the principal stresses, s_P is the distance along the P line from the point where $P=P_0$, S_P is the value of s_P at the point considered, and r_Q is the radius of curvature of the Q line at this point. Similarly, integration of eq 1b gives:

$$Q=Q_0+\int_0^{S_Q}\frac{P-Q}{r_P}ds_Q \tag{3}$$

in which s_Q is the distance along the Q line from the point where $Q=Q_0$, S_Q is the value of s_Q at the point considered, and r_P is the radius of curvature of the P line at this point. P_0 and Q_0, the constants of integration, must be separately determined.

It is to be noted that these equations are merely equations of equilibrium, and so involve no elastic constants. Hence they will apply as well to plastic as to elastic substances; and this includes substances which have been stretched beyond the elastic limit and materials like rubber, which do not conform to Hooke's law. The only restrictions are that the material be homogeneous and in a state of equilibrium.

In practical work with a plot of isoclinics and isostatics it is somewhat difficult to measure directly the values of r_Q and r_P, and it is easier to compute them from the relation $r=\text{arc}/\text{angle}=\Delta S/\Delta\phi$, where ΔS is the arc on the stress line normal to the path of integration and bounded by the isoclinics of parameters ϕ and $\phi+\Delta\phi$ in the neighborhood of the point.

Furthermore, there are a number of advantages of improved applicability in expressing results in terms of ratios of the principal stresses to some applied stress rather than in terms of the principal stresses themselves. In the first place, the results are then independent of the stress units employed. Secondly, the results are immediately applicable to cases in which the applied load is different from that which happened to be employed in the particular case under consideration. Finally, a comparison with the results of a theoretical treatment is possible at each point of the sheet in terms of merely the coordinates of the point.

Therefore, eq 2 and 3 are modified by a substitution for r and by dividing both sides by the applied stress T, defined in the present case as the ratio of the applied load to the reduced cross-sectional area of the model.

$$\frac{P}{T}=\frac{P_0}{T}-\int_0^{S_P}\frac{P-Q}{T}\frac{\Delta\phi}{\Delta s_Q}\,ds_P \tag{4}$$

$$\frac{Q}{T}=\frac{Q_0}{T}+\int_0^{S_Q}\frac{P-Q}{T}\frac{\Delta\phi}{\Delta s_P}\,ds_Q \tag{5}$$

An alternative modification of eq 2 and 3, suggested by Filon [10] gives:

$$\frac{P}{T}=\frac{P_0}{T}+\int_{\phi_0}^{\phi}\frac{P-Q}{T}\cot\psi_P d\phi \tag{6}$$

$$\frac{Q}{T}=\frac{Q_0}{T}-\int_{\phi_0}^{\phi}\frac{P-Q}{T}\cot\psi_Q d\phi \tag{7}$$

[10] L. N. G. Filon. *Graphical determination of stress from photoelastic observations.* Engineering **116**, 511 (1923); Reprinted in Brit. Assn. Rep. **91**, 350 (1923).

Here ψ_P and ψ_Q represent the angles through which the P line of stress and the Q line of stress, respectively, must be rotated in a counterclockwise direction to bring them upon the isoclinic, and ϕ_0 is the value of ϕ, where $P=P_0$ and $Q=Q_0$.

The photoelastic method, as shown below, makes possible the evaluation of the quantities either in eq 4 and 5 or in eq 6 and 7. The question of which method to use is a matter of judgment and depends on the configuration of isoclinics and isostatics at the point considered. The ideal case for eq 4 and 5 is where $\psi=0$, that is, where the line of stress is itself an isoclinic. The ideal case for eq 6 and 7 is that in which the isoclinics are inclined at an angle of about 45° to the lines of stress and are closely packed. If ψ is too small the errors will be large in this method. In the present work both methods were used, sometimes even along the same line of integration.

III. PHOTOELASTIC THEORY

1. STRESS-OPTICAL COEFFICIENT

When light passes at normal incidence through a sheet of isotropic transparent material stressed in its plane, it emerges, as in the case of doubly-refracting uniaxial crystals, as two plane-polarized rays called ordinary and extraordinary rays, one polarized in the plane of one of the principal stresses and the other polarized at right angles to it, in the plane of the other principal stress. The velocities of these two rays are different, and depend on the intermolecular and interatomic forces in the directions of the principal stresses. The velocity of the ordinary ray is found to be proportional to the P stress plus a constant, and the velocity of the extraordinary ray to vary in exactly the same way with Q. The difference of the velocities is then proportional to the difference of principal stresses. The difference in the velocities of the two rays introduces a phase difference as they emerge from the medium. The phase change in each ray, as it passes through the medium, is proportional to the thickness of the medium and inversely proportional to the velocity of that ray. The phase difference, or retardation of one with respect to the other, is then proportional to the thickness and to the difference of the reciprocals of the velocities. Since the difference in the two velocities is extremely small compared with the velocities themselves, the difference of the reciprocals is approximately proportional to the difference of the velocities themselves.

It can thus be seen that the retardation of the ordinary with respect to the extraordinary ray at any point in the body is proportional to the difference of the principal stresses P and Q and to the thickness of the sample. That is,

$$R=C\,(P-Q)\,t, \tag{8}$$

where R is the relative retardation, t is the thickness of the medium, and C, thus defined, is a constant known as the stress-optical coefficient.[11] When the relative retardation is expressed in angstrom units, the stress in bars (1 bar$=10^6$ dynes/cm^2$=1.0197$ kg/cm^2$=14.504$ lb/in.^{2}), and the thickness in millimeters, the stress-optical coefficient is given in brewsters. A brewster is thus 10^{-13} cm^2/dyne.

[11] E. G. Coker and L. N. G. Filon. A Treatise on Photoelasticity, p. 185 (Cambridge University Press, 1931).

When the value of C for the material is known, the value of $(P-Q)$ at any point in the medium can be obtained by a determination of the retardation and a measurement of the thickness. This law, as expressed in equation 8, has been fairly definitely established for materials like Bakelite, Celluloid, and glass, and more recently for some vulcanized rubber compounds.[12] A compound (compound B, composition given below) which conformed to this relation was selected for the present investigation.

2. LOCATION OF ISOCLINIC LINES

It will now be shown how, as previously stated, in polarized light under the proper conditions the isoclinic lines become visible and can be traced from direct observation. Light which has been polarized by passage through a nicol prism, called the polarizer, passes through the sheet and is observed through a second nicol prism, the analyzer. At all points where the vibration plane of the polarizing nicol is at right angles to the direction of one of the principal stresses, one of the usual two plane-polarized rays passing through the medium is absent, since there is then no component of vibration corresponding to the plane of vibration of this ray. Under the same conditions if the analyzing nicol is set at right angles to the polarizing nicol, the second plane-polarized ray, which is actually present in the specimen, is not observed since it can not pass the second nicol. That is, as far as the point in question is concerned, the result is the same as if the model were not interposed. Hence a dark band or brush will appear marking the locus of all points in the model where the principal stress directions correspond with the vibration directions of the nicol prisms. In order to obtain a complete map of the isoclinics it is necessary merely to rotate the nicols by stages through 90°, keeping their vibration planes at right angles and tracing out one resulting isoclinic at each setting. The orientation of the prisms at each position is the parameter of the resulting isoclinic.

IV. EXPERIMENTAL ARRANGEMENT

1. APPARATUS

The apparatus used for the photoelastic determinations consisted essentially of a light source, two nicol prisms, means for supporting and stressing the model, suitable lenses, and a screen. The light source was a 1,000-watt projection lamp, with a water filter for the reduction of heating effects. By means of condensing lenses the light rays were brought to a focus within the nicol prisms and were reduced to parallelism in the region between the nicols where the model was placed. A further refinement, the placing of divergent lenses on either side of the nicol prisms so as to transmit the rays through them in a parallel beam, was found to be unnecessary with the large nicol prisms used. Both prisms were equipped with divided circular scales so that their inclinations could be recorded.

An arrangement of two displaceable quartz wedges known as the Babinet compensator was inserted between the model and the analyzing nicol when it was desired to measure the retardation produced in

[12] Wilfred E. Thibodeau and Archibald T. McPherson. *Photoelastic properties of soft, vulcanized rubber.* J. Research NBS 13, 887 (1934) RP751. Reprinted in Rubber Chem. Tech. 8, 183 (1935).

the stressed model. The compensator itself produced a retardation in the opposite direction amounting to 11,400 angstrom units for each centimeter of displacement of the wedges. In this manner the net retardation could be reduced to zero, and measurement made of the amount of retardation required to accomplish this. The compensator was mounted so that it could be turned until its axes were parallel to the principal stresses at the point under observation. The final lens focused an image of the model on a piece of plain white paper, which served adequately as a screen.

2. MODEL

The model was a rectangular sheet of soft transparent rubber 46.0 by 29.8 by 0.651 cm, in the center of which was placed a disk of stiff rubber-flooring material, the moduli of which were very great in comparison with those of the soft rubber. The disk was 5.22 cm in diameter and 0.62 cm in thickness. The periphery of the disk was coated with rubber cement (Vulcalock), and after vulcanization the disk became firmly embedded in the model.

The composition of the soft rubber was as follows:

	Parts by weight
Rubber	100. 0
Sulphur	2. 0
Zinc oxide (Kadox brand)	1. 0
Stearic acid	1. 0
Tetramethylthiuram disulphide	0. 3

This was cured for 45 minutes at 125° C in a steam press. The weight of the model was 858 g. It was loaded vertically by means of wooden clamps bolted to each end of the model. The weight of the lower clamps and bolts was 170 g.

V. PROCEDURE

1. DETERMINATION OF STRESS-OPTICAL COEFFICIENT

For the purpose of determining the photoelastic characteristics of the rubber, a separate tensile specimen of flat dumbbell shape was prepared from the same compound, and stretched. The results of observations in the central region of uniform stress are shown in table 1. Since here $Q=0$ and $P=T$, by the application of eq 8 to this case, one finds:

$$R=CTt, \tag{9}$$

where T is the applied stress, measured on the actual cross section and t the actual thickness. If σ is the compensator constant, the retardation per unit displacement of the compensator, and X the displacement,

$$\begin{aligned} R&=\sigma X=CTt \\ T&=\frac{\sigma}{Ct}X \end{aligned} \tag{10}$$

TABLE 1.—*Data for calculation of stress-optical coefficient*

[Original thickness 0.278 cm; original width 0.632 cm]

W = Applied load.
L = Distance between gage marks.
X = Displacement of compensator.

W	L	X
kg	cm	cm
0.000	4.98	0.000
.055	5.13	.145
.123	5.31	.330
.173	5.46	.485
.223	5.62	.650
.273	5.77	.815
.323	5.98	.970
.373	6.18	1.140
.423	6.40	1.345
.473	6.63	1.510

For pure gum rubber vulcanizate, which was used here, Poisson's ratio has been found [13] [14] to be 0.500 for elongations in the range under consideration. For an isotropic medium with a Poisson's ratio of 0.5, it may easily be shown that

$$T=T_0(1+\epsilon) \tag{11}$$

and

$$t=\frac{t_0}{\sqrt{1+\epsilon}} \tag{12}$$

where T_0 is the applied stress calculated on the original cross section, t_0 the original thickness, and ϵ the strain, or fractional elongation. Then

$$T_0(1+\epsilon)=\frac{\sigma}{Ct_0}X\sqrt{1+\epsilon} \tag{13}$$

This equation predicts proportionality between the quantity $T_0(1+\epsilon)$ and the quantity $X\sqrt{1+\epsilon}$.

A graph of the experimental data of table 1 verifies this proportionality and has a slope [15] of 2.06 kg cm^{-3}. On multiplication of this slope by the thickness, the value of σ/C is found to be 0.572 kg cm^{-2}. It is not necessary to compute the actual value of C.

Turning now to a consideration of the stretched model with the circular insertion, the mean thickness t_m of the model being 0.611 cm, one can apply eq 8 to obtain

$$P-Q=\frac{\sigma}{Ct_m}X=\frac{0.572}{0.611}X=0.936X \tag{14}$$

Since the thickness of the model varied from point to point, strictly the individual values should be used instead of a single mean thickness. This more rigorous method was applied at a number of selected

[13] Wilfred E. Thibodeau and Archibald T. McPherson. *Photoelastic properties of soft, vulcanized rubber* J. Research NBS **13**, 887 (1934) RP751. Reprinted in Rubber Chem. Tech. **8**, 183 (1935).

[14] William L. Holt and Archibald T. McPherson. *Change of volume of rubber on stretching: Effects of time, elongation, and temperature.* J. Research NBS **17**, 657 (1936) RP936. Reprinted in Rubber Chem. Tech. **10**, 412 (1937).

[15] From this slope a value of the stress-optical coefficient C may be calculated. Here t_0=2.78 mm, and σ=11,400 A/cm.

$$C=\frac{11{,}400}{(2.78)\ (2.06)\ (980)\ 10^{-3}}=2{,}030 \text{ brewsters.}$$

This result is in reasonable agreement with the value 2,096 brewsters, the average obtained over a much larger range of stresses for seven samples of this compound in the previous investigation by Thibodeau and McPherson (reference 13).

points, and was found to yield results differing from the simpler method by only about 5 percent at the most. In view of the difficulties of measurement and the increased complexity of calculation, it did not seem worth-while to utilize this more refined procedure.

The load applied near the center of the model included, in addition to an external load of 26.75 kg, the weight of the lower clamps and half the weight of the model. When this total load of 27.35 kg was applied, the distance between the clamps increased from 41.2 to 46.1 cm, the width of the model at the center decreased from 29.8 to 28.3 cm, and its mean thickness decreased from 0.651 to 0.611 cm. Dividing 27.35 kg by 17.3 cm^2, the reduced cross-sectional area, one obtains 1.58 kg/cm^2 as the value of T, the applied stress. Finally,

$$\frac{P-Q}{T}=\frac{0.936}{1.58}X=0.593X \tag{15}$$

This is the relation employed in the calculations involving the data obtained with the compensator.

2. LOCATION OF ISOCLINIC LINES

With the plane of vibration of the polarizing nicol vertical and the plane of vibration of the analyzing nicol horizontal, the external load of 26.75 kg was applied to the model along the vertical direction. The isoclinic with parameter $\phi=0°$ appeared as a dark line on the screen and was traced on the paper. Both nicols were then rotated 1° and the corresponding isoclinic was traced. This process was repeated until the complete pattern of isoclinics shown in figure 2 was obtained.

3. LOCATION OF ISOSTATIC LINES

When the complete family of isoclinics had been traced, the paper was removed and the Q isostatics shown in figure 2 were drawn in by the method already outlined and illustrated in figure 1.

4. EVALUATION OF STRESSES

The paper screen was again inserted in the optical system, and the Babinet compensator was introduced between the model and the analyzing nicol. For each determination the axes of the compensator were turned so as to be parallel with the lines of principal stress at the point considered. The nicol prisms, with their axes still perpendicular to each other, were turned so that the axes made positive and negative angles of 45° with the vertical. At every point where an isostatic was crossed by an isoclinic and at other suitable points, measurements were made of the compensator displacement necessary to nullify the retardation produced in the model. From these values, which are proportional to the differences of principal stresses, as has just been shown, the magnitudes of $(P-Q)/T$ were determined by the use of eq 15.

In all this work, when the load was removed the rubber showed no evidence of double refraction even after repeated cycles of stress. This fact proved the absence of initial residual stresses, the presence of which is one of the commonest faults of most model materials.

Sufficient data were now available for the evaluation of the principal stresses by the use of one or more of the eq 4, 5, 6, and 7. For example, in the data which were taken along the x-axis and which are given in table 2, the isostatic is itself an isoclinic, and, as already stated, this

is the ideal case for the application of eq 5. The logical place to begin the integration is at a free boundary, where the Q stress is known to be zero. Unfortunately, in the present instance no observation was made at the boundary. Therefore, the value -0.055, obtained by the theoretical solution for an infinite sheet as given in the section below, was taken for Q_0/T at the first point of observation. The magnitude of such an assumed value is likely to be slightly too large because of the finite size of the sheet.

At successive points along the isostatic, four observations were made: (1) S_Q, the distance along the Q stress line from the point of commencement of the integration to the point considered; (2) ΔS_P, the distance, measured along the P stress line through the point, between the two nearest isoclinics lying on opposite sides of the Q

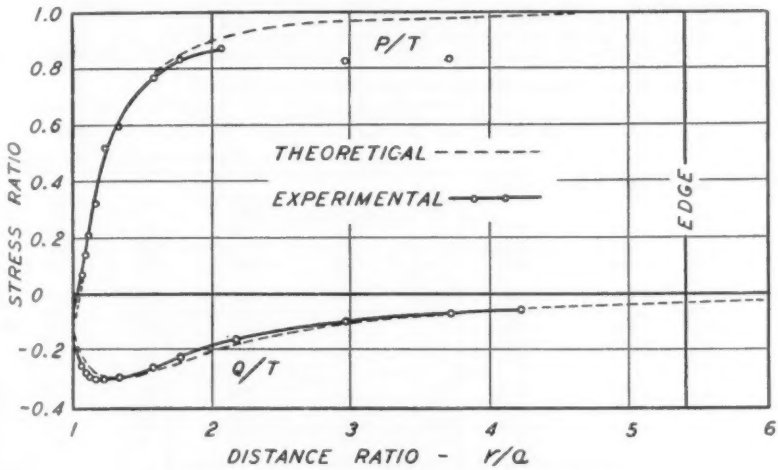

FIGURE 3.—*Principal stresses along the x-axis.*

Later independent observations failed to indicate as large a discrepancy between experimental and theoretical values as is indicated for the values of P/T at $r/a=2.97$ and $r/a=3.72$. Therefore, the experimental curve has not been continued through these points.

line and approximately equidistant from it, this approximate equality being brought about, if necessary, by the proper selection of the point to be considered; (3) $\Delta\phi$, the amount in radians by which these isoclinics differ; and (4) $(P-Q)/T$ from the compensator reading.

Graphic evaluation of the integral in eq 5 could be made by measurement of the area under the curve whose coordinates were $\left[\left(\frac{P-Q}{T}\right)\frac{\Delta\phi}{\Delta S_P}\right]$ and S_Q. These curves were not actually drawn in the present work, but the value of the integral was obtained for each interval as the product of mid-ordinate by the interval length.

The addition of values obtained in this manner yielded the results given for Q_e/T in table 2 and in figure 3. Finally, computations were made from the relation $P/T=(P-Q)/T+Q/T$ to obtain the results shown for P_e/T.

Along the y-axis, where again the isostatic is itself an isoclinic, there occurs the ideal case for the application of eq 4. The operation of obtaining P/T here was carried out in quite similar fashion to what has just been described in the application of eq 5. The value of P_0/T was taken from the theoretical solution as 1.054. The results

are shown in table 3 in the column headed P_e/T. Values of Q/T obtained from the relation $Q/T=P/T-(P-Q)/T$ are given in table 3 in the column headed Q_e/T. Since these values are obtained as the differences of two quantities which are much larger than these differences, the accuracy would not be expected to be so good as if they were obtained more directly.

TABLE 2.—*Principal stresses along the x-axis*

S_q = Distance along the Q isostatic, measured in arbitrary units of such size that the radius of the disk (a=2.61 cm) is equal to 30 units.
S_p = Distance along the P isostatic, measured in the same units as S_q. Since eq 5 and 6 involve merely the ratio of these quantities, the size of the unit is immaterial.
X = compensator displacement.
ϕ = parameter of the isoclinic, namely, the angle from the direction of the applied tension to the direction of the P stress.
r = distance from the center of the disk.
a = radius of the disk.
T = applied tension.
Q_e/T = experimental value of principal stress ratio Q/T, calculated by eq 5.
Q_t/T = theoretical value of principal stress ratio Q/T, calculated by eq 17 to 22.
P_e/T = experimental value of principal stress ratio P/T, calculated from Q_e/T and the relation $P/T=(P-Q)/T+Q/T$.
P_t/T = theoretical value of principal stress ratio P/T, calculated by eq 17 to 22.

S_q	X	$\Delta\phi/\Delta S_p$	r/a	Q_e/T	Q_t/T	P_e/T	P_t/T
Units	*cm*	*Radians/unit*					
			∞		0.000		1.000
0.0			4.23	[a]−0.055	−.055		.988
15.2	1.509	−0.0013	3.72	−.064	−.070	0.831	.983
37.8	1.554	−.0018	2.97	−.096	−.106	.826	.969
61.8	1.749	−.0035	2.17	−.159	−.179	.878	.924
73.8	1.779	−.0056	1.77	−.216	−.238	.839	.855
79.5	1.734	−.0060	1.58	−.250	−.261	.778	.780
86.8	1.499	−.0050	1.33	−.289	−.297	.600	.618
89.9	1.384	.0000	1.23	−.296	−.290	.525	.497
92.0	1.044	.0050	1.16	−.293	−.271	.326	.379
93.5	0.834	.0233	1.11	−.282	−.246	.212	.272
94.0	.699	.0700	1.09	−.272	−.233	.142	.224
95.0	.534	.1050	1.06	−.241	−.207	.076	.141
96.8	.419		1.00	[b]−.170	−.133	[b]−.04	−.067

[a] Theoretical value.
[b] Extrapolated value.

For the purpose of obtaining values of the principal stresses around the circumference of the disk and for obtaining independent values of Q/T on the y-axis, integrations were carried out along most of the Q isostatics shown in figure 2. Along lines A to G eq 5 was used for about the first six points and eq 7 for the remaining points. For line G' and all those below it eq 7 alone was employed. For those points where eq 5 was used, the method of calculation was identical with that performed along the x-axis.

With eq 7 three observations were made: (1) ψ_Q, the angle through which the line of stress must be rotated in a counterclockwise direction to bring it upon the isoclinic, the value being obtained most accurately by measuring the angle between the isoclinic and the horizontal, and subtracting from this angle the parameter of the isoclinic; (2) ϕ, the parameter of the isoclinic; (3) $(P-Q)/T$ from the compensator reading. The integrations here also were carried out by the multiplication of mid-ordinates and interval lengths. In all these integrations, except along the x-axis, the value of Q_0/T was taken as zero. P/T was calculated in the same manner as was done along the x-axis. Some of the results obtained at the last points of each integration are given in table 4 in columns headed Q_e/T and P_e/T, and the others in the columns headed Q_{et}/T and P_{et}/T in table 3.

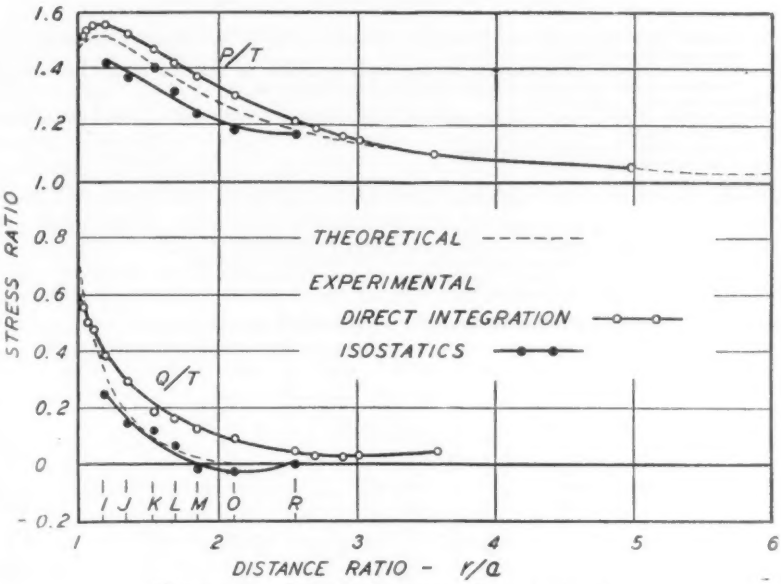

FIGURE 4.—*Principal stresses along the y-axis.*

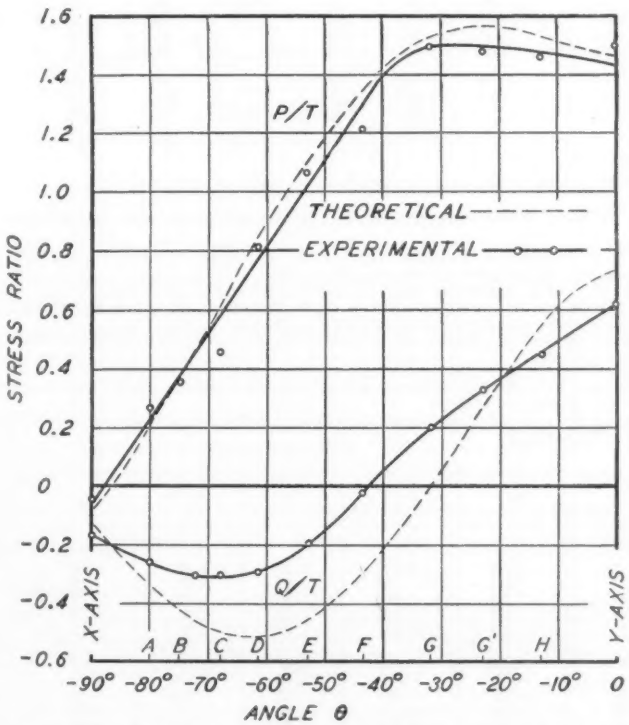

FIGURE 5.—*Principal stresses at the circumference of the disk.*

TABLE 3.—*Principal stresses along the y-axis*

S_P=distance along the P isostatic, measured in arbitrary units of such size that the radius of the disk (a=2.61 cm) is equal to 30 units.
S_Q=distance along the Q isostatic, measured in the same units as S_P. Since eq 5 and 6 involve merely the ratio of these quantities, the size of the unit is immaterial.
X=compensator displacement.
ϕ=parameter of the isoclinic, namely, the angle from the direction of the applied tension to the direction of the P stress.
r=distance from the center of the disk.
a=radius of the disk.
T=applied tension.
Q_e/T=experimental value of principal stress ratio Q/T, calculated from P_e/T and the relation $Q/T=P/T-(P-Q)/T$.
Q_{ei}/T=experimental value of principal stress ratio Q/T, calculated by eq 7 with $Q_0/T=0$, and with separate integrations along isostatics R, O, M, L, K, J, and I in figure 2.
Q_t/T=theoretical value of principal stress ratio Q/T, calculated by eq 17 to 22.
P_e/T=experimental value of principal stress ratio P/T, calculated by eq 4.
P_{ei}/T=experimental value of principal stress ratio P/T, calculated from Q_{ei}/T, and the relation $P/T=(P-Q)/T+Q/T$.
P_t/T=theoretical value of principal stress ratio P/T, calculated by eq 17 to 22.

S_P	X	$\Delta\phi/\Delta S_Q$	r/a	Q_e/T	Q_{ei}/T	Q_t/T	P_e/T	P_{ei}/T	P_t/T
Units	cm	*Radians/unit*							
			∞			0.000			1.000
0.0			4.98			−.005	[a] 1.054		1.054
42.2	1.773	−0.0019	3.58	0.045		−.008	1.096		1.098
59.0	1.880	−.0035	3.02	.031		−.008	1.146		1.139
62.6	1.923	−.0040	2.90	.021		−.007	1.16		1.15
68.3	1.959	−.0047	2.71	.029		−.006	1.19		1.17
72.8	1.975	−.0052	2.56	.045	0.003	−.004	1.22	1.17	1.19
85.8	2.046	−.0066	2.12	.095	−.030	.007	1.31	1.18	1.26
94.0	2.110	−.0073	1.85	.127	−.012	.028	1.38	1.24	1.32
98.8	2.126	−.0080	1.69	.164	.058	.052	1.42	1.32	1.37
103.3	2.169	−.0083	1.54	.186	.118	.089	1.47	1.41	1.42
109.0	2.074	−.0073	1.35	.297	.140	.180	1.53	1.37	1.48
113.8	1.971	−.0034	1.19	.389	.248	.330	1.56	1.42	1.52
116.6	1.808	.0083	1.095	.479		.487	1.55		1.51
117.3	1.761	.0165	1.073	.497		.531	1.54		1.51
117.7	1.741	.0159	1.060	.502		.564	1.54		1.50
118.5	1.618	.0270	1.033	.559		.644	1.52		1.48
119.5	1.320		1.000	[b] .62		.733	[b] 1.50		1.47

[a] Theoretical value.
[b] Extrapolated value.

TABLE 4.—*Principal stresses at the circumference of the disk*

θ=angle from the direction of applied tension to the line joining the center of the disk with the point considered. It is negative in the quadrant chosen.
Q_e/T=experimental value of principal stress ratio Q/T calculated by eq 5 or eq 7 with $Q_0/T=0$, and with separate integrations along isostatics H, G', G, F, E, D, C, B, A, and X in figure 2.
Q_t/T=theoretical value of principal stress ratio Q/T, calculated by eq. 17 to 22.
P_e/T=experimental value of principal stress ratio P/T, calculated from Q_e/T and the relation $P/T=(P-Q)/T+Q/T$.
P_t/T=theoretical value of principal stress ratio P/T, calculated by eq 17 to 22.
ϕ_e=experimental value of angle from direction of applied tension to direction of P stress, as observed from the isoclinics of figure 2.
ϕ_t=theoretical value of angle from direction of applied tension to direction of P stress, calculated from eq 17, 18, 19, and 22.

θ	Q_e/T	Q_t/T	P_e/T	P_t/T	ϕ_e	ϕ_t
Degrees					*Degrees*	*Degrees*
0	0.62	0.734	1.50	1.47	0	0
−13	.45	.548	1.46	1.53	9	10
−23	.33	.267	1.48	1.57	7	8
−32	.20	−.001	1.50	1.53	5	3
−43.5	−.02	−.287	1.22	1.35	1	−5
−53	−.19	−.449	1.07	1.12	−4	−12
−61.5	−.29	−.508	0.82	0.854	−8	−19
−68	−.30	−.489	.46	.625	−10	−24
−75	−.30	−.419	.36	.379	−12	−30
−80	−.25	−.329	.27	.217	−15	−33
−90	−.17	−.133	−.04	−.066	0	0

VI. THEORETICAL SOLUTION

The theory of the problem of the stresses in an infinite plate with a heterogeneous circular insertion has been treated by Sezawa and Nishimura,[16] who give a general solution in terms of the elastic constants of the plate and of the insertion. The constants used are λ, the plane stress constant [17] (not the Lamé constant of three-dimensional problems) and μ, the rigidity modulus.[18] In the present application the insertion is to be considered as completely rigid. Therefore, the elastic constants for it may be taken as equal to each other and infinite. This assumption reduces very materially the complexity of the general equations given by Sezawa and Nishimura. Furthermore, the terms involving the elastic constants of the plate may be expressed as functions of Poisson's ratio η by the following equation [19] from the general theory of elasticity;

$$\eta=\frac{\lambda}{\lambda+2\mu} \tag{16}$$

As previously stated, Poisson's ratio for rubber has been found [20] to be 0.500 for elongations in the present range.

Under these conditions the general equations of Sezawa and Nishimura reduce to the following:

$$\frac{\widehat{rr}}{T}=\frac{1}{2}\left\{1+\frac{1}{3}\frac{a^2}{r^2}+\left[1+\frac{12}{5}\frac{a^2}{r^2}-\frac{9}{5}\frac{a^4}{r^4}\right]\cos 2\theta\right\} \tag{17}$$

$$\frac{\widehat{\theta\theta}}{T}=\frac{1}{2}\left\{1-\frac{1}{3}\frac{a^2}{r^2}+\left[1-\frac{9}{5}\frac{a^4}{r^4}\right]\cos 2\theta\right\} \tag{18}$$

$$\frac{\widehat{r\theta}}{T}=-\frac{1}{2}\left[1-\frac{6}{5}\frac{a^2}{r^2}+\frac{9}{5}\frac{a^4}{r^4}\right]\sin 2\theta \tag{19}$$

Here θ is the angle between the direction of applied stress T and the line r from the center of the disk to the point under consideration; a is the radius of the disk; $\widehat{rr}$ and $\widehat{r\theta}$ are, respectively, the radial and tangential stresses across a section normal to r, while $\widehat{\theta\theta}$ is the stress normal to a section parallel to r.

The general theory of plane stresses yields equations [21] giving stresses referred to any axes rotated by a given angle with respect to selected axes. These equations can be applied to obtain the principal stress ratios P/T and Q/T in terms of the stress ratios $\widehat{rr}/T$, $\widehat{\theta\theta}/T$, and $\widehat{r\theta}/T$. The angle of rotation of axes, namely, the angle between r and P, is the difference between ϕ, the angle from the direction of applied stress

[16] K. Sezawa and G. Nishimura. *Stresses in a stretched plate containing a circular insertion.* Rep. Aeron. Research Inst., Tokyo Imp. Univ. **6**, 25 (1931).
[17] E. G. Coker and L. N. G. Filon. A Treatise on Photoelasticity, see page 115 (Cambridge Univ. Press, 1931).
[18] See footnote 17.
[19] See page 116 of reference 17.
[20] Wilfred E. Thibodeau and Archibald T. McPherson. *Photoelastic properties of soft, vulcanized rubber.* J. Research NBS **13**, 887 (1934) RP751. Reprinted in Rubber Chem. Tech. **8**, 183 (1935): William L. Holt and Archibald T. McPherson. *Change of volume of rubber on stretching: Effects of time, elongation, and temperature.* J. Research NBS **17**, 657 (1936) RP936. Reprinted in Rubber Chem. Tech. **10**, 412 (1937).
[21] E. G. Coker. *Photoelasticity for engineers.* Gen. Elec. Rev. **23**, 873 (1920).

to P, and θ, the angle from the direction of applied stress to r. In this manner one finds:

$$\frac{P}{T}=\frac{1}{2}\left[\frac{\widehat{rr}}{T}+\frac{\widehat{\theta\theta}}{T}+\frac{\widehat{rr}-\widehat{\theta\theta}}{T\cos 2(\phi-\theta)}\right] \tag{20}$$

$$\frac{Q}{T}=\frac{1}{2}\left[\frac{\widehat{rr}}{T}+\frac{\widehat{\theta\theta}}{T}-\frac{\widehat{rr}-\widehat{\theta\theta}}{T\cos 2(\phi-\theta)}\right] \tag{21}$$

and

$$\tan 2(\phi-\theta)=\frac{2\widehat{r\theta}}{\widehat{rr}-\widehat{\theta\theta}} \tag{22}$$

Equations 17 to 22 can then be used to obtain at any point the theoretical values of P/T, Q/T, and ϕ in terms of the coordinates (r, θ). The results are shown in tables 2, 3, and 4 in the columns headed P_t/T, Q_t/T, and ϕ_t, and in graphic form in figures 3, 4, and 5.

VII. DISCUSSION OF RESULTS

As might be expected, both P/T and Q/T can be seen to have their largest values in the region of the circumference of the disk near the axis in the direction of the applied load. The largest value of Q/T, according to both theory and observation, is found at the intersection of the circumference and this axis. The maximum of P/T along this axis, however, by both theory and experiment, is found displaced somewhat from this point in the direction away from the disk. The maximum of P/T around the circumference is also displaced somewhat from this point. The maximum of $(P-Q)/T$ at the circumference is found roughly halfway around the circumference of the quadrant.

What is not so obviously expected is the vanishing of the P/T and Q/T values on the boundary of the disk. Near the axis perpendicular to the direction of applied load the P/T values become negative, thereby indicating a slight compression. Q/T also has both positive and negative values, changing sign on the circumference about midway around the quadrant.

The maximum value of P is about 50 percent greater than T, the applied tensile stress, while the value of Q attains a maximum of the order of two-thirds of the applied tension.

Errors in the observed values, where they occur, may be ascribed to one or more of the following factors: (*a*) Errors inherent in the method used—(1) the admitted limitations of precision inherent in photoelastic determinations; (2) the difficulties of a graphic method of attack; and (3) the necessity of an extensive graphic integration to obtain some single points; (*b*) Errors entering into this particular investigation—(1) The difficulty of making photoelastic observations at the interface between the disk and the soft rubber, with the consequent necessity of some degree of extrapolation in a region where the stress variation is rapid; (2) the use of a single mean thickness instead of the actual thickness at each observed point; and (3) the uncertainty arising from the fact that the first observed point was not at the edge of the model.

The theoretical treatment involved assumptions contrary to the facts of the actual case in the following respects: (1) The sheet was assumed to be infinite in extent in both directions; (2) the deformations

were assumed to be infinitesimal; and (3) the effect of the clamps at the ends was neglected.

In view of all these factors involving possible causes of discrepancy, only the first four of which may be regarded as defects of the photoelastic method, agreement between observed and theoretical values is considered very satisfactory on the whole. The qualitative characters of the variations are the same in all cases. The locations of all critical values are identical, with the exception of Q/T in figure 5. The quantitative agreement seems as satisfactory as could be expected, except for those values of Q/T in figure 4, which were obtained as the difference of two nearly equal quantities, and except for Q/T in figure 5. In the latter case, not only were the observations difficult, but as the circumference of the disk is approached, there is a very rapid variation of Q/T, as can be seen in figures 3 and 4.

VIII. CONCLUSIONS

This work outlines a method of experimental procedure and demonstrates, by a reasonably close agreement with the theoretical treatment of a problem of complex stresses, that rubber can be employed as a model material in photoelastic work. Unlike most model materials it remains free from residual stresses, and, although it exhibits comparatively large deformations when stressed, it has such a large stress-optical coefficient that good results can be obtained with very small applied loads, less than one one-hundredth the size of those usually employed. Stress problems in rubber itself, for which theoretical treatment is often very difficult, can be readily solved in this manner. The application of results obtained with rubber models to cases involving steel and other engineering materials should be made with caution, however, on account of the difference in the values of Poisson's ratio.

Acknowledgment is made of the valuable assistance rendered by Dr. H. B. Maris and Mr. R. B. Carleton of the U. S. Naval Research Laboratory, Bellevue, D. C., in providing for the use of their unusually fine equipment in this work.

WASHINGTON, December 28, 1937.

U. S. DEPARTMENT OF COMMERCE NATIONAL BUREAU OF STANDARDS

RESEARCH PAPER RP1084

Part of Journal of Research of the National Bureau of Standards, Volume 20, March 1938

FIRE-CLAY LADLE SLEEVES

By Raymond A. Heindl and George J. Cooke *

ABSTRACT

Eight brands of fire-clay ladle sleeves, representing the product of practically all manufacturers in the United States except those on the Pacific Coast, were tested for service life in a steel foundry and certain properties of these sleeves were determined in the laboratory. The tests made in the laboratory included pyrometric cone equivalent, porosity, Young's modulus, transverse strength, extensibility, and linear thermal expansion.

In coordinating the service results with the results of the laboratory tests, it was evident that much of the trouble experienced in the foundry with the sleeves was due to lack of refractoriness of the sleeves and also to nonuniformity of some of the product, as indicated by the variation in certain of the properties of different specimens of the same brand of sleeves.

CONTENTS

	Page
I. Introduction	411
II. Samples and specimens	412
III. Laboratory tests of materials	412
1. Chemical composition	412
2. Pyrometric cone equivalents	413
3. Porosity	413
4. Young's modulus and strength	413
5. Linear thermal expansion	414
IV. Foundry service tests	414
1. Description of service	414
2. Results	415
V. Correlation and discussion of results of service tests and properties of materials as found by laboratory tests	415
VI. Summary and conclusions	417

I. INTRODUCTION

Bottom-pouring ladles are equipped with stopper rods to control the flow of metal during casting. These metal stopper rods are pivoted at the top of the ladle and pass vertically through the molten metal to the nozzle at the bottom. To prevent stopper rods from being attacked by the molten metal they are incased in fire-clay sleeves. The number of sleeves required (from 5 to 9) on a rod varies according to the depth of the ladle. The sleeves are joined by fire-clay cement and any space between the rod and the sleeve may or may not be filled with sand, ground firebrick, or similar material.

The manufacture of fire-clay sleeves is limited to a very few plants because the consumption of this specialty is small. However, such sleeves are of great importance since a product which cannot resist

* Mr. Cooke is Quarterman at the U. S. Naval Gun Factory, Washington, D. C.

the thermal shock and also meet the high temperature requirements may mean the loss of the heat or may cause severe injury or loss of life to those engaged in casting the steel.

Recently, difficulties were experienced due to sleeve failures in the steel foundry of the United States Navy Yard in Washington, D. C. As a result of these failures the National Bureau of Standards was requested to cooperate in a study of this fire-clay product. Sample sleeves selected at random from lots purchased by the foundry were studied to determine whether the performance to be expected in service from such sleeves could be evaluated from properties measured in the laboratory.

The problem is of particular interest because it was found possible to correlate results of laboratory tests and actual service results and, as a consequence, to indicate specifications by means of which products of good and poor quality can be readily distinguished on the basis of simple laboratory measurements.

II. SAMPLES AND SPECIMENS

Eight lots of 150 sleeves each were obtained for foundry testing from seven manufacturers or distributors, which represented most of the brands available in the eastern and central parts of the United States. An additional sample furnished on a bid request was tested only in the laboratory. Service data were recorded on approximately 60 of these sleeves selected at random. The sleeves, or hollow cylinders, have a wall thickness of 1¼ inches and are approximately 9 inches long and 5 inches in outside diameter. The ends are shaped to fit into each other, forming a modified taper joint.

For laboratory testing, at least two sleeves were selected in the case of six of the eight brands. The sleeves were cut in half lengthwise, and specimens were cut from the halves for porosity, Young's modulus, transverse strength and thermal expansion tests.

III. LABORATORY TESTS OF MATERIALS

1. CHEMICAL COMPOSITION

In general, the methods described by Finn and Klekotka,[1] and Lundell and Hoffman [2] were followed in making the chemical analyses. The results are given in table 1. The silica ranges from 55.42 to 65.99 percent, the alumina from 25.82 to 38.40 percent, the calcium oxide from 0.14 to 0.30 percent, and the iron, titanium oxides, etc., from 3.39 to 5.27 percent.

TABLE 1.—*Chemical composition (after ignition) of fire-clay sleeves*

Brand	1	2	3	4	5	6	7	8
SiO_2	55.42	58.58	59.62	64.30	65.99	65.48	65.31	65.95
Al_2O_3	38.40	31.77	34.90	27.24	25.82	27.53	26.27	26.76
CaO	0.14	0.21	0.30	0.14	0.26	0.14	0.19	0.17
$Fe_2O_3+T_iO_2$, etc	4.15	5.27	3.85	3.86	3.93	3.30	4.08	3.63

[1] *On a modified method for decomposing aluminous silicates for chemical analysis.* BS J. Research 4, 809 (1930) RP180.

[2] *Analysis of bauxite and of refractories of high alumina content.* BS J. Research 1, 91 (1928) RP5.

2. PYROMETRIC CONE EQUIVALENT

The pyrometric cone equivalents (pce or softening points) were determined according to the American Society for Testing Materials[3] standard method, serial designation C24–35. The values given in table 2 range from slightly above 20 to below 33.

3. POROSITY

The porosity determinations were made in accordance with the test method adopted by the American Ceramic Society.[4] The specimens weighed approximately 200 grams and the results of tests are given in table 2.

4. YOUNG'S MODULUS AND STRENGTH

The apparatus for determining Young's modulus of elasticity as well as the transverse strength of the fire-clay sleeves has been described by Heindl and Pendergast.[5] The specimens were tested over an 8-inch span. In general, the same types of curves were obtained as those illustrated in an earlier report.[6]

TABLE 2.—*Pyrometric cone equivalent, porosity, Young's modulus, strength, extensibility, linear thermal expansion, and service classification of fire-clay sleeves.*

Brand[a]	Pyrometric cone equivalent[b]	Porosity	Young's modulus	Transverse strength	Extensibility[c]	Linear thermal expansion		Service classification[d]
						25 to 1,000° C	Volume change between, approximately	
	Cone	*Percent*	*1,000 lb/in.²*	*lb/in.²*	*Percent*	*Percent*	*°C.*	
1	32-33 (1,725)	21.8	1,842	1,020	0.553	0.570	100 to 200 small	Very good (8).
2	27 (1,605)	11.4	4,964	1,820	.365	.545	550 to 600 small	Very good (2). Good (2). Fair (2). Poor (1).
2A	29 (1,640)	20.6	3,000	1,520	.506	.545	550 to 600 small	
3	32-33 (1,725)	13.6	3,580	1,850	.515	.670	100 to 200 large	Very good (4). Good (3). Fair (1).
4	23 (1,580)	15.9	3,682	1,775	.486	.620	550 to 600 large	Fair (8).
5	23 (1,580)	20.9	1,898	1,160	.620	.605	550 to 600 large	Fair (8).
6	26 (1,595)	16.1	3,883	1,740	.449	.580	550 to 600 small	Very good (3). Good (1). Fair (1). Poor (3).
7	20-23 (1,555) 27-28 (1,610)	14.5 16.9	3,120 3,590	1,610 2,310	.450 .644	.630 .554	550 to 600 large 550 to 600 small	Very good (1). Good (4). Fair (1). Poor (2).
8	23-26 (1,590)	17.0	2,942	1,500	.511	.615	550 to 600 large	Very good (1). Good (2). Fair (2). Poor (3).

[a] Only 1 sleeve available for all laboratory tests of brands 1 and 6, although a refractoriness test was made of a section of a second sleeve of brand 1 and the value obtained was not different from that shown; brands 4 and 5 made by the same manufacturer but marketed as of different quality; brand 7 was received as one shipment but because of differences in appearance two lots of sleeves were tested in the laboratory. For brand 2 the more refractory sample (2A) was received subsequent to the less refractory sample; it was not tested for service life. In comparison with other brands for which more than 1 sleeve was available for test this brand showed by far the greatest range in porosity, namely 9.0 to 20.6 percent.

[b] The numbers in parentheses following the cone numbers are the approximate temperature equivalents in ° C.

[c] Young's modulus divided by the transverse strength.

[d] The numbers in parentheses refer to the number of heats.

[e] Except for the range given, the expansion was fairly uniform between 25 and 1,000° C.

[3] Am. Soc. Testing Materials, Book of Standards, pt. 2, p. 229 (1936).

[4] J. Am. Ceram. Soc. 11, 456 (1928).

[5] *Young's modulus of elasticity at several temperatures for some refractories of varying silica content.* J. Research NBS 13, 851 (1934) RP747.

[6] *Progress report on investigation of fire-clay bricks and clays used in their preparation.* BS J. Research 3, 691 (1929) RP114.

The modulus of rupture was obtained after completion of the elastic measurements by gradually increasing the load until rupture occurred. The results of the tests are given in table 2.

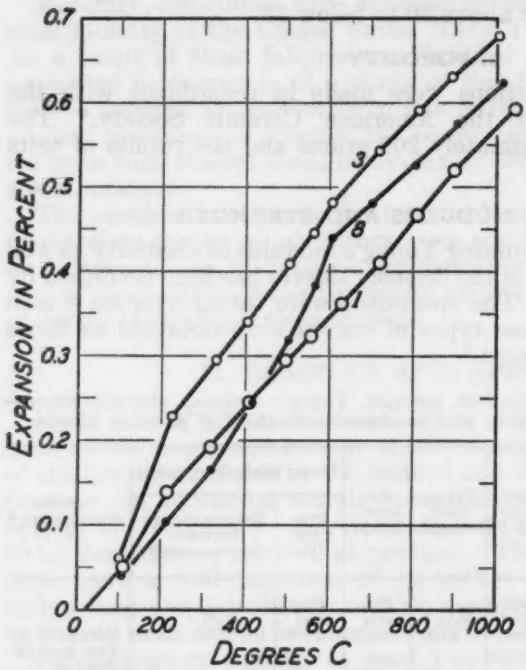

FIGURE 1.—*Linear thermal expansion curves for fire-clay sleeves, brands 1, 3, and 8, showing the three different types obtained.*

5. LINEAR THERMAL EXPANSION

The linear thermal expansion from room temperature to 1,000° C was determined by an indirect method[7] on specimens approximately ⅞ by ⅞ by 6 inches cut from the sleeves. For comparative purposes the total expansion obtained from room temperature to 1,000° C for each brand is given in table 2. It is also noted whether the rate of expansion increased appreciably either below or near 250 and 600° C, owing to crystalline silica inversions. The curves shown in figure 1 illustrate the three types of thermal expansions which were found in tests of the sleeves.

IV. FOUNDRY SERVICE TESTS

1. DESCRIPTION OF SERVICE

In the particular foundry in which the service tests were made, the ladles ranged in capacity from 8 to 30 tons. The average length of time of a pour is about 18 minutes, although on occasion this time may be exceeded by as much as 12 or 15 minutes, depending on the number and size of castings made. Sleeves are never used a second time. As far as type of material is concerned, no differentiation is made between basic or acid steel slags since the same type of fire-clay sleeves are used for either. The temperature of the metal as it leaves the furnace ranges from 1,605 to 1,670° C. The higher temperature is considered desirable to counteract the too rapid chilling of the metal when a great many castings are to be made.

The rod, stopper, and sleeves are dried at a low temperature after assembling. The ladles are preheated by means of an oil burner just before being filled with the molten metal. The temperature, within the ladle and about 6 inches from the wall at a point approximating

[7] J. Am. Ceram. Soc. 9, 555 (1926); BS J. Research 3, 691 (1929) RP114.

the position where the stopper rod would be, was observed to be approximately 675° C just previous to placing the stopper rod in position. The assembled rod, at room temperature, is placed in position immediately after the preheating of the ladle is completed. The ladle is then moved to the furnace and filled with the molten metal. The time interval between the discontinuance of preheating and the flow of the metal probably would not exceed 5 or 6 minutes. The fire-clay sleeves are thus subjected to two thermal shocks; the first, when placed in the heated ladle and the second, when the molten metal is run into the ladle.

In making the foundry tests the several brands of sleeves were subjected to the same service as far as practicable. The majority of the heats were made in an electrically heated basic type furnace. However, the number of heats made in the acid open hearth during the test period was sufficient to give some indication as to the durability of the sleeves used in that type of service.

2. RESULTS

An effort was made to differentiate between the service results obtained when the sleeves were preheated before being placed in the ladle. However, the temperatures of preheating, approximately 40 and 175° C for different assemblies, were apparently too low to have any significant effect on the life of the sleeves.

The results gained from observations made in the foundry are given in table 2. The classification (1) very good; (2) good; (3) fair; and (4) poor, is based entirely on observation of the relative resistance of the sleeves to cracking or spalling and to the cutting action of the slag. Sleeves classed "very good" were those in contact with the metal and slag for the longest periods and which showed very little attack; those classed "good" were in contact with the metal and slag for short periods and which showed only slight attack and no cracking; those classed "fair" showed appreciable cutting by slag, but such cutting while undesirable was not sufficient to cause the loss of the heat; those classed "poor" were badly attacked by slag, cracked or spalled and, in some instances, were the cause of losing the heat.

V. CORRELATION AND DISCUSSION OF RESULTS OF SERVICE TESTS AND PROPERTIES OF MATERIALS AS FOUND BY LABORATORY TESTS

The range in temperature of the metal leaving the furnace, as previously mentioned, is from 1,605 to 1,670° C. During the casting operation the temperature of the metal may drop 50 or 75° C. The point of interest in this connection is that in all but two of the cases given in table 2 the pyrometric cone equivalent (softening point) of the sleeves is below the temperature of the molten steel. The extreme case (brand 7), when the approximate temperature equivalent of the cone and the maximum metal temperature are considered, shows the metal to be hotter by 115° C. On occasion, it has been noted that the lowest sleeve has become bell-shaped by the end of the casting operation owing to deformation caused by the weight of the sleeves resting on it during long exposure at high temperatures. The excessive cutting and pitting shown by some of the sleeves is undoubtedly partially accounted for by the low softening points of those sleeves.

The average porosity of sleeves of the various brands ranges from 11.4 to 21.8 percent. The nonuniformity of sleeves of brand 2 is unusually great since the range in porosity (9.0 to 20.6) in that case is almost as great as the range for all other samples. In some instances this brand of sleeves spalled badly in the foundry and the built-up rod and sleeve assembly could not be used. Spalling and cracking would occur when the warm rod and sleeve assembly was placed in the heated ladle. Pieces remaining from these sleeves were found to have a porosity of 9.2 percent, indicating a porosity as low as that to be undesirable. A high porosity, as in the case of brand 1, does not necessarily mean a low resistance to slag attack; the high refractoriness has apparently an important bearing on such resistance since brand 1 showed excellent resistance to slag in spite of being the most porous.

A low value for Young's modulus in bending and a high value for modulus of rupture would be desirable since it would result in a high extensibility which, as shown in a previous publication,[8] is very desirable from the standpoint of resistance to thermal shock. Table 2 shows brand 2 to range in extensibility from 0.365 to 0.506 percent. The lower value is decidedly lower than the second lowest value. As already stated, brand 2 was the only one which spalled badly when the rod and sleeve assembly was placed in the heated ladle. The low extensibility or "ultimate stretch" of certain sleeves of this brand undoubtedly was a contributing factor to the readiness with which they spalled.

Other properties being equal, it would be expected that sleeves of uniform and low thermal expansion between room temperature and 1,000° C would resist failure due to thermal shock much better than sleeves having a high expansion in either or both of the temperature ranges approximating 150 to 250° C and 550 to 600° C. In the case of fire-clay sagger bodies, the importance of the extent of the expansion between room temperature and 250° C was pointed out by Heindl.[9] In the present case any abrupt change in expansion between 550 and 600° C due to the alpha to beta quartz inversion probably would be equally as important a factor in causing cracking of sleeves as the abrupt change occurring between 150 and 250° C due to the alpha to beta cristobalite inversion, because of the rapidity with which the changes must take place. The inversion at the lower temperature occurs when the rod and sleeve assembly is placed in the hot ladle and the other inversion when the hot steel contacts the sleeves. In table 2 are noted the total expansions up to 1,000° C. It is also noted whether the expansion was greater between the 150 to 250° C and 500 to 600° C ranges than at other temperature ranges between 20 and 1,000° C. In all but two cases (brands 1 and 3) the rate of expansion apparently does not change in the 150 to 250° C range. The rate increased slightly within this range in the case of brand 1 and increased greatly in the case of brand 3. On the other hand, all brands except 1 and 3 showed increased rates of expansion between 500 and 600° C. There is little doubt that the not unfavorable expansion characteristics exhibited by brand 1 contributed to the satisfactory results obtained in service. It is difficult to evaluate the effect of the increased expansion between 500 and 600° C shown by most of the

[8] Raymond A. Heindl. *A study of sagger clays and sagger bodies.* J. Research NBS 15, 255 (1935) RP827.
[9] *A study of sagger clays and sagger bodies.* J. Research NBS 15, 255 (1935) RP827.

brands because of the other properties for which values are given and which undoubtedly contribute to unsatisfactory results obtained in service.

Any rating of "poor" in the service-classification column, table 2, indicates that the particular brand of sleeve would be classed as unsatisfactory even though some of the "heats" gave no trouble and are classed "good". This procedure is justified on the basis of the possibility of the partial or complete loss of a heat whenever such sleeves are used. In other words, sleeves should be of such quality that the consumer may have complete confidence in their ability to perform the service expected of them. From table 2 it may be inferred that four of the brands did not give the expected service. The classification ranging from "very good" to "poor" on some brands may be attributed mainly to the nonuniformity of sleeves in the same lot, to the possibility that the sleeves classified as "very good" had the advantage of steel closer to the lower temperature rather than the higher in the range 1,605 to 1,670° C, and also to the possibility that the length of time that the metal was in contact with the sleeves may have been relatively short in certain cases.

In table 2 are given duplicate values for the properties of brands 2 and 7. Differences in these sleeves were so obvious from visual inspection that in the tests they were treated as different types. In both cases, the range in properties from unfavorable to favorable could readily account for the range in service classification from "poor" to "very good".

The chemical composition of the sleeves was determined to learn whether the sleeves highest in silica would be less resistant to attack by basic slag. The data obtained are too meager to warrant drawing definite conclusions, but the results do show that in all cases (approximately 18 percent of total) of acid slag the sleeves gave satisfactory service.

VI. SUMMARY AND CONCLUSIONS

A study was undertaken of eight brands of sleeves made by seven manufacturers. It is believed the product of all manufacturers except those on the Pacific Coast was represented. Certain properties of these sleeves were determined in the laboratory and records were obtained of the behavior of the sleeves in steel foundry service. The results obtained in each of eight heats was recorded for most brands.

The chemical composition, pyrometric cone equivalent, porosity, Young's modulus, strength, extensibility, and linear thermal expansion were determined.

The results obtained in the laboratory are coordinated with the service results obtained in the foundry and the following conclusions appear justified:

1. The temperature of softening of the sleeves in all but two cases was below the temperature of the molten steel surrounding them. In the extreme case the metal was hotter by approximately 115° C.
2. Excessive cutting and pitting during the casting of heats (average time 18 minutes, maximum about 30 minutes) was noted in many of the sleeves of low refractoriness.

3. The average porosity of all brands of sleeves ranged from 11.4 to 21.8 percent, although one brand showed a range in porosity from 9.2 to 20.6 percent for the different sleeves. Those of lowest porosity in this brand gave serious trouble as a result of spalling and cracking.

4. The range in Young's modulus was from 1,842,000 to 4,964,000 lb/in.^{2} The modulus of rupture ranged from 1,020 to 2,310 lb/in.^{2} and the extensibility ranged from 0.365 to 0.644 percent. The highest value for Young's modulus accompanied by the lowest value for extensibility was found in the brand of sleeves which caused much trouble due to spalling and cracking in foundry service.

5. The silica content ranged from 55.42 to 65.99 percent. Service results on the sleeves in contact with acid open hearth slags were satisfactory in all of the limited number of heats observed.

6. The total linear thermal expansions from 25 to 1,000° C ranged from 0.545 to 0.670 percent. All curves showed some inflection due to crystalline silica inversions in either the 100 to 200° C or 500 to 600° C temperature range, although the inflection was small in some cases.

7. The brand of sleeves which gave the most satisfactory results in service was very refractory, had fairly high porosity, a fairly uniform and not high expansivity, and a moderately high extensibility.

8. A great deal of variation in the properties and service results was noted in different sleeves of some of the brands indicating lack of uniformity in the product.

9. There is a sharp dividing line in the degree of refractoriness between the two brands of highest refractoriness and the remainder of the brands. In the purchase of sleeves for the type of steel foundry practice followed by some United States Navy Yards, it would appear desirable to specify a refractoriness requirement. The specified pyrometric cone equivalent expressed in approximate temperature equivalent should be greater than, or at least equivalent to, the maximum temperature of the molten metal as it enters the ladle. It would also seem desirable to specify a porosity requirement of not less than 15 percent. A minimum extensibility value and a linear thermal expansion without erratic changes due to silica inversions are also possible and desirable requirements, but because of the lack of equipment at present in most laboratories for determining the numerical values, it is doubtful that manufacturers could conveniently determine whether their product complied with such requirements. If a refractoriness requirement is specified, not much appears to be gained by specifying limits in the chemical composition.

WASHINGTON, October 28, 1937.

○